Antibiotic Uptake into Bacteria: Negamycin Translocation Across the Outer and Cytoplasmic Membranes of *Escherichia coli*

Dissertation

der Mathematisch-Naturwissenschaftlichen Fakultät

der Eberhard Karls Universität Tübingen

zur Erlangung des Grades eines

Doktors der Naturwissenschaften

(Dr. rer. nat.)

vorgelegt von

Daniel Hörömpöli

aus Böblingen

Tübingen

2022

Gedruckt mit Genehmigung der Mathematisch-Naturwissenschaftlichen Fakultät der Eberhard Karls Universität Tübingen

Tag der mündlichen Prüfung:	28.02.2023
Dekan:	Prof. Dr. Thilo Stehle
1. Berichterstatter:	Prof. Dr. Heike Brötz-Oesterhelt
2. Berichterstatter:	Prof. Dr. Samuel Wagner

Table of contents

Abbreviations

µ	micro
ATP	adenosine triphosphate
CFU	colony forming units
CM	cytoplasmic membrane
Da	Dalton
DNA	desoxyribonucleic acid
DOPG	1,2-dioleoyl-phosphatidylglycerol
e.g.	*exempli gratia*
FES	free energy surface
g	gram
h	hour
HPLC	high performance liquid chromatography
i.e.	*id est*
ITC	isothermal titration calorimetry
K_d	disassociation constant
l	liter
LPS	lipopolysaccharide
MIC	minimal inhibitory concentration
min	minute
MS	mass spectrometry
NMR	nuclear magnetic resonance
OD_{600}	optical density at 600 nm
OM	outer membrane
Omp	outer membrane protein
POPC	1-palmitoyl-2-oleoyl-phosphatidylcholine
POT	proton-dependent oligopeptide transporter
PP	polypeptone medium
RNA	ribonucleic acid
RND	resistance-nodulation cell division transporters
SAW	surface acoustic wave
TLC	thin layer chromatography
tRNA	transfer RNA
v/v	volume per volume
WT	wildtype
w/v	weight per volume

Zusammenfassung

Viele Antibiotika gegen Gram-positive Bakterien zeigen keine Aktivität gegen Gram-negative Spezies, da die Aufnahme durch eine weitere, äußere Membran verhindert wird. Sofern sich die Zielstruktur des Antibiotikums innerhalb des Zytoplasmas befindet, so muss das Antibiotikum sowohl die äußere Membran als auch die Zytoplasmamembran überwinden. Zur Diffusion über die äußere Membran durch Porine müssen Moleküle klein, hydrophil und geladen sein, wohingegen für passive Diffusion über die Zytoplasmamembran Moleküle hydrophob und ungeladen sein sollten. Negamycin ist ein Antibiotikum, welches in vorherigen Publikationen gute Aktivität gegen Gram-negative und Gram-positive Spezies zeigte. Diese Eigenschaft macht es zu einem interessanten Molekül für Aufnahmeversuche, da es sowohl die äußere als auch innere Membran passieren muss, um seine Zielstruktur am Ribosom zu erreichen. Negamycin bindet sowohl an die kleine ribosomale Untereinheit als auch an die benachbarte tRNA, wodurch die Translokation behindert und die Bindung zu unspezifischen tRNAs stabilisiert wird, was zu *Miscoding* führt. In Derivatisierungs-Studien zeigten die meisten Negamycin-Analoga keine verbesserte Aktivität gegen Bakterien, obwohl manche Analoga eine stärkere Interaktion mit der Zielstruktur aufwiesen, was auf eine verringerte Aufnahme in Bakterien hindeutet. Wir waren daher am Aufnahmemechanismus von Negamycin interessiert und haben hierfür *Escherichia coli* als Modellorganismus verwendet.

Die erste Barriere für Antibiotika ist die äußere Membran. Da Negamycin klein, hydrophil und bei neutralem pH positiv geladen ist, hat es ideale Moleküleigenschaften zur Diffusion durch Porine, die als wassergefüllte Kanäle die ganze äußere Membran durchspannen. Im Rahmen dieser Arbeit konnte zum ersten Mal gezeigt werden, dass ein Aminoglykosid-Antibiotikum die *E. coli* Porine OmpF und OmpC verwendet, da die Translokation von Kanamycin durch diese Porine nachgewiesen wurde. Im Fall von Negamycin konnte nur eine sehr schwache Abnahme der Bioaktivität festgestellt werden, wenn die beiden Poringene *ompF* und parallel *ompC* in *E. coli* deletiert wurden. Ein alternativer Aufnahmeweg über die äußere Membran, wie der sogenannte *Self-Promoted Uptake*-Mechanismus, konnte für Negamycin nicht beobachtet werden. Deletionen anderer Poringene, die bislang nicht im Zusammenhang mit Antibiotika-Aufnahme standen, zeigten einen Effekt auf die Negamycinempfindlichkeit, und zwar bei den Porinen OmpN, ChiP, LamB, OmpG, OmpW und OmpA. *In vitro* konnte in elektrophysiologischen Experimenten die Diffusion von Negamycin durch die gereinigten Porine OmpN, ChiP, OmpF und OmpC gezeigt werden. Im direkten Vergleich konnten Ertapenem, Cefotaxim und Kanamycin OmpN nicht passieren. Die selektive Barriere von OmpN wurde weiter untersucht. Hierzu wurde die Kristallstruktur von OmpN aufgelöst. OmpN zeigte zwar in der *Constriction Region*, der engsten Stelle eines Porins, einen ähnlichen Durchmesser wie OmpF und OmpC, aber die Anordnung der Aminosäuren innerhalb von OmpN sorgt für eine elektrostatische Barriere. Diese elektrostatische Barriere verhinderte die Passage von Kanamycin, ermöglichte aber den Durchtritt von Negamycin durch OmpN, was anhand von Simulationen berechnet und gezeigt werden

konnte. Das Transkriptom von *E. coli* BW25113 wurde untersucht und die Expression von *ompN* und *chiP* war zwar sehr gering, aber *E. coli* BW25113 erhöhte die Expression dieser Poringene, wenn es mit Negamycin behandelt wurde. Diese erhöhte Expression reichte jedoch nicht aus, um die zugehörigen Porinproteine im Western Blot nachzuweisen.

An der inneren Membran konnten mehrere Aufnahmewege und der Einfluss der Zusammensetzung von Nährmedien auf die Aktivität von Negamycin demonstriert werden. In einem Peptid-freien Medium nutzt Negamycin bevorzugt den ATP-abhängigen Dipeptid-Transporter Dpp. Eine verringerte zytoplasmatische Akkumulation von Negamycin konnte durch Messung von [^{3}H]negamycin in *dppA*-defizienten Mutanten gezeigt werden. Weiterhin wurde beobachtet, dass Mutanten, die auf Peptid-freiem Agar selektiert wurden, dem Negamycin zugesetzt worden war, Veränderungen im *dpp* Operon zeigten. Außerdem konnte der Einfluss von weiteren ATP-abhängigen Transportern sowie Protonen-abhängigen Oligopeptid-Transportern auf die Negamycinaufnahme nachgewiesen werden. Der Effekt von Salzen auf Negamycin wurde untersucht, und es wurde beobachtet, dass die Zugabe von $CaCl_2$ die Aktivität von Negamycin erhöht. Andere Salze, wie $MgCl_2$, NaCl, KCl und NH_4Cl, erhöhten die Negamycinaktivität jedoch nicht. Bei hohen Konzentrationen von NaCl, KCl oder NH_4Cl wurde sogar eine Verringerung der Negamycinaktivität festgestellt. Ein basischer pH erhöhte die Negamycinaktivität, und ein additiver Effekt wurde beobachtet, wenn $CaCl_2$ zu einem Peptid-reichen Medium mit pH 8,5 gegeben wurde. Akustische Oberflächenwellen-Messungen zeigten, dass $CaCl_2$ die Bindung von Negamycin an Phospholipide erhöhte. Negamycin und Ca^{2+} bilden einen Komplex, was durch eine Verringerung des Retentionsfaktors von Negamycin bei der Dünnschichtchromatographie und bei Affinitätsversuchen mit der Isothermen Titrationskalorimetrie gezeigt wurde. Die Aktivität von Negamycin war auch beeinträchtigt, wenn Gene der Atmungskette deletiert wurden oder unter anaeroben Wachstumsbedingungen, jedoch nur in Peptid-reichen Nährmedien, da hier der Dpp-abhängige Aufnahmeweg nicht zur Verfügung stand. Diese Ergebnisse deuten darauf hin, dass die Aktivität von Negamycin durch das Membranpotential der Zytoplasmamembran beeinflusst wird, was mit den Beobachtungen bei den pH-Experimenten im Einklang steht. Diese Abundanz der verschiedenen Aufnahmewege führte zu sehr geringen Resistenzraten, wenn *E. coli* mit einer Negamycinkonzentration behandelt wurde, die der vierfachen minimalen Hemmkonzentration entsprach.

Schließlich wurde noch ein Protokoll für die Biosynthese und Batch-Aufreinigung von Negamycin etabliert. Aus dem Überstand einer *Streptomyces purpeofuscus*-Kultur wurde in zwei Schritten mit Hilfe von Kationaustauschchromatographien Negamycin aufgereinigt. Das aufgereinigte Negamycin war weniger verunreinigt als kommerziell erworbenes Negamycin aus der chemischen Totalsynthese, wie Ergebnisse der Dünnschichtchromatographie und Hochleistungsflüssigkeitschromatograhie zeigten. Eine Reinheit von über 95% konnte für das biosynthetisch gewonnene Negamycin durch Kernspinresonanzspektroskopie nachgewiesen werden.

Diese Arbeit bietet neue Erkenntnisse zu den Aufnahmemöglichkeiten von Negamycin in *E. coli*. Neue Aufnahmewege konnten identifiziert werden, sowohl an der äußeren als auch inneren Membran. Diese Ergebnisse verbessern unser Verständnis der Aufnahme von pseudo-peptidischen Naturstoffen in Bakterien und können bei der weiteren Entwicklung von Negamycinderivaten helfen.

Summary

Many antibiotics against Gram-positive bacteria show no activity against Gram-negative species, as uptake is hindered by the additional outer membrane. If the antibiotic's target is within the cytoplasm, the antibiotic has to overcome both the outer and cytoplasmic membranes. For diffusion across these two membranes, ideal molecule attributes are strongly opposing. For outer membrane diffusion through porins, molecules should be small, hydrophilic and charged, whereas for passive diffusion across the cytoplasmic membrane, molecules should be hydrophobic and uncharged. Negamycin is a natural product antibiotic, which showed better activity against Gram-negative than Gram-positive species, which makes it an interesting molecule for uptake studies, as it has to overcome both outer and inner membranes to reach its target binding site at the ribosome. Negamycin binds both the small ribosomal subunit as well as the nearby tRNA, inhibiting translocation and stabilizing unspecific tRNAs, which leads to a miscoding activity. In derivatization studies, most negamycin analogues did not show improved whole cell activity, although some showed stronger target interactions, indicating that uptake was reduced upon modification. We were therefore interested in studying the uptake pathways of negamycin and used *Escherichia coli* as a model organism.

The first barrier for antibiotics is the outer membrane. As negamycin is small, hydrophilic and positively charged at neutral pH, it has the ideal molecular properties to diffuse through porins, which are water-filled channels spanning the whole outer membrane. In this thesis, it could be shown for the first time that an aminoglycoside antibiotic uses the major *E. coli* porins OmpF and OmpC, as kanamycin translocation through these porins was demonstrated. For negamycin, only a small decrease in bioactivity was detected when both porin genes *ompF* and *ompC* were deleted. Alternative pathways across the outer membrane, like the self-promoted uptake mechanism, could not be observed for negamycin. The deletion of the genes of other porins, which so far have not been associated with antibiotic translocation, had an effect on negamycin susceptibility, namely of OmpN, ChiP, LamB, OmpG, OmpW and OmpA. *In vitro*, electrophysiological experiments showed translocation of negamycin through the purified proteins OmpN, ChiP, OmpF and OmpC. When measured in parallel, ertapenem, cefotaxime and kanamycin were not able to pass through OmpN. The selective barrier of OmpN was investigated further. To this end, the crystal structure of OmpN was resolved. The constriction region of OmpN, which is the narrowest region of a porin, showed a similar size as OmpF and OmpC. However, amino acid residues ranging inside the barrel structure of the OmpN protein create an electrostatic barrier, which hinders the passage of, e.g., kanamycin, but not of negamycin, as molecular dynamics simulations could show. Investigations of the *E. coli* BW25113 transcriptome revealed that the expression of the *ompN* and *chiP* genes was low, but increased when *E. coli* was treated with negamycin. These increased transcript levels, however, did not raise the protein amounts to an extent, where the proteins could be detected by Western blot analysis.

At the inner membrane, multiple uptake pathways and environmental conditions affecting negamycin activity could be identified. In a peptide-free medium, negamycin preferably uses the ATP-dependent dipeptide transporter Dpp. A decrease in negamycin accumulation was shown by [^{3}H]negamycin measurements in a *dppA*-deficient mutant. Additionally, all mutants selected on peptide-free agar containing negamycin showed alterations in the *dpp* operon. Further ATP-dependent peptide transporters and proton-dependent oligopeptide transporters are involved in negamycin uptake as well. The effect of salts on negamycin was investigated and it could be observed that $CaCl_2$ increases negamycin activity. Other salts, like $MgCl_2$, NaCl, KCl or NH_4Cl, did not increase negamycin activity, but NaCl, KCl or NH_4Cl actually decreased susceptibility at high salt concentrations. A shift to alkaline pH increased negamycin activity and an additive effect could be observed, when $CaCl_2$ was added to a peptide-rich medium at pH 8.5. $CaCl_2$ increases binding of negamycin to phospholipids, which was shown by surface acoustic wave measurements. Negamycin forms a complex with Ca^{2+}, which was demonstrated by a reduction of the retardation factor during thin layer chromatography in the presence of $CaCl_2$ and by binding studies using isothermal titration calorimetry. Negamycin activity was also affected by the deletion of genes involved in the respiratory chain and in an anaerobic growth environment, but only in a growth medium with peptides, as here the Dpp-mediated uptake pathway is not available. These results indicate that negamycin activity could be affected by the membrane potential across the cytoplasmic membrane, which may also explain the observations in the pH experiments. This abundance of multiple uptake pathways resulted in very low resistance rates, when *E. coli* cells were treated with negamycin concentrations equivalent to four times the minimal inhibitory concentration.

Finally, a protocol for negamycin fermentation and batch purification could be established. From the supernatant of a *Streptomyces purpeofuscus* culture, negamycin was purified in two steps using cation exchange chromatography. The purified negamycin was less impure than material generated by total synthesis, as judged by thin layer chromatography and high-performance liquid chromatography. For the biosynthetic negamycin, a purity of >95% could be confirmed by nuclear magnetic resonance spectroscopy.

The work summarized in this thesis provides new insights into the uptake of pseudopeptidic natural products into Gram-negative bacteria and on the opportunities of negamycin for entering *E. coli*. New uptake routes could be identified, both at the outer as well as the inner membranes, which so far have not been associated with negamycin accumulation. These findings improve our understanding of uptake of peptide-like natural products into bacteria and can support the further development of negamycin derivatives.

List of publications

Accepted publications

Publication 1

The antibiotic negamycin crosses the bacterial cytoplasmic membrane by multiple routes

Hörömpöli, D.*, Ciglia, C.*, Glüsenkamp, K. H., Haustedt, L. O., Falkenstein-Paul, H., Bendas, G., Berscheid, A.[#], & Brötz-Oesterhelt, H.[#] (2021). *Antimicrobial Agents and Chemotherapy, 65*(4).

Publication 2

Kanamycin uptake into *Escherichia coli* is facilitated by OmpF and OmpC porin channels located in the outer membrane

Bafna, J. A.*, Sans-Serramitjana, E.*, Acosta-Gutiérrez, S.*, Bodrenko, I. V., Hörömpöli, D., Berscheid, A., Brötz-Oesterhelt, H., Winterhalter, M., & Ceccarelli, M. (2020). *ACS infectious diseases, 6*(7), 1855-1865.

Manuscripts in preparation

Manuscript 1

Porin-mediated passage of negamycin across the outer membrane of *Escherichia coli*

Hörömpöli, D., Bafna, J. A., Harbig, T., Bhamidimarri, S., Paul, E., Bodrenko, I., Hettich, A., van den Berg, B., Nieselt, K., Ceccarelli, M., Winterhalter, M., Berscheid, A., Brötz-Oesterhelt, H.

Manuscript 2

Two-step batch purification of negamycin from biosynthesis using cation exchange chromatography

Hörömpöli, D., Kulik, A., Glüsenkamp, K.-H., Saad, H., Helmle, I., Gross, H., Berscheid, A., Brötz-Oesterhelt, H.

Manuscript 3[+]

Uptake of aminoglycosides through outer membrane porins of *Escherichia coli*

Paul, E., Ghai, I., Hörömpöli, D., Brötz-Oesterhelt, H., Winterhalter, M., Bafna,. J. A.

*shared first author, [#]shared senior author, [+]listed for completeness but not summarized in this thesis

Declaration of personal contribution

Publication 1

The study concept was designed by Anne Berscheid and Heike Brötz-Oesterhelt. Negamycin was synthesized by Karl-Heinz Glüsenkamp. Strains and plasmids were generated by me, Catherine Ciglia, Melanie Dostert and Annika Hettich under guidance of Anne Berscheid and Heike Brötz-Oesterhelt. MIC determinations were performed by me, Catherine Ciglia and Anne Berscheid. [^{3}H]negamycin uptake measurements were done by me. Negamycin resistant mutants were selected by Catherine Ciglia and analyzed by Anne Berscheid. Determination of resistance rates and TLC analysis was performed by me. ITC was done by me and Anne Berscheid. SAW measurements were performed by Hildegard Falkenstein-Paul and analyzed by Gerd Bendas. Microspecies analysis was done by Lars Ole Haustedt. Cell membrane integrity and membrane potential assays were performed and analyzed by Anne Berscheid. Data was interpreted by me, Catherine Ciglia, Anne Berscheid and Heike Brötz-Oesterhelt. Statistical analysis was performed by me. Figures, figure legends and methods for the manuscript were prepared and written by me and Anne Berscheid. The remaining manuscript was written by Anne Berscheid, edited by me and Heike Brötz-Oesterhelt and approved by all authors.

Publication 2

I generated the *E. coli* Δ*ompF*Δ*ompC* strain and performed all *E. coli* antibacterial susceptibility experiments. The plasmid pASK IBA 5-*ompN* was cloned by me. Electrophysiological experiments were performed and analyzed by Jayesh Arun Bafna, Eulàlia Sans-Serramitjana and Mathias Winterhalter. Molecular dynamics simulations were performed by Silvia Acosta-Gutiérrez, Igor Bodrenko and Matteo Ceccarelli. I was involved in the interpretation of the data, performed the statistical analysis of the biological data and wrote parts of the manuscript under the guidance of Anne Berscheid and Heike Brötz-Oesterhelt.

Manuscript 1

Under my guidance, Annika Hettich generated the *E. coli* BW25113 Δ*ompN*Δ*chiP*, ATCC 25922 Δ*ompN*, ATCC 25922 Δ*chiP*, ATCC 25922 Δ*ompN*Δ*chiP*, ATCC 25922 Δ*acrAB* strains and determined the MICs for the *E. coli* ATCC 25922 background. I performed all the susceptibility determinations within the *E. coli* BW25113, HN817 and C600 backgrounds. The experiments for the self-promoted uptake mechanism, Western blot analysis and [^{3}H]negamycin accumulation were done by me. I prepared the samples for RNA-Seq and was involved in the transcriptomic data analysis, which was done by Theresa Harbig and Kay Nieselt. Electrophysiological experiments were performed and analyzed by Jayesh Arun Bafna, Eshita Paul and Mathias Winterhalter. The crystal structure of OmpN was resolved by Satya Bhamidimarri and Bert van den Berg. Molecular dynamics simulations were performed by Igor Bodrenko and Matteo Ceccarelli. The manuscript was outlined by me, edited by Anne Berscheid and Heike Brötz-Oesterhelt and finalized by all authors.

Manuscript 2

I performed the negamycin biosynthesis and batch purification experiments. Purified negamycin samples were analyzed by susceptibility measurements and TLC by me. MS analysis was done by Andreas Kulik. HPLC analysis was performed by Hamada Saad and Harald Gross. NMR was done by Irina Helmle, Harald Gross and Karl-Heinz Glüsenkamp. The manuscript was written by me and edited by Anne Berscheid.

Manuscript 3

I performed all *E. coli* antibacterial susceptibility experiments. Electrophysiological experiments were performed and analyzed by Eshita Paul, Jayesh Arun Bafna and Mathias Winterhalter. I was involved in the interpretation of the data, performed the statistical analysis of the biological data and wrote parts of the manuscript under the guidance of Heike Brötz-Oesterhelt.

1. Introduction

1.1. Antibiotics

Antibiotics are molecules which inhibit growth of or kill microorganisms (Schofield 2015) and were famously first described by Alexander Fleming (Lalchhandama 2020). Health standards increased rapidly after his discovery and isolation of penicillin (Adedeji 2016). But mass application and bad handling of antibiotics, both in human as well as in veterinary medicine, led to the development of antibiotic resistant microorganisms (Davies *et al.* 2013). According to a report by the World Health Organization, the rise of resistant strains leads to 700.000 deaths per year and a predicted rise to 10 million deaths per year by 2050 (O'Neill 2014). Some pathogens are already difficult to treat, since strains of, e.g., pathogenic *Enterobacteriaceae* or *Pseudomonas* acquired resistance against nearly all clinically used antibiotics (Livermore 2004). *P. aeruginosa* infections occur frequently in a clinical environment or when immune systems are weakened, and multidrug-resistant *P. aeruginosa* strains are marked as a serious threat by the Centers for Disease Control and Prevention (CDC 2019). Especially Gram-negative bacteria are difficult to treat, as active efflux and the two membranes form a strong barrier against antibiotic permeation (Nikaido 2003).

Discoveries of new antimicrobial substances are rare. After the 'golden age' of antibiotic discovery between 1940 and 1970, a long gap of 40 years had to be endured before a new antibiotic class against Gram-negative bacteria was approved (Brötz-Oesterhelt and Sass 2010). The most recently discovered antibiotic class against Gram-negative bacteria are the quinolones, which were first used in clinical treatment in 1967 (Emmerson and Jones 2003). Despite the imminent threat, most big pharmaceutical companies ended their research on new antimicrobial agents and currently no members of new compound classes with an unique mode of action are being tested in clinical trials (Theuretzbacher *et al.* 2020).

Most clinically important antibiotics were found in antibiotic producing microorganisms (Berdy 2005; Katz and Baltz 2016). Companies focused on high-throughput screenings to test hundreds of thousands of molecules against established and new target structures of antibiotics, but most searches failed, as this strategy mostly led to findings of unsuitable or already known agents (Brötz-Oesterhelt and Sass 2010). Especially for agents derived from total synthesis, passage of the bacterial cell envelope turned out to be a major hurdle. New sources for antibiotics are needed, and as over 99% of all bacteria living in soil or water currently cannot be cultivated in a laboratory setup, new approached are being tested. New cultivation methods are being developed (Lefevre *et al.* 2008) and more efficient genomic sequencing and analysis techniques are applied for genome mining (Scheffler *et al.* 2013; Ziemert *et al.* 2016). These approaches could have the potential to open doors to completely new biosynthetic

products. Additionally, researchers use previously discovered, but under-explored natural products as a basis for new, improved antimicrobial agents.

1.2. Negamycin

Negamycin was first isolated from a *Streptomyces purpeofuscus* culture in 1970 (Hamada *et al.* 1970). The antibiotic showed promising features, as it exhibited activity against a variety of strains, including clinically relevant *Pseudomonas aeruginosa* strains. Negamycin actually showed stronger inhibition of Gram-negative than Gram-positive strains, which led to its name-giving. The first results with mice and rabbits showed low toxicity upon injection (Hamada *et al.* 1970). Its low toxicity was confirmed in a more recent study with rats and dogs, and potential reactive metabolites, which had previously been discussed as a caveat, were found in the urine only at very low levels (Guo *et al.* 2015).

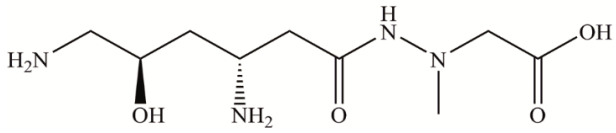

Figure 1. Structure of negamycin.

Negamycin is a small (248.28 g/mol), hydrophilic ($logD_{7.4} < -1$), dipeptide-like (Figure 1) molecule (Uehara *et al.* 1972; Guo *et al.* 2015). First results indicated that negamycin interfered with protein biosynthesis, but the exact mode of action remained unclear. Various inhibitory mechanisms of negamycin in protein biosynthesis were discussed, including the possibility to inhibit initiation (Mizuno *et al.* 1970a), a miscoding activity (Mizuno *et al.* 1970b; Uehara *et al.* 1972) or inhibiting the termination of protein biosynthesis (Uehara *et al.* 1974). The inhibition of the termination of protein biosynthesis was shown in a follow-up study (Uehara *et al.* 1976b). Crystal structures revealed that negamycin simultaneously interacts with the 16S rRNA and the anticodon site of the tRNA (Polikanov *et al.* 2014). This leads to the stabilization of nearby, unspecific tRNAs, resulting in a miscoding activity by incorporating the wrong amino acids in the peptide chain (Olivier *et al.* 2014; Polikanov *et al.* 2014). Although the binding site of tetracycline at the 16S rRNA overlaps with the binding site of negamycin, tetracycline shows a different mode of action, as it prevents binding of the tRNA and inhibits translocation this way (Chopra 1985). In direct competition for binding at the 16S rRNA, negamycin displaces tetracycline (Olivier *et al.* 2014). Mutations of the 16S rRNA could thereby lead to resistance to both antibiotics, but do not necessarily have to affect both antibiotics at the same time. In an *E. coli* strain carrying only one allele for 16 rRNA, the amino acid change U1060A increased resistance against both negamycin and tetracycline, whereas U1052G only enhanced resistance against negamycin and at the same time increased susceptibility against tetracycline strongly (Cocozaki *et al.* 2016). Nevertheless, cross-resistance in clinical pathogens seems unlikely, as bacteria possess multiple copies of rRNA genes (Klappenbach Joel *et al.* 2000).

Although negamycin had activity against various Gram-negative strains (Hamada *et al.* 1970), its activity needs to be improved for clinical usage. Almost all efforts towards improved analogs led to molecules with reduced activity against bacteria, although some showed increased binding to the target structure (Kondo *et al.* 1976; Uehara *et al.* 1976a; Raju *et al.* 2003). It has to be noted, that previous attempts at improved analogs had to be done without knowing details on how negamycin binds to its target structures. So far only the analog N6-aminopropyl negamycin has shown improved activity, with an up to four times increased activity (McKinney *et al.* 2015c).

The miscoding mode of action of negamycin combined with its low toxicity makes negamycin an interesting candidate for other applications than treatment of bacteria. Duchenne muscular dystrophy, a muscle-wasting disease, is caused by a premature stop codon in the dystrophin gene (Arakawa *et al.* 2003). Aminoglycosides have been proposed to be used for read-through of this premature stop codon, but are also associated with high toxicity (Munckhof *et al.* 1996). First experiments to treat Duchenne disease with negamycin showed that the expression of dystrophin could be restored (Arakawa *et al.* 2003). Negamycin might be of interest for similarly caused diseases, like cancer caused by premature termination codons, and aminoglycosides were used as an treatment option (Floquet *et al.* 2011).

Clinical usage of negamycin would require high amounts of the natural product. The initial publication and patent of negamycin described purification methods based on biosynthesis from a *S. purpeofuscus* culture (Hamada *et al.* 1970; Umezawa *et al.* 1972). Further studies focused on total synthesis of negamycin, but chemical synthesis of negamycin is expensive (Shibahara *et al.* 1972; Streicher *et al.* 1978; Hayashi *et al.* 2008; Hayashi *et al.* 2009). So far, no study investigated further how to optimize fermentation and the follow-up purification.

1.3. *Escherichia coli* as a model organism for antibiotic uptake

Escherichia coli is a Gram-negative, rod-shaped, facultative anaerobic bacterium, usually found in the lower intestine (Escherich 1885; Eitinger and Schlegel 2007). Most *E. coli* strains are harmless and can be beneficial as a part of the human microbiome (LeBlanc *et al.* 2013). Research on treatment options for *E. coli* is necessary, as pathogenic *E. coli* strains, e.g., enterotoxigenic *E. coli* (ETEC), enteropathogenic *E. coli* (EPEC) or enterohemorrhagic *E. coli* (EHEC), are a problem, especially in areas where hygienic standards are low (Nataro and Kaper 1998; Torres *et al.* 2005). Within the last decades, *E. coli* strains with resistances against all major antibiotic classes have been observed, including strains producing carbapenemases, extended-spectrum beta-lactamases and strains with resistances against fluoroquinolones, colistin, trimethoprim or aminoglycosides (Pitout 2012; Liu *et al.* 2016). This development makes it necessary to study *E. coli* and how antibiotics can be used as therapeutics. Additionally, the fast growth of *E. coli* and its easy handling in the laboratory, the availability of various genetic tools as well as genomic data makes *E. coli* an ideal organism to study general features of Gram-negative bacteria.

For an antibiotic against Gram-negative bacteria to reach its target in the periplasm, it has to overcome the outer membrane. If the target is within the cytoplasm, the antibiotic has to additionally cross the cytoplasmic membrane (Figure 2). For passage across both membranes, a molecule has to be small, hydrophilic and positively charged to diffuse through porin channels in the outer membrane and at the same time, the molecule should be hydrophobic and uncharged for passive diffusion across the cytoplasmic membrane (Nikaido 2003; Balaz 2012). As bacteria have to take up nutrients and these ideal molecule properties for translocation across both membranes are totally opposing, bacteria need to have additional pathways and mechanisms for uptake.

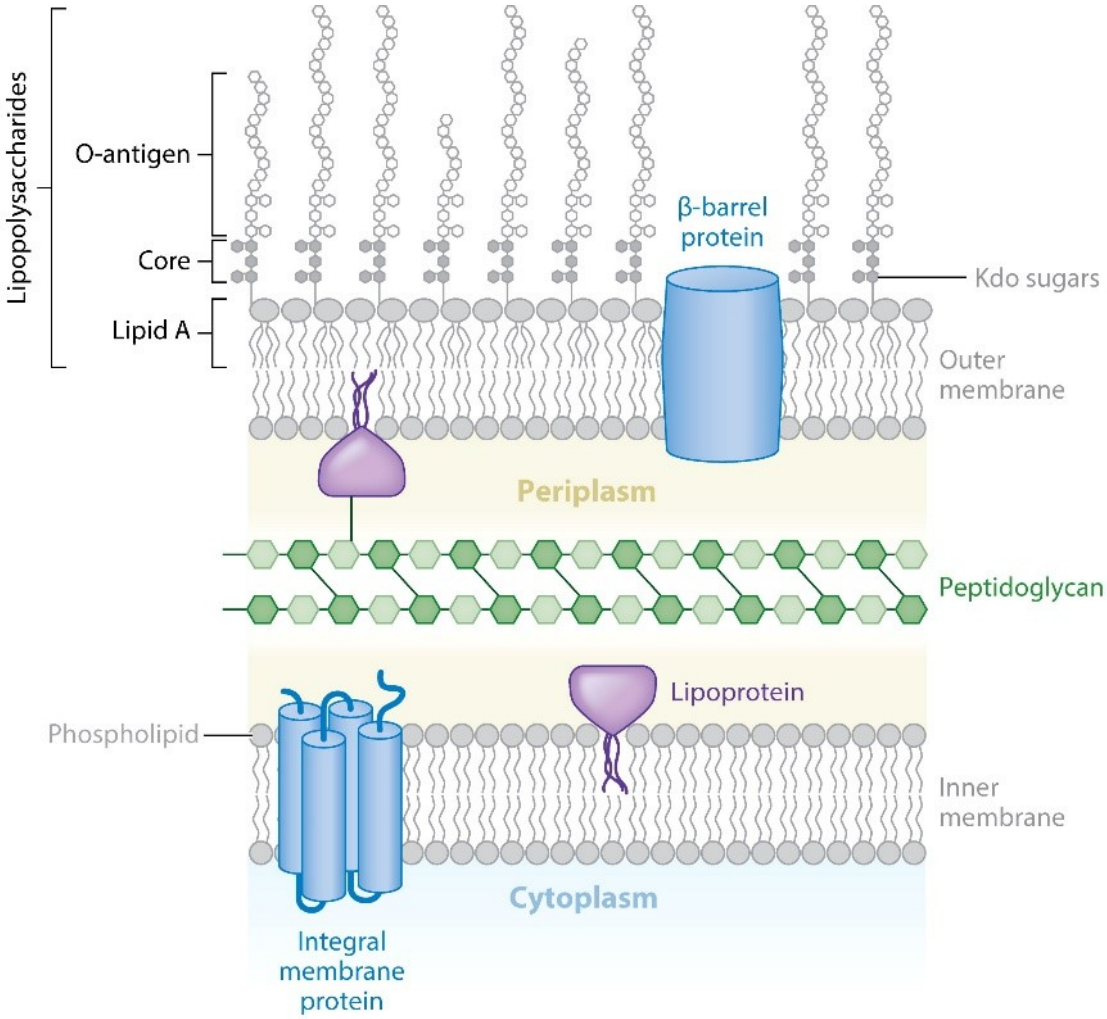

Figure 2. Schematic overview of the cell envelope of Gram-negative bacteria. The asymmetric outer membrane consists of lipopolysaccharides in the outer leaflet and phospholipids in the inner leaflet. β-barrel proteins are integrated in the outer membrane. One class of β-barrel proteins are porins which allow diffusion of hydrophilic molecules through these water-filled channels. In contrast, the inner membrane consists of two phospholipid layers and separates the periplasm and cytoplasm. Image was adapted from Henderson *et al.* 2016.

1.3.1. The outer membrane as a barrier

The outer membrane of Gram-negative bacteria is the first barrier against antibiotics. It is an asymmetric bilayer, with phospholipids as the inner leaflet and lipopolysaccharides (LPS) as the outer leaflet (Nikaido 2003). The LPS molecule is composed of the hydrophobic lipid A and a hydrophilic polysaccharide portion, which is made of the inner and outer core as well as the O-antigen, a sugar chain with up to 40 repetitions of the same oligosaccharide motif (Palva and Mäkelä 1980). The composition of each of these elements varies between species and strains (Nikaido 2003). Within the outer membrane of *E. coli* K-12, a strain widely used in laboratory work, the O-antigen is missing completely (Prehm *et al.* 1976). The rigid structure of the LPS, which is usually cross-linked by magnesium ions, hinders diffusion of hydrophilic and lipophilic molecules through this barrier (Nikaido 2003). This is not only an effective barrier against antibiotics, but also hinders nutrient uptake.

Therefore, Gram-negative bacteria possess porin proteins, which are water-filled diffusion channels spanning the outer membrane (Pagès *et al.* 2008). Porins have a β-barrel structure, which is usually made of 16 antiparallel β-sheets in *E. coli* organized as trimers (Figure 3). The channels enable passive diffusion, driven by the concentration gradient across the outer membrane. Although some porins are described to be unspecific in substrate selectivity, even these unspecific porins limit the entry of molecules by size and charge. This selective barrier is formed by specific amino acidic residues within the barrel structure, most notably in the middle of the porin by the loop L3, protruding into the barrel. Together with the residues at the opposite wall, the amino acid residues of L3 form the narrowest spot along the porin channel, the so-called constriction region (Nikaido 2003; Pagès *et al.* 2008; Acosta-Gutiérrez *et al.* 2018). Besides the size exclusion mediated by the constriction region, the charge of the amino acid residues forms an electrostatic barrier. In *E. coli*, the porins OmpF and OmpC are among the most strongly expressed proteins, with up to 100,000 copies per cell (Lugtenberg and Van Alphen 1983). As a rule of thumb, diffusion through these *E. coli* porins has been described to be limited to positively charged, hydrophilic molecules of up to 600 Da (Nikaido 1992), but recently more defined molecule properties have been proposed. More specifically, not only charge and size, but also the dipole moment and the minimal projection area are of importance (Acosta-Gutiérrez *et al.* 2018). *E. coli* encodes further general porin channels, e.g. OmpN, OmpW or OmpG, although the role of these porins is not fully understood yet (Nikaido 2003). Other porins, like LamB and ChiP, have higher substrate specificity and enable the uptake of maltose and chito-oligosaccharides, respectively (Charbit 2003; Soysa and Suginta 2016). Additionally, some porins do not only enable transport of nutrients but have been associated with additional functions. OmpA is described to be important for cell integrity, as it connects the outer membrane to the cell wall (Samsudin *et al.* 2016). In recent studies, OmpC has been proposed to take part in maintenance of the outer membrane integrity by transporting phospholipids from the outer to the inner leaflet (Chong *et al.* 2015).

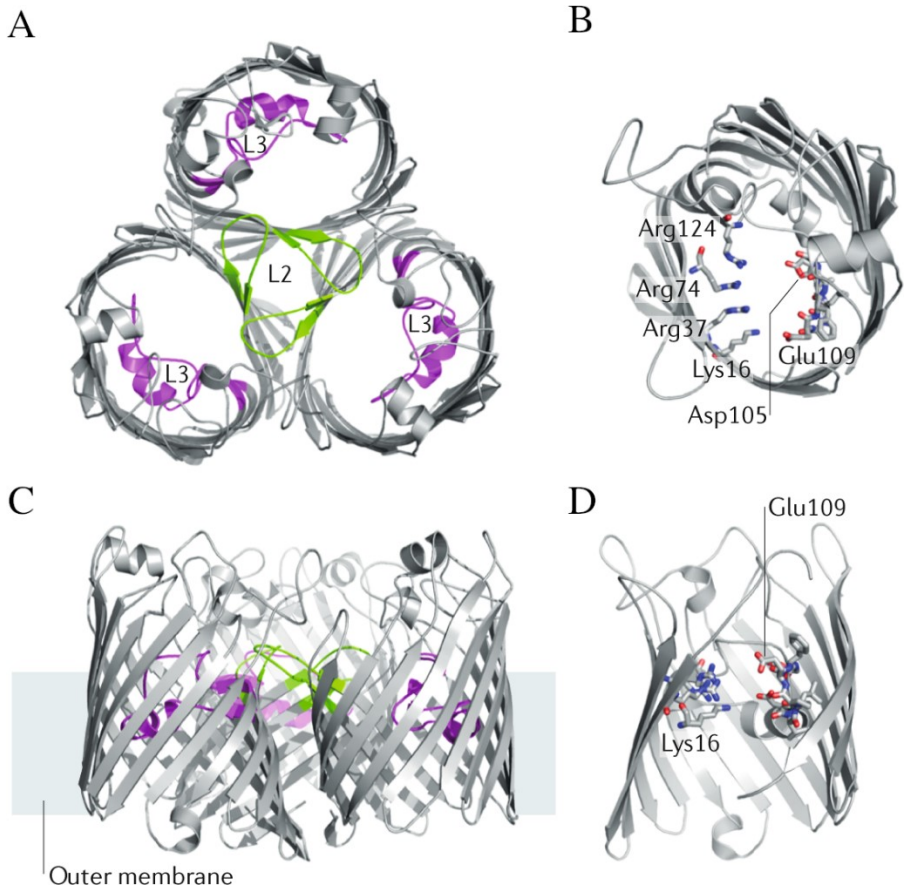

Figure 3. Structure of the *E. coli* porin OmpC. (A) The major porins of *E. coli* are organized as trimers. The loop (L2, marked in green) between the first and second β-sheet of the porin protein connects the monomers. The third loop (L3, marked in purple) ranges inside the porin channel and narrows the size of the channel. The porin is shown from the top, looking from outside the cell into the periplasm. (B) Amino acids in the constriction region are highlighted in one monomer of the OmpC porin. The narrowest region of the porin is determined by the amino acids of the loop L3 (Asp105, Glu109) and the amino acids on the opposing side (Lys16, Arg37, Arg74, Arg124) of the protein. (C & D) This constriction region is located in the middle of the porin barrel. Image was adapted and modified from Vergalli *et al.* 2019.

Antibiotic translocation through *E. coli* porins has been shown for multiple antibiotic classes. Tetracyclines, quinolones and β-lactams have been reported to translocate through OmpF or OmpC (Nikaido 2003; Pagès *et al.* 2008; Masi *et al.* 2019; Vergalli *et al.* 2020). Porins from clinical *E. coli* isolates showed alterations in their peptide sequence, especially within the constriction region, which could be linked to a reduction in antibiotic translocation (Pagès *et al.* 2008). These alterations also led to a deficit in fitness, but seemed to be overall beneficiary when exposed to antibiotics (Phan and Ferenci 2017).

Structural variations among porins result in different substrate preferences. Bacteria use these different types of porins to adjust to different environmental conditions by changing the expression of these porins (Lugtenberg and Van Alphen 1983; Nikaido 2003). *E. coli* reacts to different environments by adjusting the ratio of expression of OmpF to OmpC, as OmpF is less restrictive than OmpC in substrate specificity. Regulation of porin expression is highly complex and occurs on multiple levels (Pratt *et al.* 1996; De la Cruz and Calva 2010). Over a dozen regulator genes have been described for *E. coli* porins, with

additional post-transcriptional regulation by small antisense RNA (sRNA). These different factors of porin expression enable quick adjustment to environmental changes, e.g., in the event that bacteria are exposed to antibiotics. Shifting the expression to more restrictive porins reduces antibiotic influx into bacteria. Total absence of certain porins has been observed in clinical isolates (Pagès *et al.* 2008; Vergalli *et al.* 2020). Although general fitness and growth rates are decreased for these strains (Phan and Ferenci 2017), pathogens gain more time to react to the antibiotic exposition, for instance by upregulating efflux pumps (Zgurskaya *et al.* 2011).

For this purpose, *E. coli* possesses different classes of efflux pumps (Anes *et al.* 2015). In the context of antibiotic resistance, the efflux pump systems of the class resistance-nodulation cell division transporters (RND) are the most important. The RND are tripartite efflux pump systems, with the pump integrated in the inner membrane, a periplasmic adaptor protein and an outer membrane protein, forming a channel through the outer membrane. This outer membrane channel in *E. coli* is the TolC protein, which forms complexes with various efflux pump systems, including the five most important ones called AcrAB, AcrAD, AcrEF, MdtAB and MdtEF (Anes *et al.* 2015). The RND efflux pumps are driven by the proton motive force, which enables them to flux substances out from the cytoplasmic and periplasmic space.

General resistance mechanisms, which do not target one antibiotic specifically by modifying the antibiotic or the antibiotic's target, can function at multiple levels. The reduced uptake through porin alterations in combination with the efflux systems can have a synergistic effect against antibiotics. It has been reported, that reduced uptake through porins is not the main resistance mechanism of *E. coli*, but rather occurs in combination with other resistance mechanisms (Vergalli *et al.* 2020).

Porins are the main uptake pathways for small, hydrophilic antibiotics. For other antimicrobial compounds, alternative, porin-independent translocation mechanisms have been observed. Aminoglycosides and polymyxins destabilize the outer membrane by displacing cations, like Ca^{2+} and Mg^{2+}, which stabilize the outer membrane by linking LPS molecules, which leads to brief disruption and enables their so called self-promoted uptake (Hancock *et al.* 1991; Vaara 1992). Antibiotics with targets inside the cytoplasm must not only overcome the outer membrane, but the inner membrane of Gram-negative bacteria as well.

1.3.2. The cytoplasmic membrane as a barrier

The cytoplasmic membrane is made of a phospholipid bilayer (Silhavy *et al.* 2010). Its arrangement favors diffusion of hydrophobic molecules, whereas diffusion of hydrophilic molecules is hindered. As very lipophilic molecules interact strongly with the phospholipids, their uptake is slowed down as well (Hansch and Fujita 1964). Additionally, diffusion is favored for uncharged molecules (Shore *et al.* 1957). As nutrients need to get in the cytoplasm, bacteria use a range of active transporters for uptake

across the cytoplasmic membrane (Silver 2016). Additionally, weakly charged molecules can use the proton motive force to cross the cytoplasmic membrane (Zarfl *et al.* 2008).

Different translocation mechanisms across the cytoplasmic membrane have been described for antibiotics, both carrier-dependent and –independent, as antibiotics using the porin-mediated pathway through the outer membrane cannot diffuse easily through the cytoplasmic membrane. Some antimicrobial compounds can use peptide transporters of *E. coli* for cell entry. For instance, the nucleoside blasticin S has been associated with DtpA- and DtpD-dependent uptake (Kitamura *et al.* 2017) and the aminocephalosporins cephradine, cephalexin and cefadroxil can use DtpA (Weitz *et al.* 2007). For the tetrapeptide-antibiotic GE81112, cell entry via Opp has been shown (Maio *et al.* 2016) and the aminoglycoside kasugamycin is dependent on Dpp (Shiver *et al.* 2016). In general, antibiotics using these peptide transporters compete with peptides for uptake and some lose activity upon removal of the respective transporter genes. For fosfomycin uptake into *E. coli*, the two active transporters GlpT and UhpT, i.e., transporters for glycerol-3-phosphate and hexose phosphate, respectively, are of importance (Maloney *et al.* 1990; Kadner *et al.* 1993; Hall and Maloney 2001).

Although aminoglycosides are already in clinical usage and their uptake has been investigated by multiple groups, the exact translocation mechanism through the cytoplasmic membrane is still not fully understood. It has been reported that uptake is transporter-independent and occurs in two phases, which are both affected by energy metabolism (Taber *et al.* 1987). Within the first phase, some aminoglycoside molecules translocate across the cytoplasmic membrane, driven by the proton motive force, which enables their binding to the ribosome, miscoding and consequently defective proteins (Bryan and Van Den Elzen 1977b; Taber *et al.* 1987). It has been proposed, that these mistranslated proteins insert into the cytoplasmic membrane, which destabilizes barrier integrity and enables uptake of further aminoglycosides within this so called second energy-dependent phase (Bryan and Elzen 1976).

Diffusion of tetracyclines into the cytoplasm is also described to be carrier-independent and energy-dependent (Chopra *et al.* 1991). For the prototype compound tetracycline, different microspecies, charged and neutral, exist in an equilibrium in the periplasm. At pH 7.4, 7.1% of tetracycline microspecies are net uncharged and therefore able to diffuse through the phospholipid bilayer (Nikaido and Thanassi 1993). Interestingly, to cross the outer membrane, protonated tetracyclines chelate Mg^{2+}, which leads to a net positively charged complex that favors diffusion through porins. Within the periplasm, Mg^{2+} disassociates, which enables diffusion through the cytoplasmic membrane (Nikaido and Thanassi 1993).

First investigations on negamycin uptake into *E. coli* demonstrated that in peptide-free medium the dipeptide transporter Dpp plays a role in negamycin uptake and susceptibility (Rafanan *et al.* 2003; McKinney *et al.* 2015b). A crystal structure of negamycin bound to Dpp could not be determined, but computational simulations showed interactions between negamycin and the periplasmic binding protein DppA (McKinney *et al.* 2015b). Additional uptake routes, driven by the proton motive force, were hypothesized but not elucidated.

These examples demonstrate the complexity of antibiotic uptake across the cell envelope of Gram-negative bacteria. For structural optimization of a new antimicrobial compound in the course of lead optimization, understanding of the uptake pathways is desirable, as intracellular compound levels strongly impact antibacterial activity.

1.4. Research objectives

Negamycin is an antibiotic of interest, as it showed activity against Gram-negative bacteria, potential in infection models and low toxicity. For clinical application, an analogue with improved activity would be desirable, but with the exception of one analogue (McKinney *et al.* 2015c), all derivatization studies failed. Multiple negamycin analogues showed improved efficacy at the target structure, but tested against bacterial cells, their activity did not increase, indicating that uptake into the bacterial cells might be hindered. Therefore, understanding the molecular uptake mechanisms across both membranes is crucial for further optimization of the negamycin molecule structure.

The first objective of this work was to understand translocation pathways of negamycin across the cytoplasmic membrane of *E. coli*. Transporters important for negamycin uptake should be identified by gene deletions and measuring negamycin susceptibility. Previously, *dpp* genes were shown to affect negamycin activity (Rafanan *et al.* 2003; McKinney *et al.* 2015a), but uptake was only shown indirectly by activity measurements without proof of transport. In order to demonstrate the negamycin uptake route via the investigated transporters, negamycin was to be directly quantified in these gene deletion mutants measuring intracellular levels of radiolabeled negamycin. Based on the peptide-like structure of negamycin, further peptide transporter genes of the proton-dependent oligopeptide transporter family could be linked to negamycin activity. Another observation was the beneficial effect of calcium to negamycin activity. For this purpose, complex formation of negamycin and calcium as well as interaction with phospholipids should be investigated to elucidate how calcium facilitates negamycin uptake.

The second goal of this thesis was to identify translocation mechanisms of negamycin across the outer membrane of *E. coli*. No results have been previously published on the permeation of negamycin through the outer membrane. Therefore, the aim was to identify porins involved in negamycin translocation by targeted gene deletions and negamycin susceptibility determinations. Porins of interest should be examined in detail by investigating their structure, physiology, intracellular expression levels and molecular interaction with negamycin. Uptake into whole cells should again be directly measured with radiolabeled negamycin. Prior to this work, translocation of aminoglycosides through porins could not directly be shown, although this compound class is in clinical use for decades. As a side project, kanamycin translocation through the outer membrane of *E. coli* was investigated, studying purified porin proteins by electrophysiology and kanamycin sensitivity in the absence of the respective porin genes.

The third goal was to establish an optimized fermentation protocol for negamycin biosynthesis. The original patent (Umezawa *et al.* 1972) describes multiple methods to purify negamycin from a *Streptomyces* culture, but it requires multiple steps of ion exchange chromatography. In this thesis, yield from biosynthesis was to be improved by adjusting growth conditions, media composition and comparing negamycin producing strains. In parallel, I tried to improve the purification procedure.

2. Summary of results & discussions

This section is structured by publications and manuscripts. Within each section of chapter 2., the results and corresponding discussions of one publication or manuscript are summarized separately.

2.1. The antibiotic negamycin crosses the bacterial cytoplasmic membrane by multiple routes (publication 1)

2.1.1. Results

Negamycin targets the ribosome, therefore it does not only need to translocate across the outer membrane of Gram-negative bacteria, but across the cytoplasmic membrane as well (Olivier *et al.* 2014; Polikanov *et al.* 2014). As diffusion of such a hydrophilic molecule through the phospholipid bilayer of the cytoplasmic membrane is unlikely, uptake pathways through the inner membrane were investigated. Two minimal media of different composition were used in this study, as negamycin is not active in rich media (Table 1, publication 1). On the one hand, we used 0.5% polypeptone (PP), which is a mixture of peptides. On the other hand, we employed M9, a medium solely composed of glucose and salts. M9 lacks peptides or amino acids, which might compete for uptake with negamycin due to its dipeptide-like structure. A negamycin MIC of 4 and 8 µg/ml could be determined for *E. coli* BW25113 in M9 and PP, respectively (Table 1, publication 1).

The dipeptide-like structure of negamycin suggested the dipeptide transporter Dpp and other peptide or amino acid transporters as possible uptake pathways for cell entry. To follow this hypothesis, multiple single gene deletion mutants from the Keio collection were investigated (Baba *et al.* 2006), and multiple gene deletion strains were generated. The strongest effect on the negamycin MIC was observed, when one of the genes of the ABC transporter Dpp was deleted and when the MIC was determined in the peptide-free medium M9 (Table 2, publication 1). The deletion of *dppA*, *dppB*, *dppC*, *dppD* or *dppF* increased the MIC four-fold from 4 µg/ml to 16 µg/ml. This effect of the *dppA* gene deletion could be complemented by expressing *dppA* on a plasmid (Figure S1, publication 1). This observation on negamycin sensitivity could be linked to reduced uptake, as experiments with radioactively labeled negamycin showed a significant decrease in [^{3}H]negamycin accumulation, when comparing *E. coli* Δ*dppA* to its isogenic wild type strain (Figure 2D, publication 1).

As *E. coli* Δ*dppA* was only four-fold less susceptible to negamycin, other uptake opportunities must be available. The deletion of *sapA*, a paralog of *dppA*, increased the MIC from 4 to 8 µg/ml in M9 (Table 2, publication 1). Gene deletions of subunits of the oligopeptide transporter Opp showed no effect on negamycin susceptibility. Further single gene deletions of amino acid and peptide transporters did not affect the negamycin MIC in M9 (Table 2, publication 1). As the substrates of these paralogs are

structurally similar molecules, the deletion of single genes might be compensated by other transporters. To investigate this hypothesis, multiple gene deletion strains were generated and the negamycin MIC was determined. The double knockout strains *E. coli* Δ*dppA*Δ*oppA* and *E. coli* Δ*dppA*Δ*sapA* did not show higher negamycin resistance compared to *E. coli* Δ*dppA* (Table 2 and Figure 2A, publication 1). As negamycin was still active in the triple deletion strain, other uptake routes across the cytoplasmic membrane must be available. As a comparative example, the tripeptide herbicide bialaphos was strongly dependent on Dpp and Opp in our study. The double deletion of both *oppA* and *dppA* increased the bialaphos MIC more than 64,000 fold (Figure 2B, publication 1). Within the same strain background, the negamycin MIC increased only by four-fold (Figure 2A, publication 1). Negamycin activity was not only affected by the Dpp ABC transporter, but also by a proton-dependent oligopeptide transporter (POT). The deletion of *dtpD* increased the negamycin MIC in M9 up to two-fold and this effect was even more pronounced in PP (Table 2, publication 1). The additional deletion of *dtpD* within the multiple deletion strain led to *E. coli* Δ*dppA*Δ*oppA*Δ*sapA*Δ*dtpD*, which had a significantly higher negamycin MIC (32 µg/ml) than *E. coli* Δ*dppA*. The contribution of peptide transporters to negamycin uptake and the competition by nutrient peptides could be shown by peptide addition to M9 medium. PP added at a concentration of 0.005% increased the negamycin MIC significantly from 4 to 8 µg/ml and the addition of 0.05% PP was enough to even increase the MIC to 64 µg/ml (Figure 2C, publication 1). This observation correlated with [^{3}H]negamycin uptake studies, in which negamycin accumulation was reduced markedly by the addition of 0.05% PP to M9 (Figure 2D, publication 1).

Mutants selected on M9 agar with negamycin added reflect these trends. At 2x MIC of negamycin added to the agar, the resistance frequency of *E. coli* BW25113 was 6 x 10^{-7} and therefore quite high. As described above, the deletion of *dppA* is sufficient for growth up to 4x MIC (Table 2, publication 1). Investigations of the genome of these mutants revealed that all 12 mutants grown at 2x MIC of negamycin showed variations in the *dpp* operon, with 9 mutants showing a large chromosomal deletion comprising the whole operon plus flanking regions (Figure 3, publication 1). This result emphasizes the importance of the Dpp transporter as the primary entry point for negamycin in peptide-free medium. In contrast, mutants selected at 2x MIC on PP had a similarly high resistance frequency of 5 x 10^{-7}, but all 8 mutants investigated showed no alterations in the *dpp* operon. In both media, no mutants could be selected at a negamycin concentration corresponding to 4x MIC, corresponding to a resistance rate below 7 x 10^{-9}. The fact that single mutations did not lead to high-level negamycin resistance, confirms that multiple uptake pathways must be available.

To investigate if other environmental conditions could play a role in negamycin activity, further conditions were tested. The two minimal media M9 and PP do not only differ in their peptide content, but also in the presence of salts, which PP is lacking. The negamycin MIC was lower in M9, which is due to the absence of competing peptides at the peptide transporters, but salts could also play a role in intracellular negamycin accumulation. To investigate this, the effect of salts on the activity of negamycin

was investigated using PP. $CaCl_2$ increased negamycin activity against *E. coli* BW25113, with the lowest MIC occurring at a concentration of 2.5 mM $CaCl_2$ (Table 3, publication 1). With 2.5 mM $CaCl_2$ added, the MIC dropped from 8 to 2 µg/ml, corresponding to a four-fold change in activity. A similar effect could be observed with *Pseudomonas aeruginosa* PAO1 and *Staphylococcus aureus* ATCC 29213, where the addition of 2.5 mM $CaCl_2$ decreased the MIC from 32-64 to 8 µg/ml and from >64 to 16 µg/ml, respectively (Figure 4A, publication 1). The effect of $CaCl_2$ was not limited to Gram-negative strains, indicating that the effect of $CaCl_2$ on the activity probably happens at the cytoplasmic membrane. $MgCl_2$ added to the medium showed no effect on the negamycin MIC of *E. coli* BW25113, implying that calcium and not chloride was causing the MIC shift (Table 3, publication 1). Other salts, i.e., NaCl, KCl or NH_4Cl, did not improve negamycin activity, but rather increased the MIC at high salt concentrations (Table 3, publication 1). The improvement of negamycin activity by Ca^{2+} addition is probably not attributed to a disturbance of the integrity of the outer or inner membrane, as $CaCl_2$ and $MgCl_2$ did not decrease MICs of ciprofloxacin, tetracycline or gentamicin against *E. coli* BW25113, and at high salt concentrations of 50 mM negamyin MICs were even increased, further precluding membrane destabilization (Table S1, publication 1). Neither did the addition of $CaCl_2$ affect the IC_{50} of negamycin in an *in vitro* translation assay, suggesting that the improvement of activity by $CaCl_2$ is not due to better target affinity, but rather based on improved uptake. As $CaCl_2$ also improved negamycin activity against *Staphylococcus aureus* (Figure 4A, publication 1), we studied the interactions of negamycin and $CaCl_2$ with the cytoplasmic membrane in more detail.

The interaction between negamycin and phospholipids was investigated by surface acoustic wave (SAW) biosensor measurements by our cooperation partners. Binding experiments with a mixture of 90% 1-palmitoyl-2-oleoyl-phosphatidylcholine (POPC) and 10% 1,2-dioleoyl-phosphatidylglycerol (DOPG) was used to resemble the negatively charged cytoplasmic membrane of bacteria. Binding events of negamycin to this lipid mixture increased when 2.5 mM $CaCl_2$ was added (Figure 5C). As 2.5 mM $MgCl_2$ affected binding of negamycin to the phospholipids only slightly (Figure 5D, publication 1), the effect of increased binding can be accounted specifically to calcium. Previous MIC measurements had shown a similar trend, with only $CaCl_2$, but not $MgCl_2$, increasing negamycin activity (Table 3, publication 1).

The interaction of negamycin and $CaCl_2$ was further characterized. First, negamycin was mixed with $CaCl_2$ in different concentration ratios and subjected to thin layer chromatography (TLC). At a molar ratio of 1:1, negamycin's retardation factor was slightly increased compared to the sample without salts (Figure 6A, publication 1). At a fivefold molar excess of Ca^{2+}, migration of negamycin was slowed down substantially, and negamycin remained at the baseline, when the molarity of Ca^{2+} was ten times higher than negamycin. This shift in running behavior suggests direct interactions between negamycin and calcium. A similar trend could be observed with $MgCl_2$, and spot shifting of negamycin seemed even stronger with negamycin staying at the baseline at a molar ratio of 1:5 of negamycin to $MgCl_2$

(Figure 6A, publication 1). Spot shifting could only be observed with the divalent cations Ca^{2+} and Mg^{2+}, but not with Na^{+}, and even a ten-fold higher concentration of NaCl did not change migration of negamycin on the TLC plate. Notably, although $MgCl_2$ had a strong effect on the running behavior of negamycin on the TLC plate, the previous SAW experiment had shown only a marginal effect of $MgCl_2$ on the binding of negamycin to phospholipids (Figure 5D, publication 1) and the addition of $MgCl_2$ did not affect the MIC of negamycin (Table 3, publication 1). Thus, $CaCl_2$ seemed more relevant for negamycin uptake.

As the TLC experiment did not reveal quantitative data on binding affinity and stoichiometry, isothermal titration calorimetry (ITC) was performed next. Determining the binding affinity of negamycin to $CaCl_2$ was difficult and due to the low affinity, a stoichiometry of the interaction could not be determined. Therefore, for further analysis, the stoichiometry was set manually to 1:1 and a dissociation constant (K_d) of 7.98 mM could be obtained (Figure 6B and C, publication 1). The K_d did not change strongly when the stoichiometry was varied between 0.5:1 and 2:1, leading to K_d values of 8.62 or 7.36 mM, respectively. Under alkaline conditions the K_d improved, e.g., to 4.1 mM at pH 8.5. The charges of the carboxyl and amine groups of negamycin vary with pH (Figure S4, publication 1), which could explain a shift in binding affinity. Binding between $MgCl_2$ and negamycin could not be investigated by ITC measurements, as the background signal of $MgCl_2$ interacting with the buffer solution was too high compared to the low levels of heat released by negamycin and $MgCl_2$.

Also, the pH influences the activity of negamycin. When PP was shifted from neutral to basic pH, the negamycin MIC improved from 8 to 2-4 µg/ml (Figure 4B, publication 1). The addition of $CaCl_2$ had an additive positive effect on negamycin activity, as the combination of pH 8.5 and 0.5 mM $CaCl_2$ lowered MIC to 2 µg/ml. The previously determined "ideal" concentration for negamycin activity of 2.5 mM $CaCl_2$ (Table 3, publication 1) could not be applied under basic conditions, as calcium precipitated at higher pH. Ca^{2+} and basic pH did not only have an effect on *E. coli*, but on *P. aeruginosa* and *S. aureus* as well, where the MIC of negamycin dropped under these ideal conditions to 4 µg/ml (Figure 4A, publication 1). Therefore, the pH does not only have an effect on Gram-negative bacteria, suggesting that the benefit results predominately from an interaction with the cytoplasmic membrane.

The beta-amino group of negamycin has a pK_a of 8.0, which results in a larger proportion of zwitterionic molecules present at pH 8.5 compared to pH 7 (Figure S4, publication 1). As uncharged molecules permeate easier than charged molecules through phospholipids, a higher pH might increase the uptake of the net neutral subfraction of negamycin into the cytoplasm. Additionally, a shift to basic pH increases the membrane potential, as the electrical potential difference $\Delta\Psi$ between the periplasm and the cytoplasm is more negative at alkaline pH (Krulwich *et al.* 2011). This increase of the trans-negative membrane potential could work as sort of a pull for the translocation of the positively charged fraction of negamycin across the cytoplasmic membrane. A control experiment, where efflux pumps might be affected by the change of pH, did not show an increase in negamycin sensitivity, neither at pH 7 nor 8.5

(Table S2, publication 1). The increase in negamycin sensitivity at alkaline pH could be linked to an increased accumulation of radioactive [^{3}H]negamycin. When uptake of tritium-labeled negamycin into *E. coli* BW25113 was determined after 15 min of incubation, an increase of 46% of accumulated [^{3}H]negamycin was detected when comparing alkaline growth conditions at pH 8.5 to neutral growth conditions at pH 7 in PP (Figure 4C, publication 1).

The membrane potential of bacteria is dependent on the activity of the respiratory chain complexes (Krulwich *et al.* 2011). Therefore, the dependency of negamycin activity on genes involved in the respiratory chain was investigated by determining the MIC of gene deletion mutants, namely *E. coli* Δ*ndh*, Δ*sdhA*, Δ*sdhC*, Δ*cyoA*, Δ*cyoB*, Δ*ubiG*, Δ*ubiI* or Δ*ubiX*. The antibacterial activity of negamycin in M9 was not increased, when one of these genes was deleted (Figure 7A, publication 1). The previously described uptake pathway by the ATP-dependent Dpp transporter (Figure 2, publication 1) must still be sufficiently powered by ATP, when single genes from the respiratory chain are missing. On the other hand, the deletion of *sdhA*, *cyoA* or *cyoB* led to a two-fold increase in the negamycin MIC when determined in PP (Figure 7B, publication 1). In the peptide-rich medium, the peptide transporters are less available to negamycin, as shown above, and the peptide transporter-independent uptake route seems to be influenced by the membrane potential. This trend of MIC increase upon gene deletion of components of the respiratory chain was even more pronounced in cation-adjusted Mueller-Hinton broth, where the negamycin MIC was increased two times or more, when either *ndh*, *sdhA*, *cyoA*, *cyoB*, *ubiG*, *ubiI* or *ubiX* was deleted (Figure 7C, publication 1). Although deletions of these genes clearly affected negamycin susceptibility, it remains an open question if this membrane potential-dependent uptake pathway is carrier dependent or independent or if metabolic changes triggered by the respiratory chain defect influence negamycin uptake in a more indirect manner.

The respiratory chain depends on the presence of oxygen. We were interested in how the reduction of oxygen could affect negamycin activity. Therefore, the activity of negamycin was investigated against *E. coli* under anaerobic growth conditions. In PP, the negamycin MIC increased significantly from 8 µg/ml to 64 µg/ml under anaerobic growth conditions (Figure 8A, publication 1). This decrease in negamycin activity could also be observed at pH 8.5, where the MIC increased from 2-4 µg/ml to 32 µg/ml. Similar observations were made for the aminoglycosides kanamycin and gentamicin, where the activity decreased under anaerobic growth conditions, both in PP and M9 (Figure S5, publication 1). In M9 medium, however, the activity of negamycin was not affected by a shift from aerobic to anaerobic growth conditions (Figure 8A, publication 1). The negamycin MIC against *E. coli* BW25113 remained at 4 µg/ml. This result suggests, that negamycin uses a membrane potential-dependent uptake route when peptides are present, but in a peptide-free medium as M9, peptide transporters are still available for translocation inside the cytoplasm and do not seem strongly affected by the membrane potential decrease. The impact of gene deletions of peptide transporters on negamycin sensitivity was more pronounced under anaerobic growth conditions (Figure 8B, publication 1). In the anaerobic

environment, the *dppA* deletion increased the negamycin MIC to 32 µg/ml. Additionally, the double gene deletion of Δ*dppA*Δ*oppA* in *E. coli* showed a slight trend towards further increased negamycin resistance (MIC: 32-64 µg/ml), here demonstrating a small but reproducible contribution of Opp, which could not be detected under aerobic growth conditions. The effect of multiple gene deletions of peptide transporters was also more pronounced under anaerobic growth conditions, where *E. coli* Δ*dppA*Δ*oppA*Δ*sapA* and *E. coli* Δ*dppA*Δ*oppA*Δ*sapA*Δ*dtpD* were even less susceptible to negamycin and MIC increased to 64 µg/ml (Figure 8B, publication 1). This observation of the combining effect of the anaerobic growth conditions and peptide transporter gene deletions further reinforces the many uptake opportunities of negamycin.

2.1.2. Discussion

In this study, we described translocation mechanisms of negamycin across the cytoplasmic membrane, emphasizing its many uptake options to reach its target in the cytoplasm. When uptake opportunities are limited to a one predominant transporter, a quick rise of resistance is likely, as we could observe with bialaphos. The single deletion of *oppA* increased the bialaphos MIC by 1,000-fold and the additional gene deletion of *dppA* increased the MIC of bialaphos over 64,000 fold (Figure 2B, publication 1). The dependency on *oppA* was also reflected in the high resistance rates even at 100x MIC of bialaphos (resistance frequencies of 7×10^{-7} at 100x MIC). A similar dependency on transporters was described for the tetrapeptide antibiotic GE81112, which lost activity in *E. coli* strains without Opp (Maio *et al.* 2016). On the contrary, negamycin is able to use multiple peptide transporters and even after deletion of four relevant peptide transporter genes, the negamycin MIC increased only eight-fold (Figure 8B, publication 1). As negamycin targets ribosomal RNA, which is encoded in multiple gene copies in most organisms (e.g., seven rRNA operons in *E. coli*), quick development of high-level resistance is unlikely.

We could show that [^{3}H]negamycin accumulation is decreased in *E. coli* Δ*dppA* in a peptide-free environment (Figure 2D, publication 1). This is in accordance with previous reports, where Dpp was described to play a role in negamycin activity against *E. coli* (Rafanan *et al.* 2003; McKinney *et al.* 2015a). In a mouse thigh infection model, the presence of DppA was not required for the activity of negamycin, but it has to be noted, that the effective antibiotic concentration was two times higher, when *E. coli* ATCC 25922 Δ*dppA* was compared to its isogenic wildtype strain (McKinney *et al.* 2015a). Although negamycin does not strictly depend on Dpp-mediated transport, its importance in a peptide-free environment could clearly be seen by resistance development (Figure 3, publication 1). Using PP, negamycin competes with peptides for Dpp-mediated uptake, and other peptide transporters, or components thereof, are also important for negamycin translocation, namely the POT DtpD and SapA, the periplasmic binding protein of the the Sap transporter (Table 2, publication 1). The deletion of other subunits of the Sap transporter showed no effect on negamycin activity. SapA might therefore interact with permease domains of other transporters for negamycin uptake. Interaction between different

periplasmic binding proteins and permeases has been described before (Park James *et al.* 1998; Létoffé *et al.* 2006). DtpD belongs to the class of proton-dependent oligopeptide transporters (POTs) (Paulsen and Skurray 1994). Uptake of aminocephalosporins has been previously described for the POT DtpA (Weitz *et al.* 2007). These POTs are also present in mammalian cells (Newstead 2017), which might be of interest to the application of negamycin against Duchenne disease, which is caused by a premature stop codon (Arakawa *et al.* 2003; Taguchi *et al.* 2012).

In the peptide containing environment of PP, further factors contributing to negamycin activity could be observed. The activity of negamycin could be improved by $CaCl_2$ addition, with an ideal concentration of 2.5 mM (Table 3, publication 1). This concentration is of interest, as it resembles the concentration of calcium in the human blood (Walker *et al.* 1990; Enna and Bylund 2008). $MgCl_2$ did not improve the activity of negamycin, but at the same time did not increase the MIC (Table 3, publication 1). This observation is in contrast to other antibiotics tested, namely ciprofloxacin, tetracycline and gentamicin, where the MICs increased when salts were added to the medium (Table S1, publication 1). The addition of divalent cations has previously been linked to reduced activity of quinolones and tetracycline against *E. coli* (Chapman and Georgopapadakou 1988; Valisena *et al.* 1990; Lecomte *et al.* 1994; Marshall and Piddock 1994). The aminoglycoside streptomycin accumulated less in *E. coli* and *P. aeruginosa* in the presence of divalent cations (Bryan and Van Den Elzen 1977a). The reduced uptake of streptomycin could also be observed for the Gram-positive bacterium *S. aureus,* indicating an effect at the cytoplasmic membrane. It has been generally described, that calcium and magnesium improve the stability of membranes, especially the outer membrane, by binding to the negatively charged LPS (Nikaido 2003; Silhavy *et al.* 2010). In contrast, activity of daptomycin increased in the presence of calcium, but decreased when substituted with magnesium, nickel or manganese (Jones and Barry 1987; Weitz *et al.* 2007). Similarly, we could observe substantially facilitated binding of negamycin to phospholipids by SAW measurements in the presence of calcium but not magnesium (Figure 5, publication 1). Interactions of negamycin with magnesium could be shown by TLC (Figure 6A, publication 1), which might play a more important role for binding to the ribosome than for uptake (Polikanov *et al.* 2014). Binding of negamycin to $CaCl_2$ was also investigated by ITC. The high K_d of 7.98 mM at neutral pH hindered determination of the binding stoichiometry, but was comparable to ofloxacin binding to magnesium or tetracycline binding to calcium with reported K_d values of 1.1 mM at pH 6.5 and 0.59 mM at pH 7.5, respectively (Lecomte *et al.* 1994; Jin *et al.* 2007). Although we could clearly show direct interactions between negamycin and calcium and improved negamycin activity on the whole-cell level by calcium addition, cellular uptake measurements over a time period of 60 min with [^{3}H]negamycin did not correlate with these binding and activity studies, as no increase in uptake could be observed (Figure 4C, publication 1). It cannot be excluded, that the beneficial effect of calcium is more important at later time points. The binding of calcium to negamycin could also have an impact on the physicochemical behavior of negamycin, altering the distribution behavior of negamycin during sample processing in the radioactive experiment series.

Negamycin activity against *E. coli* could also be linked to the membrane potential. The MIC increased at acidic pH, in energy mutants and under anaerobic growth conditions (Figures 4, 7 & 8, publication 1), indicating that a membrane potential dependent pathway plays a role in negamycin accumulation. This dependency was only seen in peptide rich media, where the main uptake routes of negamycin through peptide transporters was restricted. A similar trend for pH-dependent activity was shown for aminoglycosides, although for this compound class the exact translocation mechanism across the cytoplasmic membrane remains elusive (Damper and Epstein 1981). Physicochemical calculations predict that a shift to alkaline pH leads to a bigger fraction of zwitterionic negamycin molecules (Figure S4, publication 1), which could facilitate diffusion through the phospholipids of the cytoplasmic membrane. Similarly, it has been observed that uncharged fluoroquinolones and tetracyclines diffused better through lipids (Nikaido and Thanassi 1993).

In conclusion, this study provided new insights on the various uptake opportunities of negamycin across the cytoplasmic membrane of *E. coli*. This knowledge could help in further derivatization campaigns of the antibiotic, as for this antibiotic not only binding to its target structure is of importance, but also the translocation mechanisms to reach the cytoplasmic space.

2.2. Kanamycin uptake into *Escherichia coli* is facilitated by OmpF and OmpC porin channels located in the outer membrane (publication 2)

2.2.1. Results

The porins OmpF, OmpC and OmpN of *E. coli* were investigated as possible uptake pathways for the aminoglycoside kanamycin. The porins OmpF and OmpC were previously associated with antibiotic translocation (Nikaido 2003). OmpN was selected as an additional porin of interest, as it is structurally closely related to the major porin OmpC (Prilipov *et al.* 1998). Purified porin proteins were used to determine their permeability for kanamycin. A concentration gradient of kanamycin was applied and by determining the reversal potential, the permeability ratio of kanamycin compared to SO_4^{2-} was determined for OmpF, OmpC and OmpN (Table 1, publication 2). The permeability ratios of kanamycin to sulfate were 1 : 14 and 1 : 4.2 for OmpF and OmpC, respectively. This means that kanamycin could permeate easier through OmpC than OmpF. At the same time, kanamycin permeation through OmpN was very low, as a ratio of 1 : >600 indicated no translocation of kanamycin through OmpN. In a next step, kanamycin translocation events through single channels were investigated at different voltage levels (Figure 1, publication 2). High event rates could be observed for all three porins tested, but it is important to note that this observation does not necessarily mean translocation (Mahendran *et al.* 2010). Decreasing dwell times with increasing voltage levels indicate translocation of molecules through porins. For OmpF and OmpC, lower dwell times were observed at higher voltage, indicating translocation through these porins (Figure 2B, publication 2). In contrast for OmpN, dwell times were voltage independent, therefore indicating no translocation of kanamycin through OmpN (Figure 2B, publication 2).

Molecular dynamics simulations were conducted to investigate the translocation mechanism of kanamycin through the porins OmpF and OmpC. Key regions for molecule interaction within the porin barrel structure and therefore translocation through a porin are the preorientation and constriction regions. The constriction region is located in the middle of the porin, separating the top and bottom halves of the porin protein (Figure 3C & D). This is the narrowest spot within the porin, as the loop L3 ranges inside the porin and therefore reduces the inner diameter of the barrel. The preorientation region is located between the entry of the porin on the extracellular side and the constriction region. In OmpF and OmpC it is a zone ranging from 5 to 10 Å before the constriction region. Both constriction and preorientation regions are identified by a strong electric field, with a stronger electric field at the constriction region. As the name implies, molecules interact at the preorientation region with the amino acid residues of the porin protein, before moving to the constriction region where molecules orientate their dipole moment to fit through the porin channel.

The simulation could show translocation of kanamycin through OmpF and OmpC (Figure 3, publication 2). The first minimum for kanamycin is within the preorientation region of OmpF (S0 in Figure 3A, publication 2), where kanamycin already interacts with the negatively charged residues E117 and D121 of the loop L3 within the constriction region (Figure 4B, publication 2). Although the dipole moment of kanamycin is aligned to the transversal electric field of the porin, the flux through the OmpF porin is not blocked completely. In the second minimum (S1 in Figure 3A, publication 2), kanamycin is interacting with multiple residues from the constriction region (Figure 4E, publication 2). By interacting with R42, R82, R132, D113, E117 and D121, kanamycin's dipole moment is aligned again to the transversal electric field and here now blocking the porin. For OmpC, no interactions with the loop L3 could be observed, when kanamycin was located in the preorientation region (Figure S4, publication 2). This could be attributed to the smaller electric field of OmpC, when compared to OmpF (Figure 3 & S4, publication 2). Within the constriction region of OmpC, kanamycin interacts with the residues R37, R74, D105, E109 and D113 (Figure 4G, publication 2). Similar to OmpF, kanamycin's dipole moment is here aligned to the transversal electric field and blocking the pore (Figure 4F, publication 2). These two blocking states within OmpF and OmpC were further investigated by simulating a flux of K^+ or Cl^-. For both porins, flux of the cation K^+ was reduced strongly, from 33 K^+ to 1 K^+ and 39 K^+ to 3 K^+ in OmpF and OmpC, respectively (Figure S5B & Table S2, publication 2). Interestingly, at the same time, anions are not blocked but the numbers of anions crossing these porins are even increased by kanamycin binding. Compared to empty trimeric porins, the passage of Cl^- anions increased from 5 to 8 and 3 to 15 for OmpF and OmpC, respectively (Figure S5B & Table S2, publication 2).

These observations from *in vitro* experiments and the computational setup were checked for relevance using *E. coli* cells. To this end, kanamycin susceptibility was investigated in *E. coli* lacking either *ompF*, *ompC* or both genes. Susceptibility was determined either by standardized MIC testing or streaking *E. coli* cells on agar plates with a linear kanamycin gradient. With both methods, a decrease in kanamycin susceptibility was only observed, when the genes of both *ompF* and *ompC* were deleted (Figure 5, publication 2). Single gene deletions of either *ompF* or *ompC* had no effect when compared to the wild type strain, indicating that both porins are involved in kanamycin accumulation, as suggested by the electrophysiology and molecular dynamics results. A similar trend was observed for other aminoglycosides like paromomycin, amikacin and gentamicin (Figure S6, publication 2). It has to be noted, that for all aminoglycosides tested, the MIC increased by only one dilution step in the *E. coli* Δ*ompF*Δ*ompC* mutant compared to the wild type. For other antibiotics, as the cephalosporin cefoxitin, the deletion of both porin genes had a stronger effect, and the MIC increased from 1-2 µg/ml to 8-16 µg/ml (Figure S6, publication 2). The results from this study suggest that kanamycin is able to diffuse through OmpF and OmpC, but the activity of kanamycin is not strictly dependent on the presence of these two porins, indicating further uptake opportunities into *E. coli*.

2.2.2. Discussion

The translocation of kanamycin through the *E. coli* porins OmpF and OmpC was shown for both porins by electrophysiological experiments and molecular dynamics simulations. Porin translocation requires molecules to be small and kanamycin is quite bulky, with a minimal projection area of 71 $Å^2$ (Table S3, publication 2). Other small antibiotics, which are used to treat Gram-negative pathogens, usually do not exceed a projection area of 60 $Å^2$, with the exception of ceftazidime and piperacillin with sizes of 68 and 77 $Å^2$, respectively, which are in a similar size range as kanamycin (Malloci *et al.* 2015). Kanamycin is able to diffuse through OmpF and OmpC, as it aligns perfectly to the structure of the pore. Kanamycin's dipole moment is oriented transversal to the long axis of the molecule, which enables it to place its long axis parallel to the axis of diffusion and with the dipole oriented to the transversal electric field of the porin (Figure 4, publication 2).

The cation selectivity of OmpF and OmpC is due to the negative electrostatic potential within the porins, especially caused by the anionic residues of the loop L3 (Nikaido 2003; Acosta-Gutiérrez *et al.* 2018). The reversal potential method showed, that kanamycin is able to pass through both OmpF and OmpC (Table 1, publication 2). The even more cationic-selective porin OmpN was investigated for kanamycin diffusion as well, but the reversal potential method showed no translocation through this porin (Table 1, publication 2). The structure of OmpN was not resolved at the time of this publication, but based on K_2SO_4 conductivity measurements, it was estimated that OmpN has a pore radius smaller than 1 Å, which would be significantly smaller than the pore sizes of OmpF and OmpC, with radii of 3.1 ± 1.1 and 2.8 ± 1.1 Å, respectively (Acosta-Gutiérrez *et al.* 2018). The recent structural analysis of OmpN revealed, however, that the constriction zone of OmpN (2.8 ± 1.1 Å) has a similar size to OmpF and OmpC (Figure 3, manuscript 1). The selective filter of OmpN must therefore be based on an electrostatic barrier.

Kanamycin does not only interact with OmpF at the constriction region, but also in the preorientation region, as shown by an additional minimum of the free energy surface determined by molecular dynamics (Figure 3A, publication 2). This region is exactly where previously interactions between ampicillin and norfloxacin have been reported (Ziervogel and Roux 2013; Bajaj *et al.* 2017). The preorientation region is wider than the constriction region, which results in an incomplete blockage of the ion flux by kanamycin, which was seen by single channel measurements (Figure 1A, publication 2).

On the cellular level, kanamycin susceptibility was affected by the gene deletion of *ompF* and *ompC*, but only when both porin genes were removed (Figure 5A, publication 2). This result fits the previous observations by the electrophysiological experiments and computational analyses, indicating that kanamycin is able to translocate through both porins (Table 1 & Figure 3, publication 2). The change in susceptibility was only weakly seen in the standardized determination of the MIC, but showed significantly when *E. coli* strains were grown on agar with a linear kanamycin concentration gradient, a method offering better resolution (Figure 5B, publication 2). In previous publications investigating the

effect of OmpF and OmpC on kanamycin susceptibility, results were contradictory. An OmpF-deficient *E. coli* strain showed an increase in kanamycin resistance, but was at the same time polymyxin B-resistant, indicating that other resistance mechanisms at the outer membrane could play a role as well (Foulds and Chai 1978). In another study, in which the expression of both *ompF* and *ompC* was reduced by deletion of a regulator of both porins, kanamycin susceptibility was not affected (Hancock *et al.* 1991). Slight differences in susceptibility might be overlooked when expression is not reduced completely, in contrast to our markerless gene deletions ensuring full prevention of expression. It has to be noted, that even when both porin genes were deleted, only one dilution step in difference could be determined by MIC measurements. This indicates that kanamycin activity does not depend on the presence of these porins, as other uptake pathways must be available. For polycationic aminoglycosides, it has been reported repeatedly that translocation across the outer membrane is possible by the self-promoted uptake pathway (Taber *et al.* 1987; Mingeot-Leclercq *et al.* 1999; Serio *et al.* 2018a; Serio *et al.* 2018b). Here, polycationic antibiotics displace cations between lipopolysaccharides, which destabilizes the outer membrane briefly and enables translocation. These multiple uptake opportunities minimize the risk of resistance development. Previous clinical observations on aminoglycoside resistance development reported that aminoglycoside-modifying enzymes or 16S rRNA methyltransferases are the predominant resistance mechanism in the clinical environment (Garneau-Tsodikova and Labby 2016).

Although permeation rates of kanamycin through OmpF and OmpC were low, the abundance of these porins could lead to quick equilibration between concentrations outside the bacterial cell and the periplasm. As a rough estimate, ten to twenty molecules/s/monomer diffuse through OmpF or OmpC at a 10 µM concentration gradient. Still, the importance of porins for aminoglycoside accumulation inside *E. coli* cells needs further investigation, as other uptake pathways were reported as more important previously (Hancock *et al.* 1991). Although aminoglycosides have been in clinical use for decades, the uptake pathways into the cells to reach their cytoplasmic target are not fully understood. In our study, the translocation of an aminoglycoside through porins could clearly been shown for the first time.

2.3. Porin-mediated passage of negamycin across the outer membrane of *Escherichia coli* (manuscript 1)

2.3.1. Results

Negamycin's size and hydrophilicity makes the molecule an ideal candidate for translocation through porins. These water-filled channels enable permeation of small, hydrophilic molecules, in *E. coli* up to a size of about 600 Da (Nikaido 2003). Therefore, the role of porins for negamycin uptake was investigated, using *E. coli* as a model organism. Additionally, further outer membrane translocation mechanisms and the influence of efflux pumps on negamycin activity were explored.

The absence of the major *E. coli* porins OmpF and OmpC has been linked to antibiotic resistance of different classes of antibiotics (Nikaido 2003; Vergalli *et al.* 2020). Therefore, in our study, the gene deletion mutants lacking either *ompF*, *ompC* or both genes were tested for negamycin susceptibility, but no decrease in activity could be determined by the broth microdilution method (Table 1, manuscript 1). When negamycin susceptibility of these *E. coli* mutants was tested on a linear negamycin concentration gradient in agar, a weak growth advantage of *E. coli* Δ*ompF*Δ*ompC* could be observed (Figure 1A & B, manuscript 1). Although negamycin is not dependent on the presence of these two porins, the outer membrane of *E. coli* BW25113 seems to be, at least in 0.5% polypeptone (PP) medium, a rate limiting barrier for negamycin uptake, as the addition of the outer membrane permeabilizer polymyxin B nonapeptide (PMBN) decreased the MIC from 8 µg/ml to 2 µg/ml (Table 2, manuscript 1). Therefore, other translocation pathways across the outer membrane must exist. The self-promoted uptake mechanism, which enables permeation across the outer membrane by displacing divalent cations, which enhance binding between LPS molecules, could not be observed for negamycin (Table S7, manuscript 1). Additionally, uptake does not seem to be hindered by efflux in *E. coli*, as the deletion of multiple efflux pump genes did not increase negamycin activity markedly (Table S1, manuscript 1). As these other factors did not explain how negamycin crosses the outer membrane of *E. coli* cells and negamycin is an ideal candidate for porin translocation, further porin genes were investigated. The deletion of either *ompN*, *chiP*, *lamB*, *ompG*, *ompW* or *ompA* increased the negamycin MIC by one dilution step (Table 2, manuscript 1). This effect on the MIC could be reversed by the addition of PMBN, which indicates that the observed MIC increase is based on outer membrane translocation (Table 2, manuscript 1). Our study focused on the two porin genes *ompN* and *chip*. *ompN* was selected for further investigations as it showed high similarity to *ompF* and *ompC* and was previously proposed to be a backup porin for these two major porins (Pagès *et al.* 2008). ChiP was chosen, as the MIC shift occurred in both minimal media used in this study, which was not the case for all the other porin gene deletion mutants (Table 2, manuscript 1). Deletions of *ompN* or *chiP* did not only affect negamycin susceptibility in the *E. coli* K-12 derivative strain *E. coli* BW25113, but also in the clinical isolate *E. coli* ATCC 25922 (Table 2,

manuscript 1). Surprisingly, no additive effect on negamycin activity could be observed when both *ompN* and *chiP* genes were deleted, neither with *E. coli* BW25113, nor *E. coli* ATCC 25922.

Negamycin uptake was reduced in the absence of the *ompN* or *chiP* gene. The gene deletion of either *ompN* or *chiP* in *E. coli* ATCC 25922 led to a decrease in [^{3}H]negamycin accumulation, measured 15 min after the addition of radioactively labeled negamycin (Figure 1C & S1, manuscript 1). Again, the double deletion strain Δ*ompN*Δ*chiP* showed no additive effect on negamycin uptake.

Uptake through the porins OmpN, ChiP, OmpF and OmpC was also investigated with purified proteins in an electrophysiological assay setup. The passage of negamycin through OmpN, ChiP, OmpF and OmpC could be clearly observed (Table 3, manuscript 1). As controls, ertapenem and cefotaxime translocation through OmpN was probed, but these beta-lactams could not pass through OmpN (Table 3, manuscript 1). Single channel measurements could not detect blockage of the ion current (Figure S5, manuscript 1), which is why a translocation rate of negamycin through OmpN could not be quantified. But a rough estimate of ten to hundred molecules/s/OmpN monomer at a 1 μM negamycin gradient shows fast translocation through this porin.

To understand the selectivity of the OmpN porin for negamycin, the X-ray crystal structure of *E. coli* OmpN was resolved. As proposed by comparison of the amino acid sequence (Prilipov *et al.* 1998), the structure of OmpN is similar to OmpC (Figure S6, manuscript 1). One difference is the elongation of the loop L7 in OmpN, ranging outside the cell. Additionally, at the loop L3, responsible for the constriction region within the barrel structure, Thr101 is replaced with Glu102 in OmpN (Figure 2 & S6, manuscript 1). Furthermore, OmpN has His173, Asp248 and Asp250 protruding into this constriction region, making the porin more cation selective (Figure 2, manuscript 1). These changes could explain a shift in the electrostatic barrier, as the observation of kanamycin impermeability (Bafna *et al.* 2020) cannot be justified by size comparison of the constriction region between OmpN (2.8 ± 1.1 Å), OmpF (3.1 ± 1.1 Å) and OmpC (2.8 ± 1.1 Å) (Acosta-Gutiérrez *et al.* 2018).

The resolved structure of OmpN allowed further investigations on the translocation mechanisms and interactions of negamycin with OmpN by molecular dynamics. The free energy surface (FES) of negamycin through the porin was determined and two minima could be detected (Figure 3A & 3B, manuscript 1). The minimal FES near the constriction region, labeled Min-CR, showed stronger interactions of negamycin with the protein and was closer to the constriction region than the minimal FES at Min-Above, located just above the constriction region. Therefore Min-CR was considered to be more relevant for negamycin translocation through the porin, as stronger interactions indicate the bottleneck for negamycin translocation through this OmpN. Still, the change in FES was low (-4 kcal/mol compared to outside), indicating only weak interactions of the antibiotic with the amino acid residues of the porin. The calculated flux through the OmpN porin was high, the residence time inside the pore being less than 0.1 μs, and saturation was only reached with millimolar concentrations (Figure 3C, manuscript 1). For comparison, kanamycin interactions with OmpN using the same

molecular dynamics simulations were performed. Kanamycin showed stronger interactions with the OmpN porin, especially at the constriction region (Figure 3D, 3E, 4C & 4D, manuscript 1). This was also reflected in the flux of kanamycin through OmpN, which was three orders of magnitude lower and saturation was already reached at µM concentrations (Figure 3F, manuscript 1). Overall, the calculations predicted kanamycin to permeate poorly through OmpN, which is in accordance with previous experimental data, where no diffusion of kanamycin through OmpN could be measured (Bafna *et al.* 2020).

Negamycin translocation through OmpF and OmpC could clearly be shown on the protein level (Table 3, manuscript 1), but the respective genes did not have an impact on the negamycin MIC (Table 1, manuscript 1). To investigate the global response of *E. coli* to negamycin treatment, the transcriptome was investigated by transcriptome sequencing. Among the most strongly down-regulated transcripts was the dipeptide transporter operon *dpp* (Table 4, manuscript 1), which is known to be involved in negamycin uptake across the cytoplasmic membrane of *E. coli*, as reported in publication 1. The most strongly increased transcript was *soxS*, a transcriptional activator known to be induced upon oxidative stress (Table 4, manuscript 1). Negamycin susceptibility is not influenced by *soxS* levels, as *E. coli* Δ*soxS* showed the same negamycin MIC of 8 µg/ml in PP as its isogenic wild type strain *E. coli* BW25113. Transcripts of porin genes were affected as well. *ompF* expression was reduced 2.6-fold, and at the same time, *ompN* and *chiP* expressions were increased 3.6- and 5.1-fold, respectively. More OmpN is available for outer membrane translocation, but it has to be noted, that although *ompF* expression is reduced, there are still many more *ompF* than *ompN* transcripts (Table 4, manuscript 1). Western blots never detected the OmpN or ChiP protein, neither with nor without negamycin treatment (Figure S9, manuscript 1).

To determine possible side effects of the porin gene deletions, the transcriptomes of *E. coli* Δ*ompN*, *E. coli* Δ*chiP* and *E. coli* Δ*ompN*Δ*chiP* were investigated. Most other porin transcripts were not affected by these gene deletions (Table S6, manuscript 1). Only in *E. coli* Δ*ompN*, the *chiP* transcript was reduced 2.3 times. Notably, the expression of *ompN* was low in wildtype *E. coli* BW25113, as the deletion of *ompN* did not significantly decrease *ompN* transcript amounts.

Although the expression levels of *ompN* and *chiP* were generally low and the respective protein could not be detected in Western blot analysis, the role of these porins in negamycin translocation could be shown by susceptibility determinations, electrophysiological measurements and computational simulations.

2.3.2. Discussion

Multiple uptake pathways of negamycin through porins across the outer membrane could be shown in this study. An increase in negamycin MIC could be observed when either *ompN*, *chiP*, *lamB*, *ompG*, *ompW* or *ompA* were deleted (Table 2, manuscript 1). Most importantly, the small and hydrophilic molecule was able to diffuse through various porins, which could be shown on the protein level for OmpN, ChiP, OmpF and OmpC (Table 3, manuscript 1). Negamycin permeated through these porins at rates comparable to NaCl and easier through OmpF than previously reported for kanamycin and ampicillin (Ghai *et al.* 2018; Bafna *et al.* 2020).

Previous conductance measurements led to the assumption that the OmpN pore must be smaller than OmpF or ChiP (Bafna *et al.* 2020), but the resolved structure of OmpN showed a similar pore size (Figure 2, manuscript 1) as of OmpF and OmpC (Acosta-Gutiérrez *et al.* 2018). Therefore, the antibiotic selectivity must not solely rely on pore size but on other mechanisms, like an electrostatic barrier. Within clinical *E. coli* isolates, differences in *ompC* sequences have been linked to the reduction of antibiotic translocation, although the pore size was barely affected, but rather the transversal field inside the OmpC porin (Lou *et al.* 2011). Within the structure of OmpN, Asp248 and Asp250 have been identified to protrude into the barrel, which increases cation selectivity (Figure 2C, manuscript 1).

OmpN and ChiP have not been associated with antibiotic translocation in *E. coli,* so far, as mainly OmpF and OmpC are affected by antibiotic resistance development (Vergalli *et al.* 2020). The development of high negamycin resistance at the outer membrane seems unlikely, as multiple pathways are available for translocation. The situation at the cytoplasmic membrane is different. Here, it was previously observed, that treatment with negamycin led to genomic changes of genes associated with peptide transport or energy metabolism, depending on the growth medium composition (McKinney *et al.* 2015b; Hörömpöli *et al.* 2021). Within our transcriptome study, we could also observe that negamycin treatment had strong effects on transporter transcripts at the cytoplasmic membrane (Table 4, manuscript 1). At the outer membrane, the major *E. coli* porin gene *ompF* was affected and *ompF* transcripts were reduced compared to the untreated cells. The increase of *ompN* and *chip* expression (Table 4, manuscript 1) could enable additional uptake opportunities for negamycin across the outer membrane. Negamycin might therefore be an interesting option for treatment when other antibiotics are affected by reduced uptake by the lowered expression of the major porins OmpF and OmpC (Vergalli *et al.* 2020). Although *ompN* transcripts increased by negamycin treatment, the OmpN protein was still too low to be detected by Western blot analysis (Figure S9, manuscript 1).

Previously, it was proposed that a bicistronic *ydbK-ompN* operon exists (Fàbrega *et al.* 2012). In the transcriptome data in this study, multiple copies of the *ydbK* transcript were found in untreated *E. coli* BW25113, but none of *ompN*, indicating that there is a single transcript of *ydbK* (Supplemental information 2, manuscript 1). Additionally, a transcription start site was found upstream of the *ompN* gene, indicating a monocistronic *ompN* transcript (Ettwiller *et al.* 2016). It was also proposed that the

ydbK-ompN operon might be induced in response to oxidative stress, although only the *ydbK* gene seemed relevant when exposed to oxidative stress inducing agents (Fàbrega *et al.* 2012). In another study, the *ompN* promotor was reported to be induced by carbapenems and cephalosporins (Dam and Masi 2017). In this work, the whole region between the *ompN* and *micC* genes was used for a reporter construct, which responded by an increase in fluorescence when cells were exposed to certain antibiotics. Notably, also these authors did not detect the OmpN protein on Western blots, even when the promoter signal increase was strong (Dam and Masi 2017).

The high number of translocation options of negamycin across the outer membrane and its lack of dependency on a single porin make negamycin interesting for applications against various pathogens. In *Klebsiella pneumoniae*, porins are described to be more permeable to β-lactams and sugars than porins in *E. coli* (Sugawara *et al.* 2016). This fact might explain why porin loss in *K. pneumoniae* has been associated strongly with antibiotic resistance. It could be observed, that some clinical *Klebsiella* isolates react to antibiotic exposition by reduced expression of their major porins OmpK35 and OmpK36, which was compensated be an increase in expression of OmpK37 (Doménech-Sánchez *et al.* 1999). Structurally, OmpK35, OmpK36 and OmpK37 of *K. pneumoniae* are similar to OmpF, OmpC and OmpN of *E. coli*, respectively. Negamycin as an antimicrobial treatment might be of use here to counter resistance development, although further research on permeability within other bacteria would be necessary.

Our study provides first evidence that porins other than OmpF or OmpC could be of interest in regard to antibiotic accumulation in *E. coli*. The physiological role of OmpN and ChiP needs to be further investigated to determine if these alternative pathways across the outer membrane might be of interest in clinical treatment.

2.4. Two-step batch purification of negamycin from biosynthesis using cation exchange chromatography (manuscript 2)

2.4.1. Results

The in-depth biological characterization of natural product antibiotics depends on effective production of these molecules. Chemical synthesis of natural compounds can be demanding and expensive. At the time of this study, negamycin was available to us from total synthesis, but amounts were limited. To support the multitude of studies conducted by us and our external collaboration partners in the course of this thesis project, we produced negamycin by fermentation. The purification protocol of the negamycin patent (Umezawa *et al.* 1972) was adapted and improved. Although negamycin was already discovered in 1970, it recently re-gained attention of academical and industrial research groups, as it is a promising candidate for an antimicrobial drug to combat Gram-negative pathogens (Rafanan *et al.* 2003; McKinney *et al.* 2015a; McKinney *et al.* 2015c; Hörömpöli *et al.* 2021).

Prior to this work, a biosynthesis and purification protocol for negamycin was described, using multiple ion exchange chromatography columns (Umezawa *et al.* 1972). In the current study, the strain *Streptomyces purpeofuscus* ATCC 21477 was used for fermentation, as it showed the highest yield of negamycin among three putative negamycin producer strains (Hörömpöli 2016). The negamycin production medium (NPM) proposed in the original negamycin publication and patent was used (Hamada *et al.* 1970; Umezawa *et al.* 1972), only the soybean meal was exchanged by soybean flour, as it led to higher negamycin production (Hörömpöli 2016).

Here, one exemplary isolation process is described. The first step for negamycin biosynthesis was the inoculation of a culture with a spore suspension (Figure 1, manuscript 2). After cultivation for four days at 27°C, this culture was used to inoculate the main production culture of 2.2 l, which was further incubated at 27°C for four days. This procedure led to a negamycin concentration of about 125 mg/l within the supernatant of the production culture. The sample was centrifuged, the supernatant was filtered and applied to the cation exchange chromatography material Amberlite IRC-50 (Na^+ form). After washing, negamycin was eluted with 0.25% NH_4OH and fractions with bioactivity against *E. coli* BW25113 were pooled and concentrated under low pressure to a volume of ~10 ml (Table 1, manuscript 2). This sample was applied to the second cation exchange chromatography column, Amberlite CG50 (Figure 2, manuscript 2). Negamycin was eluted with deionized H_2O and fractions of 15 ml were collected. Eluates showing similar bioactivity were pooled (Table 2) and were freeze-dried. This procedure led to three pooled samples with a total of ~72 mg of a white powder. This powder was dissolved in water and the MIC against *E. coli* BW25113 was determined. A pool of 12.98 mg showed similar activity as the negamycin available from total synthesis (Pool 2, Table 2, manuscript 2). Furthermore, 58.79 mg were only a factor of two less active than negamycin from total synthesis.

The purity of the batch of 12.98 mg with highest activity was further investigated. This sample was compared side by side with the negamycin from chemical synthesis by TLC and HPLC. The purified biosynthetic product showed only one spot by ninhydrin staining, whereas the total synthetic negamycin had three spots, and only the strongest signal had the same retention factor as the purified biosynthetic negamycin sample (Figure 3A, manuscript 2). The additional spots of the total synthetic sample correspond probably to residual material from chemical synthesis, in particular negamycin still carrying protection groups that could not be removed. Comparing the samples by HPLC on a Luna Omega Polar column, both samples showed the strongest peak at the retention time of 11 min (Figure 3B, manuscript 2) and each a minor, additional signal at different retention times, but with a much lower peak compared to the negamycin signal.

Purity of the purified fermentation product was further investigated by nuclear magnetic resonance (NMR). Compared to total synthetic negamycin, various additional peaks could be detected in the material isolated from biosynthesis (Figure 4, manuscript 2). Most smaller peaks could not be assigned to organic material. One additional peak at 3.25 ppm indicated a residual natural product impurity. Based on signal strength, purity of the biosynthetic sample was calculated to be above 95%.

2.4.2. Discussion

The procedure for negamycin purification from a *S. purpeofuscus* culture, based on the previous patent (Umezawa *et al.* 1972), could be established as a method in our lab. Additionally, the protocol was improved, as the method was reduced from four ion exchange chromatography steps to only two.

The yield of negamycin produced by the culture varied between different fermentation runs between 60 and 150 µg/ml within the fermentation supernatant. The yield of pure negamycin per 2.2 l fermentation was between 12 and 15.5 mg. In the exemplarily isolation described in this study, about 13 mg of pure negamycin (>95% purity) could be purified from a culture of 2.2 liter (Table 2, manuscript 2). Additional ~59 mg of semi-pure negamycin was extracted. This led to a yield of 72 mg negamycin, which corresponds to about 26% of the estimated total 275 mg in the production culture. This yield is comparable to the original patent, where 39 mg negamycin from a total 210 mg was purified (19%). Taking the higher fermentation volume of the 6 l culture into account, the purified amounts of negamycin per fermentation volume was lower in the original publication. But the proportion of pure negamycin, with 20 mg from the total 39 mg, was higher in the original patent (Umezawa *et al.* 1972).

Further optimization of negamycin fermentation and purification can be achieved by scaling up and by replacing or adding chromatography steps after the first cation exchange chromatography. One promising column material could be the Luna Omega Polar, which was used for analysis in this study (Figure 3B, manuscript 2). Here, a single peak at a retention time of 13 min could be observed, while many other column materials tested, did not retain the highly polar negamycin. This method must first

be applied to a larger, semi-preparative setup, but looks promising. Increasing negamycin amounts within the production culture might be difficult with classical methods, as so far alternative media or other potential producer strains did not increase the negamycin concentration in the supernatant (Hörömpöli 2016). The gene cluster for negamycin biosynthesis has not been identified, yet. Therefore, the search for new negamycin producer strains or genetic modifications of the gene cluster are not possible yet. However, the negamycin gene cluster is currently being studied by colleagues in our department.

The isolation of hydrophilic natural products is, in general, a difficult task, as large amounts of water have to be removed, which is a time-consuming task (Berlinck *et al.* 2019). Additionally, residual salts, sugars and amino acids are difficult to remove during the isolation process. New column materials, like the hydrophilic interactions liquid chromatography (HILIC), have been developed but so far have been only successfully applied for analysis (Berlinck *et al.* 2019).

For most previous studies on negamycin conducted to date, negamycin was obtained by chemical total synthesis (Shibahara *et al.* 1972; Streicher *et al.* 1978; Wang *et al.* 1982; Hayashi *et al.* 2008; Hayashi *et al.* 2009). These chemical synthesis procedures require multiple steps, varying from 13 to 19 working steps to achieve a yield of up to 26% (Wang *et al.* 1982; Hayashi *et al.* 2009). Although a more efficient procedure, with eight steps leading to a yield of 42% has been described (Hayashi *et al.* 2008), our isolation protocol from biosynthesis with only two purification steps might offer a convenient alternative for obtaining negamycin.

3. References

Acosta-Gutiérrez, Silvia, Luana Ferrara, Monisha Pathania, Muriel Masi, Jiajun Wang, Igor Bodrenko, Michael Zahn, Mathias Winterhalter, Robert A. Stavenger, Jean-Marie Pagès, James H. Naismith, Bert van den Berg, Malcolm G. P. Page, and Matteo Ceccarelli. 2018. 'Getting Drugs into Gram-Negative Bacteria: Rational Rules for Permeation through General Porins', *ACS Infectious Diseases*, 4: 1487-98.

Adedeji, W. A. 2016. 'The Treasure called Antibiotics', *Annals of Ibadan postgraduate medicine*, 14: 56-57.

Anes, João, Matthew P. McCusker, Séamus Fanning, and Marta Martins. 2015. 'The ins and outs of RND efflux pumps in Escherichia coli', *Frontiers in microbiology*, 6.

Arakawa, Masayuki, Masataka Shiozuka, Yuki Nakayama, Takahiko Hara, Masa Hamada, Shin'ichi Kondo, Daishiro Ikeda, Yoshikazu Takahashi, Ryuichi Sawa, and Yoshiaki Nonomura. 2003. 'Negamycin restores dystrophin expression in skeletal and cardiac muscles of mdx mice', *Journal of biochemistry*, 134: 751-58.

Baba, Tomoya, Takeshi Ara, Miki Hasegawa, Yuki Takai, Yoshiko Okumura, Miki Baba, Kirill A Datsenko, Masaru Tomita, Barry L Wanner, and Hirotada Mori. 2006. 'Construction of Escherichia coli K-12 in-frame, single-gene knockout mutants: the Keio collection', *Molecular systems biology*, 2: 2006.0008.

Bafna, Jayesh Arun, Eulàlia Sans-Serramitjana, Silvia Acosta-Gutiérrez, Igor V. Bodrenko, Daniel Hörömpöli, Anne Berscheid, Heike Brötz-Oesterhelt, Mathias Winterhalter, and Matteo Ceccarelli. 2020. 'Kanamycin Uptake into Escherichia coli Is Facilitated by OmpF and OmpC Porin Channels Located in the Outer Membrane', *ACS Infectious Diseases*, 6: 1855-65.

Bajaj, Harsha, Silvia Acosta Gutierrez, Igor Bodrenko, Giuliano Malloci, Mariano Andrea Scorciapino, Mathias Winterhalter, and Matteo Ceccarelli. 2017. 'Bacterial outer membrane porins as electrostatic nanosieves: exploring transport rules of small polar molecules', *ACS nano*, 11: 5465-73.

Balaz, Stefan. 2012. 'Does transbilayer diffusion have a role in membrane transport of drugs?', *Drug discovery today*, 17: 1079-87.

Berdy, Janos. 2005. 'Bioactive microbial metabolites', *The Journal of antibiotics*, 58: 1-26.

Berlinck, Roberto G. S., Afif F. Monteiro, Ariane F. Bertonha, Darlon I. Bernardi, Juliana R. Gubiani, Juliano Slivinski, Lamonielli F. Michaliski, Luciane A. C. Tonon, Victor A. Venancio, and Vitor F. Freire. 2019. 'Approaches for the isolation and identification of hydrophilic, light-sensitive, volatile and minor natural products', *Natural product reports*, 36: 981-1004.

Brötz-Oesterhelt, Heike, and Peter Sass. 2010. 'Postgenomic strategies in antibacterial drug discovery', *Future microbiology*, 5: 1553-79.

Bryan, L.E., and H.M. Van Den Elzen. 1977a. 'Effects of membrane-energy mutations and cations on streptomycin and gentamicin accumulation by bacteria: a model for entry of streptomycin and gentamicin in susceptible and resistant bacteria', *Antimicrob.Agents Chemother.*, 12: 163-77.

Bryan, LE, and HM Van Den Elzen. 1976. 'Streptomycin accumulation in susceptible and resistant strains of Escherichia coli and Pseudomonas aeruginosa', *Antimicrobial Agents and Chemotherapy*, 9: 928-38.

Bryan, LE, and HM Van Den Elzen. 1977b. 'Effects of membrane-energy mutations and cations on streptomycin and gentamicin accumulation by bacteria: a model for entry of streptomycin and gentamicin in susceptible and resistant bacteria', *Antimicrobial Agents and Chemotherapy*, 12: 163-77.

CDC. 2019. "Biggest threats and data. 2019 AR threats report." In.: CDC Atlanta, GA.

Chapman, John S, and Nafsika H Georgopapadakou. 1988. 'Routes of quinolone permeation in Escherichia coli', *Antimicrobial Agents and Chemotherapy*, 32: 438-42.

Charbit, A. 2003. 'Maltodextrin transport through lamb', *Front Biosci*, 8: s265-74.

Chong, Z. S., W. F. Woo, and S. S. Chng. 2015. 'Osmoporin OmpC forms a complex with MlaA to maintain outer membrane lipid asymmetry in Escherichia coli', *Mol Microbiol*, 98: 1133-46.

Chopra, I. 1985. 'Mode of action of the tetracyclines and the nature of bacterial resistance to them.' in, *The tetracyclines* (Springer).

Chopra, I, S Ismail, and B Oliva. 1991. 'Lack of evidence for a saturable tetracycline transport system in Staphylococcus aureus', *Antimicrobial Agents and Chemotherapy*, 35: 2643-44.

Cocozaki, Alexis I, Roger B Altman, Jian Huang, Ed T Buurman, Steven L Kazmirski, Peter Doig, D Bryan Prince, Scott C Blanchard, Jamie HD Cate, and Andrew D Ferguson. 2016. 'Resistance mutations generate divergent antibiotic susceptibility profiles against translation inhibitors', *Proceedings of the National Academy of Sciences*, 113: 8188-93.

Dam, Sushovan, and Muriel Masi. 2017. 'Dual regulation of the small RNA MicC and the quiescent porin OmpN in response to antibiotic stress in Escherichia coli', *Antibiotics*, 6: 33.

Damper, P.D., and W. Epstein. 1981. 'Role of the membrane potential in bacterial resistance to aminoglycoside antibiotics', *Antimicrob.Agents Chemother.*, 20: 803-08.

Davies, Sally C, Tom Fowler, John Watson, David M Livermore, and David Walker. 2013. 'Annual Report of the Chief Medical Officer: infection and the rise of antimicrobial resistance', *The Lancet*, 381: 1606-09.

De la Cruz, M. A., and E. Calva. 2010. 'The complexities of porin genetic regulation', *J Mol Microbiol Biotechnol*, 18: 24-36.

Doménech-Sánchez, Antonio, Santiago Hernández-Allés, Luis Martínez-Martínez, Vicente J. Benedí, and Sebastián Albertí. 1999. 'Identification and Characterization of a New Porin Gene of *Klebsiella pneumoniae*: Its Role in β-Lactam Antibiotic Resistance', *Journal of Bacteriology*, 181: 2726-32.

Eitinger, Thomas, and Hans Günter Schlegel. 2007. *Allgemeine mikrobiologie* (Georg Thieme Verlag).

Emmerson, A. M., and A. M. Jones. 2003. 'The quinolones: decades of development and use', *Journal of Antimicrobial Chemotherapy*, 51: 13-20.

Enna, SJ, and David B Bylund. 2008. "Xpharm: the comprehensive pharmacology reference." In.: Elsevier Boston, MA, USA:.

Escherich, T. 1885. 'Die darmbakterien des neugeborenen und Säuglings Fortschritte des medizin', *München*, 3: 512-22.

Ettwiller, Laurence, John Buswell, Erbay Yigit, and Ira Schildkraut. 2016. 'A novel enrichment strategy reveals unprecedented number of novel transcription start sites at single base resolution in a model prokaryote and the gut microbiome', *BMC Genomics*, 17: 199.

Fàbrega, Anna, Judah L Rosner, Robert G Martin, Mar Solé, and Jordi Vila. 2012. 'SoxS-dependent coregulation of ompN and ydbK in a multidrug-resistant Escherichia coli strain', *FEMS microbiology letters*, 332: 61-67.

Floquet, Celia, Jules Deforges, Jean-Pierre Rousset, and Laure Bidou. 2011. 'Rescue of non-sense mutated p53 tumor suppressor gene by aminoglycosides', *Nucleic acids research*, 39: 3350-62.

Foulds, JOHN, and TJ Chai. 1978. 'New major outer membrane proteins found in an Escherichia coli tolF mutant resistant to bacteriophage TuIb', *Journal of Bacteriology*, 133: 1478-83.

Garneau-Tsodikova, Sylvie, and Kristin J. Labby. 2016. 'Mechanisms of resistance to aminoglycoside antibiotics: overview and perspectives', *MedChemComm*, 7: 11-27.

Ghai, Ishan, Harsha Bajaj, Jayesh Arun Bafna, Hussein Ali El Damrany Hussein, Mathias Winterhalter, and Richard Wagner. 2018. 'Ampicillin permeation across OmpF, the major outer-membrane channel in Escherichia coli', *Journal of Biological Chemistry*, 293: 7030-37.

Guo, J., E. W. Miele, A. Chen, R. A. Luzietti, M. Zambrowski, R. L. Walsky, and E. T. Buurman. 2015. 'Pharmacokinetics of the natural antibiotic negamycin', *Xenobiotica*, 45: 625-33.

Hall, Jason A, and Peter C Maloney. 2001. 'Transmembrane Segment 11 of UhpT, the Sugar Phosphate Carrier ofEscherichia coli, Is an α-Helix That Carries Determinants of Substrate Selectivity', *Journal of Biological Chemistry*, 276: 25107-13.

Hamada, M., T. Takeuchi, S. Kondo, Y. Ikeda, and H. Naganawa. 1970. 'A new antibiotic, negamycin', *J Antibiot (Tokyo)*, 23: 170-1.

Hancock, R E, S W Farmer, Z S Li, and K Poole. 1991. 'Interaction of aminoglycosides with the outer membranes and purified lipopolysaccharide and OmpF porin of Escherichia coli', *Antimicrobial Agents and Chemotherapy*, 35: 1309-14.

Hansch, Corwin, and Toshio Fujita. 1964. 'p-σ-π Analysis. A method for the correlation of biological activity and chemical structure', *Journal of the American Chemical Society*, 86: 1616-26.

Hayashi, Yoshio, Shigenobu Nishiguchi, Magne O Sydnes, Thomas Regnier, Jun-ya Hasegawa, Takahiro Katoh, Tetsuya Kajimoto, Manabu Node, and Yoshiaki Kiso. 2009. 'A New Synthesis of (+)-Negamycin and Its Derivatives as a Potential Therapeutic Agent for Duchenne Muscular Dystrophy Treatment.' in, *Peptides for Youth* (Springer).

Hayashi, Yoshio, Thomas Regnier, Shigenobu Nishiguchi, Magne O Sydnes, Daisuke Hashimoto, Junya Hasegawa, Takahiro Katoh, Tetsuya Kajimoto, Masataka Shiozuka, and Ryoichi Matsuda. 2008. 'Efficient total synthesis of (+)-negamycin, a potential chemotherapeutic agent for genetic diseases', *Chemical communications*: 2379-81.

Hörömpöli, Daniel. 2016. 'Das Pseudopeptid-Antibiotikum Negamycin: Produktion in Streptomyces purpeofuscus und Rolle von Porinen bei der Aufnahme in *Escherichia coli* (Master thesis)', *Universität Tübingen*.

Hörömpöli, Daniel, Catherine Ciglia, Karl-Heinz Glüsenkamp, Lars Ole Haustedt, Hildegard Falkenstein-Paul, Gerd Bendas, Anne Berscheid, and Heike Brötz-Oesterhelt. 2021. 'The Antibiotic Negamycin Crosses the Bacterial Cytoplasmic Membrane by Multiple Routes', *Antimicrobial Agents and Chemotherapy*, 65: e00986-20.

Jin, Lihua, Xylenia Amaya-Mazo, Matthew E Apel, Sudha S Sankisa, Elissa Johnson, Monika A Zbyszynska, and Alexander Han. 2007. 'Ca2+ and Mg2+ bind tetracycline with distinct stoichiometries and linked deprotonation', *Biophysical chemistry*, 128: 185-96.

Jones, Ronald N, and ARTHUR L Barry. 1987. 'Antimicrobial activity and spectrum of LY146032, a lipopeptide antibiotic, including susceptibility testing recommendations', *Antimicrobial Agents and Chemotherapy*, 31: 625-29.

Kadner, Robert J, Carol A Webber, and Michael D Island. 1993. 'The family of organo-phosphate transport proteins includes a transmembrane regulatory protein', *Journal of bioenergetics and biomembranes*, 25: 637-45.

Katz, Leonard, and Richard H Baltz. 2016. 'Natural product discovery: past, present, and future', *Journal of Industrial Microbiology and Biotechnology*, 43: 155-76.

Kitamura, Kenji, Eldaa Zefany Banami Kinsui, and Fumiyoshi Abe. 2017. 'Critical role of the proton-dependent oligopeptide transporter (POT) in the cellular uptake of the peptidyl nucleoside antibiotic, blasticidin S', *Biochimica et Biophysica Acta (BBA) - Molecular Cell Research*, 1864: 393-98.

Klappenbach Joel, A., M. Dunbar John, and M. Schmidt Thomas. 2000. 'rRNA Operon Copy Number Reflects Ecological Strategies of Bacteria', *Applied and Environmental Microbiology*, 66: 1328-33.

Kondo, S., K. Iinuma, K. Yoshida, K. Yokose, and Y. Ikeda. 1976. 'Syntheses and properties of negamycin analogs modified the delta-hydroxy-beta-lysine moiety', *J Antibiot (Tokyo)*, 29: 208-11.

Krulwich, Terry A, George Sachs, and Etana Padan. 2011. 'Molecular aspects of bacterial pH sensing and homeostasis', *Nature Reviews Microbiology*, 9: 330-43.

Lalchhandama, K. 2020. 'Reappraising Fleming's snot and mould', *Mizo Academy of Sciences*, 20: 29-42.

LeBlanc, Jean Guy, Christian Milani, Graciela Savoy De Giori, Fernando Sesma, Douwe Van Sinderen, and Marco Ventura. 2013. 'Bacteria as vitamin suppliers to their host: a gut microbiota perspective', *Current opinion in biotechnology*, 24: 160-68.

Lecomte, S, MH Baron, M Th Chenon, C Coupry, and NJ Moreau. 1994. 'Effect of magnesium complexation by fluoroquinolones on their antibacterial properties', *Antimicrobial Agents and Chemotherapy*, 38: 2810-16.

Lefevre, Fabrice, Patrick Robe, Cyrille Jarrin, Aurélien Ginolhac, Caroline Zago, Daniel Auriol, Timothy M Vogel, Pascal Simonet, and Renaud Nalin. 2008. 'Drugs from hidden bugs: their discovery via untapped resources', *Research in microbiology*, 159: 153-61.

Létoffé, Sylvie, Philippe Delepelaire, and Cécile Wandersman. 2006. 'The housekeeping dipeptide permease is the Escherichia coli heme transporter and functions with two optional peptide binding proteins', *Proceedings of the National Academy of Sciences*, 103: 12891.

Liu, Yi-Yun, Yang Wang, Timothy R Walsh, Ling-Xian Yi, Rong Zhang, James Spencer, Yohei Doi, Guobao Tian, Baolei Dong, and Xianhui Huang. 2016. 'Emergence of plasmid-mediated colistin resistance mechanism MCR-1 in animals and human beings in China: a microbiological and molecular biological study', *The Lancet infectious diseases*, 16: 161-68.

Livermore, DM. 2004. 'The need for new antibiotics', *Clinical microbiology and infection*, 10: 1-9.

Lou, Hubing, Min Chen, Susan S Black, Simon R Bushell, Matteo Ceccarelli, Tivadar Mach, Konstantinos Beis, Alison S Low, Victoria A Bamford, and Ian R Booth. 2011. 'Altered antibiotic transport in OmpC mutants isolated from a series of clinical strains of multi-drug resistant E. coli', *PloS one*, 6: e25825.

Lugtenberg, Ben, and Loek Van Alphen. 1983. 'Molecular architecture and functioning of the outer membrane of Escherichia coli and other gram-negative bacteria', *Biochimica et Biophysica Acta (BBA) - Reviews on Biomembranes*, 737: 51-115.

Mahendran, Kozhinjampara R., Eric Hajjar, Tivadar Mach, Marcos Lovelle, Amit Kumar, Isabel Sousa, Enrico Spiga, Helge Weingart, Paula Gameiro, Mathias Winterhalter, and Matteo Ceccarelli. 2010. 'Molecular Basis of Enrofloxacin Translocation through OmpF, an Outer Membrane Channel of Escherichia coli - When Binding Does Not Imply Translocation', *The Journal of Physical Chemistry B*, 114: 5170-79.

Maio, Alessandro, Letizia Brandi, Stefano Donadio, and Claudio O Gualerzi. 2016. 'The oligopeptide permease Opp mediates illicit transport of the bacterial P-site decoding inhibitor GE81112', *Antibiotics*, 5: 17.

Malloci, Giuliano, Attilio Vittorio Vargiu, Giovanni Serra, Andrea Bosin, Paolo Ruggerone, and Matteo Ceccarelli. 2015. 'A database of force-field parameters, dynamics, and properties of antimicrobial compounds', *Molecules*, 20: 13997-4021.

Maloney, PC, SV Ambudkar, V Anatharam, LA Sonna, and ATUL Varadhachary. 1990. 'Anion-exchange mechanisms in bacteria', *Microbiological reviews*, 54: 1-17.

Marshall, AJH, and LJV Piddock. 1994. 'Interaction of divalent cations, quinolones and bacteria', *Journal of Antimicrobial Chemotherapy*, 34: 465-83.

Masi, Muriel, Mathias Winterhalter, and Jean-Marie Pagès. 2019. 'Outer membrane porins', *Bacterial cell walls and membranes*: 79-123.

McKinney, D., N. Bezdenejnih-Snyder, K. Farrington, J. Guo, R. McLaughlin, A. Ruvinsky, R. Singh, G. Basarab, S. Narayan, and E. T. Buurman. 2015a. 'Illicit Transport via Dipeptide Transporter Dpp is Irrelevant to the Efficacy of Negamycin in Mouse Thigh Models of Escherichia coli Infection', *ACS Infect. Dis.*, 1: 222-30.

McKinney, David C, Natascha Bezdenejnih-Snyder, Krista Farrington, Jian Guo, Robert E McLaughlin, Anatoly M Ruvinsky, Renu Singh, Gregory S Basarab, Sridhar Narayan, and Ed T Buurman. 2015b. 'Illicit transport via dipeptide transporter Dpp is irrelevant to the efficacy of negamycin in mouse thigh models of Escherichia coli infection', *ACS Infectious Diseases*, 1: 222-30.

McKinney, David C., Gregory S. Basarab, Alexis I. Cocozaki, Melinda A. Foulk, Matthew D. Miller, Anatoly M. Ruvinsky, Clay W. Scott, Kumar Thakur, Liang Zhao, Ed T. Buurman, and Sridhar Narayan. 2015c. 'Structural Insights Lead to a Negamycin Analogue with Improved Antimicrobial Activity against Gram-Negative Pathogens', *ACS Medicinal Chemistry Letters*, 6: 930-35.

Mingeot-Leclercq, Marie-Paule, Youri Glupczynski, and Paul M. Tulkens. 1999. 'Aminoglycosides: Activity and Resistance', *Antimicrobial Agents and Chemotherapy*, 43: 727-37.

Mizuno, S., K. Nitta, and H. Umezawa. 1970a. 'Mechanism of action of negamycin in Escherichia coli K12. I. Inhibition of initiation of protein synthesis', *J Antibiot (Tokyo)*, 23: 581-8.

Mizuno, S., K. Nitta, and H. Umezawa. 1970b. 'Mechanism of action of negamycin in Escherichia coli K12. II. Miscoding activity in polypeptide synthesis directed by snythetic polynucleotide', *J Antibiot (Tokyo)*, 23: 589-94.

Munckhof, Wendy J, M Lindsay Grayson, and John D Turnidge. 1996. 'A meta-analysis of studies on the safety and efficacy of aminoglycosides given either once daily or as divided doses', *Journal of Antimicrobial Chemotherapy*, 37: 645-63.

Nataro, James P, and James B Kaper. 1998. 'Diarrheagenic escherichia coli', *Clinical Microbiology Reviews*, 11: 142-201.

Newstead, Simon. 2017. 'Recent advances in understanding proton coupled peptide transport via the POT family', *Current opinion in structural biology*, 45: 17-24.

Nikaido, H, and DG Thanassi. 1993. 'Penetration of lipophilic agents with multiple protonation sites into bacterial cells: tetracyclines and fluoroquinolones as examples', *Antimicrobial Agents and Chemotherapy*, 37: 1393-99.

Nikaido, H. 1992. 'Porins and specific channels of bacterial outer membranes', *Mol Microbiol*, 6: 435-42.

Nikaido, Hiroshi. 2003. 'Molecular Basis of Bacterial Outer Membrane Permeability Revisited', *Microbiology and Molecular Biology Reviews*, 67: 593-656.

O'Neill, J. 2014. "Antimicrobial resistance: tackling a crisis for the health and wealth of nations. Review on antimicrobial resistance." In.

Olivier, N. B., R. B. Altman, J. Noeske, G. S. Basarab, E. Code, A. D. Ferguson, N. Gao, J. Huang, M. F. Juette, S. Livchak, M. D. Miller, D. B. Prince, J. H. Cate, E. T. Buurman, and S. C. Blanchard. 2014. 'Negamycin induces translational stalling and miscoding by binding to the small subunit head domain of the Escherichia coli ribosome', *Proc Natl Acad Sci U S A*, 111: 16274-9.

Pagès, Jean-Marie, Chloë E. James, and Mathias Winterhalter. 2008. 'The porin and the permeating antibiotic: a selective diffusion barrier in Gram-negative bacteria', *Nature Reviews Microbiology*, 6: 893-903.

Palva, E Tapio, and P Helena Mäkelä. 1980. 'Lipopolysaccharide heterogeneity in Salmonella typhimurium analyzed by sodium dodecyl sulfate/polyacrylamide gel electrophoresis', *European Journal of Biochemistry*, 107: 137-43.

Park James, T., Debabrata Raychaudhuri, Hongshan Li, Staffan Normark, and Dominique Mengin-Lecreulx. 1998. 'MppA, a Periplasmic Binding Protein Essential for Import of the Bacterial Cell Wall Peptidel-Alanyl-γ-d-Glutamyl-meso-Diaminopimelate', *Journal of Bacteriology*, 180: 1215-23.

Paulsen, I. T., and R. A. Skurray. 1994. 'The POT family of transport proteins', *Trends Biochem Sci*, 19: 404.

Phan, Katherine, and Thomas Ferenci. 2017. 'The fitness costs and trade-off shapes associated with the exclusion of nine antibiotics by OmpF porin channels', *The ISME journal*, 11: 1472-82.

Pitout, Johann. 2012. 'Extraintestinal pathogenic Escherichia coli: a combination of virulence with antibiotic resistance', *Frontiers in microbiology*, 3: 9.

Polikanov, Y. S., T. Szal, F. Jiang, P. Gupta, R. Matsuda, M. Shiozuka, T. A. Steitz, N. Vazquez-Laslop, and A. S. Mankin. 2014. 'Negamycin interferes with decoding and translocation by simultaneous interaction with rRNA and tRNA', *Mol Cell*, 56: 541-50.

Pratt, L. A., W. Hsing, K. E. Gibson, and T. J. Silhavy. 1996. 'From acids to osmZ: multiple factors influence synthesis of the OmpF and OmpC porins in Escherichia coli', *Mol Microbiol*, 20: 911-7.

Prehm, Peter, Günter Schmidt, Barbara Jann, and Klaus Jann. 1976. 'The Cell-Wall Lipopolysaccharide of Escherichia coli K-12: Structure and Acceptor Site for O-Antigen and Other Substituents', *European Journal of Biochemistry*, 70: 171-77.

Prilipov, Alexej, Prashant S Phale, Ralf Koebnik, Christine Widmer, and Jurg P Rosenbusch. 1998. 'Identification and Characterization of Two Quiescent Porin Genes, nmpC and ompN, in Escherichia coli BE', *Journal of Bacteriology*, 180: 3388-92.

Rafanan, N., P. Margolis, A. Kubo, R. Saxena, C. Rosenow, R. White, and J. Trias. 2003. "F-1682 Resistance to VRC4219 in Escherichia coli." In *ICAAC* Chicago.

Raju, B., Kathleen Mortell, Sampathkumar Anandan, Hardwin O'Dowd, Hongwu Gao, Marcela Gomez, Corinne Hackbarth, Charlotte Wu, Wen Wang, Zhengyu Yuan, Richard White, Joaquim Trias, and Dinesh V. Patel. 2003. 'N- and C-terminal modifications of negamycin', *Bioorganic & Medicinal Chemistry Letters*, 13: 2413-18.

Samsudin, F., M. L. Ortiz-Suarez, T. J. Piggot, P. J. Bond, and S. Khalid. 2016. 'OmpA: A Flexible Clamp for Bacterial Cell Wall Attachment', *Structure*, 24: 2227-35.

Scheffler, RJ, S Colmer, H Tynan, AL Demain, and VP Gullo. 2013. 'Antimicrobials, drug discovery, and genome mining', *Applied microbiology and biotechnology*, 97: 969-78.

Schofield, Christopher. 2015. "Antibiotics: Current innovations and future trends. Edited by Sergio Sánchez and Arnold L. Demain." In.: Wiley Online Library.

Serio, A, T Keepers, L Andrews, and K Krause. 2018a. 'Aminoglycoside Revival: Review of a Historically Important Class of Antimicrobials Undergoing Rejuvenation', *EcoSal Plus*.

Serio, Alisa W., Tiffany Keepers, Logan Andrews, Kevin M. Krause, and Karen Bush. 2018b. 'Aminoglycoside Revival: Review of a Historically Important Class of Antimicrobials Undergoing Rejuvenation', *EcoSal Plus*, 8.

Shibahara, Seiji, Shinichi Kondo, Kenji Maeda, Hamao Umezawa, and Masaji Ohno. 1972. 'Total syntheses of negamycin and the antipode', *Journal of the American Chemical Society*, 94: 4353-54.

Shiver, Anthony L, Hendrik Osadnik, George Kritikos, Bo Li, Nevan Krogan, Athanasios Typas, and Carol A Gross. 2016. 'A chemical-genomic screen of neglected antibiotics reveals illicit transport of kasugamycin and blasticidin S', *PLoS genetics*, 12: e1006124.

Shore, Parkhurst A, Bernard B Brodie, and C Adrain M Hogben. 1957. 'The gastric secretion of drugs: a pH partition hypothesis', *Journal of Pharmacology and Experimental Therapeutics*, 119: 361-69.

Silhavy, Thomas J, Daniel Kahne, and Suzanne Walker. 2010. 'The bacterial cell envelope', *Cold Spring Harbor perspectives in biology*, 2: a000414.

Silver, Lynn L. 2016. 'A Gestalt approach to Gram-negative entry', *Bioorganic & medicinal chemistry*, 24: 6379-89.

Soysa, H. S., and W. Suginta. 2016. 'Identification and Functional Characterization of a Novel OprD-like Chitin Uptake Channel in Non-chitinolytic Bacteria', *J Biol Chem*, 291: 13622-33.

Streicher, Wolfgang, HELLMUTHR EINSHAGEN, and FRIEDERIKTEU RNOWSKY. 1978. 'Total synthesis of rac. negamycin and of negamycin analogs', *The Journal of antibiotics*, 31: 725-28.

Sugawara, Etsuko, Seiji Kojima, and Hiroshi Nikaido. 2016. 'Klebsiella pneumoniae major porins OmpK35 and OmpK36 allow more efficient diffusion of β-lactams than their Escherichia coli homologs OmpF and OmpC', *Journal of Bacteriology*, 198: 3200-08.

Taber, Harry W, John P Mueller, Paul F Miller, and AS Arrow. 1987. 'Bacterial uptake of aminoglycoside antibiotics', *Microbiological reviews*, 51: 439-57.

Taguchi, Akihiro, Shigenobu Nishiguchi, Masataka Shiozuka, Takao Nomoto, Mayuko Ina, Shouta Nojima, Ryoichi Matsuda, Yoshiaki Nonomura, Yoshiaki Kiso, and Yuri Yamazaki. 2012. 'Negamycin analogue with readthrough-promoting activity as a potential drug candidate for duchenne muscular dystrophy', *ACS Medicinal Chemistry Letters*, 3: 118-22.

Theuretzbacher, Ursula, Karen Bush, Stephan Harbarth, Mical Paul, John H. Rex, Evelina Tacconelli, and Guy E. Thwaites. 2020. 'Critical analysis of antibacterial agents in clinical development', *Nature Reviews Microbiology*, 18: 286-98.

Torres, Alfredo G, Xin Zhou, and James B Kaper. 2005. 'Adherence of diarrheagenic Escherichia coli strains to epithelial cells', *Infection and immunity*, 73: 18-29.

Uehara, Y., M. Hori, and H. Umezawa. 1974. 'Negamycin inhibits termination of protein synthesis directed by phage f2 RNA in vitro', *Biochim Biophys Acta*, 374: 82-95.

Uehara, Y., S. Kondo, H. Umezawa, K. Suzukake, and M. Hori. 1972. 'Negamycin, a miscoding antibiotic with a unique structure', *J Antibiot (Tokyo)*, 25: 685-8.

Uehara, Yoshimasa, MAKOTO HORI, SHINICHI KONDO, MASA HAMADA, and HAMAO UMEZAWA. 1976a. 'Structure-activity relationships among negamycin analogs', *The Journal of antibiotics*, 29: 937-43.

Uehara, Yoshimasa, Makoto Hori, and Hamao Umezawa. 1976b. 'Specific inhibition of the termination process of protein synthesis by negamycin', *Biochimica et Biophysica Acta (BBA)-Nucleic Acids and Protein Synthesis*, 442: 251-62.

Umezawa, Hamao, Shinichi Kondo, Kenji Takeuchi Maeda, and Masa Hamada. 1972. 'Negamycin (Patent US3679742 A)'.

Vaara, Martti. 1992. 'Agents that increase the permeability of the outer membrane', *Microbiological reviews*, 56: 395-411.

Valisena, S, M Palumbo, C Parolin, G Palu, and GA Meloni. 1990. 'Relevance of ionic effects on norfloxacin uptake by Escherichia coli', *Biochemical pharmacology*, 40: 431-36.

Vergalli, Julia, Igor V. Bodrenko, Muriel Masi, Lucile Moynié, Silvia Acosta-Gutiérrez, James H. Naismith, Anne Davin-Regli, Matteo Ceccarelli, Bert van den Berg, Mathias Winterhalter, and Jean-Marie Pagès. 2020. 'Porins and small-molecule translocation across the outer membrane of Gram-negative bacteria', *Nature Reviews Microbiology*, 18: 164-76.

Walker, H Kenneth, W Dallas Hall, and J Willis Hurst. 1990. 'Clinical methods: the history, physical, and laboratory examinations'.

Wang, Yi Fong, Toshio Izawa, Susumu Kobayashi, and Masaji Ohno. 1982. 'Stereocontrolled synthesis of (+)-negamycin from an acyclic homoallylamine by 1,3-asymmetric induction', *Journal of the American Chemical Society*, 104: 6465-66.

Weitz, Dietmar, Daniel Harder, Fabio Casagrande, Dimitrios Fotiadis, Petr Obrdlik, Bela Kelety, and Hannelore Daniel. 2007. 'Functional and Structural Characterization of a Prokaryotic Peptide Transporter with Features Similar to Mammalian PEPT1*', *Journal of Biological Chemistry*, 282: 2832-39.

Zarfl, Christiane, Michael Matthies, and Jörg Klasmeier. 2008. 'A mechanistical model for the uptake of sulfonamides by bacteria', *Chemosphere*, 70: 753-60.

Zgurskaya, H. I., G. Krishnamoorthy, A. Ntreh, and S. Lu. 2011. 'Mechanism and Function of the Outer Membrane Channel TolC in Multidrug Resistance and Physiology of Enterobacteria', *Front Microbiol*, 2: 189.

Ziemert, Nadine, Mohammad Alanjary, and Tilmann Weber. 2016. 'The evolution of genome mining in microbes–a review', *Natural product reports*, 33: 988-1005.

Ziervogel, Brigitte K, and Benoît Roux. 2013. 'The binding of antibiotics in OmpF porin', *Structure*, 21: 76-87.

4. Appendix

4.1. Publication 1

AMERICAN SOCIETY FOR MICROBIOLOGY | Antimicrobial Agents and Chemotherapy®

EXPERIMENTAL THERAPEUTICS

The Antibiotic Negamycin Crosses the Bacterial Cytoplasmic Membrane by Multiple Routes

Daniel Hörömpöli,[a,b] Catherine Ciglia,[c] Karl-Heinz Glüsenkamp,[d] Lars Ole Haustedt,[e] Hildegard Falkenstein-Paul,[f] Gerd Bendas,[f] Anne Berscheid,[a,b,c] Heike Brötz-Oesterhelt[a,b,c,g]

[a]Interfaculty Institute of Microbiology and Infection Medicine, Department of Microbial Bioactive Compounds, University of Tuebingen, Tuebingen, Germany
[b]German Center of Infection Research (DZIF), Partner Site Tuebingen, Tuebingen, Germany
[c]Institute of Pharmaceutical Biology, University of Duesseldorf, Duesseldorf, Germany
[d]Squarix GmbH, Marl, Germany
[e]AnalytiCon Discovery GmbH, Potsdam, Germany
[f]Pharmaceutical Institute, Department of Pharmaceutical & Cell Biological Chemistry, University of Bonn, Bonn, Germany
[g]Cluster of Excellence 2124: Controlling Microbes to Fight Infection, Tuebingen, Germany

Daniel Hörömpöli and Catherine Ciglia contributed equally to this work. Author order was determined by mutual verbal consent.
Heike Brötz-Oesterhelt and Anne Berscheid share senior authorship.

ABSTRACT Negamycin is a natural pseudodipeptide antibiotic with promising activity against Gram-negative and Gram-positive bacteria, including *Enterobacteriaceae*, *Pseudomonas aeruginosa*, and *Staphylococcus aureus*, and good efficacy in infection models. It binds to ribosomes with a novel binding mode, stimulating miscoding and inhibiting ribosome translocation. We were particularly interested in studying how the small, positively charged natural product reaches its cytoplasmic target in *Escherichia coli*. Negamycin crosses the cytoplasmic membrane by multiple routes depending on environmental conditions. In a peptide-free medium, negamycin uses endogenous peptide transporters for active translocation, preferentially the dipeptide permease Dpp. However, in the absence of functional Dpp or in the presence of outcompeting nutrient peptides, negamycin can still enter the cytoplasm. We observed a contribution of the DppA homologs SapA and OppA, as well as of the proton-dependent oligopeptide transporter DtpD. Calcium strongly improves the activity of negamycin against both Gram-negative and Gram-positive bacteria, especially at concentrations around 2.5 mM, reflecting human blood levels. Calcium forms a complex with negamycin and facilitates its interaction with negatively charged phospholipids in bacterial membranes. Moreover, decreased activity at acidic pH and under anaerobic conditions points to a role of the membrane potential in negamycin uptake. Accordingly, improved activity at alkaline pH could be linked to increased uptake of [^{3}H]negamycin. The diversity of options for membrane translocation is reflected by low resistance rates. The example of negamycin demonstrates that membrane passage of antibiotics can be multifaceted and that for cytoplasmic anti-Gram-negative drugs, understanding of permeation and target interaction are equally important.

KEYWORDS Dpp, DtpD, *Escherichia coli*, antibiotic, calcium, membrane, natural product, negamycin, peptide transporters, uptake

Bacterial infections and the increase in antibiotic resistance are among the main health issues of today (1). Discovering and developing new antibiotics against Gram-negative bacteria is particularly challenging. This difficulty is not based on a lack of suitable targets but caused by the strict penetration prerequisites of the Gram-negative cell envelope. In recent years it has become increasingly clear that the failure in identifying new antibiotics with whole-cell activity against Gram-negatives is related to

Citation Hörömpöli D, Ciglia C, Glüsenkamp K-H, Haustedt LO, Falkenstein-Paul H, Bendas G, Berscheid A, Brötz-Oesterhelt H. 2021. The antibiotic negamycin crosses the bacterial cytoplasmic membrane by multiple routes. Antimicrob Agents Chemother 65:e00986-20. https://doi.org/10.1128/AAC.00986-20.

Address correspondence to Anne Berscheid, anne.berscheid@uni-tuebingen.de, or Heike Brötz-Oesterhelt, heike.broetz-oesterhelt@uni-tuebingen.de.

Received 15 May 2020
Returned for modification 13 June 2020
Accepted 12 January 2021
Accepted manuscript posted online 19 January 2021
Published 18 March 2021

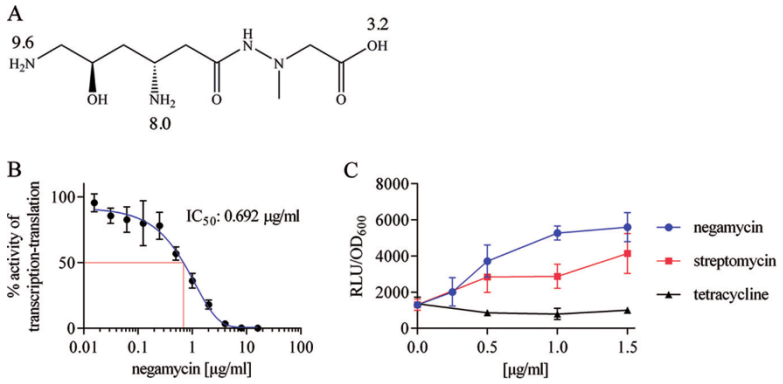

FIG 1 Negamycin structure and mode of action. (A) Structure of negamycin with pKa values (8). (B) Effect of negamycin on coupled *in vitro* transcription-translation using an *E. coli* S30 extract and plasmid-based *Photinus pyralis* luciferase as reporter. Error bars showing standard deviation (SD) of five independent experiments. (C) Effect of negamycin, streptomycin (positive control), or tetracycline (negative control) in a whole-cell miscoding assay demonstrating the readthrough of a stop codon within the luciferase gene. Error bars indicating SD of two independent experiments. RLU, relative luminescence units.

the incomplete understanding of the mechanisms underlying permeation of bacterial membranes (2). An antibiotic needs special characteristics to translocate through the Gram-negative cell envelope, as the outer membrane and cytoplasmic membrane have orthogonal penetration requirements (3–6).

To learn from nature, we studied the uptake of the natural product antibiotic negamycin across the cytoplasmic membrane of *Escherichia coli*. Negamycin is a pseudopeptide with hydroxy-β-lysine as the central amino acid (Fig. 1A). It is a small, hydrophilic compound with a molecular weight of 248.3 g/mol and a positive net charge at neutral pH, discovered already in 1970 in culture filtrates of strains closely related to *Streptomyces purpeofuscus* (7). In animal models, negamycin cured systemic infections with *E. coli*, *Klebsiella pneumoniae*, *Salmonella enterica* serotype Typhi, *Pseudomonas aeruginosa*, and *Staphylococcus aureus* and demonstrated low acute toxicity (7, 8). Interestingly, it is more potent against Gram-negative than against Gram-positive bacteria. Due to its high polarity, it showed low oral bioavailability (6% in rats), low plasma protein binding (10%), and low hepatic clearance, and it was excreted almost entirely via the kidneys in an unmodified form (8).

Negamycin inhibits translation. Early studies reported an inhibition of ribosome translocation, stabilization of polysomes, disturbance of the termination process, and miscoding (9–13). In crystal structures, the compound was found bound to several sites of the small and large ribosomal subunits (14–16). Resistance mutations in a strain carrying only one rRNA allele mapped the primary site of antibiotic action to helix 34 of the 16S rRNA, a position that overlaps with the tetracycline binding site. However, in contrast to tetracycline, negamycin also establishes contacts with the aminoacyl-tRNA and increases the residency time of noncognate tRNAs (14). In accordance with this miscoding activity, negamycin is bactericidal (10). Negamycin triggers miscoding at the eukaryotic ribosome as well and cured Duchenne muscular dystrophy in mice, which carried a nonsense mutation in the dystrophin gene (17, 18).

In an attempt to improve the efficacy of negamycin, several derivatization campaigns were conducted by companies and academic groups, which almost exclusively resulted in a loss of activity (19–21). Only a single recently reported derivative, N6-(3-aminopropyl) negamycin, showed 4-fold improved antibacterial activity (22). Notably, among the derivatives generated over the years, several were active in ribosomal extracts but failed in whole-cell MIC assays, suggesting uptake issues (23). This

TABLE 1 Antimicrobial activity of negamycin and the reference antibiotics ciprofloxacin, tetracycline, and gentamicin in different growth media

	MIC (μg/ml)															
	Negamycin				Ciprofloxacin				Tetracycline				Gentamicin			
	MHB	LB	M9	PP	MHB	LB	M9	PP	MHB	LB	M9	PP	MHB	LB	M9	PP
E. coli BW25113	64	64	4	8	0.016	0.016	0.008	0.008	1	2	1−2	2	0.5	4	0.25	0.06
E. coli ATCC 25922	>64	>64	2[a]	16	0.008	0.008	0.008[a]	0.004	1	1	0.5[a]	1	1	8	0.5[a]	0.125
P. aeruginosa PAO1	>64	>64	64	32	0.06	0.06	0.06	0.06	16	16	16	8	0.25	2	2	0.25
S. aureus ATCC 29213	>64	>64	ng	>64	0.25	0.25	ng	0.125	0.5	0.5	ng	1	0.25	4	ng	0.25
B. subtilis 168 *trpC2*	>64	>64	ng	>64	0.06	0.06	ng	0.06	4	8	ng	8	0.06	0.25	ng	0.03

[a]M9 minimal medium supplemented with thiamine (1 mg/liter) for *E. coli* ATCC 25922. ng, no growth.

observation and the fact that negamycin activity had displayed strong media dependency (7) stimulated our interest in studying the uptake process of the agent across the cell envelope. For optimization of negamycin, a thorough understanding of the uptake mechanism seems equally important as detailed insight into the target interaction.

When we started our investigations, we were aware of a poster presented by Versicor Inc. at the Interscience Conference on Antimicrobial Agents and Chemotherapy (ICAAC) already in 2002 (24) demonstrating that *E. coli* mutants with a defective dipeptide permease Dpp or deficient in components of the electron transport chain show low-level resistance to negamycin. While our work was in progress, a publication by AstraZeneca confirmed these findings and showed that Dpp plays a minor role in negamycin uptake during treatment of an *E. coli* mouse thigh infection (25).

In our studies, with a mechanistic focus in mind, we compared growth media of entirely different composition, on the one hand, M9 minimal medium rich in salt and glucose but free of peptides, versus on the other hand, 0.5% polypeptone (PP) in water containing a nondefined mixture of peptides but no externally added sugars, salts, or buffer. Here, we report on the passage of negamycin across the cytoplasmic membrane of *E. coli* and demonstrate that more than one route can be used, with their respective contributions determined by the environment. The complex uptake process of negamycin shows that more than one entry mechanism should be considered when studying natural product passage into bacterial cells. Evolution can bestow natural products with a variety of interactions facilitating entry, which makes them valuable models for studying antibiotic uptake.

RESULTS

Media conditions significantly affect negamycin activity. Negamycin used in this study was of synthetic origin and inhibited translation in an *E. coli* cell-free system with a half-maximal inhibitory concentration (IC_{50}) of 2.8 μM (0.69 μg/ml, Fig. 1B), in accordance with previously published values (20, 22, 26). The compound also induced stop codon readthrough in an *E. coli* whole-cell miscoding assay (Fig. 1C). The antibacterial activity of negamycin against *E. coli* varied substantially in growth media of different compositions. In rich media, such as Mueller-Hinton broth (MHB) and lysogeny broth (LB), MICs were greater than or equal to 64 μg/ml (Table 1). Markedly stronger antibacterial activity was detected in M9 or PP, corresponding to MICs of 4 μg/ml and 8 μg/ml for *E. coli* strain BW25113, respectively. *Pseudomonas aeruginosa* strain PAO1 was also inhibited, although at higher concentrations (32 to 64 μg/ml), while the Gram-positive bacteria tested (i.e., *Staphylococcus aureus* strain ATCC 29213, *Bacillus subtilis* strain 168 *trpC2*) were not inhibited up to 64 μg/ml under these conditions (Table 1), demonstrating that negamycin is stronger against Gram-negatives. As comparators, we used the antibiotics ciprofloxacin, tetracycline, and gentamicin for MIC determinations in the same set of media. We did not detect any large differences in activity between the four media for these reference antibiotics, with the exception of the decreased activity of gentamicin in media containing a larger amount of salt (i.e., LB and M9), which was

TABLE 2 Negamycin MICs of various *E. coli* BW25113 transporter mutants in M9 or 0.5% polypeptone (PP)

	Negamycin MIC (μg/ml)[d]	
***E. coli* strain**	**M9**	**PP**
BW25113 wild type	4	8
Single transporter deletions[a]		
ATP-dependent oligopeptide transporters		
Δ*dppA*, Δ*dppB*, Δ*dppC*, Δ*dppD*, Δ*dppF*	**16**	8
Δ*oppA*, Δ*oppB*, Δ*oppC*, Δ*oppD*, Δ*oppF*	4	8
Δ*sapA*	**8**	**16**
Δ*sapB*, Δ*sapC*, Δ*sapF*	4	8
Δ*sapD*	2	8
Δ*ddpA*, Δ*gsiB*, Δ*mppA*, Δ*nikA*, Δ*ygiS*	4	8
Proton-dependent oligopeptide transporters		
Δ*dtpD* (Δ*ybgH*)[b]	**4–8**	**16**
Δ*dtpA* (Δ*tppB*), Δ*dtpB* (Δ*yhiP*), Δ*dtpC* (Δ*yjdL*)	4	8
Amino acid transporters		
Δ*lysP*, Δ*hisP*	4	nd
Δ*cadB*, Δ*hisQ*, Δ*hisJ*, Δ*argT*	4	nd
Δ*hisM*	2–4	nd
Multiple transporter deletions[c]		
Δ*dppA*Δ*oppA*	**16**	**8–16**
Δ*dppA*Δ*sapA*	**16**	8
Δ*dppA*Δ*dtpD*	**16**	8
Δ*dppA*Δ*oppA*Δ*sapA*	**16–32**	8
Δ*dppA*Δ*oppA*Δ*sapA*Δ*dtpD*	**32**	8

[a]Strains originating from the Keio collection (76).
[b]In cases where genes of previously unknown function were later renamed according to their function, the names in parentheses refer to names employed in the Keio collection.
[c]Strains generated in the course of this work. nd, not determined.
[d]Numbers in bold indicate increases in the MIC compared to the parent strain *E. coli* BW25113.

observed across different species (Table 1). The activity of negamycin in media of orthogonal composition was a first indication of the use of multiple entry routes into the bacterial cytoplasm. To dissect these uptake mechanisms, we chose M9 as well as PP for all further experiments.

Negamycin crosses the cytoplasmic membrane via different endogenous *E. coli* peptide transporters. Due to its pseudopeptide-like structure and previous reports on the dipeptide permease Dpp as an entry route into *E. coli* (24, 25), we investigated whether negamycin is capable of using one or more additional peptide transporters. Aiming at a comprehensive picture, we tested a large variety of *E. coli* peptide as well as amino acid transporter mutants (Table 2). Dpp mutants elicited the strongest effect. Single knockouts of each of the genes encoding the different subunits of the ABC transporter Dpp displayed a 4-fold increase in the negamycin MIC in M9 medium (Table 2), which is in accordance with previous reports (24, 25). Expressing *dppA* from a plasmid complemented the *dppA* deletion (Fig. S1). To prove that the decreased negamycin susceptibility observed in MIC determinations is directly linked to a reduced antibiotic uptake, we performed experiments with radiolabeled negamycin. Here, we detected a significantly decreased [^{3}H]negamycin uptake into the Δ*dppA* mutant compared to its isogenic parent strain, with a 15% smaller amount after 15 min and a 20% smaller amount after 60 min of treatment (Fig. 2D). Since negamycin is still capable of inhibiting the growth of *dpp* knockout mutants, additional uptake routes into the cytoplasm must be available. The knockout of *sapA*, a paralog of *dppA*, led to a 2-fold increase in the negamycin MIC, while the deletion of the other genes encoding the Sap ABC transporter (i.e., permease domains *sapB* and *sapC*, ATPase domains *sapD* and *sapF*) did not reduce negamycin susceptibility (Table 2). No clear effects were detected

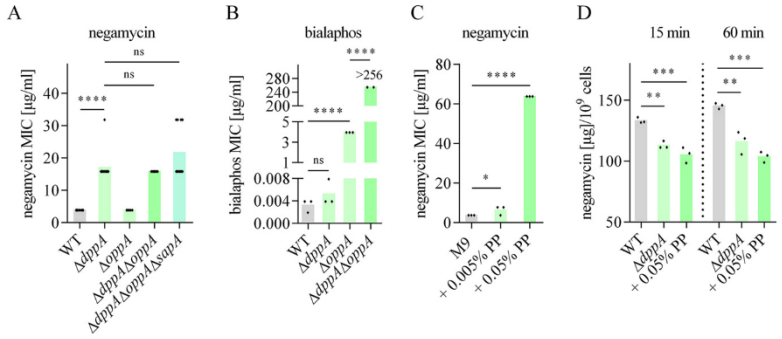

FIG 2 Negamycin uses multiple peptide transporters and competes with peptides for uptake, whereas entry options for bialaphos are limited to Opp and Dpp transporters. (A and B) Impact of single or multiple ABC peptide transporter deletions in the *E. coli* BW25113 background on negamycin (A) or bialaphos (B) susceptibility in M9 medium. (C) Impact of peptide addition on negamycin MICs in M9. Negamycin susceptibility of *E. coli* BW25113 in M9 decreases with supplemented polypeptone (PP) in a concentration-dependent manner. (D) Uptake of [^{3}H]negamycin into *E. coli* BW25113 wild type or its isogenic Δ*dppA* mutant in M9. [^{3}H]negamycin (specific activity: 0.052 Ci/mmol) was added to the cells at a concentration of 32 μg/ml. One sample of the wild type was supplemented with 0.05% PP concurrently with negamycin addition. Samples were taken after 15 (left) or 60 (right) min of incubation at 37°C with shaking. Negamycin uptake is significantly reduced in M9 with the addition of 0.05% PP or the deletion of the peptide transporter gene *dppA*. Each diamond represents an independent MIC determination (A to C) or [^{3}H]negamycin uptake measurement (D). Statistical significance was determined using unpaired Student's *t* test with Holm-Bonferroni correction. ns, $P > 0.05$; *, $P \leq 0.05$; **, $P \leq 0.01$; ***, $P \leq 0.001$; ****, $P \leq 0.0001$.

in single-knockout mutants of the genes encoding the different subunits of the main *E. coli* oligopeptide transporter Opp (Table 2). SapA and OppA share 36% and 25% amino acid identity with DppA, respectively. The deletion of the genes encoding DppA paralogs like DdpA, GsiB, MppA, NikA, and YgiS did not reduce negamycin susceptibility (Table 2). To detect putative cross talk or compensatory effects due to redundancy of paralogous periplasmic binding proteins of different ABC transporters, double and triple knockout mutants were generated. The double knockouts Δ*dppA*Δ*oppA* and Δ*dppA*Δ*sapA* did not display a higher negamycin resistance than Δ*dppA* alone. The Δ*dppA*Δ*oppA*Δ*sapA* triple deletion mutant showed a marginal, nonsignificant increase in the negamycin MIC compared to the Δ*dppA* single-knockout (Table 2 and Fig. 2A). The herbicide bialaphos (L-alanyl-L-alanyl-phosphinothricin) is a tripeptide that has been described as a substrate of mainly the Opp transporter, but it can also use Dpp as a second route for cell entry (27). When comparing bialaphos to negamycin, it became apparent that bialaphos has limited options for cell entry apart from the two main *E. coli* peptide ABC transporters Opp and Dpp. Single deletion of *oppA* already increased the MIC dramatically (1,000-fold), and, although a single deletion of *dppA* did not show a significant effect, the MIC rose more than 64,000-fold in a Δ*oppA*Δ*dppA* double mutant (Fig. 2B). In contrast, only a 4-fold increase in negamycin MIC was observed in both the Δ*dppA* single as well as the Δ*dppA*Δ*oppA* double knockout mutants (Fig. 2A), confirming that negamycin has considerably more options of entering the cytoplasm than bialaphos. In addition to the ABC transporters mentioned above, the deletion of one of the four *E. coli* proton-dependent oligopeptide transporters (POTs), namely, DtpD (YbgH), led to a 2-fold decrease in negamycin susceptibility (Table 2). When we additionally deleted *dtpD* in the Δ*dppA*Δ*oppA*Δ*sapA* mutant background, the resulting quadruple mutant showed a 2-fold negamycin MIC increase compared to that of Δ*dppA* and consequently an 8-fold MIC increase compared to that of the wild type in M9 medium (Table 2). Notably, none of the multiple knockout mutants showed complete negamycin resistance, indicating the presence of further negamycin uptake routes and revealing the highly promiscuous nature of this natural product antibiotic.

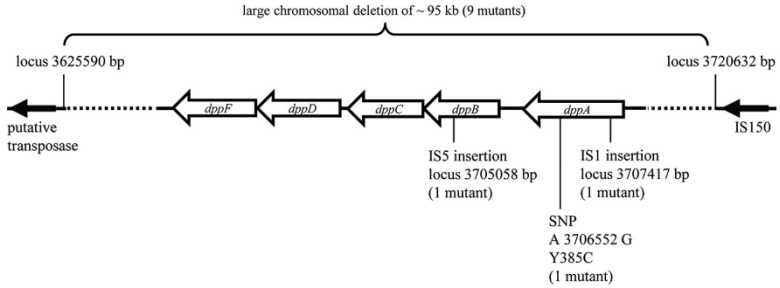

FIG 3 Schematic overview of the *dpp* operon in *E. coli* and spontaneous mutations induced by negamycin exposure. Indicated deletions, IS element insertions, and a point mutation were detected in spontaneous negamycin resistant mutants isolated from M9 agar plates containing 2× MIC negamycin. Locus numbers based on *E. coli* K-12 MG1655 (GenBank access no. U00096.3). SNP, single nucleotide polymorphism.

Generally, the effects of peptide transporter deletions on negamycin susceptibility were significantly more pronounced in M9 than in PP medium (Table 2). Here, the orthogonal composition of our two growth media is relevant. In M9 lacking any peptide ingredient, negamycin has free access to peptide transporters. In contrast, in PP, where peptides represent the sole carbon and nitrogen source, nutrient peptides are highly abundant, and negamycin is under strong competition with them at the transporters. The unaltered negamycin susceptibility of the *dpp* mutants in PP compared to that of the wild type demonstrates that here, negamycin entry is not dominated by passage through Dpp. Accordingly, when peptides (i.e., polypeptone) were added to M9 medium, the negamycin MIC increased in a concentration-dependent manner (Fig. 2C) and to a level surpassing that of the *dppA* knockout, which suggests a role of peptide transporters unrelated to Dpp. Likewise, we observed that significantly less [^{3}H]negamycin accumulated in *E. coli* after addition of 0.05% polypeptone to M9 medium in radioactive uptake experiments (Fig. 2D). The activity of negamycin against multiple peptide transporter knockouts as well as in peptide-containing media indicates that negamycin must enter the cell via at least one additional uptake route.

Negamycin resistance frequencies reflect the availability of multiple uptake routes. Strong preference for a single uptake route versus the option of multiple entry routes is also reflected by the risk of acquiring high-level resistance. Thus, we next compared the mutation frequencies of negamycin in our two selected growth media and first concentrated on the situation close to the MIC. In M9, the resistance frequency at 2× MIC for negamycin in *E. coli* BW25113 was 6×10^{-7}. As *dpp* deletion had shown the strongest impact on negamycin activity in M9 (Table 2), we next analyzed the *dpp* operon of 12 *E. coli* BW25113 mutants isolated from M9 agar at 2× MIC. No PCR product was obtained for 9 of the 12 selected mutants when using primers flanking the *dpp* operon (dppA-F-2 and dppA-F rev2). Whole-genome sequencing of one of these mutants revealed a large chromosomal deletion of approximately 95 kB, containing the entire *dpp* operon plus large flanking regions (Fig. 3). This large deletion was subsequently also identified in the 8 other mutants that initially had not yielded a PCR product for the *dpp* operon. Interestingly, two mobile genetic elements (putative transposase *yhhI* upstream and IS150 downstream) flank the deleted region, which might have facilitated excision. The deletion had occurred at the start of a REP260 element and fused this part to the inverted repeat left (IRL) of IS150. A similar deletion (approximately 100 bp smaller) had been detected in negamycin resistant mutants in an *E. coli* W3110 background (25). When we conducted a BLAST search, we found that the same deletion had also occurred in an *E. coli* K-12 MG1655 strain during exposure to subinhibitory concentrations of the antibacterial phenolic monoterpene carvacrol (sequence ID CP026026.1 [28]). According to the Profiling of *E. coli* Chromosome database (PEC; shigen.nig.ac.jp/ecoli/pec), no essential genes are found in this 95-kB region of the chromosome (29). With regard to our three remaining mutants isolated from M9 agar

TABLE 3 Negamycin activity against *E. coli* BW25113 in the presence of different concentrations of salts added to 0.5% polypeptone medium

	Negamycin MIC (μg/ml)[a]				
Salt concentration	$CaCl_2$	$MgCl_2$	NaCl	KCl	NH_4Cl
0 mM	8	8	8	8	8
0.5 mM	**4**	8	8	8	8
2.5 mM	**2**	8	8	8	8
5 mM	**2–4**	8	8	**8–16**	**8–16**
10 mM	**4**	8	8	**8–16**	**16**
50 mM	8	8	**32–64**	**32**	**64**

[a]Numbers in bold indicate changes in the MIC compared to activity without salts.

under negamycin selection pressure, one mutant harbored a point mutation in *dppA* that led to a Y385C amino acid exchange, while two of the mutants had insertions of mobile genetic elements in the *dpp* operon. Among these, one mutant carried an insertion of the insertion element IS1 in *dppA*, and in the second mutant, IS5 had integrated into *dppB* (Fig. 3). In total, all 12 out of 12 *E. coli* BW25113 mutants isolated on M9 agar at 2× MIC showed alterations in the *dpp* operon, confirming Dpp as the preferential uptake route for negamycin in peptide-free media. The negamycin MIC of all mutants was increased by 4-fold in M9 (MIC, 16 μg/ml), in agreement with the genetic knockout of *dppA* and other genes of the *dpp* operon. In PP medium, the MIC of all mutants was unchanged.

While the resistance frequency for negamycin was high at 2× MIC in M9, it already strongly decreased at 4× MIC ($<7 \times 10^{-9}$). This number reflects our limit of detection and might be even lower. For comparison, for the tripeptide bialaphos, mutation frequencies in M9 were high even at 100× MIC (frequencies of 4×10^{-6} at 4× MIC, 4×10^{-7} at 10× MIC, and 7×10^{-7} at 100× MIC). This result confirms that loss of function of a single transporter already leads to a large decrease in bialaphos activity, i.e., a 1,000× MIC increase in a Δ*oppA* strain (Fig. 2B). On PP agar, negamycin resistance frequencies were similar to those on M9, with a high frequency of 5×10^{-7} at 2× MIC and less than 7×10^{-9} at 4× MIC. However, in contrast to M9, no alterations in the *dpp* operon were detected in 8 mutants isolated from PP agar, confirming that Dpp does not play a prominent role in negamycin transport in peptide-containing media. Importantly, the low mutation rate at 4× MIC in both very different media indicates that no high-level negamycin resistance can be obtained by mutation of a single transporter, as other uptake routes remain available.

Negamycin activity is significantly improved by calcium. Next, we investigated the impact of different salt conditions on negamycin activity in PP medium, which does not contain salts *a priori*. The addition of 0.5 mM $CaCl_2$ to the medium improved the negamycin MIC in *E. coli* BW25113 by 2-fold, while a concentration of 2.5 mM was the most effective and led to a 4-fold decrease of the negamycin MIC (Table 3). Calcium also had a beneficial effect on negamycin activity against other species, e.g., *P. aeruginosa* and *S. aureus* (Fig. 4A). MICs dropped by 2- to 4-fold when cation-adjusted MH broth (MHBII) compared to standard MHB was used. MHBII contains calcium at a concentration of 20 to 25 μg/ml, corresponding to approximately 0.5 mM. Magnesium, on the other hand, had no significant effect. Other divalent cations (i.e., Mn^{2+}, Zn^{2+}, and Ni^{2+}) could not be tested in the same concentration range as calcium and magnesium due to toxicity for the *E. coli* cells. Low concentrations of NaCl did not improve negamycin activity, and the addition of 50 mM NaCl was even inhibitory, as were other monovalent cations like K^+ and NH_4^+ (Table 3). On a side note, when reducing the total salt concentration of M9 to one-fourth of its regular content (and leaving the glucose amount unchanged), the negamycin MIC dropped from 4 μg/ml to 1 μg/ml for *E. coli*. M9 contains monovalent cations (Na^+, K^+, NH_4^+), the sum of which amounts to approximately 145 mM. Thus, the monovalent cations present in M9 may negatively affect activity in this medium, especially the Dpp unrelated routes. For

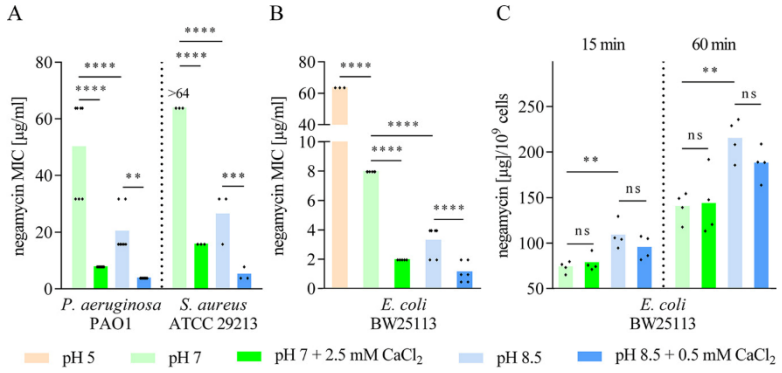

FIG 4 Basic pH and calcium are additive in improving negamycin activity. Negamycin MICs of *P. aeruginosa* PAO1 and *S. aureus* ATCC 29213 (A) and of *E. coli* BW25113 (B) in 0.5% PP medium adjusted to different pH values and in combination with $CaCl_2$. (C) Influence of pH and $CaCl_2$ on [^{3}H]negamycin uptake in *E. coli* BW25113 in PP. A total amount of 32 μg/ml of [^{3}H]negamycin (specific activity: 0.052 Ci/mmol) was added to the cells. $CaCl_2$ and [^{3}H]negamycin were added to the cultures in parallel. Samples were taken after 15 (left) or 60 (right) min of incubation with [^{3}H]negamycin at 37°C with shaking. Alkaline pH increased [^{3}H]negamycin uptake, while we could not detect such an effect after the addition of $CaCl_2$. Each diamond represents an independent MIC determination (A and B) or [^{3}H]negamycin uptake measurement (C). Statistical significance was determined using unpaired Student's *t* test with Holm-Bonferroni correction. ns, $P > 0.05$; **, $P \leq 0.01$; ***, $P \leq 0.001$; ****, $P \leq 0.0001$.

comparison, the MICs of ciprofloxacin, tetracycline, and gentamicin were also determined in PP in the presence of different salts. Here, $CaCl_2$ and $MgCl_2$ did not improve activity of these compounds and rather increased their MICs at 50 mM respective salts (Table S1). As observed for negamycin, NaCl decreased the activity of the aminoglycoside gentamicin, while ciprofloxacin and tetracycline MICs remained unaffected (Table S1).

In a published ribosome cocrystal structure, negamycin established contacts to the rRNA as well as the tRNA by coordinating a magnesium ion (14). Not to overlook a potential benefit of calcium at the target level, we performed the *E. coli in vitro* translation assay and added 1 to 8 μM calcium to the assay mixture. The IC_{50} of negamycin remained unchanged. *E. coli* keeps its cytoplasmic free Ca^{2+} concentration low and tightly regulated (steady-state levels of 200 to 300 nM), even when exposed to external Ca^{2+} concentrations in the millimolar range (30), while cytoplasmic magnesium concentrations are much higher (1 to 5 mM free Mg^{2+} [31]). Therefore, it was unlikely that the beneficial effect that external calcium exerted on negamycin activity was related to target binding.

Calcium enhances binding of negamycin to phospholipid membranes. To investigate the interaction of negamycin with a phospholipid membrane, we performed surface acoustic wave (SAW) biosensor measurements. A model membrane bilayer consisting of a lower lipid layer immobilized at the sensor surface and an upper phospholipid layer was exposed to negamycin in a flow chamber, and binding events were recorded. As phospholipids, we compared, on the one hand, 1-palmitoyl-2-oleoyl-phosphatidylcholine (POPC) and, on the other hand, a mixture of 90% POPC (net neutral)/10% 1,2-dioleoyl-phosphatidylglycerol (DOPG, net negative) to provide the negative charge common to bacterial cytoplasmic membranes. Each experiment started with the injection of negamycin at nanomolar concentrations, and further negamycin was added to the system by serial injections up to the micromolar range. SAW experiments showed that negamycin already has a certain binding tendency to an uncharged POPC model membrane indicated by the small phase change starting at the fourth injection (Fig. 5A). Binding of negamycin was substantially increased by adding 10% of DOPG to the POPC membrane, as shown by the earlier onset and the higher degree of binding (Fig. 5B). Furthermore, the presence of 2.5 mM $CaCl_2$ strongly improved the interaction of negamycin with the membrane, clearly indicated by the

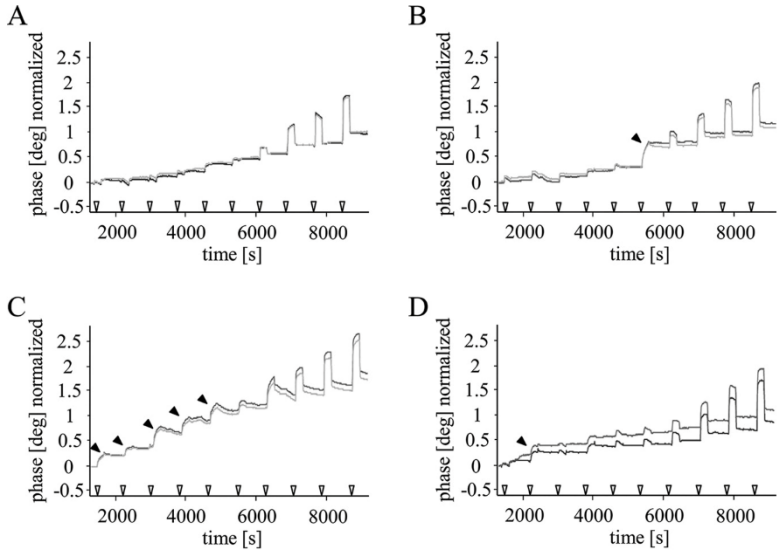

FIG 5 Calcium supports the binding of negamycin to phospholipid membranes. Surface acoustic wave (SAW) sensorgrams comparing the interaction of negamycin with a POPC membrane (A), a POPC/DOPG membrane (B), or a POPC/DOPG membrane in the presence of 2.5 mM $CaCl_2$ (C) or with a POPC/DOPG membrane in the presence of 2.5 mM $MgCl_2$ (D). The empty triangles at the *x* axis indicate the injection steps of negamycin. The total concentration of negamycin ranges from 7.5×10^{-8} M (outermost left triangle) to 1×10^{-5} M (outermost right triangle). Filled arrows at the curves indicate binding events. The large phase shifts at high negamycin concentrations which drop back after injection are a consequence of increased viscosity and do not indicate real binding events.

rapid onset of binding already at the lowest negamycin concentration and the larger phase change (Fig. 5C). The cation species appears to be crucial for the membrane-binding affinity, as the addition of 2.5 mM $MgCl_2$ had only a marginal effect on the binding process (Fig. 5D). The observation that $CaCl_2$ improved negamycin activity not only against Gram-negative but also against Gram-positive bacteria (Fig. 4A) suggests that calcium facilitates negamycin uptake at the cytoplasmic membrane. However, an additional beneficial effect at the outer membrane cannot be excluded at this point.

To rule out secondary antibiotic effects emerging from the interaction of negamycin with phospholipid membranes stimulated by calcium, we determined the membrane potential and permeability in *E. coli* upon negamycin treatment. The membrane potential was unaffected up to 4× MIC of negamycin over a time course of 180 min in the absence and presence of calcium (Fig. S2). We also could not observe an increased membrane permeability within 60 min of negamycin treatment as monitored by staining with the DNA-binding, cell-impermeant fluorescent dye SYTOX Green (Fig. S3). In contrast, colistin increased membrane permeability within 10 to 20 min of treatment. After 90 to 120 min of negamycin treatment, the SYTOX Green assay signaled a beginning impairment of membrane integrity, an effect probably related to the miscoding activity of this compound (Fig. S3). Importantly, the addition of calcium did not promote the disruption of membrane integrity; on the contrary, it rather seemed to have a stabilizing effect on the cells.

Negamycin forms a complex with calcium. We further tested the capacity of negamycin to interact with calcium directly. Mainly the carboxyl, but also the carbonyl and amine groups within the flexible negamycin molecule, indicate that it may be able to chelate cations. In thin-layer chromatography (TLC), the addition of Ca^{2+} in a molar ratio of 1:1 reduced negamycin migration (spot-shift), implying complex formation (Fig. 6A). At 5-fold molar surplus of Ca^{2+} over negamycin, the antibiotic was almost completely retained at the origin. The addition of Mg^{2+} influenced negamycin migration to

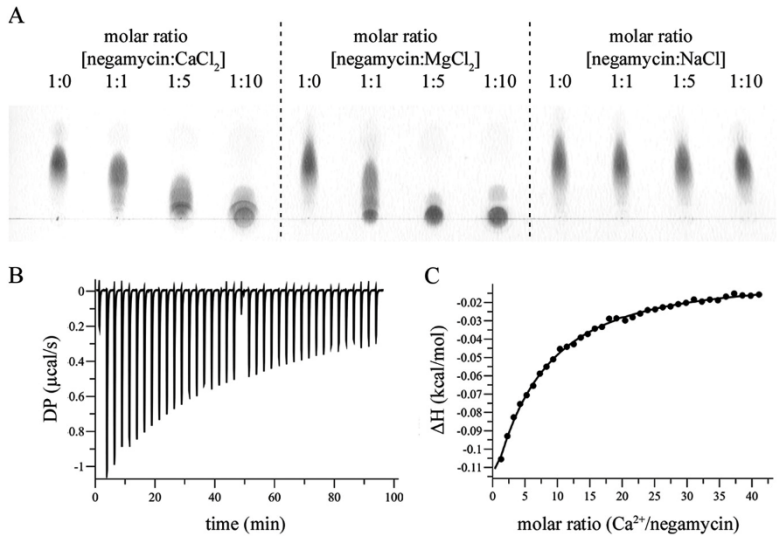

FIG 6 Negamycin forms a complex with calcium. (A) Thin-layer chromatography (TLC) analysis of negamycin with $CaCl_2$, $MgCl_2$, or NaCl at different molar ratios. (B and C) Isothermal titration calorimetry (ITC) of negamycin titrated with $CaCl_2$. (B) Heat differences monitored by differential power (DP) measurements upon two consecutive series of 19 injections of $CaCl_2$ after baseline correction and subtraction of control experiments of $CaCl_2$ titration into buffer, buffer titration into buffer, and negamycin titration into buffer. (C) Binding enthalpies (ΔH) against the Ca^{2+}/negamycin molar ratio. ITC data were fitted to the one-site binding model. Due to the low binding affinity, fitting required to preset stoichiometry manually, which we set to 1:1. With these settings, a K_d of 7.98 mM was obtained.

a similar extent, while NaCl at a molar surplus of 1:10 showed no effect (Fig. 6A). The ability of negamycin to form a complex with calcium could be confirmed by isothermal titration calorimetry (ITC). Here, binding of Ca^{2+} to negamycin was clearly detected (Fig. 6B), but the affinity of the interaction was low. Due to the low affinity of binding (low c-value titration), ITC did not allow us to determine the stoichiometry of the complex. When manually setting the stoichiometry to 1:1, a binding affinity (K_d) of 7.98 mM was obtained in Tris buffer pH 7.0 (Fig. 6C). Although the stoichiometry of negamycin and calcium could not be determined with certainty, the K_d is not largely dependent on this parameter. When imposing a stoichiometry of 0.5:1 or 2:1, K_d values of 8.62 mM or 7.36 mM were obtained, respectively. Furthermore, an effect of the pH on the binding affinity of negamycin and calcium was observed. At pH 8.5, a slightly improved K_d of 4.1 mM was determined when fixing the stoichiometry to 1:1. The charges of the different groups (carboxyl, amine) within the negamycin molecule vary with pH as their protonation changes (Fig. S4), which may explain why binding affinities change with pH. Of note, we were not able to detect binding of Mg^{2+} to negamycin by ITC. Most likely, the large heat of dilution resulting from the titration of $MgCl_2$ into buffer containing negamycin masked the small quantity of heat released by the binding.

pH has a substantial impact on negamycin activity. Negamycin activity was also strongly influenced by the pH of the medium. The pH of 0.5% PP is around 7, and the medium is not buffered. By adjusting the pH of PP to pH 5, an 8-fold reduction in negamycin activity was observed for *E. coli*, while on the other hand, the MIC improved 2- to 4-fold at pH 8.5 (Fig. 4B). The beneficial effect of calcium on negamycin activity was additive to the alkaline pH, leading to a MIC of 1 μg/ml in *E. coli* under these optimized conditions (pH 8.5 and 0.5 mM $CaCl_2$). Of note, since a $CaCl_2$ concentration of 2.5 mM, which had shown the strongest effect on negamycin MIC at pH 7, could not be tested at pH 8.5 due to precipitation, the concentration of $CaCl_2$ was lowered to 0.5 mM.

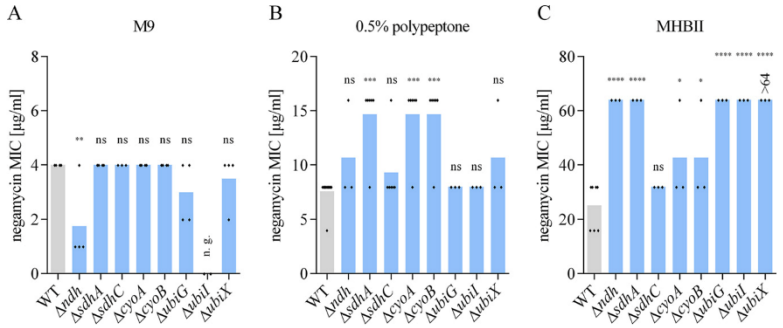

FIG 7 Mutations affecting the respiratory chain reduce negamycin sensitivity in peptide-rich media. Negamycin MICs of different energy mutants of *E. coli* BW25113 in M9 (A), 0.5% PP (B), or MHBII (C). Each diamond represents an independent MIC determination. Statistical significance was determined using unpaired Student's *t* test with Holm-Bonferroni correction, comparing the various deletion strains to the wild type (WT). ns, $P > 0.05$; *, $P \leq 0.05$; **, $P \leq 0.01$; ***, $P \leq 0.001$; ****, $P \leq 0.0001$; n. g., no growth under this condition.

Improvement of negamycin activity at pH 8.5/0.5 mM $CaCl_2$ was not limited to *E. coli* but also affected *P. aeruginosa* and *S. aureus*, where the negamycin MIC dropped to 4 μg/ml (Fig. 4A).

The pH of the surrounding medium affects the membrane potential of bacteria (32). The electrical potential $\Delta\psi$ across the cytoplasmic membrane of *E. coli* is more negative at alkaline pH than at acidic pH. The passage of positively charged negamycin molecules across the cytoplasmic membrane may be facilitated by the trans-negative (i.e., surplus negative charge inside) electrical potential gradient. With increasing $\Delta\psi$ at alkaline pH, more negamycin molecules may pass the cytoplasmic membrane in a given time period than at neutral pH, leading to an increased accumulation of negamycin inside the cell. Such behavior has also been reported for the positively charged aminoglycosides (33). However, for the negamycin structure, an additional pH-dependent aspect should be considered. The beta-amino group of negamycin has a pK_a of 8.0, meaning that at pH 8.5, the number of negamycin molecules that are zwitterionic is considerably higher than that at pH 7.0 (Fig. S4). At pH 7.0, approximately 99% of negamycin molecules contain a net charge of +1, while only 1% of negamycin is present in its zwitterionic form. At pH 8.5, the two different zwitterionic species of negamycin together make up about 30% of the total amount of molecules, and this net neutral state may contribute to passage across the cytoplasmic membrane, putatively by passive diffusion.

In this regard, we also determined the negamycin MIC of isogenic Δ*acrA*, Δ*acrB*, and Δ*acrAB* mutants under our media conditions. We did not detect a decrease in negamycin MIC in these mutants devoid of the main *E. coli* efflux pump, neither at pH 7 nor at pH 8.5 plus 0.5 mM $CaCl_2$ (Table S2). In contrast, novobiocin MICs were affected heavily by the deletion of this efflux pump, also under alkaline conditions in the presence of $CaCl_2$.

By performing experiments with tritium-labeled negamycin, we measured a significantly increased uptake of negamycin at pH 8.5 than at pH 7 (Fig. 4C). At alkaline pH, the amount of accumulated [^{3}H]negamycin was increased by 46% and 53% after 15 min and 60 min, respectively. The uptake data directly explain the improved negamycin activity observed at pH 8.5. However, with our experimental setup, we could not detect an increased [^{3}H]negamycin accumulation over 60 min when adding $CaCl_2$ to the cultures, neither at pH 7 nor at pH 8.5 (Fig. 4C). Similar to the situation at neutral pH, we did not observe a dissipation of the membrane potential or disruption of membrane integrity upon negamycin treatment at pH 8.5, neither in the absence nor presence of $CaCl_2$ (Fig. S2 and S3).

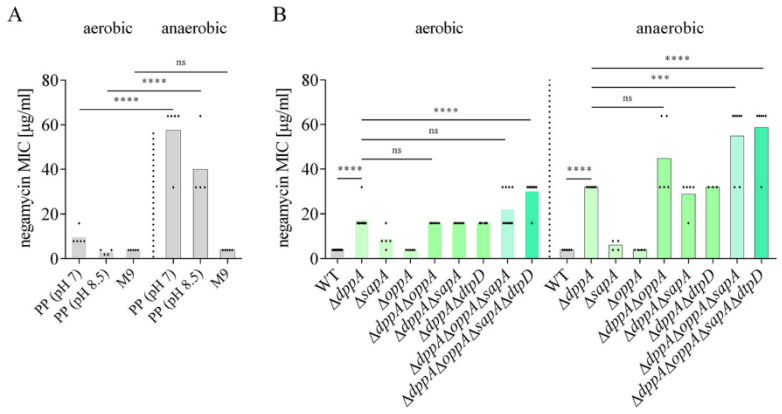

FIG 8 Anaerobic growth conditions reduce negamycin susceptibility in peptide-containing media and in peptide transporter mutants. (A) Negamycin MICs of *E. coli* BW25113 wild type in different media under aerobic and anaerobic conditions. Statistical significance was determined using Student's *t* test comparing anaerobic to aerobic growth conditions. (B) Effect of peptide transporter deletions in the *E. coli* BW25113 background on negamycin susceptibility under aerobic *versus* anaerobic growth conditions in M9 medium. Each diamond represents an independent MIC determination. Statistical significance was determined using unpaired Student's *t* test with Holm-Bonferroni correction. ns, $P > 0.05$; *, $P \leq 0.05$; ***, $P \leq 0.001$; ****, $P \leq 0.0001$.

Negamycin susceptibility is reduced in *E. coli* energy mutants. The membrane potential $\Delta\psi$ is dependent on the activity of the respiratory chain complexes (32). Thus, we analyzed several strains of the *E. coli* Keio collection lacking proteins involved in different stages of the respiratory chain for their susceptibility to negamycin under our media conditions (Fig. 7). In M9 medium, all of the energy mutants tested remained fully susceptible (Fig. 7A). The glucose level in M9 seems sufficient to ensure activity of the ATP-fueled Dpp also in energy mutants, and this transporter is the preferred uptake route in M9. In polypeptone, we observed a 2-fold negamycin MIC increase in some of the mutants (Fig. 7B). Overall, the effects of energy mutations on negamycin susceptibility detected by us were lower than previously reported. Versicor had noted a 2- to 4-fold MIC increase for a negamycin derivative in Δ*hemB*, Δ*ubiD*, and Δ*cydAB* mutants, and more recently, McKinney and coworkers reported an over-4-fold MIC increase of an *ubiX* mutant (24, 25). As we did not observe such substantial effects of the energy mutants under our assay conditions (using M9 or PP), we repeated the MIC determination in MHBII, the medium that had been used before (25). For MHBII, we confirm more pronounced changes with up to 4-fold MIC increase for several of the mutants (Δ*ndh*, Δ*sdhA*, Δ*ubiG*, Δ*ubiI*, Δ*ubiX*) (Fig. 7C). One obvious difference between the three media is their peptide content (0 g/liter in M9, 5 g/liter in 0.5% polypeptone, 17.5 g/liter casein hydrolysate, plus 2 g/liter beef infusion in MHBII). Peptide transporter-based entry routes are less available for negamycin the higher the competition with nutrient peptides, with a stronger impact on Dpp than on DtpD, which puts more emphasis on alternative uptake mechanisms that are more dependent on a certain membrane potential threshold. In addition, it cannot be excluded that metabolic changes in *E. coli* while growing in the different media play a role.

Negamycin activity is reduced under anaerobic conditions in peptide-rich media. We also investigated negamycin activity under anaerobic conditions. *E. coli* BW25113, when growing in PP in the absence of oxygen, was substantially less susceptible to negamycin, and the MIC increased from 8 μg/ml to 32 to 64 μg/ml (Fig. 8A). The same trend was observed for kanamycin and gentamicin in PP (Fig. S5), and it is well described that aminoglycoside activity is strongly impaired under anaerobic conditions (34). Vice versa, when performing the MIC determination in ambient air while shaking the microplate, negamycin MIC was improved by 2-fold in PP most likely as a consequence of the increased oxygen availability (Fig. S6). On the other hand, and in

contrast to that of aminoglycosides, the negamycin MIC remained unchanged in M9 minimal medium when incubating the cells under anaerobic conditions (Fig. 8A and Fig. S5). Similar to the results obtained for the energy mutants in M9, the unaltered negamycin MIC probably reflects the availability of Dpp and other peptide transporters for uptake in M9 also under anaerobic conditions. When comparing the set of our single and multiple peptide transporter mutants in M9 under aerobic versus anaerobic conditions, we observed that peptide transporters have a higher impact on negamycin uptake in the latter case (Fig. 8B). Here, the contribution of the two further periplasmic binding proteins OppA and SapA, as well as of the POT DtpD, to negamycin uptake became clearly visible (Fig. 8B). Anaerobiosis also raised the MIC of the quadruple peptide transporter knockout, indicating that at least one further negamycin entry route exists and that this route is oxygen-dependent. An explanation would be the membrane potential-dependent uptake in an aminoglycoside-like manner.

DISCUSSION

The initial publication on the discovery of negamycin had already described a media dependency of its antibacterial activity (7), providing a first indication that bacterial uptake of this compound may be influenced by the environment. On a molecular level, we now found that the dipeptide-like antibiotic has multiple options to cross the cytoplasmic membrane. In the absence of peptides, negamycin preferably enters the cell by active transport via the dipeptide permease Dpp. Versicor had previously reported a 4-fold MIC increase of a fluorinated negamycin analog in a *dpp* mutant in M9, and the same observation was also made later for unmodified negamycin by AstraZeneca (24, 25). We confirm this primary uptake route by uptake assays using tritium-labeled negamycin (Fig. 2D) as well as by the exclusive selection of Dpp mutants at 2× MIC in M9. Dpp is one of the main *E. coli* peptide transporters and preferably transports dipeptides composed of L-amino acids along with some tripeptides (27, 35, 36). Its periplasmic binding protein DppA was further shown to be involved in the uptake of 5-aminolevulinic acid as well as heme, proving that Dpp can transport substrates that do not contain a peptide bond (37, 38). It has been postulated that modification of the peptide bond atoms in peptide analogs may lower their binding affinities to DppA (39), a potential explanation for our observation that negamycin uptake is outcompeted at DppA by nutrient peptides.

It is clear that Dpp is not the only uptake route used by negamycin in M9, as only a maximal 4-fold decrease in susceptibility was detected in *dpp* mutants. We found a second periplasmic binding protein, SapA, to be involved in negamycin uptake. Among the seven paralogs of DppA in *E. coli*, SapA shares the highest homology with DppA and was the only paralog that showed decreased negamycin activity in a single-knockout mutant. The Sap ABC transporter was described to be involved in antimicrobial peptide (AMP) resistance in *Salmonella enterica* serotype Typhimurium and *Haemophilus influenzae* (40, 41). In *E. coli*, the function of the SapA protein in *E. coli* is unclear. Even though Sap from *E. coli* shares high amino acid identity with its homolog in *Salmonella*, a function in AMP resistance could not be detected in *E. coli*. Furthermore, SapBCDF, but not SapA, was shown to contribute to the export of the polyamine putrescine (42). As negamycin activity was decreased, when *sapA* was deleted but not the other subunits of the Sap transporter, SapA may interact with the permease domains of another transporter to support negamycin uptake. Cross talk between periplasmic binding proteins and noncognate permease domains has been described before, e.g., MppA interacts with Dpp for heme transport (38) as well as with Opp for recycling of the cell wall murein (43). Due to the redundancy of transport systems, contributions of single transporters may only become visible when preferred routes are not available. While no decrease in negamycin susceptibility was visible in Δ*oppA* to Δ*oppE* single and Δ*dppA*Δ*oppA* double knockouts in M9, a Δ*dppA*Δ*oppA*Δ*sapA* triple mutant showed a small increase in negamycin MIC compared to that of Δ*dppA*. The contribution of OppA was more clearly visible under

anaerobic conditions (Fig. 8B), demonstrating that OppA also plays a minor role in negamycin uptake.

Besides the contribution of different ABC transporters, a decreased susceptibility was also identified in a *dtpD* (*ybgH*) mutant, representing one of the four *E. coli* proton-dependent oligopeptide transporters (POTs). POTs are found in all kingdoms of life except archaea, and they transport mainly di- and tripeptides but are remarkably promiscuous concerning their substrate specificity (44). Interestingly, POTs play an important role in the absorption of several peptide-like drugs, i.e., the human POT homologs PEPT1 and PEPT2 present in the mammalian brush border and renal membranes transport orally administered beta-lactam antibiotics (45, 46). POTs are less well described for the uptake of antimicrobials by bacteria, but it has been shown in competition assays that *E. coli* DtpA (YdgR) has a similar substrate specificity as PEPT1, interacting with the aminocephalosporins cefadroxil, cephalexin, and cephradine (47). It has also been suggested recently that uptake of the peptidyl nucleoside blasticidin S could be mediated by POT transporters, especially DtpA and DtpD (48). The presence of a peptide bond is not a prerequisite for substrate recognition by human PEPT1 (49), and the minimal features were described to be a positively charged amino terminus and a negatively charged carboxy terminus separated by at least 4 methyl groups (50), further substantiating that negamycin may serve as a substrate for the *E. coli* homolog DtpD. Due to redundancy in substrate specificities among the four POTs of *E. coli*, it cannot be excluded that other POTs besides DtpD contribute to negamycin uptake.

Illicit transport was described for several antimicrobial compounds with peptide-like structural elements, among them pacidamycin and kasugamycin (51, 52). GE81112, a natural tetrapeptide antibiotic, which inhibits protein biosynthesis, was shown to enter the cell via Opp (53). The compound shows very good MICs in minimal media. However, its activity is completely abolished in rich media containing peptides (*E. coli* MG1655, MIC $>512\,\mu$g/ml in MHB), and *E. coli* strains lacking Opp were described to be resistant to GE81112 (53). Similarly, bialaphos, which we used as a comparator for negamycin in this study, is mainly transported via Opp and, to a lesser extent, via Dpp. The deletion of *oppA* increased the bialaphos MIC by 1,000-fold, and a Δ*dppA*Δ*oppA* double mutant showed complete resistance in M9. Comparison with GE81112 and bialaphos emphasizes the particular strength of negamycin in promiscuous uptake. Negamycin is active in minimal salt as well as peptide-containing media, and a quadruple knockout mutant (Δ*dppA*Δ*oppA*Δ*sapA*Δ*dtpD*) still has only an 8-fold reduced susceptibility. This diversity of options is directly reflected by the mutation rates. While negamycin mutation frequencies were high at 2× MIC, they immediately dropped to low rates at 4× MIC. Notably, the risk of spontaneous target mutations is also extremely low. All contacts of negamycin to its target site are established to rRNA (14, 15), and most bacterial species harbor multiple rRNA gene alleles (e.g., 7 rRNA gene copies in *E. coli*).

Negamycin even showed good activity in PP medium, i.e., when competing with natural peptide substrates at the peptide transporters. Impressively, negamycin can still use peptide transporters under these highly competitive conditions, as indicated by our observation that increasing the amount of polypeptone from 0.5% to 2% raised the negamycin MIC by 4-fold. This observation leads to the question of whether peptide transporters can play a role in negamycin uptake *in vivo*. McKinney and colleagues reported that Dpp was not relevant for negamycin efficacy in a mouse thigh infection (25); nonetheless, the total dose that they required for an equivalent reduction of the bacterial load was increased by 2-fold for the Δ*dppA* mutant compared to that for the wild type. In our MIC assays, we could still detect effects of peptide transporter deletions when peptides were present (e.g., Δ*dtpD* and Δ*sapA*). Thus, although it is clear that negamycin is much less dependent on a single specific peptide transporter than agents that solely rely on illicit transport by a particular route, it still might use such transporters for uptake *in vivo*. However, negamycin also certainly has alternatives to

illicit uptake, and the specific environment at the site of infection determines its preferred uptake route.

In peptide-containing media, we detected a substantial impact of calcium on negamycin activity (Table 3), which was particularly beneficial in the concentration range of human blood calcium levels (54, 55). Substituting calcium with magnesium was not effective, but importantly the latter ion also did not negatively affect negamycin activity. In contrast to those of negamycin, aminoglycoside MICs rise in the presence of divalent cations (33). A decreased uptake of streptomycin following the addition of $MgCl_2$ and $CaCl_2$ was reported for *E. coli* and *P. aeruginosa* but also for the Gram-positive *S. aureus* (56). Divalent cations also hampered the intracellular accumulation of quinolones in *E. coli* and *S. aureus* (57–60), and magnesium ions inhibited the uptake of tetracycline in *E. coli* (61). When testing ciprofloxacin, tetracycline, and gentamicin against *E. coli* under our experimental conditions, we observed the same trends (Table S1). On the other hand, enhancing effects of calcium on bioactivity have been shown for daptomycin (62). In this case, the substitution of calcium with other divalent cations like Mg^{2+}, Ni^{2+}, or Mn^{2+} increased daptomycin MICs by at least 32-fold (63). Mechanism-wise, it was suggested that Ca^{2+} is more effective than Mg^{2+} in bridging daptomycin and negatively charged phospholipid headgroups (64), based on the finding that Ca^{2+} seems to fit better between phospholipid headgroups and to interact more strongly with phosphate and carbonyl groups than Mg^{2+} (65). These observations match our data obtained by SAW experiments, where we observed a substantially better binding of negamycin to phospholipid membranes in the presence of Ca^{2+} than of Mg^{2+} (Fig. 5), although a direct interaction of negamycin in solution with both calcium and magnesium was detected by TLC (Fig. 6A). We obtained K_d values of 7.98 mM or 4.1 mM by low c-value titration via ITC for calcium binding to negamycin at pH 7 or pH 8.5, respectively. Previously determined binding affinities of other antibiotics to divalent cations were in a similar range, i.e., the quinolone ofloxacin bound Mg^{2+} with a K_d of 1 mM as determined by nuclear magnetic resonance (NMR) and tetracycline showed a pH-dependent binding affinity to Ca^{2+} with K_d values of 1.1 mM and 0.59 mM at pH 6.5 and pH 7.5, respectively (60, 66). We were not able to determine the stoichiometry of the complex of negamycin and calcium in this study. Tetracycline was shown to bind calcium and magnesium with distinct stoichiometries, namely, one Ca^{2+} or 0.5 Mg^{2+} per tetracycline molecule (66). Since the negamycin-ribosome cocrystal structure revealed a magnesium-mediated contact of negamycin via its carboxylic moiety to the 16S rRNA (14), complex formation of negamycin with Ca^{2+} or Mg^{2+} in solution may involve the carboxyl and also putatively the carbonyl and amine groups. Complexation of quinolones with Mg^{2+} frequently involves both the ketone and deprotonated carboxylate groups (60), while they more rarely bind the metal ion via the two carboxyl oxygen atoms (67). Taken together, calcium significantly improves negamycin activity in Gram-negative and Gram-positive bacteria, in contrast to other antibiotics with intracellular targets (aminoglycosides, fluoroquinolones, tetracyclines), which were shown to be antagonized by divalent cations (Table S1). Enhanced binding to phospholipid membranes mediated by calcium may suggest a role of this cation in negamycin uptake. However, an effect of $CaCl_2$ on cell entry did not emerge in our uptake studies with [^{3}H]negamycin over a time course of 60 min (Fig. 4C). As calcium binding modifies the physicochemical behavior of negamycin, we cannot exclude an altered distribution behavior of this compound during sample processing in our radioactive assay setup. In addition, we cannot rule out that the beneficial effect of calcium comes into play at a later point in time, which would be difficult to dissect as mixed effects are expected due to the miscoding mode of action of negamycin. On the other hand, our data clearly show that the interaction of negamycin with bacterial membranes stimulated by calcium does not enhance membrane permeability or disturb the membrane potential as a secondary, translation-independent mode of action (Fig. S2 and S3). Thus, the specific molecular mechanisms on how calcium improves negamycin activity needs further investigation.

Our results of decreased negamycin activity at acidic pH, in energy mutants, and under anaerobic conditions indicate that at least one uptake route is affected by the membrane potential. The negative impact of acidic pH on negamycin uptake had previously been noted for *E. coli* and attributed to the correspondingly lower membrane potential, a characteristic also known for aminoglycosides (25, 68). However, our studies with different growth media emphasize that the impact of the membrane potential on negamycin activity is dependent on the environment. The lack of effect of respiratory chain mutations (Fig. 7A) and oxygen depletion (Fig. 8A) in M9 medium underline that negamycin has entry options that do not rely on a certain membrane potential threshold, such as Dpp. A significant increase in negamycin MICs in different energy mutants was only observed in peptide-containing media (Fig. 7B and C), and the effects were more pronounced in MHBII than in PP. The higher peptide content of MHBII compared to that of PP seems to render peptide transporter routes less accessible and the membrane potential more crucial. Although it has been known for decades that aminoglycoside uptake is membrane potential-dependent, the specific molecular mechanism of translocation of these highly cationic, hydrophilic compounds across the cytoplasmic membrane is not fully elucidated. It remains unclear if yet unidentified transporters or carriers are involved. For negamycin, we have identified a proton-dependent oligopeptide transporter to contribute to uptake. The main driving force of this secondary active transporter family is the membrane potential, as these transporters couple substrate translocation to proton flux down an electrochemical proton gradient (47).

With regard to increased uptake at alkaline pH (Fig. 4C), a second factor deserves consideration besides the membrane potential, namely, microspeciation of negamycin. The number of net neutral negamycin molecules increases with pH, reaching about 30% at pH 8.5 (Fig. S4). Fluoroquinolones and tetracyclines have been proposed to diffuse passively through the lipid bilayer in their uncharged forms (69). At physiological pH, zwitterionic ciprofloxacin is predominant over the neutral (uncharged) form. It was proposed that zwitterionic molecules form stacks, which reduces their polarity and favors insertion into the bilayer. Neutralization is achieved by the intramolecular transfer of protons favored by partial solvation loss, and ciprofloxacin crosses the membrane by passive diffusion as a neutral monomer (70). Whether a zwitterionic fraction of negamycin might also be able to cross the cytoplasmic membrane without an active transport process remains speculative considering that negamycin is notably more hydrophilic than ciprofloxacin.

In summary, our data show that negamycin is exceptional in its capacity to employ multiple, independent uptake routes across the bacterial cytoplasmic membrane, which highlights the very promiscuous nature of this small natural product, thereby decreasing the risk of high-level resistance by transporter mutations.

MATERIALS AND METHODS

Bacterial strains and growth conditions. Bacterial strains used in this study are listed in Table S3. Strains were grown in either 0.5% polypeptone (PP) in water (BD BBL polypeptone, catalog no. 211910), M9 minimal medium (47.74 mM $Na_2HPO_4 \times 2H_2O$, 22.04 mM KH_2PO_4, 8.56 mM NaCl, 18.7 mM NH_4Cl, 2 mM $MgSO_4$, 100 μM $CaCl_2$, 0.4% glucose), lysogeny broth (LB), Mueller-Hinton broth (MHB; BD Difco), or cation-adjusted Mueller-Hinton broth (MHBII; BD Difco) at 37°C with shaking (190 rpm) or on respective agar. Antibiotics, salts, or PP were added as indicated. Negamycin (>95% purity) was synthesized by Squarix GmbH, Marl, Germany, based on published procedures (20, 71). Tritium-labeling of negamycin was performed by Hartmann Analytic GmbH, Braunschweig, Germany. Bialaphos was obtained from Alfa Aesar, tetracycline from Sigma-Aldrich Chemie GmbH, streptomycin sulfate from AppliChem, and gentamicin sulfate and kanamycin sulfate from Carl Roth. The pH was adjusted to the indicated values using 1 M HCl or 1 M NaOH. For growth curve experiments, strains were cultivated in microplates with shaking at intervals, and the optical density at 600 nm (OD_{600}) was recorded in a microplate reader (Infinite M200 PRO, Tecan).

Determination of antibacterial activity. The MIC was determined by the broth microdilution method according to the Clinical and Laboratory Standards Institute (CLSI) guidelines using the direct colony suspension method with an inoculum of 5×10^5 CFU/ml (72). In addition to the standard MHB, antimicrobial susceptibility testing was performed using different media and conditions. MICs were read after incubation at 37°C for 20 h or after 24 h when M9 minimal medium was used. Anaerobic growth

conditions were generated using the GasPAK Anaerobe Pouch System (BD), and the incubation time in M9 medium was extended to 28 h under anaerobic conditions. All values were determined in at least three independent experiments, i.e., different bacterial cultures grown on different days were subjected to the same experimental procedures. Each independent measurement is represented as a diamond in the dot plot overlaid on the bar chart, and the arithmetic mean of the single measurements is displayed as a colored, vertical bar (Fig. 2, 4, 7, and 8). Statistical analysis was performed using R (the R Foundation for Statistical Computing, version 3.6.1). Unpaired Student's *t* test was used for statistical evaluation. For multiple comparisons, the Holm-Bonferroni correction was applied. A P value ≤ 0.05 was considered statistically significant.

***In vitro* transcription-translation assay.** An *in vitro* coupled transcription/translation assay was performed to assess the potency of negamycin on bacterial translation in a cell-free system. The assay is based on S30 extracts prepared from logarithmically growing *E. coli* strain MRE600 (73), an RNase I deficient strain, according to a procedure described by Zubay (74). The system further uses the pBESTluc plasmid (Promega Corporation, Madison, USA) encoding the firefly (*Photinus pyralis*) luciferase gene under the control of a *tac* promoter as a reporter, allowing the detection of translation inhibition by measuring luminescence. Apart from S30 extract and pBESTluc plasmid, the reaction mixture contained the following supplements: 2.5 mM ATP, 0.5 mM GTP, 0.5 mM UTP, 0.5 mM CTP, 20 amino acids (0.04 mM each), an ATP regenerating system (creatine phosphokinase/phosphocreatine), 3.2% (wt/vol) polyethylene glycol 600, 8 mM putrescine, and 2 mM dithiothreitol (DTT) in an appropriate buffer system (40 mM triethylamine [pH 7.5], 140 mM potassium acetate, 8 mM magnesium acetate, 20 mM ammonium acetate, 1.4 mM spermidine). *In vitro* coupled transcription-translation reactions in the presence of a concentration series of negamycin were performed for 2 h at 25°C. After addition of the substrate luciferin, chemiluminescence was recorded in a multiplate reader (Infinite M200, Tecan). The IC_{50} was determined as the concentration of negamycin, which led to 50% reduction of luminescence compared to an untreated control.

Miscoding assay. A K31STOP mutation was introduced into the pBESTluc plasmid by site-directed mutagenesis using the primers Luc-mut_for and Luc-mut_rev (Table S4). The resulting plasmid pBESTluc-mut harbors a stop codon in the firefly luciferase gene that leads to a truncated, nonfunctional enzyme. For the miscoding assay, *E. coli* BW25113 carrying the pBESTluc-mut plasmid was grown to the exponential phase. The culture was diluted to an OD_{600} of 0.1 and treated with either negamycin, streptomycin (positive control), or tetracycline (negative control) at sub-MICs. After incubation in M9 for 5 h at 37°C, OD_{600} and chemiluminescence were measured following the addition of 2 mM luciferin in a microplate reader (Infinite M200 PRO, Tecan). Miscoding (readthrough) activity was detected as the ratio of relative light units (RLU) per OD_{600}.

Knockout of genes in *E. coli*. Knockout strains were constructed as previously described by Datsenko and Wanner (75). Briefly, the pKD3 (chloramphenicol) or pKD13 (kanamycin) resistance cassette was amplified using primers with homologous ends to the gene of interest. The used primers are listed in Table S4. *E. coli* cells were first transformed with the helper plasmid pKD46 and then with the extended resistance cassette. Recombination took place during incubation for 24 h at 37°C. The resistance cassette was subsequently deleted using the FLP-expression plasmid pCP20. Gene deletions were confirmed by PCR followed by Sanger sequencing. For the deletion of multiple genes in the same strain, the single-gene knockout strains of the Keio collection (76) were used as the templates.

Complementation of *dppA* in *E. coli*. The *dppA* gene was amplified by PCR from genomic DNA of *E. coli* BW25113 using the primers dppA-XbaI_for and dppA-XhoI_rev (Table S4) and cloned into pASK-IBA5 (IBA GmbH, Göttingen). The resulting plasmid pASK-*dppA* was used for *E. coli* strain JW3513 (Δ*dppA*) transformation. Expression of *dppA* in M9 medium was induced by adding 10 ng/ml anhydrotetracycline (Cayman Chemical, USA).

[^{3}H]negamycin uptake. Radiolabeled [^{3}H]negamycin with a specific activity of 16.6 Ci/mmol was acquired and used in all uptake assays after dilution with unlabeled compound to a final specific activity of 0.052 Ci/mmol. *E. coli* BW25113 or its isogenic Δ*dppA* mutant were grown in M9 or PP under shaking conditions at 37°C until early exponential growth phase. Cells were harvested by centrifugation at room temperature and resuspended in fresh medium to an OD_{600} of 5. The cell suspension was shaken at 37°C for 10 min before 32 μg/ml of [^{3}H]negamycin (specific activity: 0.052 Ci/mmol) were added and cells were further incubated at 37°C under shaking conditions. 500 μl samples were taken after 15 min and 60 min and quickly cooled on ice. Samples were centrifuged, washed two times with 500 μl ice-cold 3% NaCl (wt/vol), and transferred into a precooled tube containing 800 μl silicone oil (two parts of AR 200 [Sigma-Aldrich] to one part of AK 100 [Wacker]). After centrifugation, the aqueous phase and the silicone oil were removed. The cell pellet was resuspended in 100 μl ice-cold 3% NaCl (wt/vol) and transferred to a liquid scintillation counting vial. 1 ml Soluene (PerkinElmer) was added and incubated over night at room temperature. The next day, 3 ml of the liquid scintillation cocktail Ultima Gold (PerkinElmer) was added, mixed thoroughly, and incubated for 3 h at room temperature. Samples were measured (counts per minute [cpm] over 10 min) using the liquid scintillation analyzer Tri-Carb 2900TR (Packard Bioscience) with the software package QuantaSmart 1.31 (Packard Bioscience). Negamycin amounts (μg) were calculated based on a dilution series of the [^{3}H]negamycin compound standard (specific activity: 0.052 Ci/mmol) and put in relation to the *E. coli* cell number, determined by OD_{600}, which was measured in parallel when samples were taken. Statistical significance was calculated using R (the R Foundation for Statistical Computing, version 3.6.1) as described in the methods for determination of antimicrobial activity.

Isolation of spontaneous antibiotic-resistant mutants. A single *E. coli* BW25113 colony was transferred in 10 ml LB and incubated overnight at 37°C with shaking (190 rpm). The overnight culture was

centrifuged and resuspended in 0.9% saline (0.9% wt/vol of NaCl in MilliQ water), and 1×10^8 to 5×10^8 CFU were plated on M9 or PP agar, containing different concentrations of either negamycin or bialaphos. Agar plates were incubated at 37°C, and colonies grown after 24 h were transferred onto a fresh agar plate containing either negamycin or bialaphos and checked for growth. In cases where the resistance rate turned out to be high, the experiment was repeated with lower cell numbers per plate to allow for precise colony counting.

Sequencing of the *dpp* operon of negamycin resistant mutants. The *dpp* operon was amplified from genomic DNA of the negamycin resistant mutants selected on either M9 or 0.5% PP media using the primers dppA-F-2 and dppA-F rev2 (Table S4). The resulting PCR products (size approximately 8.5 kB) were subjected to Sanger sequencing (LGC Genomics, Germany) using the primers listed in Table S4. Since no PCR product was obtained for several of the negamycin resistant mutants selected on M9, one of these mutants (M9-2) was subjected to whole-genome sequencing. After detection of a large chromosomal deletion in M9-2, the same deletion was confirmed by PCR and Sanger sequencing in 8 other mutants using the primers dpp-flank_for and dpp-flank_rev (Table S4).

Whole-genome sequencing. Genomic DNA from overnight cultures of *E. coli* strains BW25113 wild type and M9-2, a negamycin resistant mutant selected on M9 agar at 2× MIC which had not yielded a PCR product for the *dpp* operon (dppA-F-2 and dppA-F rev2 primers) was purified using the MasterPure Gram-positive DNA purification kit (Epicentre Biotechnologies). Shotgun libraries with an insert size of approximately 300 bp of the different *E. coli* strains were generated by fragmentation followed by end repair of DNA (Eurofins Genomics GmbH). The libraries were sequenced on Illumina MiSeq using chemistry v3, and the obtained reads were mapped on the reference genome of *E. coli* strain K-12 substrain MG1655 (NCBI accession number NC_000913.3) (Eurofins Genomics GmbH).

SAW biosensor measurements. Surface acoustic wave (SAW) measurements were performed to investigate the membrane-binding capacity of negamycin using a sam®5 blue sensor device (SAW Instruments GmbH, Bonn, Germany) as described before (77). Binding events were measured by means of phase shifts of the acoustic wave. SAW sensor chips were cleaned as described, followed by preincubation with a chloroform solution of 10 mM hexadecanethiol overnight. After drying the quartz, a model membrane consisting of either POPC or POPC with 10 mol% DOPG was formed by Langmuir-Blodgett technique and transferred to the sensors as described before (78). After embedding the dried sensor into the device and rehydrating the model membrane with ultrapure water, binding of negamycin to the membrane was investigated in a 200 mM morpholinepropanesulfonic acid (MOPS) (pH 7) buffer flow after injecting negamycin in a dilution series ranging from 7.5×10^{-8} M to 1×10^{-5} M.

Thin-layer chromatography. Thin-layer chromatography (TLC) was performed on TLC silica gel 60 F254 (Merck) with chloroform-methanol-25% aqueous ammonia (2:2:1) as mobile phase. 6 μl of each sample containing negamycin in a concentration of 6 mM without or with the respective salts ($CaCl_2$, $MgCl_2$, or NaCl) in molar ratios of 1:1, 1:5, or 1:10 were applied to the adsorbent layer. The developed plates were dried at 60°C, treated with ninhydrin for visualization, and dried for another 15 min at 100°C.

Isothermal titration calorimetry (ITC). Binding of negamycin to Ca^{2+} was determined by isothermal titration calorimetry (ITC). Experiments were performed by titrating 50 mM $CaCl_2$ into the cell filled with 0.5 mM negamycin. Both components were dissolved in the same buffer (200 mM Tris, pH 7 or 8.5) to prevent unspecific heat caused by dilution effects. Subsequently, the first point of the isotherm and signals from three different control experiments (titration of 50 mM $CaCl_2$ into buffer, buffer into 0.5 mM negamycin, and buffer into buffer) were subtracted from the isotherm before data evaluation. All ITC experiments were performed on a Microcal PEAQ-ITC (Malvern) at 25°C with a stirring speed of 750 rpm and 2 consecutive experiments of 19 injections of 2 μl each. The two data sets of 19 injections each were combined using the Malvern MicroCal Concat tool. The resulting isotherm was integrated and fitted with the one side binding model of the corresponding Malvern MicroCal PEAQ-ITC analysis software.

Cell membrane integrity assay. The impact of antibiotic treatment on cell membrane integrity was investigated using the cell-impermeant nucleic acid dye SYTOX Green (Invitrogen). *E. coli* BW25113 was grown in PP pH 7 or pH 8.5 to the exponential growth phase, and cultures were diluted to an OD_{600} of 0.05 in fresh medium without or with $CaCl_2$ (2.5 mM at pH 7 and 0.5 mM at pH 8.5). SYTOX Green was added to the cells to a final concentration of 5 μM, and the cell suspensions were incubated for 5 min at room temperature. Samples of 100 μl were transferred to a black 96-well microplate and antibiotics were added at the indicated concentrations. Immediately after antibiotic addition, fluorescence emission at 510 to 650 nm was measured with a wavelength step size of 2 nm after excitation at 475 nm in a microplate reader (Spark, Tecan). Fluorescence emission spectra were recorded every 10 min over a time course of 3 h at 30°C, with periodic shaking before each measurement. Of note, the SYTOX Green dye showed an increased fluorescence intensity in PP pH 8.5 compared to that in PP pH 7 even in the absence of cells, correlating with the higher relative fluorescence units (RFU) measured in the untreated control samples at pH 8.5 compared to those at pH 7.

Membrane potential assay. The membrane potential upon antibiotic treatment was assessed using the $DiOC_2(3)$ dye (Molecular Probes, Fisher Scientific). To minimize dye efflux, the assay was performed using *E. coli* BW25113 Δ*acrA*. *E. coli* BW25113 Δ*acrA* was grown in PP pH 7 or pH 8.5 to the exponential growth phase, and the OD_{600} was adjusted to 0.5 in fresh medium with or without $CaCl_2$ (2.5 mM at pH 7 and 0.5 mM at pH 8.5). 30 μM $DiOC_2(3)$ was added and samples were incubated at room temperature for 15 min in the dark. Volumes of 100 μl were transferred to a black 96-well microplate and the red/green fluorescence (excitation at 485 nm, emission at 530 nm [green] and 630 nm [red]) was measured in a

microplate reader (Infinite M200 PRO, Tecan). After an initial fluorescence measurement, the program was paused and antibiotics were added at the indicated concentrations. Thereafter, the red/green fluorescence was recorded every 5 min over a time course of 3 h at 25°C.

SUPPLEMENTAL MATERIAL

Supplemental material is available online only.

SUPPLEMENTAL FILE 1, PDF file, 1.8 MB.

ACKNOWLEDGMENTS

This study was supported by the German Center of Infection Research (DZIF) projects TTU 09.812 and TTU 09.819 and the German Federal Ministry of Education and Research BMBF (project Gram-NEG-DESIGN). C.C. gratefully acknowledges a PhD scholarship of the German National Academic Foundation (Deutsche Studienstiftung). We thank Melanie Dostert and Annika Hettich for expert technical assistance.

REFERENCES

1. O'Neill J. 2014. Review on antimicrobial resistance: tackling a crisis for the health and wealth of nations. https://amr-review.org/Publications.html.
2. Tommasi R, Brown DG, Walkup GK, Manchester JI, Miller AA. 2015. ESKAPEing the labyrinth of antibacterial discovery. Nat Rev Drug Discov 14:529–542. https://doi.org/10.1038/nrd4572.
3. Nikaido H. 2003. Molecular basis of bacterial outer membrane permeability revisited. Microbiol Mol Biol Rev 67:593–656. https://doi.org/10.1128/mmbr.67.4.593-656.2003.
4. Silver LL. 2016. A Gestalt approach to Gram-negative entry. Bioorg Med Chem 24:6379–6389. https://doi.org/10.1016/j.bmc.2016.06.044.
5. Richter MF, Drown BS, Andrew P, Garcia A, Shirai T, Svec RL, Hergenrother PJ. 2017. Predictive compound accumulation rules yield a broad-spectrum antibiotic. Nature 545:299–304. https://doi.org/10.1038/nature22308.
6. O'Shea R, Moser HE. 2008. Physicochemical properties of antibacterial compounds: implications for drug discovery. J Med Chem 51:2871–2878. https://doi.org/10.1021/jm700967e.
7. Hamada M, Takeuchi T, Kondo S, Ikeda Y, Naganawa H. 1970. A new antibiotic, negamycin. J Antibiot (Tokyo) 23:170–171. https://doi.org/10.7164/antibiotics.23.170.
8. Guo J, Miele EW, Chen A, Luzietti RA, Zambrowski M, Walsky RL, Buurman ET. 2015. Pharmacokinetics of the natural antibiotic negamycin. Xenobiotica 45:625–633. https://doi.org/10.3109/00498254.2015.1006301.
9. Mizuno S, Nitta K, Umezawa H. 1970. Mechanism of action of negamycin in *Escherichia coli* K12. I. Inhibition of initiation of protein synthesis. J Antibiot 23:581–588. https://doi.org/10.7164/antibiotics.23.581.
10. Mizuno S, Nitta K, Umezawa H. 1970. Mechanism of action of negamycin in *Escherichia coli* K12. II. Miscoding activity in polypeptide synthesis directed by synthetic polynucleotide. J Antibiot 23:589–594. https://doi.org/10.7164/antibiotics.23.589.
11. Uehara Y, Hori M, Umezawa H. 1974. Negamycin inhibits termination of protein synthesis directed by phage f2 RNA in vitro. Biochim Biophys Acta 374:82–95. https://doi.org/10.1016/0005-2787(74)90201-9.
12. Uehara Y, Hori M, Umezawa H. 1976. Specific inhibition of the termination process of protein synthesis by negamycin. Biochim Biophys Acta 442:251–262. https://doi.org/10.1016/0005-2787(76)90495-0.
13. Uehara Y, Kondo S, Umezawa H, Suzukake K, Hori M. 1972. Negamycin, a miscoding antibiotic with a unique structure. J Antibiot (Tokyo) 25:685–688. https://doi.org/10.7164/antibiotics.25.685.
14. Polikanov YS, Szal T, Jiang F, Gupta P, Matsuda R, Shiozuka M, Steitz TA, Vázquez-Laslop N, Mankin AS. 2014. Negamycin interferes with decoding and translocation by simultaneous interaction with rRNA and tRNA. Mol Cell 56:541–550. https://doi.org/10.1016/j.molcel.2014.09.021.
15. Olivier NB, Altman RB, Noeske J, Basarab GS, Code E, Ferguson AD, Gao N, Huang J, Juette MF, Livchak S, Miller MD, Prince DB, Cate JHD, Buurman ET, Blanchard SC. 2014. Negamycin induces translational stalling and miscoding by binding to the small subunit head domain of the *Escherichia coli* ribosome. Proc Natl Acad Sci U S A 111:16274–16279. https://doi.org/10.1073/pnas.1414401111.
16. Schroeder SJ, Blaha G, Moore PB. 2007. Negamycin binds to the wall of the nascent chain exit tunnel of the 50S ribosomal subunit. Antimicrob Agents Chemother 51:4462–4465. https://doi.org/10.1128/AAC.00455-07.
17. Arakawa M, Shiozuka M, Nakayama Y, Hara T, Hamada M, Kondo S, Ikeda D, Takahashi Y, Sawa R, Nonomura Y, Sheykholeslami K, Kondo K, Kaga K, Kitamura T, Suzuki-Miyagoe Y, Takeda S, Matsuda R. 2003. Negamycin restores dystrophin expression in skeletal and cardiac muscles of mdx mice. J Biochem 134:751–758. https://doi.org/10.1093/jb/mvg203.
18. Taguchi A, Nishiguchi S, Shiozuka M, Nomoto T, Ina M, Nojima S, Matsuda R, Nonomura Y, Kiso Y, Yamazaki Y, Yakushiji F, Hayashi Y. 2012. Negamycin analogue with readthrough-promoting activity as a potential drug candidate for Duchenne muscular dystrophy. ACS Med Chem Lett 3:118–122. https://doi.org/10.1021/ml200245t.
19. Kondo S, Iinuma K, Yoshida K, Yokose K, Ikeda Y. 1976. Syntheses and properties of negamycin analogs modified the delta-hydroxy-beta-lysine moiety. J Antibiot (Tokyo) 29:208–211. https://doi.org/10.7164/antibiotics.29.208.
20. Raju B, Mortell K, Anandan S, O'Dowd H, Gao H, Gomez M, Hackbarth C, Wu C, Wang W, Yuan Z, White R, Trias J, Patel DV. 2003. N- and C-terminal modifications of negamycin. Bioorg Med Chem Lett 13:2413–2418. https://doi.org/10.1016/S0960-894X(03)00393-7.
21. Uehara Y, Hori M, Kondo S, Hamada M, Umezawa H. 1976. Structure-activity relationships among negamycin analogs. J Antibiot (Tokyo) 29:937–943. https://doi.org/10.7164/antibiotics.29.937.
22. McKinney DC, Basarab GS, Cocozaki AI, Foulk MA, Miller MD, Ruvinsky AM, Scott CW, Thakur K, Zhao L, Buurman ET, Narayan S. 2015. Structural insights lead to a negamycin analogue with improved antimicrobial activity against Gram-negative pathogens. ACS Med Chem Lett 6:930–935. https://doi.org/10.1021/acsmedchemlett.5b00205.
23. Raju B, Anandan S, Gu S, Herradura P, O'Dowd H, Kim B, Gomez M, Hackbarth C, Wu C, Wang W, Yuan Z, White R, Trias J, Patel DV. 2004. Conformationally restricted analogs of deoxynegamycin. Bioorg Med Chem Lett 14:3103–3107. https://doi.org/10.1016/j.bmcl.2004.04.036.
24. Rafanan N, Margolis P, Kubo A, Saxena R, Rosenow C, White R, Trias J. 27 to 30 September 2002. Resistance to VRC4219 in *Escherichia coli*. Poster presented at the 42nd ICAAC Annual meeting of the American Society for Microbiology, San Diego, CA.
25. McKinney D, Bezdenejnih-Snyder N, Farrington K, Guo J, McLaughlin R, Ruvinsky A, Singh R, Basarab G, Narayan S, Buurman ET. 2015. Illicit transport via dipeptide transporter Dpp is irrelevant to the efficacy of negamycin in mouse thigh models of *Escherichia coli* infection. ACS Infect Dis 1:222–230. https://doi.org/10.1021/acsinfecdis.5b00027.
26. Cocozaki AI, Altman RB, Huang J, Buurman ET, Kazmirski SL, Doig P, Prince DB, Blanchard SC, Cate JHD, Ferguson AD. 2016. Resistance mutations generate divergent antibiotic susceptibility profiles against translation inhibitors. Proc Natl Acad Sci U S A 113:8188–8193. https://doi.org/10.1073/pnas.1605127113.
27. Abouhamad WN, Manson M, Gibson MM, Higgins CF. 1991. Peptide transport and chemotaxis in *Escherichia coli* and *Salmonella typhimurium*: characterization of the dipeptide permease (Dpp) and the dipeptide-binding protein. Mol Microbiol 5:1035–1047. https://doi.org/10.1111/j.1365-2958.1991.tb01876.x.
28. Chueca B, Renzoni A, Berdejo D, Pagan R, Kelley WL, Garcia-Gonzalo D.

2018. Whole-genome sequencing and genetic analysis reveal novel stress responses to individual constituents of essential oils in *Escherichia coli*. Appl Environ Microbiol 84:e02538-17 https://doi.org/10.1128/AEM.02538-17.
29. Yamazaki Y, Niki H, Kato J. 2008. Profiling of *Escherichia coli* chromosome database. Methods Mol Biol 416:385–389. https://doi.org/10.1007/978-1-59745-321-9_26.
30. Holland IB, Jones HE, Campbell AK, Jacq A. 1999. An assessment of the role of intracellular free Ca^{2+} in *E. coli*. Biochimie 81:901–907. https://doi.org/10.1016/S0300-9084(99)00205-9.
31. Nierhaus KH. 2014. Mg^{2+}, K^{+}, and the ribosome. J Bacteriol 196:3817–3819. https://doi.org/10.1128/JB.02297-14.
32. Krulwich TA, Sachs G, Padan E. 2011. Molecular aspects of bacterial pH sensing and homeostasis. Nat Rev Microbiol 9:330–343. https://doi.org/10.1038/nrmicro2549.
33. Hancock RE. 1981. Aminoglycoside uptake and mode of action – with special reference to streptomycin and gentamicin. I. Antagonists and mutants. J Antimicrob Chemother 8:249–276. https://doi.org/10.1093/jac/8.4.249.
34. Schlessinger D. 1988. Failure of aminoglycoside antibiotics to kill anaerobic, low-pH, and resistant cultures. Clin Microbiol Rev 1:54–59. https://doi.org/10.1128/cmr.1.1.54.
35. Manson MD, Blank V, Brade G, Higgins CF. 1986. Peptide chemotaxis in *E. coli* involves the Tap signal transducer and the dipeptide permease. Nature 321:253–256. https://doi.org/10.1038/321253a0.
36. Smith MW, Tyreman DR, Payne GM, Marshall NJ, Payne JW. 1999. Substrate specificity of the periplasmic dipeptide-binding protein from *Escherichia coli*: experimental basis for the design of peptide prodrugs. Microbiology 145:2891–2901. https://doi.org/10.1099/00221287-145-10-2891.
37. Verkamp E, Backman VM, Bjornsson JM, Soll D, Eggertsson G. 1993. The periplasmic dipeptide permease system transports 5-aminolevulinic acid in *Escherichia coli*. J Bacteriol 175:1452–1456. https://doi.org/10.1128/jb.175.5.1452-1456.1993.
38. Létoffé S, Delepelaire P, Wandersman C. 2006. The housekeeping dipeptide permease is the *Escherichia coli* heme transporter and functions with two optional peptide binding proteins. Proc Natl Acad Sci U S A 103:12891–12896. https://doi.org/10.1073/pnas.0605440103.
39. Payne JW, Grail BM, Gupta S, Ladbury JE, Marshall NJ, O'Brien R, Payne GM. 2000. Structural basis for recognition of dipeptides by peptide transporters. Arch Biochem Biophys 384:9–23. https://doi.org/10.1006/abbi.2000.2084.
40. Parra-Lopez C, Baer MT, Groisman EA. 1993. Molecular genetic analysis of a locus required for resistance to antimicrobial peptides in *Salmonella typhimurium*. EMBO J 12:4053–4062. https://doi.org/10.1002/j.1460-2075.1993.tb06089.x.
41. Shelton CL, Raffel FK, Beatty WL, Johnson SM, Mason KM. 2011. Sap transporter mediated import and subsequent degradation of antimicrobial peptides in *Haemophilus*. PLoS Pathog 7:e1002360. https://doi.org/10.1371/journal.ppat.1002360.
42. Sugiyama Y, Nakamura A, Matsumoto M, Kanbe A, Sakanaka M, Higashi K, Igarashi K, Katayama T, Suzuki H, Kurihara S. 2016. A novel putrescine exporter SapBCDF of *Escherichia coli*. J Biol Chem 291:26343–26351. https://doi.org/10.1074/jbc.M116.762450.
43. Park JT, Raychaudhuri D, Li H, Normark S, Mengin-Lecreulx D. 1998. MppA, a periplasmic binding protein essential for import of the bacterial cell wall peptide L-alanyl-gamma-D-glutamyl-meso-diaminopimelate. J Bacteriol 180:1215–1223. https://doi.org/10.1128/JB.180.5.1215-1223.1998.
44. Newstead S. 2017. Recent advances in understanding proton coupled peptide transport via the POT family. Curr Opin Struct Biol 45:17–24. https://doi.org/10.1016/j.sbi.2016.10.018.
45. Inui K, Yamamoto M, Saito H. 1992. Transepithelial transport of oral cephalosporins by monolayers of intestinal epithelial cell line Caco-2: specific transport systems in apical and basolateral membranes. J Pharmacol Exp Ther 261:195–201.
46. Smith DE, Clemencon B, Hediger MA. 2013. Proton-coupled oligopeptide transporter family SLC15: physiological, pharmacological and pathological implications. Mol Aspects Med 34:323–336. https://doi.org/10.1016/j.mam.2012.11.003.
47. Weitz D, Harder D, Casagrande F, Fotiadis D, Obrdlik P, Kelety B, Daniel H. 2007. Functional and structural characterization of a prokaryotic peptide transporter with features similar to mammalian PEPT1. J Biol Chem 282:2832–2839. https://doi.org/10.1074/jbc.M604866200.
48. Kitamura K, Zefany E, Kinsui B, Abe F. 2017. Critical role of the proton-dependent oligopeptide transporter (POT) in the cellular uptake of the peptidyl nucleoside antibiotic, blasticidin S. Biochim Biophys Acta Mol Cell Res 1864:393–398. https://doi.org/10.1016/j.bbamcr.2016.11.030.
49. Daniel H, Kottra G. 2004. The proton oligopeptide cotransporter family SLC15 in physiology and pharmacology. Pflugers Arch 447:610–618. https://doi.org/10.1007/s00424-003-1101-4.
50. Döring F, Will J, Amasheh S, Clauss W, Ahlbrecht H, Daniel H. 1998. Minimal molecular determinants of substrates for recognition by the intestinal peptide transporter. J Biol Chem 273:23211–23218. https://doi.org/10.1074/jbc.273.36.23211.
51. Mistry A, Warren MS, Cusick JK, Karkhoff-Schweizer RR, Lomovskaya O, Schweizer HP. 2013. High-level pacidamycin resistance in *Pseudomonas aeruginosa* is mediated by an Opp oligopeptide permease encoded by the *opp-fabI* operon. Antimicrob Agents Chemother 57:5565–5571. https://doi.org/10.1128/AAC.01198-13.
52. Shiver AL, Osadnik H, Kritikos G, Li B, Krogan N, Typas A, Gross CA. 2016. A chemical-genomic screen of neglected antibiotics reveals illicit transport of kasugamycin and blasticidin S. PLoS Genet 12:e1006124-19. https://doi.org/10.1371/journal.pgen.1006124.
53. Maio A, Brandi L, Donadio S, Gualerzi CO. 2016. The oligopeptide permease Opp mediates illicit transport of the bacterial P-site decoding inhibitor GE81112. Antibiotics (Basel) 5:17. https://doi.org/10.3390/antibiotics5020017.
54. Goldstein DA. 1990. Serum calcium. *In* Walker HK, Hall WD, Hurst JW (ed), Clinical methods: the history, physical, and laboratory examinations, 3rd ed. Butterworths, Boston, MA.
55. Yee J. 2007. Hypercalcemia. *In* Enna SJ, Bylund DB (ed), xPharm: the comprehensive pharmacology reference. Elsevier, New York.
56. Bryan LE, Van Den Elzen HM. 1977. Effects of membrane-energy mutations and cations on streptomycin and gentamicin accumulation by bacteria: a model for entry of streptomycin and gentamicin in susceptible and resistant bacteria. Antimicrob Agents Chemother 12:163–177. https://doi.org/10.1128/aac.12.2.163.
57. Chapman JS, Georgopapadakou NH. 1988. Routes of quinolone permeation in *Escherichia coli*. Antimicrob Agents Chemother 32:438–442. https://doi.org/10.1128/aac.32.4.438.
58. Valisena S, Palumbo M, Parolin C, Palu G, Meloni GA. 1990. Relevance of ionic effects on norfloxacin uptake by *Escherichia coli*. Biochem Pharmacol 40:431–436. https://doi.org/10.1016/0006-2952(90)90540-2.
59. Marshall AJH, Piddock LJV. 1994. Interaction of divalent cations, quinolones and bacteria. J Antimicrob Chemother 34:465–483. https://doi.org/10.1093/jac/34.4.465.
60. Lecomte S, Baron MH, Chenon MT, Coupry C, Moreau NJ. 1994. Effect of magnesium complexation by fluoroquinolines on their antibacterial properties. Antimicrob Agents Chemother 38:2810–2816. https://doi.org/10.1128/aac.38.12.2810.
61. Yamaguchi A, Ohmori H, Kaneko-Ohdera M, Nomura T, Sawai T. 1991. Delta pH-dependent accumulation of tetracycline in *Escherichia coli*. Antimicrob Agents Chemother 35:53–56. https://doi.org/10.1128/aac.35.1.53.
62. Jones RN, Barry AL. 1987. Antimicrobial activity and spectrum of LY146032, a lipopeptide antibiotic, including susceptibility testing recommendations. Antimicrob Agents Chemother 31:625–629. https://doi.org/10.1128/aac.31.4.625.
63. Ho SW, Jung D, Calhoun JR, Lear JD, Okon M, Scott WRP, Hancock REW, Straus SK. 2008. Effect of divalent cations on the structure of the antibiotic daptomycin. Eur Biophys J 37:421–433. https://doi.org/10.1007/s00249-007-0227-2.
64. Straus SK, Hancock REW. 2006. Mode of action of the new antibiotic for Gram-positive pathogens daptomycin: comparison with cationic antimicrobial peptides and lipopeptides. Biochim Biophys Acta 1758:1215–1223. https://doi.org/10.1016/j.bbamem.2006.02.009.
65. Garidel P, Blume A. 1999. Interaction of alkaline earth cations with the negatively charged phospholipid 1,2-dimyristoyl-sn-glycero-3-phosphoglycerol: a differential scanning and isothermal titration calorimetric study. Langmuir 15:5526–5534. https://doi.org/10.1021/la990217a.
66. Jin L, Amaya-Mazo X, Apel ME, Sankisa SS, Johnson E, Zbyszynska MA, Han A. 2007. Ca^{2+} and Mg^{2+} bind tetracycline with distinct stoichiometries and linked deprotonation. Biophys Chem 128:185–196. https://doi.org/10.1016/j.bpc.2007.04.005.
67. Uivarosi V. 2013. Metal complexes of quinolone antibiotics and their applications: an update. Molecules 18:11153–11197. https://doi.org/10.3390/molecules180911153.
68. Damper PD, Epstein W. 1981. Role of the membrane potential in bacterial resistance to aminoglycoside antibiotics. Antimicrob Agents Chemother 20:803–808. https://doi.org/10.1128/aac.20.6.803.

69. Nikaido H, Thanassi DG. 1993. Penetration of lipophilic agents with multiple protonation sites into bacterial cells: tetracyclines and fluoroquinolones as examples. Antimicrob Agents Chemother 37:1393–1399. https://doi.org/10.1128/aac.37.7.1393.
70. Cramariuc O, Rog T, Javanainen M, Monticelli L, Polishchuk AV, Vattulainen I. 2012. Mechanism for translocation of fluoroquinolones across lipid membranes. Biochim Biophys Acta 1818:2563–2571. https://doi.org/10.1016/j.bbamem.2012.05.027.
71. Wang YF, Izawa T, Kobayashi S, Ohno M. 1982. Stereocontrolled synthesis of (+)-negamycin from an acyclic homoallylamine by 1,3-asymmetric induction. J Am Chem Soc 104:6465–6466. https://doi.org/10.1021/ja00387a060.
72. Patel JB, Cockerill FR, Bradford PA, Eliopoulos GM, Hindler JA, Jenkins SG, Lewis JS, Limbago B, Miller LA, Nicolau DP, Powell M, Swenson JM, Turnidge JD, Weinstein MP, Zimmer BL. 2015. Methods for dilution antimicrobial susceptibility tests for bacteria that grow aerobically. Approved Standard - Tenth Edition, vol 35. Clinical and Laboratory Standards Institute, USA.
73. Wade HE, Robinson HK. 1966. Magnesium ion-independent ribonucleic acid depolymerases in bacteria. Biochem J 101:467–479. https://doi.org/10.1042/bj1010467.
74. Zubay G. 1973. *In vitro* synthesis of protein in microbial systems. Annu Rev Genet 7:267–287. https://doi.org/10.1146/annurev.ge.07.120173.001411.
75. Datsenko KA, Wanner BL. 2000. One-step inactivation of chromosomal genes in *Escherichia coli* K-12 using PCR products. Proc Natl Acad Sci U S A 97:6640–6645. https://doi.org/10.1073/pnas.120163297.
76. Baba T, Ara T, Hasegawa M, Takai Y, Okumura Y, Baba M, Datsenko KA, Tomita M, Wanner BL, Mori H. 2006. Construction of *Escherichia coli* K-12 in-frame, single-gene knockout mutants: the Keio collection. Mol Syst Biol 2:1–11. https://doi.org/10.1038/msb4100050.
77. Schlesinger M, Simonis D, Schmitz P, Fritzsche J, Bendas G. 2009. Binding between heparin and the integrin VLA-4. Thromb Haemost 102:816–822. https://doi.org/10.1160/TH09-01-0061.
78. Reder-Christ K, Schmitz P, Bota M, Gerber U, Falkenstein-Paul H, Fuss C, Enachescu M, Bendas G. 2013. A dry membrane protection technique to allow surface acoustic wave biosensor measurements of biological model membrane approaches. Sensors (Basel) 13:12392–12405. https://doi.org/10.3390/s130912392.

Supplemental Data

The antibiotic negamycin crosses the bacterial cytoplasmic membrane by multiple routes

Daniel Hörömpöli[a,b]+, Catherine Ciglia[c]+, Karl-Heinz Glüsenkamp[d], Lars Ole Haustedt[e], Hildegard Falkenstein-Paul[f], Gerd Bendas[f], Anne Berscheid[a,b,c]*#, Heike Brötz-Oesterhelt[a,b,c,g]*#

[a] Interfaculty Institute of Microbiology and Infection Medicine, Department of Microbial Bioactive Compounds, University of Tuebingen, Tuebingen, Germany

[b] German Center of Infection Research (DZIF), partner site Tuebingen

[c] Institute of Pharmaceutical Biology, University of Duesseldorf, Duesseldorf, Germany

[d] Squarix GmbH, Marl, Germany

[e] AnalytiCon Discovery GmbH, Potsdam, Germany

[f] Pharmaceutical Institute, Department of Pharmaceutical & Cell Biological Chemistry, University of Bonn, Bonn, Germany

[g] Cluster of Excellence 2124: Controlling Microbes to Fight Infection

Running Head: Negamycin passage across the cytoplasmic membrane

+ D.H. and C.C. contributed equally to this work. Author order was determined by mutual verbal consent.

* H.B.-O. and A.B. share senior authorship.

Address correspondence to Heike Brötz-Oesterhelt, heike.broetz-oesterhelt@uni-tuebingen.de; Anne Berscheid, anne.berscheid@uni-tuebingen.de

Figures

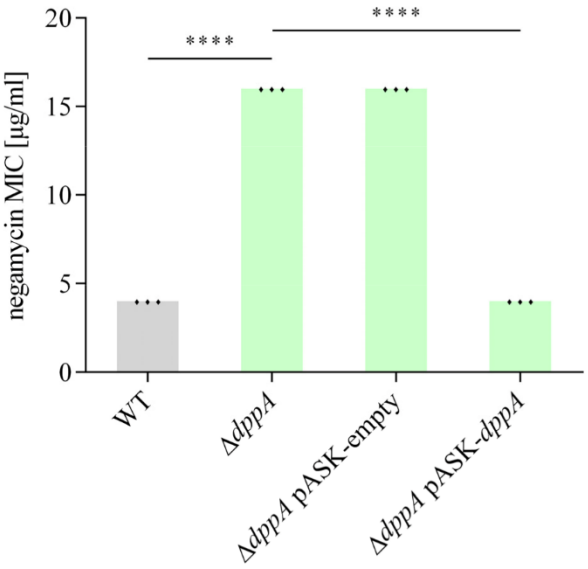

Figure S1. Deletion of chromosomal *dppA* in *E. coli* BW25113 reduces negamycin susceptibility and can be complemented by DppA expression from a plasmid (pASK-*dppA*). The same plasmid lacking *dppA* (pASK-empty) served as a negative control. Negamycin MICs were determined in M9. DppA expression was induced with 10 ng/ml anhydrotetracycline. Each diamond represents an independent MIC determination. Statistical significance was determined using unpaired Student's t-test with Holm-Bonferroni correction. ****, $P \leq 0.0001$.

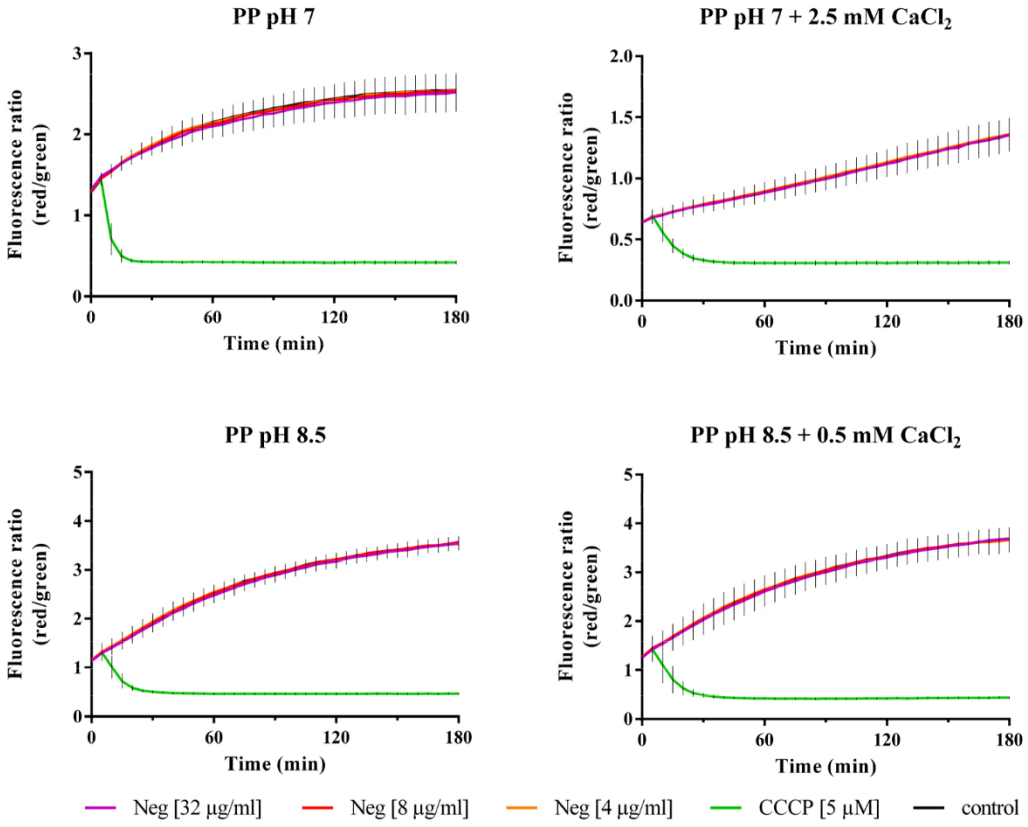

Figure S2. Negamycin treatment does not lead to rapid membrane depolarization under different media conditions. *E. coli* BW25113 Δ*acrA* was used for the $DiOC_2(3)$ dye-based membrane potential assay to minimize dye efflux. Negamycin (Neg) was applied at different concentrations up to 32 µg/ml (corresponding to 4x MIC at pH 7 and to 32-64x MIC at pH 8.5 + 0.5 mM $CaCl_2$). No dissipation of the membrane potential was observed over a time course of 180 min in 0.5% polypeptone medium (PP) at pH 7 and pH 8.5, neither in the absence nor in the presence of $CaCl_2$, while the addition of the protonophore CCCP led to a quick depolarization of the *E. coli* cells indicated by the decrease in the red/green fluorescence ratio under all media conditions. The experiment was performed in at least three biological replicates, graphs represent the mean ± standard deviation.

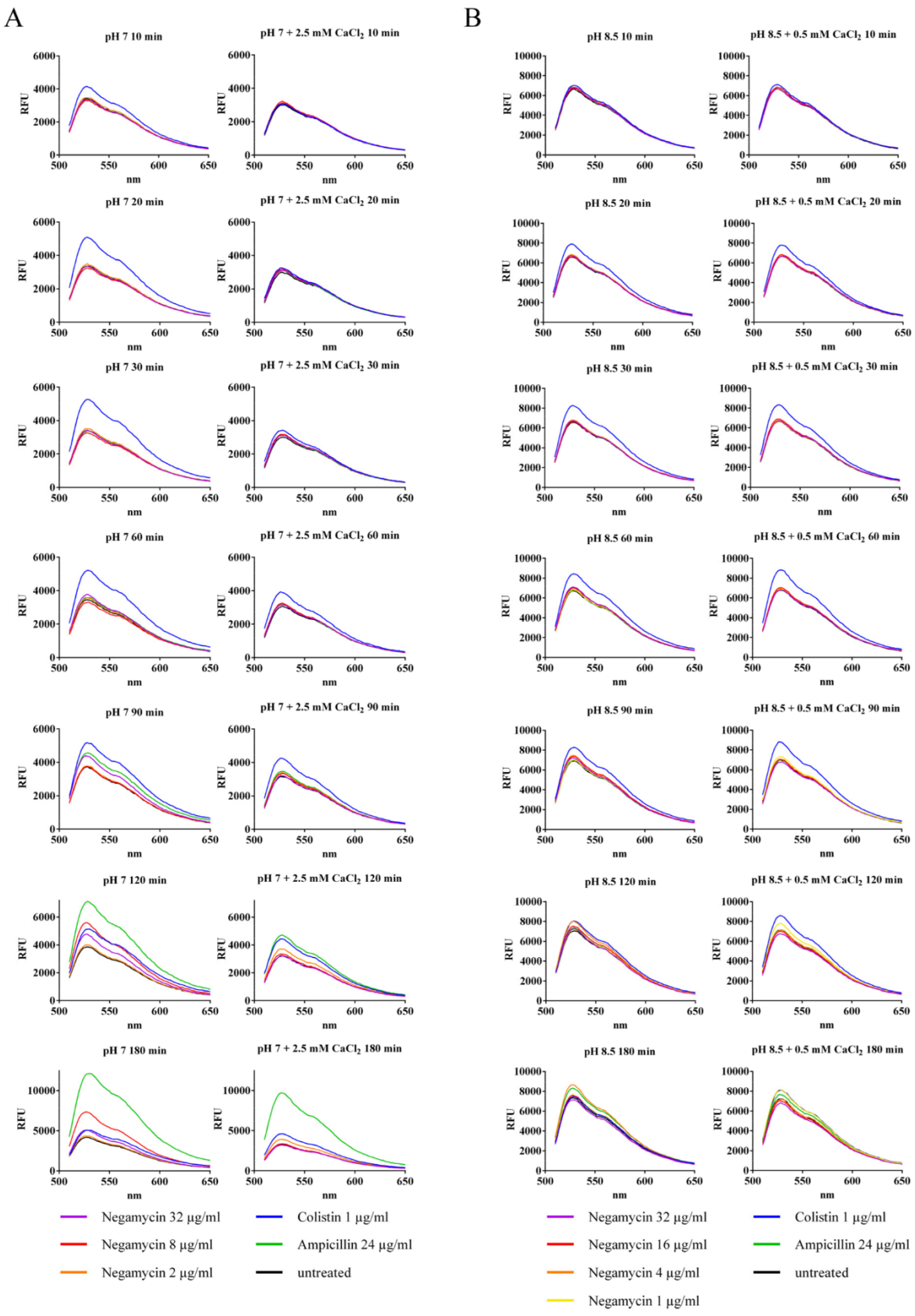
A
pH 7 10 min
pH 7 + 2.5 mM CaCl2 10 min
pH 7 20 min
pH 7 + 2.5 mM CaCl2 20 min
pH 7 30 min
pH 7 + 2.5 mM CaCl2 30 min
pH 7 60 min
pH 7 + 2.5 mM CaCl2 60 min
pH 7 90 min
pH 7 + 2.5 mM CaCl2 90 min
pH 7 120 min
pH 7 + 2.5 mM CaCl2 120 min
pH 7 180 min
pH 7 + 2.5 mM CaCl2 180 min
RFU
nm
Negamycin 32 µg/ml
Negamycin 8 µg/ml
Negamycin 2 µg/ml
Colistin 1 µg/ml
Ampicillin 24 µg/ml
untreated
B
pH 8.5 10 min
pH 8.5 + 0.5 mM CaCl2 10 min
pH 8.5 20 min
pH 8.5 + 0.5 mM CaCl2 20 min
pH 8.5 30 min
pH 8.5 + 0.5 mM CaCl2 30 min
pH 8.5 60 min
pH 8.5 + 0.5 mM CaCl2 60 min
pH 8.5 90 min
pH 8.5 + 0.5 mM CaCl2 90 min
pH 8.5 120 min
pH 8.5 + 0.5 mM CaCl2 120 min
pH 8.5 180 min
pH 8.5 + 0.5 mM CaCl2 180 min
RFU
nm
Negamycin 32 µg/ml
Negamycin 16 µg/ml
Negamycin 4 µg/ml
Negamycin 1 µg/ml
Colistin 1 µg/ml
Ampicillin 24 µg/ml
untreated

Figure S3. Negamycin treatment does not lead to a rapid permeabilization of the cytoplasmic membrane in the presence of $CaCl_2$. Membrane integrity upon antibiotic treatment was assessed using the cell membrane impermeant nucleic acid stain SYTOX Green, that emits increased fluorescence when binding to nucleic acids after having gained access through membrane pores. Negamycin concentrations up to 32 µg/ml (i.e. corresponding to 4x MIC in PP pH 7 and 16x MIC at pH 7 + 2.5 mM $CaCl_2$) did not lead to an increased permeability of *E. coli* BW25113 within 60 min of treatment, neither at pH 7 ± $CaCl_2$ (A) nor at pH 8.5 ± $CaCl_2$ (B). After 90 min of negamycin treatment, first effects on membrane integrity appeared, which, however, can be most likely attributed to the miscoding activity of this compound. The effect was best visible at concentrations reflecting the MIC in the respective media (i.e. 8 µg/ml at pH 7, 2 µg/ml in pH 7 + 2.5 mM $CaCl_2$, 4 µg/ml at pH 8.5 and 1 µg/ml at pH 8.5 + 0.5 mM $CaCl_2$), in agreement with the fact that negamycin, although having miscoding as the primary mechanism, leads to full translation inhibition at higher concentrations. Similarly, aberrant membrane proteins resulting from translational miscoding were also suggested to be responsible for membrane permeabilization during prolonged aminoglycoside exposure (1, 2). Importantly, $CaCl_2$ addition did not accelerate the permeabilization process, also not under alkaline conditions. In contrast, the membrane disrupting agent colistin disturbed the membrane integrity already after 10-20 min at 4x MIC, as indicated by the increase in fluorescence signal compared to the untreated control. Cell lysis caused by the treatment with the cell wall inhibitor ampicillin became visible after 90-120 min of treatment in accordance with the fact that peptidoglycan sacculus weakening requires some time to take effect. The graph shows the data representative of three independent biological experiments. Of note, SYTOX Green shows a higher fluorescence intensity at alkaline pH, even in the absence of cells.

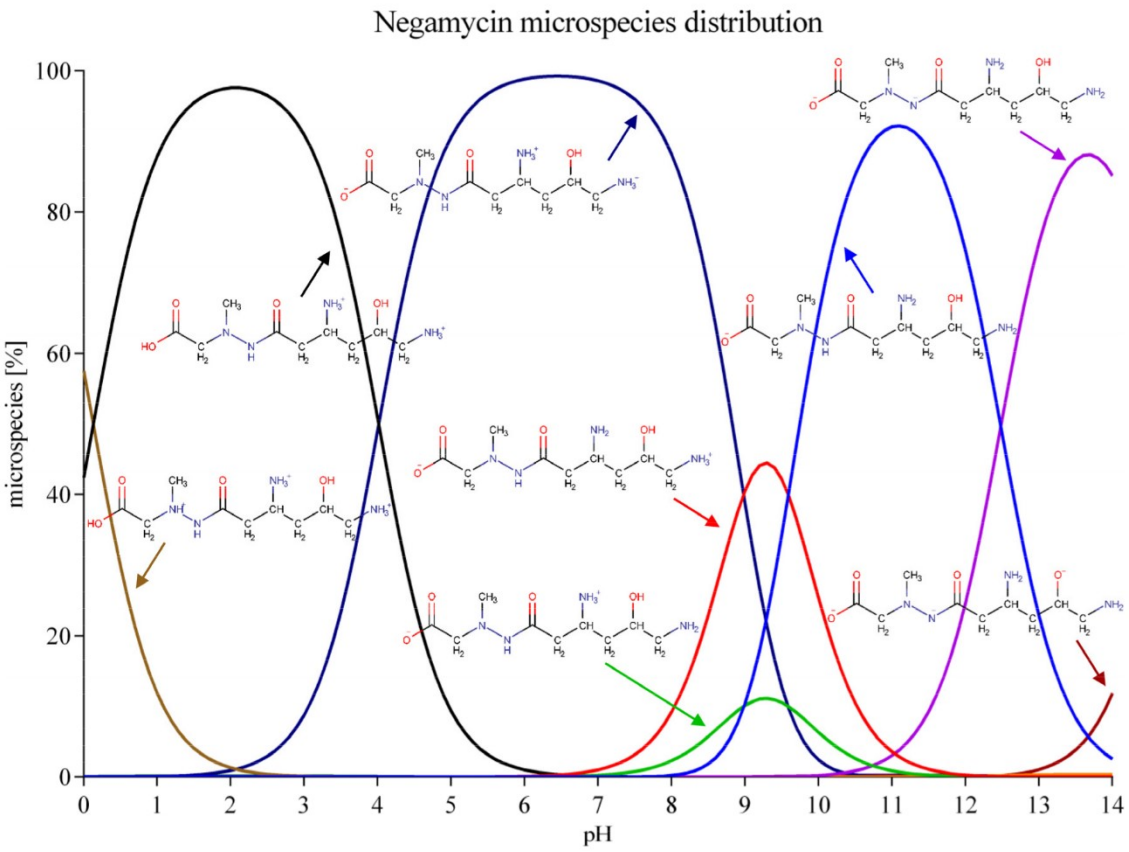

Figure S4. Negamycin microspecies distribution calculated with ChemAxon MarvinView (version 17.29.0). Calculated pKa values (4.02, 8.88 and 9.69) by ChemAxon differ slightly from the experimentally determined pKa values (3.2, 8.0 and 9.6) by Guo et al. (3).

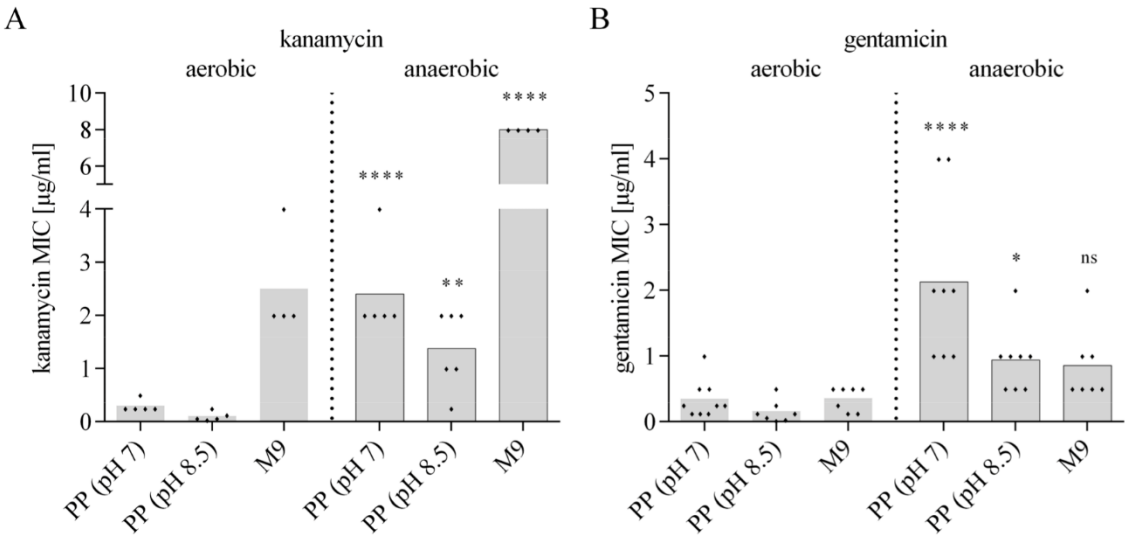

Figure S5. Susceptibility of *E. coli* BW25113 to the aminoglycosides kanamycin (A) and gentamicin (B) under aerobic and anaerobic growth conditions in 0.5% polypeptone (PP) pH 7 or pH 8.5 or in M9 minimal medium. Each diamond represents an independent MIC determination. Statistical significance was determined using unpaired Student's t-test comparing the effect of anaerobic growth conditions to the same antibiotic within the same medium under aerobic growth conditions. ns, $P > 0.05$; *, $P \leq 0.05$; **, $P \leq 0.01$; ***, $P \leq 0.001$; ****, $P \leq 0.0001$.

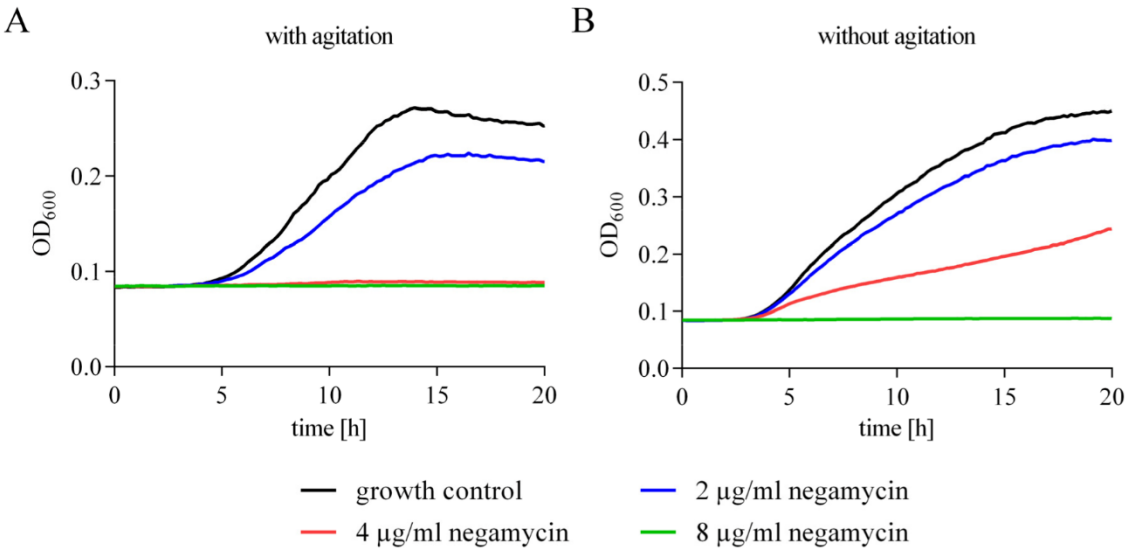

Figure S6. Effect of negamycin on the growth of *E. coli* BW25113 in 0.5% polypeptone (PP) in microplates with (A) or without (B) agitation. Microplates were either incubated with periodic shaking (218 rpm for 30 s at 5 min intervals) (A) or kept static as customary during MIC determinations (B) and OD_{600} was measured in a microplate reader (Infinite M200 pro, TECAN). Negamycin susceptibility is increased under well-aerated growth conditions in PP.

Tables

Table S1. Antimicrobial activity of ciprofloxacin, tetracycline and gentamicin against *E. coli* BW25113 in the presence of different concentrations of salts added to 0.5% polypeptone medium.

	MIC [μg/ml]									
		$CaCl_2$			$MgCl_2$			NaCl		
	0 mM	2.5 mM	10 mM	50 mM	2.5 mM	10 mM	50 mM	2.5 mM	10 mM	50
Ciprofloxacin	0.008	0.008	0.016	0.06	0.008	0.016	0.125	0.004	0.004	0.(
Tetracycline	2	4-8	4	16	8	16	>64	2	2	1
Gentamicin	0.06	0.06	0.06	1	0.06	0.06	0.25	0.06	0.25	0

Table S2. Antibacterial activity of negamycin and novobiocin in efflux deficient mutants in PP pH 7 and PP pH 8.5 with 0.5 mM $CaCl_2$. Deletion of the main *E. coli* efflux pump AcrAB did not improve negamycin activity under either growth condition, while the activity of the known AcrAB substrate novobiocin strongly increased in the pump deletion mutant.

	MIC [µg/ml]							
	Negamycin				Novobiocin			
	WT	Δ*acrA*	Δ*acrB*	Δ*acrAB*	WT	Δ*acrA*	Δ*acrB*	Δ*acrAB*
pH 7	8	8	8	16	32	1-2	1-2	0.5
pH 8.5 + 0.5 mM $CaCl_2$	0.5-1	0.5	0.5	1	>64	32	32	4-8

Table S3. Bacterial strains used in this study.

Strain	Gene function (4)	Genotype/characteristics	source
***E. coli* ATCC 25922™**		Clinical isolate, CLSI reference strain	(5)
***E. coli* BW25113**		wildtype; F-, Δ(*araD-araB*)*567*, Δ*lacZ4787*(::*rrnB*-3), *λ*-, *rph*-1, Δ(*rhaD-rhaB*)*568*, *hsdR514*	(6, 7)
E. coli* JW0422 Δ*cyoA	cytochrome bo_3 ubiquinol oxidase subunit II	F-, Δ*(araD-araB)567*, Δ*lacZ4787*(::*rrnB*-3), *λ*-, Δ*cyoA789::kan*, *rph*-1, Δ(*rhaD-rhaB*)*568*, *hsdR514*	(6, 7)
E. coli* JW0421 Δ*cyoB	cytochrome bo_3 ubiquinol oxidase subunit II	F-, Δ*(araD-araB)567*, Δ*lacZ4787*(::*rrnB*-3), *λ*-, Δ*cyoB788::kan*, *rph*-1, Δ(*rhaD-rhaB*)*568*, *hsdR514*	(6, 7)
E. coli* JW0711 Δ*sdhC	succinate:quinone oxireductase	F-, Δ*(araD-araB)567*, Δ*lacZ4787*(::*rrnB*-3), *λ*-, Δ*sdhC771::kan*, *rph*-1, Δ(*rhaD-rhaB*)*568*, *hsdR514*	(6, 7)
E. coli* JW0713 Δ*sdhA	succinate:quinone oxireductase, FAD binding protein	F-, Δ*(araD-araB)567*, Δ*lacZ4787*(::*rrnB*-3), *λ*-, Δ*sdhA773::kan*, *rph*-1, Δ(*rhaD-rhaB*)*568*, *hsdR514*	(6, 7)
E. coli* JW1095 Δ*ndh	NADH:quinone oxireductase II	F-, Δ*(araD-araB)567*, Δ*lacZ4787*(::*rrnB*-3), *λ*-, Δ*ndh771::kan*, *rph*-1, Δ(*rhaD-rhaB*)*568*, *hsdR514*	(6, 7)
E. coli* JW2226 Δ*ubiG	3-demethylubiquinone-*8* 3-*O*-methyltransferase, 2-octaprenyl-6-hydroxyphenol methylase	F-, Δ*(araD-araB)567*, Δ*lacZ4787*(::*rrnB*-3), *λ*-, Δ*ubiG785::kan*, *rph*-1, Δ(*rhaD-rhaB*)*568*, *hsdR514*	(6, 7)
E. coli* JW2874 Δ*ubiI	2-octaprenylphenol hydroxylase	F-, Δ*(araD-araB)567*, Δ*lacZ4787*(::*rrnB*-3), *λ*-, Δ*ubiI757::kan*, *rph*-1, Δ(*rhaD-rhaB*)*568*, *hsdR514*	(6, 7)
E. coli* JW2308 Δ*ubiX	flavin prenyltransferase	F-, Δ*(araD-araB)567*, Δ*lacZ4787*(::*rrnB*-3), *λ*-, Δ*ubiX732::kan*, *rph*-1, Δ(*rhaD-rhaB*)*568*, *hsdR514*	(6, 7)
E. coli* JW3513 Δ*dppA	dipeptide ABC transporter periplasmic binding protein	F-, Δ(*araD-araB*)*567*, Δ*lacZ4787*(::*rrnB*-3), *λ*-, Δ*dppA728::kan*, *rph*-1, Δ(*rhaD-rhaB*)*568*, *hsdR514*	(6, 7)
E. coli* JW3513 Δ*dppA* pASK-*dppA	dipeptide ABC transporter periplasmic binding protein	F-, Δ(*araD-araB*)*567*, Δ*lacZ4787*(::*rrnB*-3), *λ*-, Δ*dppA728*,*rph*-1, Δ(*rhaD-rhaB*)*568*, *hsdR514*, pASK-*dppA*	this study
***E. coli* JW3513 Δ*dppA* pASK-empty**	dipeptide ABC transporter periplasmic binding protein	F-, Δ(*araD-araB*)*567*, Δ*lacZ4787*(::*rrnB*-3), *λ*-, Δ*dppA728*,*rph*-1, Δ(*rhaD-rhaB*)*568*, *hsdR514*, pASK-empty	this study
E. coli* JW3512 Δ*dppB	dipeptide ABC transporter membrane subunit	F-, Δ(*araD-araB*)*567*, Δ*lacZ4787*(::*rrnB*-3), *λ*-, Δ*dppB726::kan*, *rph*-1, Δ(*rhaD-rhaB*)*568*, *hsdR514*	(6, 7)
E. coli* JW3511 Δ*dppC	dipeptide ABC transporter membrane subunit	F-, Δ(*araD-araB*)*567*, Δ*lacZ4787*(::*rrnB*-3), *λ*-, Δ*dppC725::kan*, *rph*-1, Δ(*rhaD-rhaB*)*568*, *hsdR514*	(6, 7)
E. coli* JW3510 Δ*dppD	dipeptide ABC transporter ATP binding subunit	F-, Δ(*araD-araB*)*567*, Δ*lacZ4787*(::*rrnB*-3), *λ*-, Δ*dppD724::kan*, *rph*-1, Δ(*rhaD-rhaB*)*568*, *hsdR514*	(6, 7)

E. coli* JW3509 Δ*dppF	dipeptide ABC transporter ATP binding subunit	F-, Δ(*araD-araB*)*567*, Δ*lacZ4787*(::*rrnB*-3), *λ*-, Δ*dppF723::kan*, *rph*-1, Δ(*rhaD-rhaB*)*568*, *hsdR514*	(6, 7)
E. coli* JW1287 Δ*sapA	dipeptide ABC transporter periplasmic binding protein	F-, Δ(*araD-araB*)*567*, Δ*lacZ4787*(::*rrnB*-3), *λ*-, Δ*sapA730::kan*, *rph*-1, Δ(*rhaD-rhaB*)*568*, *hsdR514*	(6, 7)
E. coli* JW1286 Δ*sapB	peptide ABC transporter membrane subunit	F-, Δ*(araD-araB)567*, Δ*lacZ4787*(::*rrnB*-3), *λ*-, *ΔsapB729::kan*, *rph*-1, Δ*(rhaD-rhaB)568*, *hsdR514*	(6, 7)
E. coli* JW1285 Δ*sapC	dipeptide ABC transporter membrane subunit	F-, Δ(*araD-araB*)*567*, Δ*lacZ4787*(::*rrnB*-3), *λ*-, Δ*sapC728::kan*, *rph*-1, Δ(*rhaD-rhaB*)*568*, *hsdR514*	(6, 7)
E. coli* JW1284 Δ*sapD	dipeptide ABC transporter ATP binding subunit	F-, Δ(*araD-araB*)*567*, Δ*lacZ4787*(::*rrnB*-3), *λ*-, Δ*sapD727::kan*, *rph*-1, Δ(*rhaD-rhaB*)*568*, *hsdR514*	(6, 7)
E. coli* JW1283 Δ*sapF	dipeptide ABC transporter ATP binding subunit	F-, Δ(*araD-araB*)*567*, Δ*lacZ4787*(::*rrnB*-3), *λ*-, Δ*sapF726::kan*, *rph*-1, Δ(*rhaD-rhaB*)*568*, *hsdR514*	(6, 7)
E. coli* JW1235 Δ*oppA	oligopeptide ABC transporter periplasmic binding protein	F-, Δ(*araD-araB*)*567*, Δ*lacZ4787*(::*rrnB*-3), *λ*-, Δ*oppA750::kan*, *rph*-1, Δ(*rhaD-rhaB*)*568*, *hsdR514*	(6, 7)
E. coli* JW1236 Δ*oppB	oligopeptide ABC transporter membrane subunit	F-, Δ(*araD-araB*)*567*, Δ*lacZ4787*(::*rrnB*-3), *λ*-, Δ*oppB751::kan*, *rph*-1, Δ(*rhaD-rhaB*)*568*, *hsdR514*	(6, 7)
E. coli* JW1237 Δ*oppC	oligopeptide ABC transporter membrane subunit	F-, Δ(*araD-araB*)*567*, Δ*lacZ4787*(::*rrnB*-3), *λ*-, Δ*oppC752::kan*, *rph*-1, Δ(*rhaD-rhaB*)*568*, *hsdR514*	(6, 7)
E. coli* JW1238 Δ*oppD	oligopeptide ABC transporter ATP binding subunit	F-, Δ(*araD-araB*)*567*, Δ*lacZ4787*(::*rrnB*-3), *λ*-, Δ*oppD753::kan*, *rph*-1, Δ(*rhaD-rhaB*)*568*, *hsdR514*	(6, 7)
E. coli* JW1239 Δ*oppF	oligopeptide ABC transporter ATP binding subunit	F-, Δ(*araD-araB*)*567*, Δ*lacZ4787*(::*rrnB*-3), *λ*-, Δ*oppF754::kan*, *rph*-1, Δ(*rhaD-rhaB*)*568*, *hsdR514*	(6, 7)
E. coli* JW1322 Δ*mppA	peptide ABC transporter periplasmic binding protein	F-, Δ(*araD-araB*)*567*, Δ*lacZ4787*(::*rrnB*-3), *λ*-, Δ*mppA767::kan*, *rph*-1, Δ(*rhaD-rhaB*)*568*, *hsdR514*	(6, 7)
E. coli* JW2988 Δ*ygiS	putative deoxycholate binding periplasmic protein	F-, Δ(*araD-araB*)*567*, Δ*lacZ4787*(::*rrnB*-3), *λ*-, Δ*ygiS790::kan*, *rph*-1, Δ(*rhaD-rhaB*)*568*, *hsdR514*	(6, 7)
E. coli* JW5111 *ΔgsiB	glutathione ABC transporter periplasmic binding protein	F-, Δ(*araD-araB*)*567*, Δ*lacZ4787*(::*rrnB*-3), *λ*-, Δ*gsiB730::kan*, *rph*-1, Δ(*rhaD-rhaB*)*568*, *hsdR514*	(6, 7)
E. coli* JW5240 *ΔddpA	putative dipeptide ABC transporter periplasmic binding protein	F-, Δ(*araD-araB*)*567*, Δ*lacZ4787*(::*rrnB*-3), *λ*-, Δ*ddpA780::kan*, *rph*-1, Δ(*rhaD-rhaB*)*568*, *hsdR514*	(6, 7)
E. coli* JW3441 *ΔnikA	nickel ABC transporter periplasmic binding protein	F-, Δ(*araD-araB*)*567*, Δ*lacZ4787*(::*rrnB*-3), *λ*-, Δ*nikA730::kan*, *rph*-1, Δ(*rhaD-rhaB*)*568*, *hsdR514*	(6, 7)
***E. coli* JW0699 Δ*dtpD* (Δ*ybgH*)**	dipeptide:H^+ symporter	F-, Δ(*araD-araB*)*567*, Δ*lacZ4787*(::*rrnB*-3), *λ*-, Δ*ybgH759::kan*, *rph*-1, Δ(*rhaD-rhaB*)*568*, *hsdR514*	(6, 7)
***E. coli* JW1626 Δ*dtpA* (Δ*ydgR*)**	dipeptide/tripeptide:H^+ symporter	F-, Δ(*araD-araB*)*567*, Δ*lacZ4787*(::*rrnB*-3), *λ*-, Δ*ydgR784::kan*, *rph*-1, Δ(*rhaD-rhaB*)*568*, *hsdR514*	(6, 7)

***E. coli* JW4091 Δ*dtpC* (Δ*yjdL*)**	dipeptide/tripeptide:H^+ symporter	F-, Δ(*araD-araB*)*567*, Δ*lacZ4787*(::*rrnB*-3), *λ*-, Δ*yjdL757::kan*, , *rph*-1, Δ(*rhaD-rhaB*)*568*, *hsdR514*	(6, 7)
***E. coli* JW3463 Δ*dtpB* (Δ*yhiP*)**	dipeptide/tripeptide:H^+ symporter	F-, Δ(*araD-araB*)*567*, Δ*lacZ4787*(::*rrnB*-3), *λ*-, Δ*yhiP752::kan*, , *rph*-1, Δ(*rhaD-rhaB*)*568*, *hsdR514*	(6, 7)
E. coli* JW2143 Δ*lysP	lysine:H^+ symporter	F-, *Δ(araD-araB)567*, *ΔlacZ4787*(::*rrnB*-3), *λ*-, *ΔlysP783::kan*, *rph-1*, *Δ(rhaD-rhaB)568*, *hsdR514*	(6, 7)
E. coli* JW2303 Δ*hisP	histidine/lysine/arginine/ornithine ABC transporter, ATP binding subunit	F-, *Δ(araD-araB)567*, *ΔlacZ4787*(::*rrnB*-3), *λ*-, *ΔhisP778::kan*, *rph-1*, *Δ(rhaD-rhaB)568*, *hsdR514*	(6, 7)
E. coli* JW4093 Δ*cadB	lysine:cadaverine antiporter	F-, *Δ(araD-araB)567*, *ΔlacZ4787*(::*rrnB*-3), *λ*-, *ΔcadB759::kan*, *rph-1*, *Δ(rhaD-rhaB)568*, *hsdR514*	(6, 7)
E. coli* JW2305 Δ*hisQ	histidine/lysine/arginine/ornithine ABC transporter, membrane subunit	F-, *Δ(araD-araB)567*, *ΔlacZ4787*(::*rrnB*-3), *λ*-, *ΔhisQ780::kan*, *rph-1*, *Δ(rhaD-rhaB)568*, *hsdR514*	(6, 7)
E. coli* JW2306 Δ*hisJ	histidine ABC transporter, periplasmic binding protein	F-, *Δ(araD-araB)567*, *ΔlacZ4787*(::*rrnB*-3), *λ*-, *ΔhisJ730::kan*, *rph-1*, *Δ(rhaD-rhaB)568*, *hsdR514*	(6, 7)
E. coli* JW2307 Δ*argT	lysine/arginine/ornithine ABC transporter, periplasmic binding protein	F-, *Δ(araD-araB)567*, *ΔlacZ4787*(::*rrnB*-3), *λ*-, *ΔargT721::kan*, *rph-1*, *Δ(rhaD-rhaB)568*, *hsdR514*	(6, 7)
E. coli* JW2304 Δ*hisM	histidine/lysine/arginine/ornithine ABC transporter, membrane subunit	F-, *Δ(araD-araB)567*, *ΔlacZ4787*(::*rrnB*-3), *λ*-, *ΔhisM779::kan*, *rph-1*, *Δ(rhaD-rhaB)568*, *hsdR514*	(6, 7)
E. coli* Δ*dppA*Δ*sapA	multiple peptide transporters	F-, Δ(*araD-araB*)*567*, Δ*lacZ4787*(::*rrnB*-3), *λ*-, Δ*dppA728::kan*, Δ*sapA::cm*, *rph*-1, Δ(*rhaD-rhaB*)*568*, *hsdR514*	this study
E. coli* Δ*dppA*Δ*oppA	multiple peptide transporters	F-, Δ(*araD-araB*)*567*, Δ*lacZ4787*(::*rrnB*-3), *λ*-, Δ*dppA728::kan*, Δ*oppA::cm*, *rph*-1, Δ(*rhaD-rhaB*)*568*, *hsdR514*	this study
E. coli* Δ*dppA*Δ*dtpD	multiple peptide transporters	F-, Δ(*araD-araB*)*567*, Δ*lacZ4787*(::*rrnB*-3), *λ*-, Δ*dppA728*, Δ*ybgH759::kan*, *rph*-1, Δ(*rhaD-rhaB*)*568*, *hsdR514*	this study
E. coli* Δ*dppA*Δ*sapA*Δ*oppA	multiple peptide transporters	F-, Δ(*araD-araB*)*567*, Δ*lacZ4787*(::*rrnB*-3), *λ*-, Δ*dppA728*, Δ*sapA730*, Δ*oppA750::kan*, *rph*-1, Δ(*rhaD-rhaB*)*568*, *hsdR514*	this study
E. coli* Δ*dppA*Δ*sapA*Δ*oppA*Δ*dtpD	multiple peptide transporters	F-, Δ(*araD-araB*)*567*, Δ*lacZ4787*(::*rrnB*-3), *λ*-, Δ*dppA728*, Δ*sapA730*, Δ*oppA750*, Δ*ybgH759::kan*, *rph*-1, Δ(*rhaD-rhaB*)*568*, *hsdR514*	this study
E. coli* Δ*acrA	Multidrug efflux pump membrane protein	F-, *Δ(araD-araB)567*, *ΔlacZ4787*(::*rrnB*-3), *λ*-, *ΔacrA7480::kan*, *rph-1*, *Δ(rhaD-rhaB)568*, *hsdR514*	(6, 7)
E. coli* Δ*acrB	Multidrug efflux pump permease	F-, *Δ(araD-araB)567*, *ΔlacZ4787*(::*rrnB*-3), *λ*-, *ΔacrB747::kan*, *rph-1*, *Δ(rhaD-rhaB)568*, *hsdR514*	(6, 7)
E. coli* Δ*acrA*Δ*acrB	Multidrug efflux pump	F-, Δ(*araD-araB*)*567*, Δ*lacZ4787*(::*rrnB*-3), *λ*-, Δ*(acrB747-acrA748)::kan*, *rph*-1, Δ(*rhaD-rhaB*)*568*, *hsdR514*	this study

***Pseudomonas aeruginosa* PAO1**	reference strain	(8, 9)
***Staphylococcus aureus* ATCC 29213**	reference strain	(5)
***Bacillus subtilis* 168 trpC2**	*trpC2*	(10)

Table S4: Oligonucleotides used in this study.

Oligonucleotide	Sequence (5'-3')
Knockout generation	
oppA-H1-pKD3	AGAGAAGTTTAGTAGCAGCTGGCGTTCTGGCTGCGCTAATGGTGTAGGCTGGAGCTGCTTC
oppA-H2-pKD3	CCGGGTATAGGTATTATCCAGCGGATCTTTGCCGGTATAGCCATATGAATATCCTCCTTAG
sapA-H1-pKD3	TGAATCTCCCCCGCATGCTGATATCCGCGACAGCGGTTTTGGTGTAGGCTGGAGCTGCTTC
sapA-H2-pKD3	CCAGCAAAGGAGGCGTTACCAAACGGGCTAAGTACCAGACCATATGAATATCCTCCTTAG
dtpD-H1-pKD13	GCGCAACTATTACGTGACGTTGCCGTCAATTGTGGAATTATTATGTGTAGGCTGGAGCTG
dtpD-H2-pKD13	GCATCAGGCATCGGTGCTGGCCTATTAAGACTCCAGCGCCAGCGCATCCGGGGATCCGT
DppA complementation	
dppA-XbaI_for	TTGGTCTAGATTGGAGCAGAATAATGCGTA
dppA-XhoI_rev	TTGCCTCGAGTTGCCTTTGCCATCAGTCTT
Dpp operon PCR amplification and sequencing	
dppA-F-2	TGACAACTCGGTGACCTATG
dppA-F-1	GATTGACGAGGGCGTATCTG
dppA-F 0	CCGCCTTATTCGACCTACAC
dppA-F 1	CTCACCGTTGGTGTAAATCC
dppA-F 2	AAGGCATGGGCTTGCCAGAG
dppA-F 3	GCTGAAAGAAGCGGGTCTGG
dppA-F 4	CCATCCGGCAGCAATACTTC
dppA-F 5	CCGTCGCCCATATGATCTTG
dppA-F 6	ATGTGCTGTCGCGCCTGATG
dppA-F 7	GCATTTCGGCGACGAAAGCG
dppA-F 8	CGCGTCACCCGTATACTCAG
dppA-F 9	CGAGCACTATGACCGCTATC
dppA-F rev	ATTGTGTCGTGCCTCATTCC
dppA-F rev2	GCAGCGATCATTGCTTATCC
Characterization and sequencing of the 95 kb deletion including the *dpp* operon	
dpp-flank_for	GCAATAGATAACCACGGGAAGG
dpp-flank_rev	TTTACGGAAGGTCGTTACCAG
dpp-flank2_for	TTATTGCTTATACATGATC
dpp-flank3_for	ATGACGGTCAGATATTAT
Miscoding assay	
Luc-mut_for	ACTGCATAAGGCTATGTAGAGATACGCCCTGGT
Luc-mut_rev	ACCAGGGCGTATCTCTACATAGCCTTATGCAGT

References

1. Davis BD, Chen LL, Tai PC. 1986. Misread protein creates membrane channels: an essential step in the bactericidal action of aminoglycosides. Proc Natl Acad Sci U S A 83:6164-8.
2. Busse HJ, Wöstmann C, Bakker EP. 1992. The bactericidal action of streptomycin: membrane permeabilization caused by the insertion of mistranslated proteins into the cytoplasmic membrane of *Escherichia coli* and subsequent caging of the antibiotic inside the cells due to degradation of these proteins. Journal of General Microbiology 138:551-61.
3. Guo J, Miele EW, Chen A, Luzietti RA, Zambrowski M, Walsky RL, Buurman ET. 2015. Pharmacokinetics of the natural antibiotic negamycin. Xenobiotica 45:625-633.
4. Keseler IM, Mackie A, Santos-Zavaleta A, Billington R, Bonavides-Martinez C, Caspi R, Fulcher C, Gama-Castro S, Kothari A, Krummenacker M, Latendresse M, Muniz-Rascado L, Ong Q, Paley S, Peralta-Gil M, Subhraveti P, Velazquez-Ramirez DA, Weaver D, Collado-Vides J, Paulsen I, Karp PD. 2017. The EcoCyc database: reflecting new knowledge about *Escherichia coli* K-12. Nucleic Acids Res 45:D543-D550.
5. Patel JB, Cockerill FR, Bradford PA, Eliopoulos GM, Hindler JA, Jenkins SG, Lewis JS, Limbago B, Miller LA, Nicolau DP, Powell M, Swenson JM, Turnidge JD, Weinstein MP, Zimmer BL. 2015. Methods for dilution antimicrobial susceptibility tests for bacteria that grow aerobically. Approved Standard - Tenth Edition, vol 35. Clinical and Laboratory Standards Institute, USA.
6. Baba T, Ara T, Hasegawa M, Takai Y, Okumura Y, Baba M, Datsenko KA, Tomita M, Wanner BL, Mori H. 2006. Construction of *Escherichia coli* K-12 in-frame, single-gene knockout mutants: the Keio collection. Molecular Systems Biology 2:1-11.
7. Datsenko KA, Wanner BL. 2000. One-step inactivation of chromosomal genes in *Escherichia coli* K-12 using PCR products. Proceedings of the National Academy of Sciences of the United States of America 97:6640-5.
8. Holloway BW. 1955. Genetic recombination in *Pseudomonas aeruginosa*. J Gen Microbiol 13:572-81.
9. Stover C, Pham X, Erwin A, Mizoguchi S, Warrener P, Hickey M, Brinkman F, Hufnagle W, Kowalik D, Lagrou M. 2000. Complete genome sequence of *Pseudomonas aeruginosa* PAO1, an opportunistic pathogen. Nature 406:959-964.
10. Anagnostopoulos C, Spizizen J. 1961. Requirements for Transformation in *Bacillus subtilis*. Journal of Bacteriology 81:741-6.

4.2. Publication 2

ACS Infectious Diseases

pubs.acs.org/journal/aidcbc Article

Kanamycin Uptake into *Escherichia coli* Is Facilitated by OmpF and OmpC Porin Channels Located in the Outer Membrane

Jayesh Arun Bafna,[¶] Eulàlia Sans-Serramitjana,[¶] Silvia Acosta-Gutiérrez,[¶] Igor V. Bodrenko, Daniel Hörömpöli, Anne Berscheid, Heike Brötz-Oesterhelt,* Mathias Winterhalter,* and Matteo Ceccarelli*

Cite This: *ACS Infect. Dis.* 2020, 6, 1855−1865 Read Online

ACCESS | Metrics & More | Article Recommendations | Supporting Information

ABSTRACT: Despite decades of therapeutic application of aminoglycosides, it is still a matter of debate if porins contribute to the translocation of the antibiotics across the bacterial outer membrane. Here, we quantified the uptake of kanamycin across the major porin channels OmpF and OmpC present in the outer membrane of *Escherichia coli*. Our analysis revealed that, despite its relatively large size, about 10−20 kanamycin molecules per second permeate through OmpF and OmpC under a 10 μM concentration gradient, whereas OmpN does not allow the passage. Molecular simulations elucidate the uptake mechanism of kanamycin through these porins. Whole-cell studies with a defined set of *E. coli* porin mutants provide evidence that translocation of kanamycin via porins is relevant for antibiotic potency. The values are discussed with respect to other antibiotics.

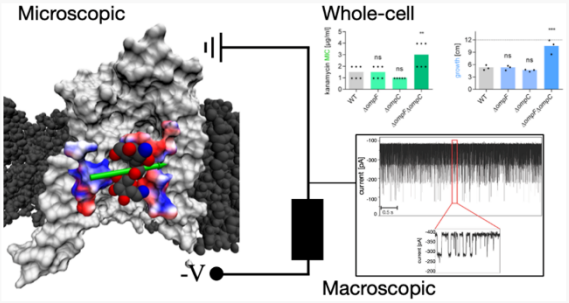

KEYWORDS: *E. coli, OmpF, OmpC, OmpN, bacterial porins, optimal transport*

The complex cell envelope of Gram-negative bacteria comprises two membranes: the outer membrane (OM) and the cytoplasmic membrane. The two membranes delimit the periplasmic space of the bacterial cell and prevent the accumulation of toxic agents in the cytosol while regulating the access of nutrients vital for growth and cell function. The OM is the first barrier during compound uptake. It is composed of an asymmetric bilayer: an inner leaflet of phospholipids and an outer leaflet of lipopolysaccharides (LPS). Both OM leaflets combined prevent the efficient diffusion of hydrophilic as well as hydrophobic molecules. Porins, water-filled channels spanning across the OM, enable passive diffusion of small, hydrophilic molecules into the periplasm. Substrate specificity is mainly defined by the constriction zone within the barrel structure of these porins, determining entry of molecules by factors such as size, shape, electric multipoles, and rigidity.[1−3]

E. coli encodes multiple porins. The major porins OmpF and OmpC are highly abundant and both cation-selective, and it has been thought that they restrict the passage to compounds with a size-exclusion limit of about 600 Da.[4] However, it has recently been suggested that this limit should be redefined using other parameters.[5,6] The translocation of several classes of antibiotics, e.g., β-lactams and fluoroquinolones, through porins has been investigated extensively. Also, porin modification emerged as antibiotic resistance mechanism in clinical isolates,[7] based on specific changes in amino acid residues or decreased expression of wild-type porins.[8]

Aminoglycosides (AGs) target the ribosome in the cytoplasm, thus they have to overcome both membranes in Gram-negative bacteria. Despite their frequent use as therapeutic agents, the mechanisms of their OM translocation remain incompletely understood. The self-promoted pathway is a proposed uptake mechanism. Here, divalent cations between LPS molecules are displaced by AGs, which leads to brief OM destabilization, thereby enabling OM translocation.[9] However, since AGs are both cationic and hydrophilic structures with a molecular size below 600 Da, they have also been hypothesized to diffuse through porins of *E. coli*. First in vitro assays using the liposome swelling technique had suggested translocation of various aminoglycosides through *E. coli* porins,[10] but whole-cell experiments were inconclusive and contradictory.[9,11]

Received: March 3, 2020
Published: May 5, 2020

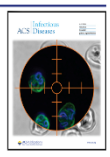

Table 1. Reversal Potential Permeability Measurements[a]

	(*trans*-side) (mM)		(GND/*cis*-side) (mM)				flux extrapolated to 10 μM ion gradient (molecules/s)	
channel	kanamycin	SO_4^{2-}	kanamycin	SO_4^{2-}	V_{rev}(mV)	$P = P_{Kan}^{4+}/P_{sulfate}^{2-}$	cations	SO_4^{2-}
OmpF	20	35	50	87.5	−8.7 ± 2.5	1:14	9	73
OmpC	20	35	50	87.5	−5.1 ± 0.6	1:4.2	16	20
OmpN	20	35	50	88.4	−12.0 ± 3	1:>600[b]	too low	
	(*trans*-side) (mM)		(GND/*cis*-side) (mM)				flux extrapolated to 10 μM ion gradient (molecules/s)	
channel	K^+	SO_4^{2-}	K^+	SO_4^{2-}	V_{rev}(mV)	$P = P_{K}^{+}/P_{sulfate}^{2-}$	cations	SO_4^{2-}
OmpF	100	50	500	250	10.7 ± 0.7	2.4:1	1,300	1,100
OmpC	100	50	500	250	13.4 ± 1.2	2.8:1	800	600
OmpN	20	10	100	50	33.5 ± 3.1	21:1	900	100

[a]Determined zero current potentials (V_{rev}) with standard deviation, calculated permeability ratios and flux-rate from the mean zero current potential. [b]Permeability ratio is too small to estimate the flux. The concentration value of SO_4^{2-} is also determined by the addition of $H_2SO_4^2$ used to adjust the buffer pH.

To elucidate the passage of AGs through *E. coli* porins, we characterized the permeability of kanamycin through three outer membrane porins of *E. coli*, namely, OmpF, OmpC, and the structurally similar OmpN. We quantified the uptake by an electrophysiological zero-current assay using concentration gradients of kanamycin under bi-ionic conditions, and combined it with single-channel measurements to determine the net flux of kanamycin.[12,13] Our single-channel study in the presence of low amounts of kanamycin revealed clear blockages. Thus, we analyzed also the change in event rates with increasing transmembrane applied voltage. To reveal the main interactions of kanamycin while diffusing along the pore, we examined the translocation event of kanamycin through OmpF and OmpC employing enhanced sampling molecular dynamics simulations. We could confirm these new insights in whole-cell assays, where the double deletion of both porin genes *ompF* and *ompC* decreased kanamycin susceptibility. A single deletion of only one of these porins had no detectable effect on kanamycin resistance, which corroborates that both major porins OmpF and OmpC play a role in kanamycin translocation across the OM of *E. coli*. Combining the electrophysiological data, all-atom simulations, and whole-cell results, we conclude that both OmpF and OmpC are permeable to kanamycin.

■ RESULTS

Experimental Flux Quantification Using Reversal Potential Measurements. We have previously shown that the net flux of charged compounds driven by a concentration gradient can be estimated from the experimentally accessible reversal potential, in combination with single channel conductance recordings.[12] In a first series of experiments, the three porins of interest from the *E. coli* outer membrane (OmpF, OmpC, and OmpN) were reconstituted into a planar bilayer, and the single channel currents in the presence of kanamycin sulfate, and potassium sulfate as control, were recorded. Table S1 summarizes the conductance measurements of the three *E. coli* porins obtained in symmetrical 20 mM kanamycin sulfate or K_2SO_4 at pH 7 and ΔV = +100 mV. Due to the diverse size of the cations (kanamycin versus K^+, see Table S3 for a comparison with pore sizes), the single trimeric channel conductance with K_2SO_4 was substantially higher than that with kanamycin sulfate: 240 pS vs 16 pS, respectively, for OmpF. Moreover, OmpF conductance was comparable to that of OmpC, whereas OmpN conductance was significantly lower (16:13:9.5 pS in case of kanamycin sulfate or 240:180:58 pS in case of KCl).

To further quantify the concentration-driven flux, we applied a concentration gradient and recorded the induced voltage to obtain the permeability ratio. The latter was obtained by fitting the experimental $I-V$ curves to the Goldman−Hodgkin−Katz (GHK) current equation.[14] Despite the fact that the assumptions of the GHK-theory (point-like noninteracting ions in a homogeneous electric field) are not fulfilled, we expect in general a reasonably good prediction for the ion permeability ratio.[12] We used a bi-ionic symmetrical 20 mM concentration of kanamycin and 35 mM of the sulfate salt on both sides of the membrane containing, respectively, OmpF, OmpC, or OmpN porins (the difference in the SO_4^{2-} concentrations is due to the titration of H_2SO_4 for adjusting the pH to 7). The *cis* compartment was then supplemented with 50 mM of kanamycin and 87.5 mM of the sulfate salt and the zero-current-potential was measured (Figure S1A−C). As summarized in Table 1, the reversal potentials, in the case of kanamycin sulfate, are negative for the same ionic concentrations *cis*/*trans* for the three porins assessed, with the maximal reversal potential value for the OmpN porin. This implies that anions permeate faster compared to cations in all three channels, with OmpN almost impermeable to kanamycin. In contrast, the reversal potentials in the case of potassium sulfate are positive for the same ionic concentration gradients *cis*/*trans* for the three porins studied, with the highest cation selectivity for OmpN. Our results are in agreement with the qualitative observation of the permeation specificities by Nikaido and Prilipov et al.[15,16]

In a second series of measurements, we recorded the permeation of single kanamycin with single channel electrophysiology. Reconstituted OmpF, OmpC, or OmpN showed a stable conductance in their open conformation. In the membrane potential range used in these experiments, from −150 to +150 mV, the channel open conductance is ohmic, with ≈4 nS for OmpF, ≈2.7 nS for OmpC, and ≈1.6 nS for OmpN, all at 1 M KCl. Throughout this study, the membrane potential was defined as positive on the *trans*-side of the chamber, the *cis*-side being the virtual ground, and the respective channel was inserted into the bilayer from the *cis*-side of the chamber, unless otherwise noted.

After successful single channel reconstitution was achieved, the ion current was recorded for 30 s at each applied potential from (+150 to −150 mV), then 10 μM of kanamycin sulfate

https://dx.doi.org/10.1021/acsinfecdis.0c00102
ACS Infect. Dis. 2020, 6, 1855−1865

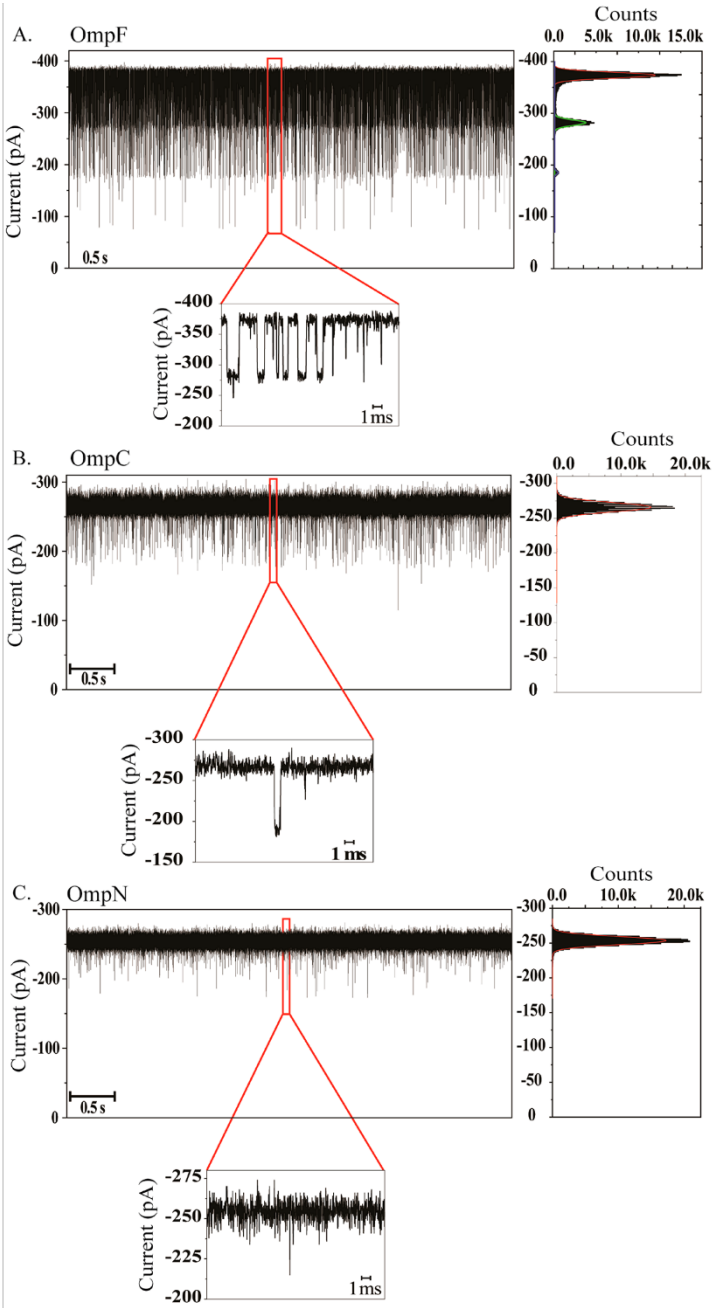

Figure 1. Ion current traces in the presence of kanamycin. Single channel measurements of (A) OmpF, (B) OmpC, and (C) OmpN in the presence of 10 μM kanamycin sulfate in 1 M KCl, 10 mM HEPES at pH 7. A is the single channel trace of OmpF in the presence of kanamycin sulfate at an applied potential of −100 mV. Its corresponding zoom of the events are below and all point histogram are on the right. Similarly, B and C show, respectively, the traces of OmpC and OmpN, with their zoomed events and all point histograms.

was added to the *cis*-side of the chamber and their translocation was investigated under the applied membrane potential (note the solution was buffered with 10 mM HEPES, the pH was stable at pH 7). The entry of kanamycin molecules into the constriction zone of the porin causes a resolvable reduction in the open pore conductance with resolvable dwell times (τ_d > 0.1 ms)), referred to as "events" in this work.

Figure 1A−C shows the current traces of the porins in the presence of 10 μM of kanamycin sulfate with resolvable events at a membrane potential of −100 mV. We analyzed the event rates f_e and mean dwell times τ_d, to assess the translocation of these molecules through these general diffusion porins, where τ_d is obtained from fitting an exponential to the distribution of dwell times and N_e is the number of events in a given time

https://dx.doi.org/10.1021/acsinfecdis.0c00102
ACS Infect. Dis. 2020, 6, 1855−1865

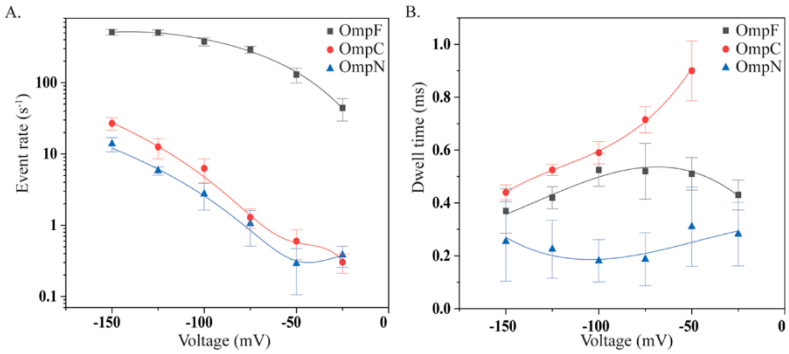

Figure 2. Event rates and dwell times. Statistical analysis of the traces measured at different applied voltages for OmpF, OmpC, and OmpN of Figure 1. (A) Event rate f_e vs applied negative voltages. Increasing the negative voltage pulls more cationic kanamycin molecules into the channel. (B) Dwell time analysis. In the case of OmpC, higher negative voltage drives kanamycin faster through the channel, whereas in OmpF only voltages above −75 mV reduce the residence time. Note that at low voltages up to −75 mV kanamycin is less prone to permeate and is rather pushed against the inner barrier. In contrast for OmpN, the dwell time is independent of the voltage indicating mainly nontranslocating events. The black, red, and blue lines are intended to serve as guidelines for the reader to follow the data points.

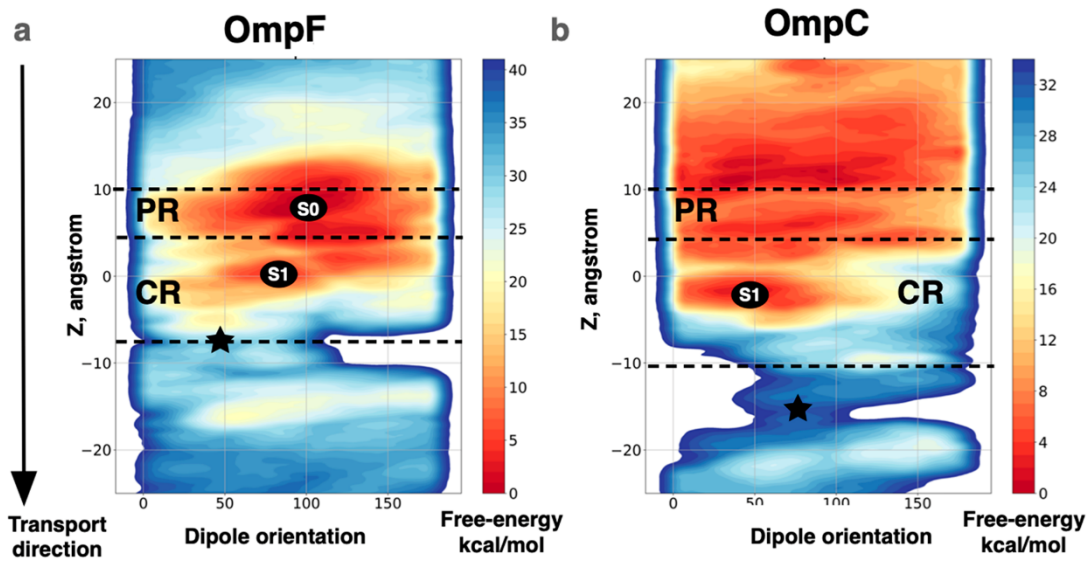

Figure 3. Kanamycin permeation path through OmpF and OmpC. Qualitative free energy surface for a single kanamycin translocation event showing the region of main interactions. The relevant conformations for kanamycin transport through OmpF (a) and OmpC (b) are highlighted. The ion current blocking states are highlighted as S1 and the bottleneck for transport (the energetic saddle point) as a star. The key regions for transport are delimited and labeled, e.g., PR (preorientation region) and CR (constriction region)

interval. For calculation of τ_d, f_e at least ∼1000 events were analyzed.

The results of the analysis of τ_d and f_e are shown in Figure 2 for OmpF, OmpC, and OmpN. The event rate increases throughout. However, an event rate itself does not allow drawing conclusions on the translocation.[17] The decrease of the dwell time at high voltage is a signature of translocation. In the case of OmpF, Figure 2B (black filled squares) shows the maximum of dwell time at around −75 mV. This may indicate that kanamycin ions translocate with higher probability through OmpF above this potential, although a significant increase in f_e is observed (Figure 2A, filled black squares).[18] In case of OmpC, we see a clear trend in the dwell time pattern (decreasing dwell time with increasing transmembrane potential), which again may hint toward the enhanced translocation of kanamycin through OmpC. From the permeability ratios obtained by reversal potential measurements of OmpF and OmpC, we see that kanamycin should permeate better through OmpC than OmpF at low concentrations (Table 1). However, the event rate f_e in OmpF shows saturation at high voltages, which is not observed for OmpC. When extrapolating the flux obtained at high concentrations (reversal potential) to low concentrations (single channel), one needs to account for the saturation of OmpF. Indeed, we expect both values to be rather similar at low kanamycin concentrations. While OmpN shows an increasing number of event rates (Figure 2A, blue filled triangles) at high voltages, their respective dwell times shown in Figure 2B (blue filled triangles) are voltage independent,

https://dx.doi.org/10.1021/acsinfecdis.0c00102
ACS Infect. Dis. 2020, 6, 1855−1865

which means rather caused by short-lived (bounce back) events.[18]

Translocation Mechanism through the Main Porins of *E. coli* (Molecular Dynamics). Starting from the available high-resolution structures of OmpF and OmpC, we used enhanced sampling molecular dynamics simulations (metadynamics) to provide an atomistic view of the main interactions of kanamycin within the channel, when translocating from CIS to TRANS. In previous works,[6,19−21] two crucial regions for small molecule translocation along the transport direction (*Z*, Figure 3) were identified in OmpF: (i) the preorientation region (PR), (from 5 Å < *Z* < 10 Å; Figure 3) with R167, R168, and D121 as key motifs allowing the binding of ampicillin and other dipolar molecules;[21,22] (ii) the constriction region (CR) (from 5 Å < *Z* < −5 Å; Figure 3) whose key motifs are the positively charged residues of the basic ladder (R42, R82, R132, K16) and the negatively charged residues of the constricting loop L3 (D113 and E117).

Both regions are characterized by a strong electric field component perpendicular to the axis of diffusion, more intense in the CR than in the PR[20,21] (Figure S2b). One striking difference between the porins is that in OmpF the transversal electric field is always higher than that in OmpC,[6] as reported in Figure S2b. In the case of kanamycin transport through OmpF, the first deep minimum (Figure 3a, state S0) is located in the PR. As it can be observed in Figure 4b,c, in this position and due to its size (71 Å^2, Figure 4a, and Table S3), kanamycin already interacts with two of the negatively charged key motifs of the CR, E117 and D121 of loop L3. Its total dipole moment is aligned to the transversal electric field of the pore (Figure 4b); however, kanamycin does not completely block the pore at this position.

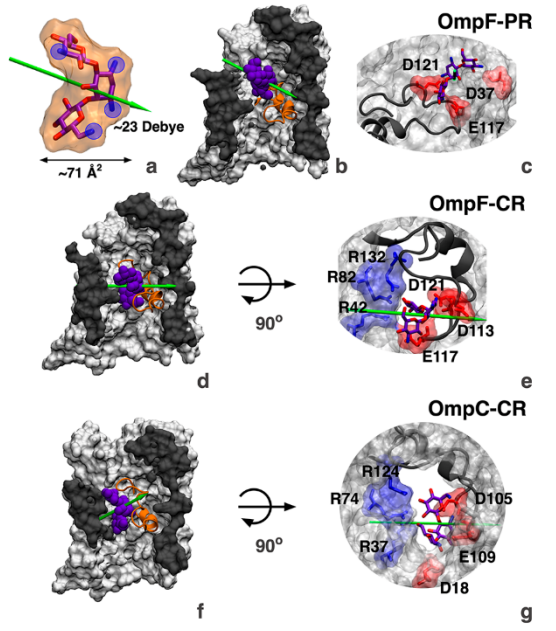

Figure 4. Structure of kanamycin and main conformations along the translocation path in OmpF and OmpC. (a) Licorice representation of kanamycin with its van der Waals surface superimposed in orange, dipole moment in green and positively charged groups highlighted in blue. Kanamycin (represented as violet van der Waals spheres) position with respect to the main diffusion axis of the pore (partial surface representation) in the main conformations during permeation through OmpF (b, d) and OmpC (f). Kanamycin interactions with charged groups from the walls of the pore are depicted in licorice for each conformation panels (c, e, g).

From this position, kanamycin misaligns its dipole moment in order to approach the CR, attracted by the other two negatively charged motifs of the loop L3, E117, and D113 (Figure S2, S3, states 2 and 3). In the second minimum S1 of Figure 3, kanamycin is located in the narrowest region of the CR (Figure 4d), again with its dipole moment fully aligned to the transversal electric field. It interacts with all key charged motifs of the eyelet, namely, the positively charged arginines R42, R82, R132 and the negatively charged D113, E117, and D121 (Figure 4e). As it can be seen now, kanamycin completely blocks the pore. The energetic bottleneck for kanamycin transport is the exit of the CR. As it can be seen from the main interactions in the saddle point conformation, Figure 3 (saddle-point indicated with a star), the interactions of kanamycin with the charged motifs of the loop L3 are very strong (Figure S3, state 0).

In the case of the kanamycin transport through OmpC, fewer steps seem to be relevant in the transport process (Figure S2c, bottom panel). The capture of kanamycin in OmpC (Figure 3, Figure S4) is less pronounced than in OmpF, probably due to the smaller electric field in the preorientation region. Conversely to OmpF, in OmpC kanamycin does not interact with the charged key motifs of the loop L3 when located in the PR, but it interacts mainly with the walls and the loop L2 of the monomer 2 (Figure S4, states 1−2). Once inside the CR (Figure 3b: S1), kanamycin aligns its dipole moment to the transversal electric field of the pore (Figure 4f), interacting with the main charged motifs of the OmpC eyelet, namely the positively charged arginines R37 and R74 and the negatively charged residues of the loop L3 (D105, E109, and D113). As in OmpF, the main energetic bottleneck is the exit from the CR, due to the strong interactions with its charged motifs (Figure S4, state 0).

In order to further investigate the two blocking-states identified respectively for OmpF and OmpC, we performed 4 single replica simulations of OmpF/OmpC with kanamycin inside the eyelet and with an applied voltage of −100 mV (Figure S5). The four replicas were stable and retained the interactions with the pore for the whole length of the simulation, as it can be observed in Figure S5a. The probability distribution of the distance of the center of mass of kanamycin to the blocking site in OmpF is centered in ∼1 Å ± (Figure S5a, upper panel). We observed that although kanamycin is predicted to block the cation (K^+, blue) passage almost completely, on average 1 K^+ translocates compared to 33 K^+ in the empty trimer (Figure S5b, upper panel, and Table S2); it does not block anions (Cl^-, red), instead it is predicted to enhance their passage, as we have 8 Cl^- on average that can pass compared to 5 in the empty trimer (Figure S5b, upper panel, and Table S2). The same is predicted with OmpC: the presence of kanamycin in the CR blocks partially the passage of cations (on average 3K^+ versus 39 K^+ in the empty trimer, Figure S5b and Table S2), while it somehow enhances the flux of anions, as on average 15 Cl^- translocate in the presence of kanamycin, while in the empty trimer 3 Cl^- go through (Figure S5b, lower panel, and Table S2).

Whole-Cell Assays. The experiments with purified proteins as well as the numerical simulations indicated

https://dx.doi.org/10.1021/acsinfecdis.0c00102
ACS Infect. Dis. 2020, 6, 1855−1865

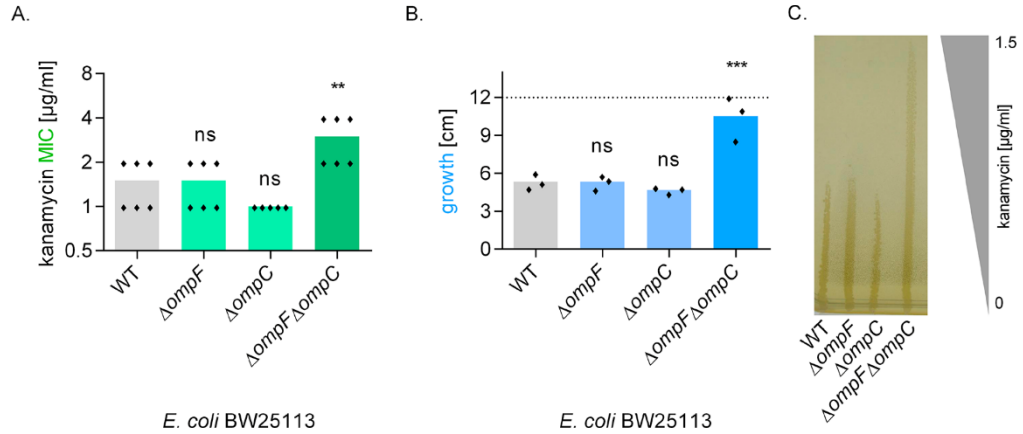

Figure 5. Role of porins in kanamycin susceptibility of *E. coli* BW25113. (A) The kanamycin MIC is significantly increased when both major porin genes *ompF* and *ompC* are deleted, while single porin knockout strains did not show increased resistance. MIC values are represented on a logarithmic scale. (B, C) The same trend could be observed when *E. coli* porin mutant strains were streaked on agar plates with a linear kanamycin gradient. The dotted line represents the maximal length of the plate. One representative biological replicate of B is shown in C. Each diamond represents one independent measurement from a different day. The vertical colored bars show the arithmetic mean of all data points. Statistical analysis was done using unpaired Student's *t*-test with Holm−Bonferroni correction, comparing the mutants to the wildtype (WT) strain. not significant (ns), $P > 0.05$; **, $P \leq 0.01$; ***, $P \leq 0.001$.

permeation of kanamycin through both major porins OmpF and OmpC. To validate the relevance of these observations in bacterial cells, we determined the kanamycin susceptibility of different porin mutants. We employed the single-gene deletion mutants of *ompF* and *ompC* from the Keio collection and generated in the current study a double deletion strain missing both of these major porin genes.[23] Kanamycin susceptibility was measured by a standard assay for the determination of the minimal inhibitory concentration (MIC) as well as by streaking of the *E. coli* strains on an agar plate containing a linear kanamycin gradient. *E. coli* missing either *ompF* or *ompC* alone (single knockout strains) showed similar susceptibility to kanamycin as the wild type parent strain *E. coli* BW25113 (Figure 5). However, the double deletion strain *E. coli* Δ*ompF*Δ*ompC* showed a clear and statistically significant decrease in kanamycin susceptibility. This result indicates that kanamycin is able to use both porins, *ompF* as well as *ompC* for outer membrane translocation and that a single deletion of either porin still leaves the other available. Similar observations were made with the further aminoglycosides paromomycin, amikacin, and gentamicin (Figures S6 and S7), and data for aminoglycosides were compared to β-lactams and fluoroquinolones, representatives of which were previously shown to pass through OmpF and OmpC (Figure S8 and Table S4). Importantly, although the susceptibility to aminoglycosides was clearly and reproducibly decreased in the Δ*ompF*Δ*ompC* double knockout strain, the absolute value of the MIC increased only about 2-fold. This finding indicates that at least one further translocation mechanism, such as self-promoted uptake[9] and/or one or more further porin(s), is still available for the AGs as option to cross the OM of *E. coli*.

■ DISCUSSION

The combination of two independent experimental techniques and molecular dynamics simulations showed that kanamycin can translocate through OmpF and OmpC, but not through OmpN. In both OmpF and OmpC, kanamycin shows strong interactions with the pore wall, especially with the anionic residues of the loop L3, due to its positive charge. Further, the orientation of its dipole, transversal to the long axis of the molecule itself (Figure 4a) allows the accommodation of kanamycin in the pore with its long axis parallel to the axis of diffusion and, at the same time, with the dipole aligned to the transversal electric field (Figure 4d,e,f,g). From a structural point of view, kanamycin adapts perfectly to the geometry of the pore and its electrostatics. The negative electrostatic potential inside both OmpF and OmpC[6] creates the condition for quite strong binding of cationic molecules such as kanamycin, as shown from the current traces in Figure 2 and simulations data in Figure 3 and Figure 4. This is not the case for OmpN. Though more selective for small cations (K^+), it has a pore not compatible with the dimension of kanamycin (the minimal pore radius is smaller than 1 Å, as it can be estimated from comparison of the K_2SO_4 conductivity for all the pores, see Table S1). The reversal potential method confirms that no translocation events occur in OmpN (Table 1).

It is worth to note that kanamycin has an average minimal projection area of 71 Å^2 (see Table S3). Among small-molecule antibiotics presented in a recent database,[24] only ceftazidime and piperacillin show the size comparable to kanamycin, respectively, 68 Å^2 and 77 Å^2, while all the other antibiotics have the minimal projection area that does not exceed 60 Å^2 (see Table S3). Interestingly, both ceftazidime and piperacillin are anionic, so they are not favored to translocate through negatively charged OmpF and OmpC. However, ceftazidime has been shown to translocate through OmpF and with low numbers through OmpC,[25] while the larger piperacillin showed extremely low permeability through both of them.[6] In our study we observed a low MIC increase for ceftazidime and none at all for piperacillin upon *ompF* and *ompC* double deletion (see Figure S8 and Table S4). Kanamycin, larger than ceftazidime, can go through OmpF and OmpC with comparable numbers thanks to a larger dipole moment, especially for the transverse component (Table S3). This is the electrostatic compensation of the steric barrier.

https://dx.doi.org/10.1021/acsinfecdis.0c00102
ACS Infect. Dis. 2020, 6, 1855−1865

The simulations of the translocation of kanamycin through OmpF showed the existence of an additional binding site in the preorientation region (Figure 4b,c), exactly where the dipolar and zwitterionic ampicillin and norfloxacin showed strong interactions.[21,22] In this conformation, kanamycin's dipole can be aligned along the transversal electric field. However, due to the relatively large pore size there, there is no complete blockage of the passage of the small ions. This correlates with the presence of two different conduction levels in OmpF, see histogram on Figure 1A. This second site works also as a reservoir, accumulating kanamycin from the solvent, thus causing the saturation seen in Figure 2A.

The insights from these biophysical and computational experiments could be transferred to and confirmed in living *E. coli* cells. *E. coli* mutants, lacking one or both major porins, were exposed to kanamycin in different experimental setups and a resistance phenotype emerged, when OmpF and OmpC were missing in parallel (Figure 5). Previous investigations on the role of OmpF and OmpC in kanamycin resistance had been contradictory. In an early publication, the OmpF-deficient strain *E. coli* JF703 displayed increased kanamycin resistance.[11] However, this strain was also polymyxin B-resistant,[11] suggesting that it might carry further mutations besides that of *ompF*. In a later study, no effects on kanamycin MICs could be observed for *E. coli* single mutants of *ompF* and *ompC* or in a regulator mutant lacking both porins.[9] In the current study, we constructed a markerless *ompF ompC* double knockout strain, and compared it to its isogenic wildtype and both markerless single knockout strains, using two different antimicrobial assay read-outs and conducting multiple experimental repetitions for statistical validation. While we corroborate that a single deletion of either *ompF* or *ompC* does not change the susceptibility of *E. coli* to different AGs, the double deletion of both major porins reduces susceptibility by a factor of 2. This finding indicates, on the one hand that both porins contribute to AG uptake in *E. coli* and on the other hand it demonstrates that their impact is rather limited. Besides OmpF and OmpC, AGs have further means of entering *E. coli*. A different porin could potentially be involved, it is also widely accepted that the polycationic AGs displace divalent cations from the LPS molecules, thereby forcing their passage across the destabilized outer membrane by self-promoted uptake.[26−28] The concept that AGs have multiple and independent means of crossing the outer membrane is reflected by the fact that uptake mutations are not the focus of clinical resistance development. Indeed, AG resistance is mostly based on acquired and plasmid-transferable AG-modifying enzymes or 16S rRNA methyltransferases.[29]

Besides, we determined additional MIC values for a number of antibiotics from different classes (see Figure S8 and Table S4). Several factors contribute to the MIC value (e.g., target affinity, efflux, porin-mediated and additional porin-unrelated uptake routes, environmental conditions). Although antibacterial agents are often grouped within the same antibiotic class according to a related pharmacophore and corresponding mode of action, they are different structural entities that are influenced by the range of these factors to a different extent. Interestingly, the change in MIC upon porin deletion of AG is in the range found for some cephalosporins and penicillins (e.g., ceftazidime, ceftriaxone, carbenicillin). In addition, kanamycin needs further translocation across the inner cell membrane to reach its target. Despite the relatively low flux value, the periplasmic space might be rapidly equilibrated and the passage through both porins has only a small effect on the activity.

Inspection of previous investigations on concentration driven flux through OmpF at a 10 μM gradient revealed 600 molecules/s for avibactam,[30] 350 molecules/s for cefotaxime (unpublished), 240 molecules/s for ampicillin,[31] and 10−20 molecules/s of kanamycin, but also substantially lower values for cefepime[32] (0.035 molecules/s, extrapolated from on-rates, without counting fast events[33]). These expected fluxes will enter the periplasm of bacteria. To estimate the number of molecules after equilibration inside bacteria, we assumed a sphere with a radius of 1 μm size mostly filled by biomass. This may allow for a few thousand antibiotics at 10 μM. Assuming further a few hundreds to thousands of channels, the concentration equilibrium will be easily achieved within a few seconds also for kanamycin. Other techniques based on single cell fluorescence using fluoroquinolones or mass spectrometry determined that the equilibrium between the inner and the outer concentration occurs within a few minutes.[5,34,35] Porins are the limiting factors for the efficacy of an antibiotic either (i) when there are no alternative uptake pathways and the number of porins is low, or (ii) when the rate of entry is very low. In the case of kanamycin, two highly abundant porins are used and further uptake routes (i.e., self-promoted uptake) contribute in addition.

■ CONCLUSIONS

Although aminoglycosides are a mainstay of clinical anti-Gram-negative therapy, their molecular uptake mechanism has remained a matter of debate. In our interdisciplinary study we tackled the problem by a complementary biophysical, computational, and microbiological approach and demonstrate the involvement of the porins OmpF and OmpC in kanamycin translocation across the OM on three different levels: the reconstituted proteins, pore structure, and growing bacterial cells. By describing and quantifying the transport of kanamycin through three different pores, with increasing size (OmpN, OmpC, OmpF) and with inverted increased selectivity to small cations, we were able to investigate the role of the steric term and the electrostatic compensation. In OmpN, the small open pore does not allow the translocation. In OmpC, the higher negative charge compared to OmpF is enough to compensate for the smaller size. Finally, the largest pore, OmpF, shows reduced flux due to the presence of an additional binding site near the mouth of the channel. This example provides a clear picture of optimal transport through a size-constricted pore combining electrostatic compensation of a steric barrier. Kanamycin with its cylindrical shape can fit perfectly well into the constriction region. At the same time, the position of the four positively charged groups provides a dipole that can align to the transversal electric field, thus allowing a binding near the constriction region and compensating the steric barrier while translocating. Eventually, about 10−20 kanamycin molecules per second can permeate through OmpF and OmpC under a 10 μM concentration gradient, and whole-cell studies provided evidence that translocation of kanamycin via porins is relevant for antibiotic potency, though other uptake mechanisms are not excluded.

■ METHODS

Materials. Kanamycin sulfate and cefoxitin sodium salt were obtained from Carl Roth (Mannheim, Germany),

https://dx.doi.org/10.1021/acsinfecdis.0c00102
ACS Infect. Dis. 2020, 6, 1855−1865

gentamicin sulfate from Applichem PanReac (Darmstadt, Germany), paromomycin sulfate from Cayman Chemical (Michigan, U.S.A.), amikacin disulfate from Acros Organics (Geel, Belgium) potassium sulfate salt from Sigma-Aldrich (Dorset, United Kingdom), and 1,2-diphytanoyl-*sn*-glycero-3-phosphocoline from Avanti Polar Lipids (Alabaster, AL), and all other chemicals used were procured from AppliChem. The proteins were produced in house following previous publications[18] and the SI.

Planar Lipid Bilayer and Electrical Recording: Single and Multichannel Measurements. Single channel recording apparatus consisted of a two-compartment Teflon chamber (~2.5 mL each) separated by a 25 μm thick Teflon partition with an aperture of ≈100 μm diameter for membrane formation. Bilayer lipid membranes were formed from 1,2-diphytanoyl-*sn*-glycero-3-phosphocholine (DPhPC) using the monolayer opposition technique.[36] The aperture was pretreated with a hexadecane/hexane solution (1% v/v) and was allowed to cure for ~20 min to achieve solvent evaporation. The *trans*- and *cis*-sides of the chambers were filled with buffer solution, 1 M KCl, 10 mM HEPES at pH 7.0. Ten μL of lipid in pentane (5 mg/mL) was added to both sides of the chamber, and a bilayer was formed after evaporation of pentane. Single channel reconstitution was achieved by addition of purified OmpF or OmpC porins into the *cis*-side of the chamber at a volume of ≈0.3 μL from their stock solutions (1 mg/mL) and diluted by ~100 fold using Genapol X-080 (1% v/v). The final protein concentration in the chamber was ≈1 pM. Channel current traces were recorded with Ag/AgCl pellet electrodes (World Precision Instruments), the *cis* side of the chamber being the virtual ground, using the Axopatch 200B (Molecular Devices, LLC) patch-clamp amplifier in V-clamp mode (whole cell β = 1) with a CV-203BU headstage. The output signal was filtered by a lowpass Bessel filter at 10 kHz and saved at a sampling frequency of 50 kHz using an Axon Digidata 1440A digitizer (Molecular Devices, LLC). Data analysis was performed with an in-house analysis suite created with the LabVIEW software suite (National Instruments).

Further, for measuring the electrophysiological reversal potential assay (Multi channel) for asymmetric condition we used commercial calomel electrodes (Metrohm). The *cis* side electrode of the cell was grounded, whereas the *trans* side electrode was linked to the headstage of an Axopatch 200B amplifier in the voltage clamp mode. Signals were filtered by an on-board low pass Bessel filter at 10 kHz with a sampling frequency of 50 kHz. Analysis of the current recordings was completed using Clampfit (Axon Instruments). The relative permeability of cations vs solute anions in the bi-ionic case ($P_{kanamycin^{4+}}/P_{sulfate^{2-}}$)) were obtained by fitting of the experimental $I-V$ curves with the Goldman−Hodgkin−Katz current equation.[37] The flux was estimated using the permeability ratios between the cation over anion flux and an estimation of the ion current induced by a reversal potential.[12,13,37]

All-Atom Molecular Dynamics Simulations. The experimental X-ray structures of OmpF and OmpC (PDB ID: 2OMF, 2J1N) were used as starting coordinates for molecular dynamics (MD) simulations. All the amino acid residues were simulated in the ionization state at neutral pH except for the E296 (OmpF) and D299 (OmpC) which were protonated (net charge 0) as suggested by Varma et al.[38] For both systems the entire trimer was embedded in a pre-equilibrated POPC (1-palmitoyl-2-oleoyl-*sn*-glycero-3-phosphocholine) bilayer of 259 lipids. The system was oriented in order to center the protein at the origin of the coordinate system and align the channel along the z-axis (positive z: extracellular side; negative z: periplasmic side). Thus, we solvated it in a 150 mM KCl solution. The selected force fields were as follows: AMBER14SB[39] for the protein, AMBER lipid14[40] for the POPC molecules, TIP3P[41] for water. After 1 ps of energy minimization (conjugate gradients), a slow heating from 10 to 300 K was carried out for 1 ns. During this stage, positional restraints were applied on the protein α-carbons (all three dimensions) as well as on the lipids phosphorus atoms (along z only). After releasing the constraints on the POPC, an equilibration stage follows for 4 ns in the NPT ensemble at 1.0 bar and 300 K. Finally, 0.6 μs MD simulations were performed in the NVT ensemble after the elimination of the protein restraints. The NPT equilibration was performed with the program NAMD,[42] with 1.0 fs time-step, and treating long-range electrostatics with the soft particle mesh Ewald (SPME) method (64 grid points and order 4 with direct cutoff at 1.0 nm and 1.0 Å grid-size). Pressure control was applied using the Nose-Hoover method (extended Lagrangian) with isotropic cell, integrated with the Langevin Dynamics (200 and 100 fs of piston period and decay, respectively). The latter was also applied for temperature control with 200 fs thermostat damping time. Production run in the NVT ensemble with a time step of 4 fs was performed through the ACEMD code[43] compiled for GPUs. The Langevin thermostat was used with 1 ps damping time. SPME was used to treat the electrostatics as for the equilibration stage.

The GAFF force-field parameters[44] were used to describe kanamycin (PubChem: CID 6032). Partial atomic charges were evaluated according to the RESP approach:[45] the molecule was first optimized at the HF/6-31G(d) level, up to a convergence in energy of 10^{-5} au, using the Gaussian03 package.[46] Atomic RESP charges were derived from the electrostatic potential using the antechamber module of the AMBER package.[47] The minimal projection area and the charge at different pH were calculated with the software Marvin.[48]

Starting from the final configuration of the OmpF and OmpC simulation described above, the molecule was placed outside the lumen of the first monomer. The difference between the z-coordinate of the center of mass (COM) of the antibiotic and the z-coordinate of the COM of the protein monomer was 32 Å. A thousand steps of energy minimization were performed. The equilibration stage followed for 1 ns in the NVT ensemble at 300 K as described hereinbefore. Well-tempered metadynamics[49,50] simulation were performed with the ACEMD code[43] combined with PLUMED,[51] until the first effective translocation through the protein constriction region (CR) was observed. Two biased collective variables were used, namely, the antibiotic position and the projection of the dipole moment of the antibiotic onto the z-axis of the channel. In practice, the "position" Δz was defined as the difference of the z-coordinate between the COM of the antibiotic and that of the porin first monomer. During the metadynamics run, energy biases were added every 50 ps to each collective variable (height 0.1 au; σ 0.25 and 5.0 au for position and dipole moment, respectively) with a bias factor of 10.0, to ensure the slow exploration of the translocation event. For the two cation-blocking conformations, 4 replicas of 100 ns were launched

https://dx.doi.org/10.1021/acsinfecdis.0c00102
ACS Infect. Dis. 2020, 6, 1855−1865

with an applied potential of −100 mV to evaluate ion current in the presence of kanamycin.

Determination of the Aminoglycoside Sensitivity of *E. coli* Porin Mutants. Minimal inhibitory concentrations (MIC) of aminoglycosides were determined according to guidelines of the Clinical Laboratory Standards Institute (CLSI)[52] using cation-adjusted Mueller Hinton broth (MHBII). Strains used in this work are listed in Table S5. Bacterial cell numbers were adjusted to an inoculum of 5×10^5 cells/mL and the lowest concentration to inhibit visible bacterial growth was determined after 18 h of incubation at 37 °C. For agar gradient plates, 7.5 g/L of agar−agar was added to the broth. The first layer was poured without kanamycin and was solidified while the plate was at an inclined position. The top layer containing kanamycin at a concentration of 1.5 μg/mL was solidified when the plate was level. Prior to use the plate was stored overnight at 4 °C. *E. coli* cells were suspended in 0.9% NaCl (w/v) and the optical density at 600 nm (OD_{600}) was adjusted to 0.1. This cell suspension was streaked on the agar gradient plates using cotton swabs and growth was read after 18 h of incubation at 37 °C. Statistical analysis was performed using R (the R foundation for Statistical Computing, version 3.6.1). Unpaired Student's *t*-test was used to determine statistical significance. For multiple comparisons, alpha was adjusted with the Holm-Bonferroni method.

Generation of Gene Deletion Strains. Porin gene deletions were performed as described by Datsenko and Wanner.[53] Briefly, the kanamycin resistance cassette was amplified from the vector pKD13, using primers (Table S6) attached to homologous ends of the porin genes of interest. *E. coli* cells were first transformed with the helper plasmid pKD46 and in a second transformation round with the constructed PCR products. The resistance cassette was removed with the helper plasmid pCP20. Gene deletions were confirmed by PCR.

■ ASSOCIATED CONTENT

Supporting Information

The Supporting Information is available free of charge at https://pubs.acs.org/doi/10.1021/acsinfecdis.0c00102.

Figures S1−S8 and Tables S1−S7 (PDF)

■ AUTHOR INFORMATION

Corresponding Authors

Heike Brötz-Oesterhelt − *Department of Microbial Bioactive Compounds, Interfaculty Institute of Microbiology and Infection Medicine, University of Tübingen, D-72076 Tübingen, Germany; German Center for Infection Research (DZIF) Partner Site, D-72076 Tübingen, Germany;* orcid.org/0000-0001-9364-1832; Email: heike.broetz-oesterhelt@uni-tuebingen.de

Mathias Winterhalter − *Department of Life Sciences and Chemistry, Jacobs University Bremen, D-28719 Bremen, Germany*; Email: m.winterhalter@jacobs-university.de

Matteo Ceccarelli − *IOM/CNR, Sezione di Cagliari, Cittadella Universitaria di Monserrato, 09042 Monserrato, Italy; Department of Physics, University of Cagliari, and CNR/IOM, Cittadella Universitaria di Monserrato, 09042 Monserrato, Italy;* orcid.org/0000-0003-4272-902X; Email: matteo.ceccarelli@dsf.unica.it

Authors

Jayesh Arun Bafna − *Department of Life Sciences and Chemistry, Jacobs University Bremen, D-28719 Bremen, Germany*

Eulàlia Sans-Serramitjana − *Department of Life Sciences and Chemistry, Jacobs University Bremen, D-28719 Bremen, Germany*

Silvia Acosta-Gutiérrez − *Department of Chemistry, University College London, WC1E 6BT London, United Kingdom;* orcid.org/0000-0002-0122-9769

Igor V. Bodrenko − *IOM/CNR, Sezione di Cagliari, Cittadella Universitaria di Monserrato, 09042 Monserrato, Italy;* orcid.org/0000-0003-1141-1449

Daniel Hörömpöli − *Department of Microbial Bioactive Compounds, Interfaculty Institute of Microbiology and Infection Medicine, University of Tübingen, D-72076 Tübingen, Germany; German Center for Infection Research (DZIF) Partner Site, D-72076 Tübingen, Germany;* orcid.org/0000-0002-5236-8443

Anne Berscheid − *Department of Microbial Bioactive Compounds, Interfaculty Institute of Microbiology and Infection Medicine, University of Tübingen, D-72076 Tübingen, Germany; German Center for Infection Research (DZIF) Partner Site, D-72076 Tübingen, Germany;* orcid.org/0000-0003-1585-8715

Complete contact information is available at: https://pubs.acs.org/10.1021/acsinfecdis.0c00102

Author Contributions

¶J.A.B., E.S.-S., and S.A.-G. contributed equally.

Notes

The authors declare no competing financial interest.

■ ACKNOWLEDGMENTS

The research leading to these results was conducted as part of the Translocation consortium (www.translocation.eu) and has received support from the Innovative Medicines Initiative Joint Undertaking under Grant Agreement No. 115525, resources which are composed of financial contribution from European Union's seventh framework program (FP7/2007−2013) and EFPIA companies. H.B.-O., D.H., and A.B. gratefully acknowledge funding by the German Center of Infection Research (DZIF), project TTU 09.819, and infrastructural support by the Deutsche Forschungsgemeinschaft (DFG, German Research Foundation) under Germany's Excellence Strategy, EXC 2124-390838134. M.C. would like to thank the partial funding from MIUR "Progetti di Ricerca di Interesse Nazionale" (2015795S5W).

■ ABBREVIATIONS

OM, outer membrane; LPS, lipopolysaccharides; AG, aminoglycosides; COM, center of mass; GHK, Goldman−Hodgkin−Katz; PR, preorientation region; CR, constriction region; MIC, minimal inhibitory concentration; WT, wildtype; MD, molecular dynamics; SPME, soft particle mesh Ewald.

■ REFERENCES

(1) Nikaido, H. (2003) Molecular Basis of Bacterial Outer Membrane Permeability Revisited. *Microbiol. Mol. Biol. Rev. 67*, 593−656.

(2) Richter, M. F., Drown, B. S., Riley, A. P., Garcia, A., Shirai, T., Svec, R. L., and Hergenrother, P. J. (2017) Predictive Compound

Accumulation Rules Yield a Broad-Spectrum Antibiotic. *Nature 545*, 299−304.
(3) Vergalli, J., Bodrenko, I. V., Masi, M., Moynié, L., Acosta-Gutiérrez, S., Naismith, J. H., Davin-Regli, A., Ceccarelli, M., van den Berg, B., Winterhalter, M., and Pagès, J.-M. (2020) Porins and Small-Molecule Translocation across the Outer Membrane of Gram-Negative Bacteria. *Nat. Rev. Microbiol. 18*, 164−176.
(4) Nakae, T. (1976) Identification of the Outer Membrane Protein of E. Coli That Produces Transmembrane Channels in Reconstituted Vesicle Membranes. *Biochem. Biophys. Res. Commun. 71*, 877−884.
(5) Ruggiu, F., Yang, S., Simmons, R. L., Casarez, A., Jones, A. K., Li, C., Jansen, J. M., Moser, H. E., Dean, C. R., Reck, F., and Lindvall, M. (2019) Size Matters and How You Measure It: A Gram-Negative Antibacterial Example Exceeding Typical Molecular Weight Limits. *ACS Infect. Dis. 5*, 1688−1692.
(6) Acosta-Gutiérrez, S., Ferrara, L., Pathania, M., Masi, M., Wang, J., Bodrenko, I., Zahn, M., Winterhalter, M., Stavenger, R. A., Pagès, J.-M., Naismith, J. H., van den Berg, B., Page, M. G. P., and Ceccarelli, M. (2018) Getting Drugs into Gram-Negative Bacteria: Rational Rules for Permeation through General Porins. *ACS Infect. Dis. 4*, 1487−1498.
(7) Lou, H., Chen, M., Black, S. S., Bushell, S. R., Ceccarelli, M., Mach, T., Beis, K., Low, A. S., Bamford, V. A., Booth, I. R., Bayley, H., and Naismith, J. H. (2011) Altered Antibiotic Transport in OmpC Mutants Isolated from a Series of Clinical Strains of Multi-Drug Resistant E. Coli. *PLoS One 6*, No. e25825.
(8) Pagès, J.-M., James, C. E., and Winterhalter, M. (2008) The Porin and the Permeating Antibiotic: A Selective Diffusion Barrier in Gram-Negative Bacteria. *Nat. Rev. Microbiol. 6*, 893−903.
(9) Hancock, R. E. W., Farmer, S. W., Li, Z. S., and Poole, K. (1991) Interaction of Aminoglycosides with the Outer Membranes and Purified Lipopolysaccharide and OmpF Porin of Escherichia Coli. *Antimicrob. Agents Chemother. 35*, 1309−1314.
(10) Nakae, R., and Nakae, T. (1982) Diffusion of Aminoglycoside Antibiotics across the Outer Membrane of Escherichia Coli. *Antimicrob. Agents Chemother. 22*, 554−559.
(11) Foulds, J., and Chai, T. J. (1978) New Major Outer Membrane Proteins Found in an Escherichia Coli TolF Mutant Resistant to Bacteriophage TuIb. *J. Bacteriol. 133*, 1478−1483.
(12) Ghai, I., Pira, A., Scorciapino, M. A., Bodrenko, I., Benier, L., Ceccarelli, M., Winterhalter, M., and Wagner, R. (2017) General Method to Determine the Flux of Charged Molecules through Nanopores Applied to β-Lactamase Inhibitors and OmpF. *J. Phys. Chem. Lett. 8*, 1295−1301.
(13) Ghai, I., Winterhalter, M., and Wagner, R. (2017) Probing Transport of Charged β-Lactamase Inhibitors through OmpC, a Membrane Channel from E. Coli. *Biochem. Biophys. Res. Commun. 484*, 51−55.
(14) Eaton, D. C. (1985) Ionic Channels of Excitable Membranes. Bertil Hille. Sunderland, Ma: Sinauer Associates, 1984. *J. Neurosci. Res. 13*, 599−600.
(15) Nikaido, H., and Vaara, M. (1985) Molecular Basis of Bacterial Outer Membrane Permeability. *Microbiol. Rev. 49*, 1−32.
(16) Prilipov, A., Phale, P. S., Koebnik, R., Widmer, C., and Rosenbusch, J. P. (1998) Identification and Characterization of Two Quiescent Porin Genes, NmpC and OmpN, in Escherichia Coli BE. *J. Bacteriol. 180*, 3388−3392.
(17) Mahendran, K. R., Hajjar, E., Mach, T., Lovelle, M., Kumar, A., Sousa, I., Spiga, E., Weingart, H., Gameiro, P., Winterhalter, M., and Ceccarelli, M. (2010) Molecular Basis of Enrofloxacin Translocation through OmpF, an Outer Membrane Channel of Escherichia Coli - When Binding Does Not Imply Translocation. *J. Phys. Chem. B 114*, 5170−5179.
(18) Lamichhane, U., Islam, T., Prasad, S., Weingart, H., Mahendran, K. R., and Winterhalter, M. (2013) Peptide Translocation through the Mesoscopic Channel: Binding Kinetics at the Single Molecule Level. *Eur. Biophys. J. 42*, 363−369.
(19) Acosta-Gutierrez, S., Scorciapino, M. A., Bodrenko, I., and Ceccarelli, M. (2015) Filtering with Electric Field: The Case of E. Coli Porins. *J. Phys. Chem. Lett. 6*, 1807−1812.
(20) Gutiérrez, S. A., Bodrenko, I., Scorciapino, M. A., and Ceccarelli, M. (2016) Macroscopic Electric Field inside Water-Filled Biological Nanopores. *Phys. Chem. Chem. Phys. 18*, 8855−8864.
(21) Bajaj, H., Acosta Gutierrez, S., Bodrenko, I., Malloci, G., Scorciapino, M. A., Winterhalter, M., and Ceccarelli, M. (2017) Bacterial Outer Membrane Porins as Electrostatic Nanosieves: Exploring Transport Rules of Small Polar Molecules. *ACS Nano 11*, 5465−5473.
(22) Ziervogel, B. K., and Roux, B. (2013) The Binding of Antibiotics in OmpF Porin. *Structure 21*, 76−87.
(23) Baba, T., Ara, T., Hasegawa, M., Takai, Y., Okumura, Y., Baba, M., Datsenko, K. A., Tomita, M., Wanner, B. L., and Mori, H. (2006) Construction of Escherichia Coli K-12 In-frame, Single-gene Knockout Mutants: The Keio Collection. *Mol. Syst. Biol.*, DOI: 10.1038/msb4100050.
(24) Malloci, G., Vargiu, A., Serra, G., Bosin, A., Ruggerone, P., and Ceccarelli, M. (2015) A Database of Force-Field Parameters, Dynamics, and Properties of Antimicrobial Compounds. *Molecules 20*, 13997−14021.
(25) Allam, A., Maigre, L., Vergalli, J., Dumont, E., Cinquin, B., Alves de Sousa, R., Pajovic, J., Pinet, E., Smith, N., Herbeuval, J.-P., Réfrégiers, M., Artaud, I., and Pagès, J.-M. (2017) Microspectrofluorimetry to Dissect the Permeation of Ceftazidime in Gram-Negative Bacteria. *Sci. Rep. 7*, 986.
(26) Mingeot-Leclercq, M. P., Glupczynski, Y., and Tulkens, P. M. (1999) Aminoglycosides: Activity and Resistance. *Antimicrob. Agents Chemother. 43*, 727−737.
(27) Serio, A. W., Keepers, T., Andrews, L., and Krause, K. M. (2018) Aminoglycoside Revival: Review of a Historically Important Class of Antimicrobials Undergoing Rejuvenation. *EcoSal Plus*, DOI: 10.1128/ecosalplus.ESP-0002-2018.
(28) Richter, M. F., and Hergenrother, P. J. (2019) The Challenge of Converting Gram-Positive-Only Compounds into Broad-Spectrum Antibiotics. *Ann. N. Y. Acad. Sci. 1435*, 18−38.
(29) Garneau-Tsodikova, S., and Labby, K. J. (2016) Mechanisms of Resistance to Aminoglycoside Antibiotics: Overview and Perspectives. *MedChemComm 7*, 11−27.
(30) Ghai, I., Pira, A., Scorciapino, M. A., Bodrenko, I., Benier, L., Ceccarelli, M., Winterhalter, M., and Wagner, R. (2017) A General Method to Determine the Flux of Charged Molecules Through Nanopores Applied to SS-Lactamase Inhibitors and OmpF. *J. Phys. Chem. Lett. 8*, 1295−1310.
(31) Ghai, I., Bajaj, H., Arun Bafna, J., El Damrany Hussein, H. A., Winterhalter, M., and Wagner, R. (2018) Ampicillin Permeation across OmpF, the Major Outer-Membrane Channel in Escherichia Coli. *J. Biol. Chem. 293*, 7030−7037.
(32) Mahendran, K. R., Kreir, M., Weingart, H., Fertig, N., and Winterhalter, M. (2010) Permeation of Antibiotics through Escherichia Coli OmpF and OmpC Porins: Screening for Influx on a Single-Molecule Level. *J. Biomol. Screening 15*, 302−307.
(33) Bodrenko, I. V., Wang, J., Salis, S., Winterhalter, M., and Ceccarelli, M. (2017) Sensing Single Molecule Penetration into Nanopores: Pushing the Time Resolution to the Diffusion Limit. *ACS Sensors 2*, 1184.
(34) Dumont, E., Vergalli, J., Conraux, L., Taillier, C., Vassort, A., Pajović, J., Réfrégiers, M., Mourez, M., and Pagès, J.-M. (2018) Antibiotics and Efflux: Combined Spectrofluorimetry and Mass Spectrometry to Evaluate the Involvement of Concentration and Efflux Activity in Antibiotic Intracellular Accumulation. *J. Antimicrob. Chemother. 74*, 58−65.
(35) Reck, F., Jansen, J. M., and Moser, H. E. (2020) Challenges of Antibacterial Drug Discovery. *ARKIVOC 2019*, 227−244.
(36) Montal, M., and Mueller, P. (1972) Formation of Bimolecular Membranes from Lipid Monolayers and a Study of Their Electrical Properties. *Proc. Natl. Acad. Sci. U. S. A. 69*, 3561−3566.

(37) Sullivan, H. (1992) Ionic Channels of Excitable Membranes, 2nd Ed. *Neurology 42*, 1439−1439.
(38) Varma, S., Chiu, S. W., and Jakobsson, E. (2006) The Influence of Amino Acid Protonation States on Molecular Dynamics Simulations of the Bacterial Porin OmpF. *Biophys. J. 90*, 112−123.
(39) Maier, J. A., Martinez, C., Kasavajhala, K., Wickstrom, L., Hauser, K. E., and Simmerling, C. (2015) Ff14SB: Improving the Accuracy of Protein Side Chain and Backbone Parameters from Ff99SB. *J. Chem. Theory Comput. 11*, 3696−3713.
(40) Dickson, C. J., Madej, B. D., Skjevik, Å. A., Betz, R. M., Teigen, K., Gould, I. R., and Walker, R. C. (2014) Lipid14: The Amber Lipid Force Field. *J. Chem. Theory Comput. 10*, 865−879.
(41) Jorgensen, W. L., Chandrasekhar, J., Madura, J. D., Impey, R. W., and Klein, M. L. (1983) Comparison of Simple Potential Functions for Simulating Liquid Water. *J. Chem. Phys. 79*, 926−935.
(42) Phillips, J. C., Braun, R., Wang, W., Gumbart, J., Tajkhorshid, E., Villa, E., Chipot, C., Skeel, R. D., Kalé, L., and Schulten, K. (2005) Scalable Molecular Dynamics with NAMD. *J. Comput. Chem. 26*, 1781−1802.
(43) Harvey, M. J., Giupponi, G., and Fabritiis, G. De. (2009) ACEMD: Accelerating Biomolecular Dynamics in the Microsecond Time Scale. *J. Chem. Theory Comput. 5*, 1632−1639.
(44) Wang, J., Wolf, R. M., Caldwell, J. W., Kollman, P. A., and Case, D. A. (2004) Development and Testing of a General Amber Force Field. *J. Comput. Chem. 25*, 1157−1174.
(45) Bayly, C. I., Cieplak, P., Cornell, W., and Kollman, P. A. (1993) A Well-Behaved Electrostatic Potential Based Method Using Charge Restraints for Deriving Atomic Charges: The RESP Model. *J. Phys. Chem. 97*, 10269−10280.
(46) Fritschy, J.-M., and Brünig, I. (2003) Formation and Plasticity of GABAergic Synapses: Physiological Mechanisms and Pathophysiological Implications. *Pharmacol. Ther. 98*, 299−323.
(47) Wang, J., Wang, W., Kollman, P. A, and Case, D. A. (2006) Automatic atom type and bond type perception in molecular mechanical calculations. *J. Mol. Graphics Modell. 25*, 247260.
(48) Marvin Sketch (2019) *ChemAxon: Software Solutions and Services for Chemistry and Biology*, Version 19.8.0.
(49) Barducci, A., Bussi, G., and Parrinello, M. (2008) Well-Tempered Metadynamics: A Smoothly Converging and Tunable Free-Energy Method. *Phys. Rev. Lett. 100*, 020603.
(50) Laio, A., and Parrinello, M. (2002) Escaping Free-Energy Minima. *Proc. Natl. Acad. Sci. U. S. A. 99*, 12562−12566.
(51) Tribello, G. A., Bonomi, M., Branduardi, D., Camilloni, C., and Bussi, G. (2014) PLUMED 2: New Feathers for an Old Bird. *Comput. Phys. Commun. 185*, 604−613.
(52) Subramaniam, P., and Nandan, N. (2011) Effect of Xylitol, Sodium Fluoride and Triclosan Containing Mouth Rinse on Streptococcus Mutans. *Contemp. Clin. Dent. 2*, 287.
(53) Datsenko, K. A., and Wanner, B. L. (2000) One-Step Inactivation of Chromosomal Genes in Escherichia Coli K-12 Using PCR Products. *Proc. Natl. Acad. Sci. U. S. A. 97*, 6640−6645.

https://dx.doi.org/10.1021/acsinfecdis.0c00102
ACS Infect. Dis. 2020, 6, 1855−1865

Supplementary Information

Kanamycin uptake into *Escherichia coli* is facilitated by OmpF and OmpC porin channels located in the outer membrane

Jayesh Arun Bafna ,[1‡] Eulàlia Sans-Serramitjana,[1‡] Silvia Acosta-Gutiérrez,[2‡] Igor V. Bodrenko[3], Daniel Hörömpöli,[4,5] Anne Berscheid,[4,5] Heike Brötz-Oesterhelt,[4,5] Mathias Winterhalter[1] and Matteo Ceccarelli[3,6].

[1] Department of Life Sciences and Chemistry, Jacobs University Bremen, D-28719 Bremen, Germany

[2] Department of Chemistry, University College London, WC1E 6BT London, United Kingdom

[3] IOM/CNR, Sezione di Cagliari, Cittadella Universitaria di Monserrato, 09042 Monserrato, Italy.

[4] Department of Microbial Bioactive Compounds, Interfaculty Institute of Microbiology and Infection Medicine, University of Tübingen, D-72076 Tübingen, Germany

[5] German Center for Infection Research (DZIF), partner site D-72076 Tübingen, Germany

[6] Department of Physics, University of Cagliari, and CNR/IOM, Cittadella Universitaria di Monserrato, 09042 Monserrato, Italy.

[‡] Equally contributed

Bacterial strains and growth conditions.

For OmpN overexpression in untagged form, we used *E. coli* BL21 (DE3) Omp8.[1] This strain lacks the major porins of *E. coli* (OmpF, OmpC, OmpA and LamB). These cells were transformed with the plasmid pASK IBA5-ompN and grown at 37°C, 250 rpm in Luria-Bertani (LB) medium (Roth, Germany) or LB agar plates supplemented with ampicillin at 100 µg/mL for plasmid maintenance. OmpF and OmpC has been purified according to the published recipe.[2,3]

Expression and purification of OmpN

An overnight preculture of *E. coli* BL21 (DE3) Omp8 containing pASK IBA5-ompN was inoculated into Luria-Bertani medium containing ampicillin at OD_{600} 0.1. When the optical density of the culture reached 0.7, the culture was induced with 200 µg/L anhydrotetracycline, and the expression was performed overnight at room temperature while shaking (250 rpm). Cells were harvested by centrifugation at 6000 g for 30 min at 4°C and stored at -20°C until purification.

For purification, a pellet from 1 L of culture was resuspended in lysis buffer (10 mM Tris pH 8, 5 mM $MgCl_2$, 1 mM PMSF, 50 µg/ml RNase A and 5 µg/ml DNase I) and disrupted by 3 passages at 4000 psi in a French Press on ice. After removing the cells debris by 40 min of centrifugation at 3220 g, 4 °C, the membrane was pelleted by ultracentrifugation (1 h, 110000 g at 4°C). The pellet was solubilized in 10 mM Tris/HCl pH 8, 0.125 % Octyl POE (N-octylpolyoxyethylene from Bachem) using a Potter homogenizer and incubated for 1 h at room temperature on the wheel. The remaining insoluble material was separated by a second ultracentrifugation (110000 g, room temperature, 1 h). OmpN was extracted by solubilization of this pellet with 10 mM Tris HCl pH 8, 3% Octyl POE and elimination of insoluble material by ultracentrifugation. This step was performed two times.

The last supernatants contained the expected protein were pooled and concentrated with an Amicon concentration unit (cut off 30 kDa).

The samples were supplemented with Laemmli sample buffer and heated at 98°C for 10 minutes (denaturing condition) or supplemented with Laemmli sample buffer lacking beta mercapto-ethanol and not heated (non-denaturing condition) and loaded on 12% SDS PAGE gel.[4] The gels were stained with Coomassie Brilliant Blue G250 (Figure S5).

Table S1. Conductivity measurements. *Experimental single channel conductance value with standard deviation of the OmpF, OmpC and OmpN trimer at low ionic strength (20 mM) under bi-ionic symmetrical addition.*

Protein	G_{trimer} (pS) trimer Vm= +100 mV 20 mM Kanamycin sulphate	G_{trimer} (pS) trimer Vm= +100 mV Control: 20 mM K_2 SO_4
OmpF	16 ± 3.7 pS	240 ± 27 pS
OmpC	13 ± 2.8 pS	180 ± 30 pS
OmpN	9.5 ± 2.2 pS	58 ± 17 pS

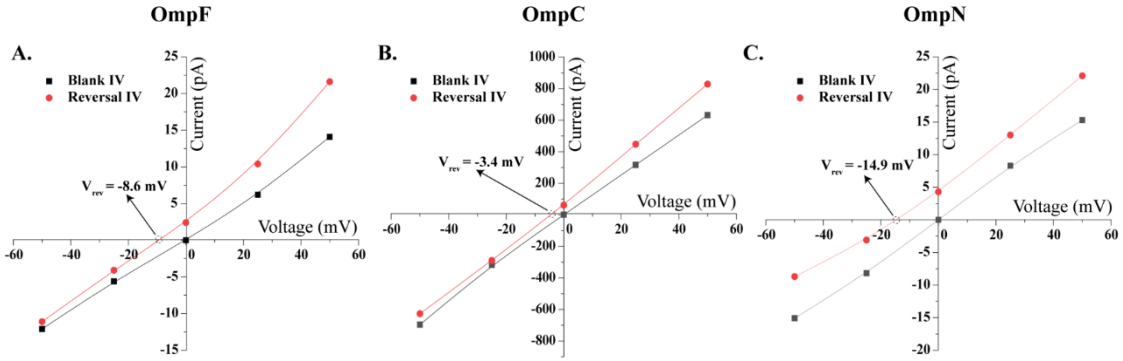

Figure S1. Reversal potentials (A) *Current recording from bilayer containing multiple reconstituted OmpF channels with symmetrical 20 mM kanamycin (GND-cis/trans) and cis 50 mM kanamycin (bi-ionic conditions).* ***(B)*** *Current recording from bilayer containing multiple reconstituted OmpC channels with symmetrical 20 mM kanamycin (GND-cis/trans) and cis 50 mM kanamycin (bi-ionic conditions).* ***(C)*** *Current recording from bilayer containing multiple reconstituted OmpN channels with symmetrical 20 mM kanamycin (GND-cis/trans) and cis 50 mM kanamycin (bi-ionic conditions).*

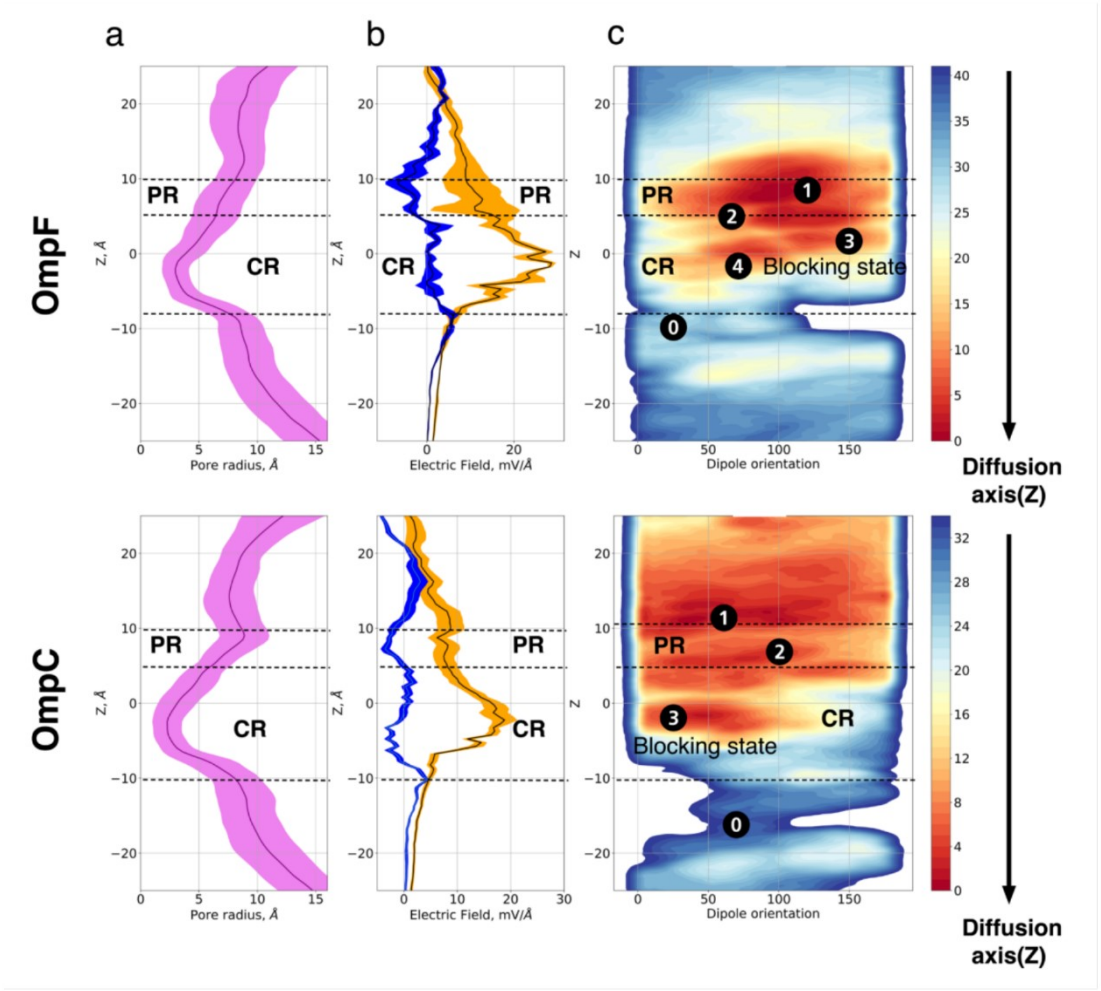

Figure S2. ***Kanamycin permeation path through OmpF and OmpC***. ***a)*** *The average pore radius with fluctuations;* ***b)*** *the internal electric field: the transversal component (orange) and the longitudinal component (blue);* ***c)*** *a qualitative free energy surface for a single kanamycin translocation event (the ion current blocking state is highlighted). The upper panel depicts OmpF and the bottom panel corresponds to OmpC.*

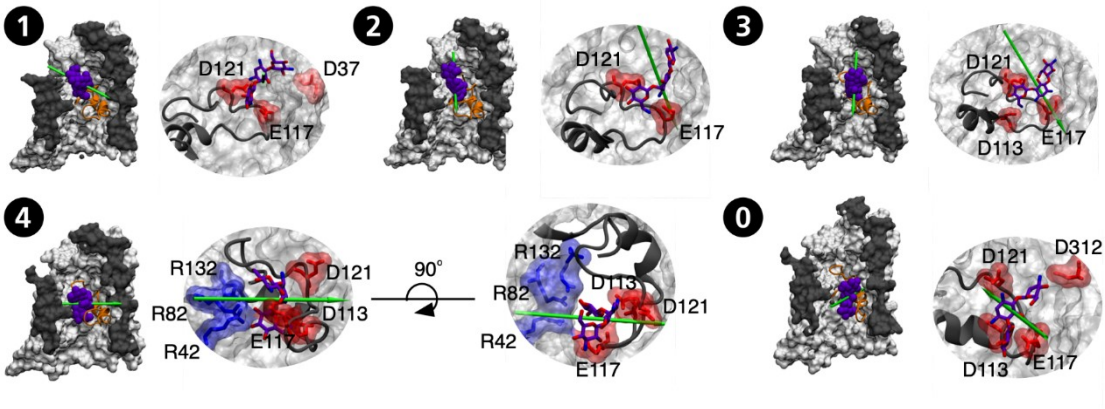

Figure S3. *Kanamycin transport path through OmpF. Kanamycin (represented as violet van der Waals spheres) positioned with respect to the main diffusion axis of the pore (partial surface representation) in the main conformations during transport through OmpF. Kanamycin interactions with charged groups from the walls of the pore are depicted in licorice for each conformation panel. States numbering refer to minima in Figure S2. Minima 1 and 4 are renamed in the main text as S0 and S1 respectively. The state labeled 0 is highlighted with star in Figure 3 of the main text.*

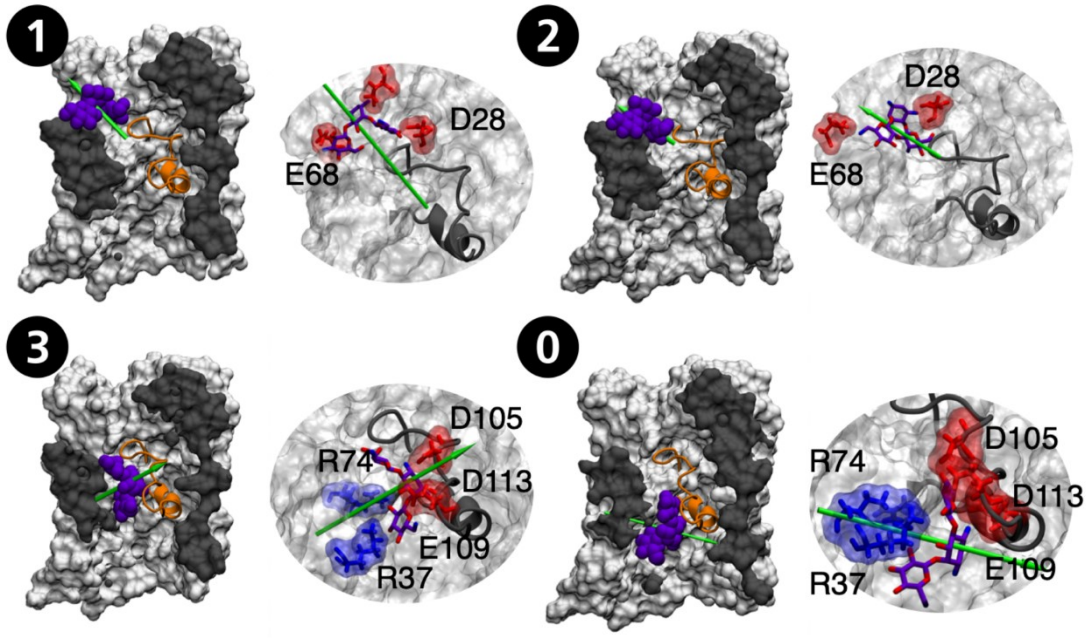

Figure S4. *Kanamycin transport path through OmpC. Kanamycin (represented as violet van der Waals spheres) positioned with respect to the main diffusion axis of the pore (partial surface representation) in the main conformations during transport through OmpF. Kanamycin interactions with charged groups from the walls of the pore are depicted in licorice for each conformation panel. States numbering refer to minima in Figure S2. Minimum 3 is renamed in the main text as S1 and the state labelled as 0 is highlighted with star in Figure 3 of the main text.*

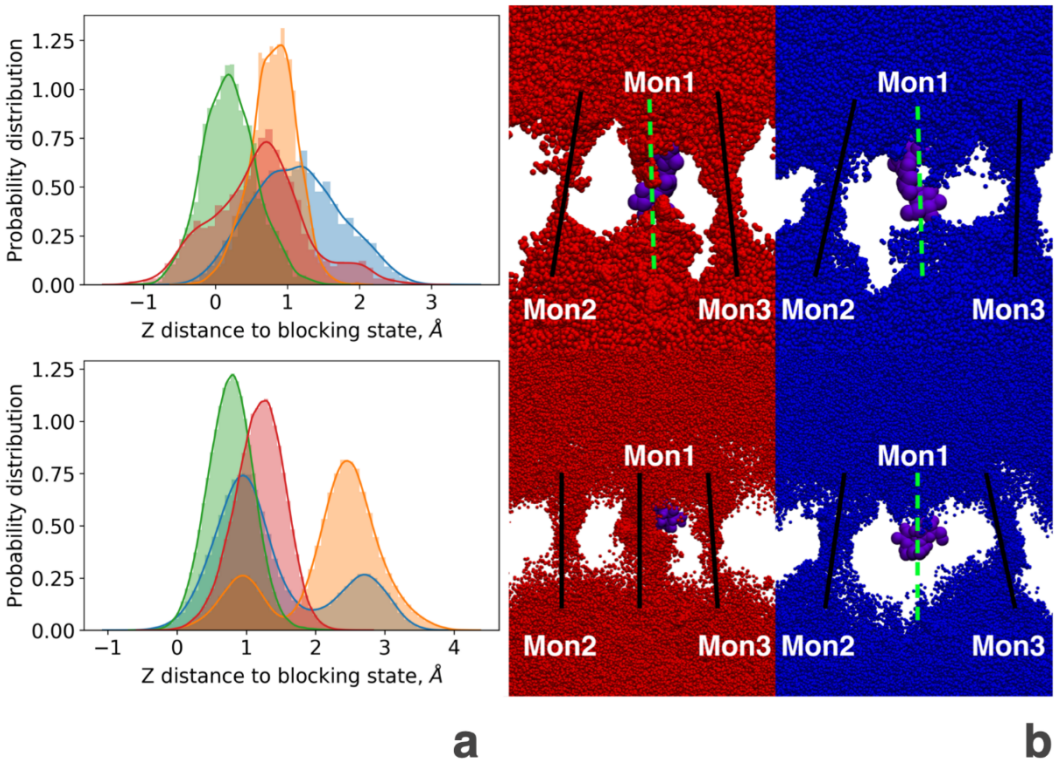

Figure S5. Kanamycin blocking states, ion current analysis*. **a)** Probability distribution function of the distance of the centre of mass of kanamycin to the blocking state site for the four independent replicas of 100 ns with an applied voltage of -100 mV, respectively, for OmpF (upper panel) and OmpC (lower panel). Each replica has a different color. **b)** Superimposition of the ions (Cl^- red, K^+ blue) along the trajectory with a kanamycin molecule (represented as violet van der Waals spheres) sitting in the constriction region of monomer 1.*

Table S2. Translocating ions. *Number of Cl^- and K^+ ions translocating through the trimer during the simulations for the 4 replicas of each system with and without kanamycin.*

	OmpF		OmpC	
	Cl^-	**K^+**	**Cl^-**	**K^+**
Empty-R1	2	34	4	42
Empty-R2	4	27	5	38
Empty-R3	8	29	1	43
Empty-R4	7	41	4	34
Average	**5.2 ± 2.4**	**32.7±5.4**	**3.5 ± 1.5**	**39.2 ± 3.5**
Kanamycin-R1	6	2	13	2
Kanamycin-R2	11	0	20	3
Kanamycin-R3	8	1	18	2
Kanamycin-R4	6	2	10	6
Average	**7.7 ± 2.0**	**1.2 ± 0.8**	**15.25 ± 3.9**	**3.2 ± 1.6**

Kanamycin is a quite large cationic molecule with an electric dipole moment (relative to its center of mass) oriented almost transversally to the long axis of the molecule itself (**Figure 4a**). The average parameters obtained by simulating kanamycin in a box of water are summarized in **Table S3** and compared with three beta-lactam antibiotics, ampicillin, piperacillin and ceftazidime. Marvin was used for drawing, displaying and characterizing chemical structures, substructures and reactions, Marvin 19.8.0, ChemAxon (https://www.chemaxon.com).

Table S3. Molecular descriptors for permeation through porins*. Molecular descriptors for antibiotics calculated by averaging the MD trajectories of molecules in water. Molecular descriptors from porins (OmpF and OmpC) as reported in Acosta-Gutierrez et al.*[5] *The size of OmpN was predicted here using the data on conductance of this work.*

Molecule	**Charge**	**Total dipole moment and its transversal component (Debye)**	**Effective average radius of the minimal projection area (Å) and minimal projection area (Å^2)**
Kanamycin	+4e	23.0 (Dxy=22.99)	4.8 (71.2)
Ampicillin	0	34.1 (Dxy=13.5)	4.0 (50.5)
Ceftazidime	-1e	18.5 (Dxy=13.0)	4.7 (68.3)
Piperacillin	-1e	28.1 (Dxy=15.6)	5.0 (77.5)
Porin	**Selectivity PK^+/PCl^-**	**Conductance (nS) 1MKCl and 50mV**	**Minimum pore radius (Å) and area (Å^2)**
OmpF	1.3	4.0	3.1 (30.2)
OmpC	2.2	2.9	2.8 (24.6)
OmpN		1.6 *(this work)*	1.0 (3.14) *(predicted)*

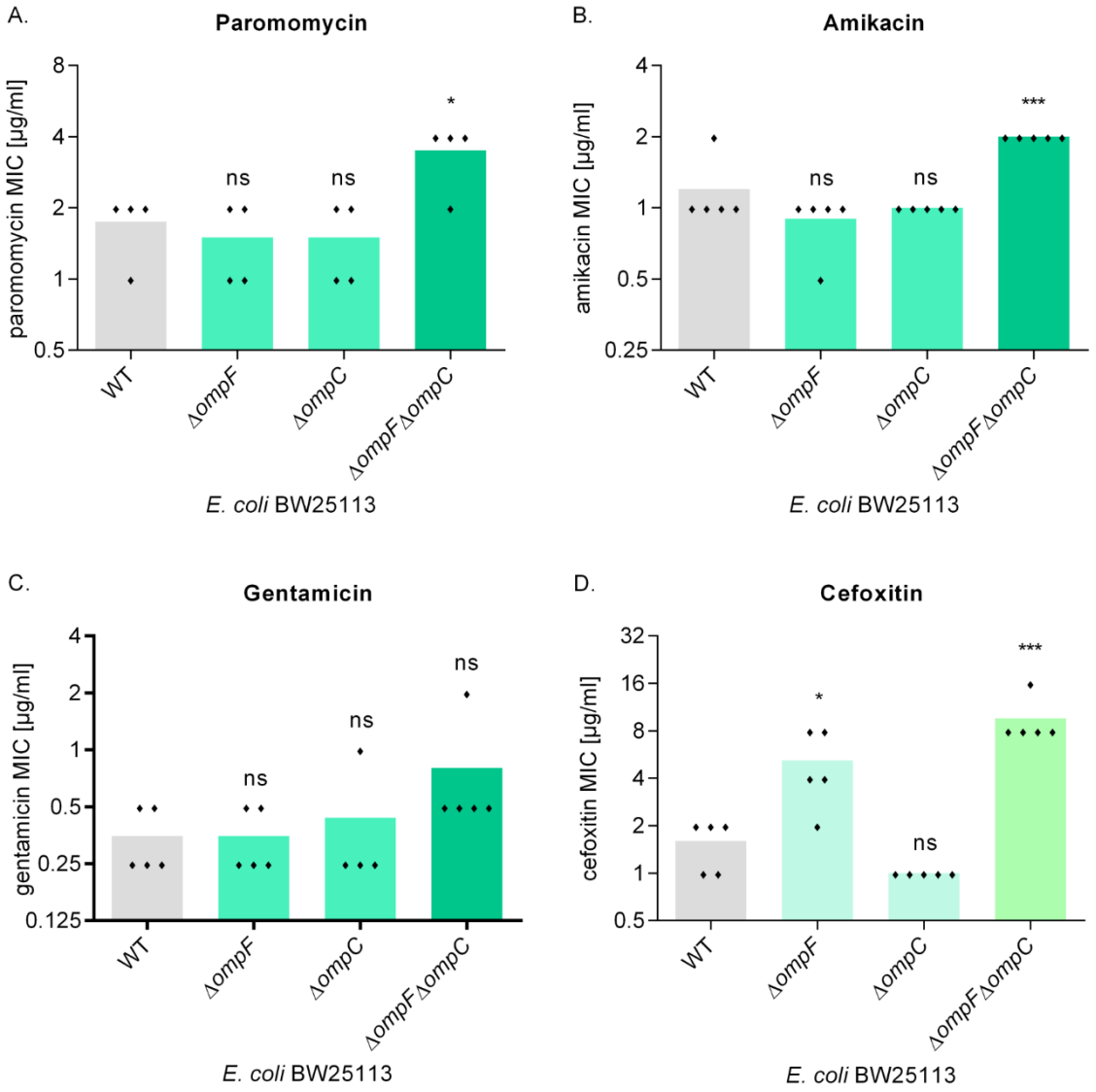

Figure S6. Effect of porin deletions on the antibiotic susceptibility of E. coli BW25113. *The deletion of both major porin genes ompF and ompC was required to significantly increase the MIC of the aminoglycosides paromomycin (A) and amikacin (B). For gentamicin (C), a trend towards reduced susceptibility of the double knockout mutant was also observed but without statistical significance. These data suggest that aminoglycosides structurally distinct from kanamycin (Figure S7) can also pass through both porins. The cephalosporin antibiotic cefoxitin (D) is known to pass through OmpF and OmpC[6] and was used as a structurally unrelated positive control. In the case of cefoxitin, already the single deletion of ompF was enough to markedly increase the MIC and the additional deletion of ompC reduced susceptibility further. The 4-fold MIC increase in the absence of both ompF and ompC indicates that this cephalosporin is more dependent on uptake via porins than aminoglycosides. MIC values are represented on a logarithmic scale. Each diamond represents one independent measurement from a different day. The vertical colored bars show the arithmetic mean of all data points. Statistical analysis was performed using unpaired Student's t-test with Holm-Bonferroni correction, comparing mutants to the wildtype (WT) strain. Not significant (ns), $P > 0.05$; *, $P \leq 0.05$; **, $P \leq 0.01$; ***, $P \leq 0.001$.*

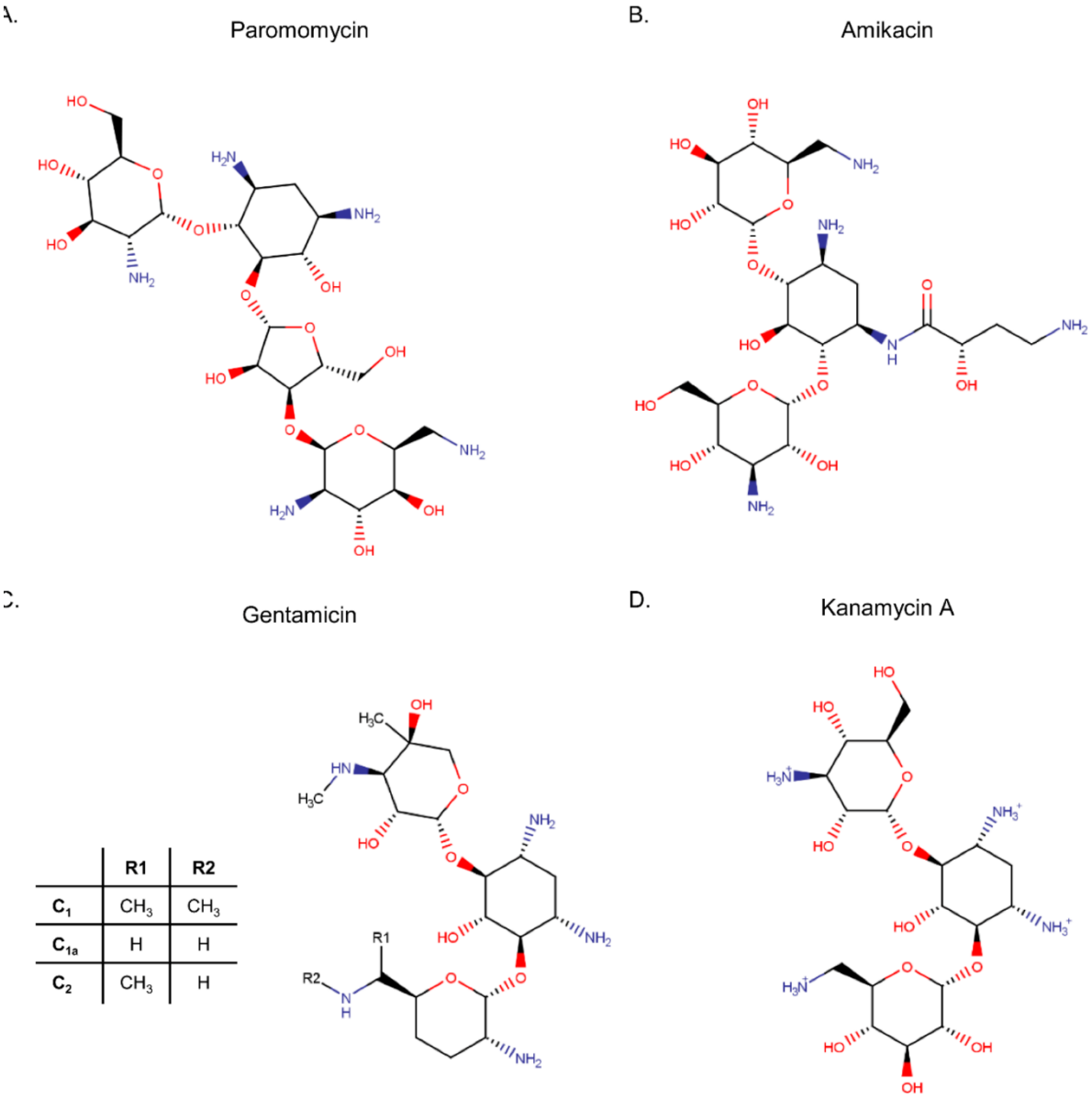

	R1	R2
C_1	CH_3	CH_3
C_{1a}	H	H
C_2	CH_3	H

Figure S7. Structural diversity of the AGs used in this study. *Although paromomycin (A), amikacin (B), gentamicin (C) and kanamycin (D) differ in their structure, they showed similar susceptibility patterns when comparing porin deletion strains to the E. coli wildtype (Fig. 5 & S6). Aminoglycoside resistance was slightly increased when both major porin genes ompF and ompC were deleted, indicating that they are involved in the outer membrane translocation of E. coli. Only the major components gentamicin C_1, C_{1a} and C_2 (C) and kanamycin A (D) of the gentamicin and kanamycin natural product complexes are shown.*

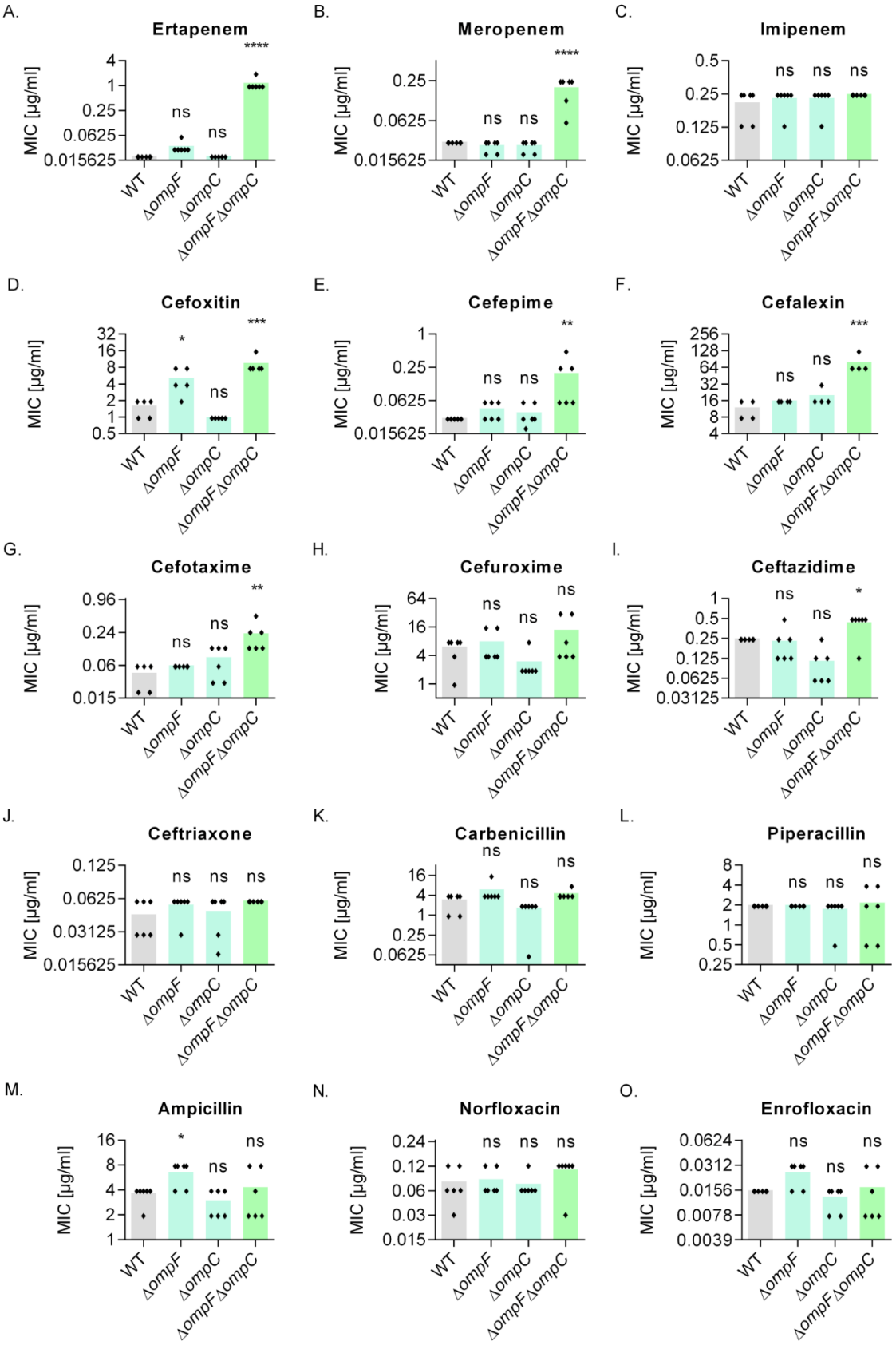

Figure S8. Determination of the effect of the deletion of the major porin genes ompF and ompC in E. coli BW25113. *The MIC of different carbapenems (A-C), cephalosporins (D-J), penicillins (K-M) and fluoroquinolones (N-O) were compared.*

*The activity of most antibiotics was affected by the absence of the ompF and ompC genes, although the porin dependency differed even within the same class of antibiotics. MIC values are represented on a logarithmic scale. Each diamond represents one independent measurement from a different day. The vertical colored bars show the arithmetic mean of all data points. Statistical analysis was performed using unpaired Student's t-test with Holm-Bonferroni correction, comparing mutants to the wildtype (WT) strain. Not significant (ns), P > 0.05; *, P ≤ 0.05; **, P ≤ 0.01; ***, P ≤ 0.001; ****, P ≤ 0.0001.*

***Table S4**. Relative MIC increase of the ΔompFΔompC double deletion strain in relation to the wildtype E. coli BW25113 for different aminoglycosides, β-lactams and fluoroquinolones. The change in the MIC was calculated by dividing the MIC of E. coli ΔompFΔompC by the MIC of the wildtype culture measured in parallel on the same day. Note that compounds commonly summarized within the same antibiotic class due to a related pharmacophore and corresponding mode of action are different structural entities with distinct size and physicochemistry, which leads to different uptake modalities. SD, standard deviation.*

Antibiotic	**Class**	**Relative MIC increase (Δ*ompF*Δ*ompC*/WT) [average ± SD]**
Ertapenem	Carbapenem	58.33 ± 20.41
Cefalexin	Cephalosporin	7 ± 2
Meropenem	Carbapenem	6.61 ± 2.77
Cefotaxime	Cephalosporin	5.53 ± 2.39
Cefepime	Cephalosporin	4.53 ± 3.47
Cefuroxime	Cephalosporin	3 ± 2.95
Paromomycin	Aminoglycoside	2.25 ± 1.26
Gentamicin	Aminoglycoside	2.2 ± 1.1
Carbenicillin	Penicillin	2.17 ± 1.47
Kanamycin	Aminoglycoside	2.17 ± 0.98
Amikacin	Aminoglycoside	1.8 ± 0.45
Ceftazidime	Cephalosporin	1.75 ± 0.6
Ceftriaxone	Cephalosporin	1.5 ± 0.55
Norfloxacin	Fluoroquinolone	1.5 ± 0.55
Ampicillin	Penicillin	1.42 ± 1.39
Imipenem	Carbapenem	1.31 ± 0.48
Piperacillin	Penicillin	1.08 ± 0.79
Enrofloxacin	Fluoroquinolone	1.08 ± 0.74

Table S5. *Bacterial strains used in this work.*

Strain	Genotype/characteristics	source
***E. coli* BW25113**	wildtype; F-, Δ(*araD-araB*)*567*, Δ*lacZ4787*(::*rrnB*-3), *λ*-, *rph*-1, Δ(*rhaD-rhaB*)*568*, *hsdR514*	[7,8]
E. coli* JW0912 *ΔompF	F-, Δ(*araD-araB*)*567*, Δ*lacZ4787*(::*rrnB*-3), *λ*-, Δ*ompF746*, *rph*-1, Δ(*rhaD-rhaB*)*568*, *hsdR514*	[7,8]
E. coli* JW2203 *ΔompC	F-, Δ(*araD-araB*)*567*, Δ*lacZ4787*(::*rrnB*-3), *λ*-, Δ*ompC768*, *rph*-1, Δ(*rhaD-rhaB*)*568*, *hsdR514*	[7,8]
E. coli ΔompFΔompC	F-, Δ(*araD-araB*)*567*, Δ*lacZ4787*(::*rrnB*-3), *λ*-, Δ*ompF746*, Δ*ompC768*, *rph*-1, Δ(*rhaD-rhaB*)*568*, *hsdR514*	this study

Table S6. Oligonucleotides used for the generation of the porin gene deletions.
Homologous regions to the plasmid pKD13 are marked in bold.

Oligonucleotide	5'-3' sequence
KO-ompF_fwd	TTAACAAAGAGGTGTGCTATTAGAACTGGTAAACGATACC **ATTCCGGGGATCCGTCGACC**
KO-ompF_rev	GCAGGTGTCATAAAAAAAACCATGAGGGTAATAAATAATG **TGTAGGCTGGAGCTGCTTCG**
KO-ompC_fwd	TGTTCGATATCAATCGAGATTAGAACTGGTAAACCAGACC **ATTCCGGGGATCCGTCGACC**
KO-ompC_rev	AAAAGCAAATAAAGGCATATAACAGAGGGTTAATAACAT **GTGTAGGCTGGAGCTGCTTCG**

Flux calculation:

To calculate the individual flux of kanamycin and its counter ion sulphate for a single OmpF channel from the reversal potential measurement, we make use of the diffusion current (Osmotic driven flux)[9] when a concentration gradient is generated across the bilayer system (see Table S7). Below is the typical IV, representing $I_{diffusion}$ and $V_{reversal}$.

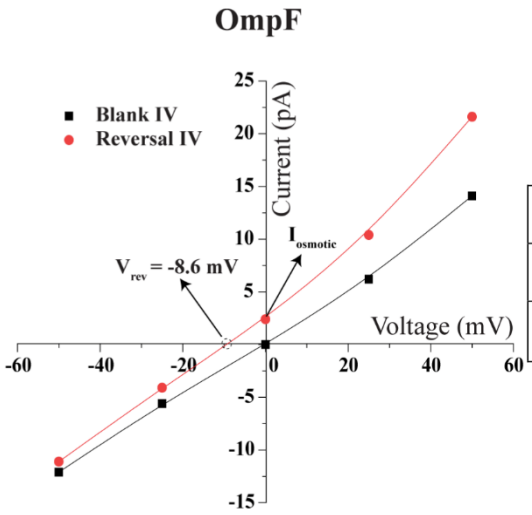

Table S7

Trans side		Cis side	
Kanamycin	**SO_4^{2-}**	**Kanamycin**	**SO_4^{2-}**
20	35	50	87.5

$$\frac{P_{Kanamycin(4+)}}{P_{Sulphate(2-)}} = \frac{1}{14}$$

By extracting the value of $I_{diffusion} = 1.8\,pA$ from the graph and simply dividing the current based on the permeability ratio, one obtains:

$I_{Kanamycin} = 0.13\,pA$

$I_{sulphate} = 1.75\,pA$

$I_{diffusion} = 1.9$ pA at the concentration difference (see Table S7)

Resulting at such ionic density, 1 µM difference inducing

$$\frac{d\,I_{diffusion(Kanamycin)}}{d[c]} = 4\,attoA \bullet \mu M^{-1}$$

Similarly, for sulphate ion we get 33.4 $attoA \bullet \mu M^{-1}$

From the above graph the conductance (slope) of the I-V (symmetric conditions) was measured to be 0.35 nS and from the steps recording of OmpF insertion at 20 mM Kanamycin sulphate, the average conductance of single $OmpF_{wt}$ channel at pH 7 is 16 ±3.7 pS

$$\text{Number of channels} = \frac{\text{Measured conductance } (\bullet)}{\text{Single channel conductance}} = \frac{0.35\,nS}{0.016\,nS} \sim 23\,channels$$

In the case of a single channel:

For Kanamycin:

$$\frac{d\, I_{diffusion,single\ channel}}{d[c]} = (4\ attoA \bullet \mu M^{-1})/23\ channels = 0.17\ \ attoA \bullet \mu M^{-1}$$

Similarly, for sulphate ion we get: $1.85\ attoA \bullet \mu M^{-1}$

To determine the number of net flux of Kanamycin ions (*N*) per second:

$$\mathrm{N/s} = \frac{\mathrm{q/s}}{e} = \frac{0.17\ \ attoA \bullet \mu M^{-1} \bullet s^{-1}}{1.6\times10^{-19} C} = 1\ \mu M^{-1} \bullet s^{-1}$$

Similarly, for sulphate ion we get: $11\ \mu M^{-1} \bullet s^{-1}$

Therefore, we calculated roughly ~1 Kanamycin and ~ 10 sulphate ions diffusing through a single OmpF normalized to 1 µM gradient of kanamycin sulphate.

References

(1) Prilipov, A.; Phale, P. S.; Van Gelder, P.; Rosenbusch, J. P.; Koebnik, R. Coupling Site-Directed Mutagenesis with High-Level Expression: Large Scale Production of Mutant Porins from E. Coli. *FEMS Microbiol. Lett.* **1998**, *163*, 65–72.

(2) Lamichhane, U.; Islam, T.; Prasad, S.; Weingart, H.; Mahendran, K. R.; Winterhalter, M. Peptide Translocation through the Mesoscopic Channel: Binding Kinetics at the Single Molecule Level. *Eur. Biophys. J.* **2013**, *42*, 363–369.

(3) Biró, I.; Pezeshki, S.; Weingart, H.; Winterhalter, M.; Kleinekathöfer, U. Comparing the Temperature-Dependent Conductance of the Two Structurally Similar E. Coli Porins OmpC and OmpF. *Biophys. J.* **2010**, *98*, 1830–1839.

(4) LAEMMLI, U. K. Cleavage of Structural Proteins during the Assembly of the Head of Bacteriophage T4. *Nature* **1970**, *227*, 680–685.

(5) Acosta-Gutiérrez, S.; Ferrara, L.; Pathania, M.; Masi, M.; Wang, J.; Bodrenko, I.; Zahn, M.; Winterhalter, M.; Stavenger, R. A.; Pagès, J.-M.; Naismith, J. H.; van den Berg, B.; Page, M. G. P.; Ceccarelli, M. Getting Drugs into Gram-Negative Bacteria: Rational Rules for Permeation through General Porins. *ACS Infect. Dis.* **2018**, *4*, 1487–1498.

(6) Livermore DM. Antibiotic Uptake and Transport by Bacteria. *Scand J Infect Dis Suppl.* **1990**, *74*, 15–22.

(7) Baba, T.; Ara, T.; Hasegawa, M.; Takai, Y.; Okumura, Y.; Baba, M.; Datsenko, K. A.; Tomita, M.; Wanner, B. L.; Mori, H. Construction of Escherichia Coli K 12 In frame, Single gene Knockout Mutants: The Keio Collection. *Mol. Syst.*

Biol. **2006**, *2*, 2006.0008.

(8) Datsenko, K. A.; Wanner, B. L. One-Step Inactivation of Chromosomal Genes in Escherichia Coli K-12 Using PCR Products. *Proc. Natl. Acad. Sci.* **2000**, *97*, 6640–6645.

(9) Ghai, I.; Winterhalter, M.; Wagner, R. Probing Transport of Charged β-Lactamase Inhibitors through OmpC, a Membrane Channel from E. Coli. *Biochem. Biophys. Res. Commun.* **2017**, *484*, 51–55.

4.3. Manuscript 1

Porin-mediated passage of negamycin across the outer membrane of *Escherichia coli*

Daniel Hörömpöli[1], Jayesh Arun Bafna[2], Theresa Harbig[3], Satya Bhamidimarri[4], Eshita Paul[2], Igor Bodrenko[5], Annika Hettich[1], Bert van den Berg[4], Kay Nieselt[3], Matteo Ceccarelli[5], Mathias Winterhalter[2], Anne Berscheid[1], Heike Brötz-Oesterhelt[1]

[1]Department of Microbial Bioactive Compounds, Interfaculty Institute of Microbiology and Infection Medicine, University of Tübingen, Tübingen, Germany

[2]Department of Life Sciences and Chemistry, Jacobs University Bremen, Bremen, Germany

[3]Center for Bioinformatics, University of Tübingen, Tübingen, Germany

[4]Institute for Cell and Molecular Biosciences, Medical School, Newcastle University, Newcastle upon Tyne, UK

[5]IOM/CNR, Sezione di Cagliari, Cittadella Universitaria di Monserrato, Monserrato, Italy

Abstract

The rise of antimicrobial resistant pathogens calls for new antibacterial treatments, but potent new compounds are scarce. Development of new antibiotics is difficult, especially against Gram-negative bacteria, as here uptake is strongly hindered by the additional outer membrane. Most antimicrobial agents against Gram-negatives, in particular small hydrophilic molecules, use the porin mediated pathway to cross the outer membrane, which limits the choice of an antibiotic, as it has to fit by size, charge and hydrophilicity. In *E. coli*, the major porins OmpF and OmpC are associated with antibiotic translocation and therefore also with non-specific antibiotic cross-resistance. In this regard, alternative uptake routes are of interest. We were interested in the uptake of the small, natural product antibiotic negamycin and discovered new uptake pathways across the outer membrane of *E. coli*. Besides OmpF and OmpC, we investigated the role of the minor porins OmpN and ChiP in negamycin translocation. We detected an effect of OmpN and ChiP on negamycin susceptibility and confirmed passage by electrophysiological assays. The structure of OmpN was solved by X-ray crystallography in order to analyze the negamycin translocation mechanism by computational simulations. As abundancy of these minor porins was low in *E. coli*, their transcript levels were analyzed by RNA-Seq. Increased transcripts levels of *ompN* and *chiP* were observed upon negamycin treatment. These new, additional uptake pathways across the outer membrane of *E. coli* highlight the antibiotic potential of negamycin, especially as resistance development is low due to availability of multiple uptake routes at both the outer and inner membranes.

Introduction

The outer membrane of Gram-negative bacteria is the first barrier for antibiotics with peri- or cytoplasmic targets. Translocation of antibiotics across the outer membrane is limited, as the asymmetrical composition of the outer membrane, with phospholipids in the inner and lipopolysaccharides (LPS) in the outer leaflet, hampers diffusion of molecules into the periplasm.[1] At the same time, bacteria need to enable nutrient uptake across this stringent barrier. Porins, water-filled channels, spanning across the whole outer membrane, allow diffusion of small, charged and polar molecules. Translocation through the major porins of *Escherichia coli*, namely OmpF and OmpC, is limited to smaller molecules, preferably positively charged and not bigger than 600 Da, although this rule of thumb is just a rough estimate,[2] as previous studies report various factors for porin translocation.[3] Although these porins have been studied for over 50 years, their role in antibiotic translocation is still not fully understood. Just recently it has been shown that aminoglycosides, already in clinical use, could diffuse through porins, as experimental data showed translocation of kanamycin through OmpF and OmpC.[4] So far, porins other than OmpF or OmpC have not been the focus of the antibiotic translocation studies in *E. coli*.

As uptake of some antibiotics is dependent on these porins, resistance can occur by modifying either channel properties or alteration in expression.[5] Although a decrease of nutrient influx could lead to reduced fitness, this tradeoff proved to be beneficial for bacteria under antibiotic exposition.[6, 7] Modifications of these rather unspecific channels could also lead to cross-resistance to other antibiotic classes, as this resistance mechanism is not specific to one structural class. In *E. coli*, this mechanism mainly affects the highly abundant porins OmpF and OmpC,[5] therefore investigations of alternative pathways for antibiotics are of interest.

We were interested in the uptake opportunities across the outer membrane of the antibiotic negamycin, as we recently could describe multiple influx pathways for this agent across the cytoplasmic membrane of *E. coli*.[8] Negamycin is a small (248.28 g/mol, 4.7 Å average minimal radius), very hydrophilic natural product, first described 1970 as a secondary metabolite of a *Streptomyces purpeofuscus* strain.[9] Negamycin interferes with protein biosynthesis, as it binds to the small

ribosomal subunit and inhibits translocation of the peptide chain.[10, 11] At the same time, negamycin stabilizes binding of unspecific tRNA, leading to a miscoding activity, resulting in a bactericidal mode of action. To reach its target in the cytoplasm, negamycin needs to cross both the outer as well as the inner membrane. Uptake studies are needed, as, with the exception of one analogue,[12] most optimizations of negamycin failed to achieve an increase in activity. Although some modifications led to higher target binding, whole-cell bioactivity was decreased, probably due to reduced uptake.[13-15] So far, negamycin translocation across the cytoplasmic membrane, but not the outer membrane, has been investigated in previous studies.[8, 16] With its molecular properties, negamycin is an ideal candidate for porin translocation. Surprisingly, our results of antibiotic susceptibility testing in different knockout mutants indicated that negamycin activity in *E. coli* is not dependent on either OmpF or OmpC, but rather on other, less studied porins, namely OmpN or ChiP. Electrophysiological studies confirmed that negamycin is able to pass through OmpN and ChiP. To uncover the structural basis of negamycin translocation by OmpN, we solved its structure by X-ray crystallography. Based on the structure, molecular simulations were performed, which gave further insights into the translocation mechanisms of negamycin through OmpN. We also compared the translocation mechanism of kanamycin through OmpN. To further understand how *E. coli* reacts to negamycin treatment, we carried out expression analyses investigating their transcript levels by RNA-Seq and porin protein levels by Western Blot detection. Our study could show new uptake pathways across the outer membrane of *E. coli*, which so far have not been associated with antibiotic translocation.

Results

Influence of porins on negamycin susceptibility. It is well known that the major *E. coli* porins OmpF and OmpC play an important role in antibiotic uptake.[1, 5] Negamycin has ideal physicochemical properties for translocation across porins,[3] as it is hydrophilic and positively charged at neutral pH, with an average dipole moment of 22.7 Debye. To investigate the roles of OmpF and OmpC in negamycin susceptibility, the minimal inhibitory concentrations (MIC) of negamycin were determined in *E. coli* BW25113 deletion strains without *ompF*, *ompC* or both major porin genes. Minimal media containing either only 0.5% polypeptone (PP) or glucose and salts (M9) were used, as negamycin competes with peptides for uptake opportunities and activity is strongly dependent on media composition.[8] The deletion of the porin genes *ompF*, *ompC* and the combinational deletion of both genes did not decrease negamycin susceptibility compared to the wildtype (Table 1). As a control, the MIC of the β-lactam cefotaxime was determined under the same conditions, and MIC increased up to 8-fold upon deletion of *ompF* or the multiple deletion of both *ompF* and *ompC*, indicating that our applied test conditions were suitable to detect effects due to porin loss (Table 1). Although we could not detect a change in negamycin MIC in Δ*ompF*Δ*ompC* by broth microdilution testing, the double deletion mutant showed a slight growth advantage compared to the wild type when streaked on a PP agar plate with a linear negamycin concentration gradient (Figure 1A & B).

Table 1. Negamycin and cefotaxime MIC determinations with porin gene deletion strains. Negamycin activity is not affected by deletion of *ompF* or *ompC*, whereas cefotaxime MIC is increased in *ompF* deletion mutants.

	negamycin MIC [µg/ml]		cefotaxime MIC [µg/ml]	
strain	PP	M9	PP	M9
E. coli BW25113 (WT)	8	4	0.031	0.008
E. coli Δ*ompF*	8	4	0.125	0.063
E. coli Δ*ompC*	8	2-4	0.031	0.008
E. coli Δ*ompF*Δ*ompC*	4-8	ng	0.125	ng

ng, no growth

To test whether the outer membrane is a rate limiting barrier for negamycin translocation in general, the integrity of the outer membrane was destabilized by addition of polymyxin nonapeptide B (PMBN) and negamycin MIC was determined. The PMBN addition decreased negamycin MIC from 8 to 2 µg/ml in PP, whereas in M9 medium it stayed at 4 µg/ml, regardless of the presence of PMBN

(Table 2). The reduced MIC in PP indicates that the outer membrane is a barrier for negamycin translocation. This trend could not be observed in M9, although the presence of high amounts of salts has to be considered, as these may at least partially antagonize the permeabilizing effect of PMBN by stabilization of the outer membrane.

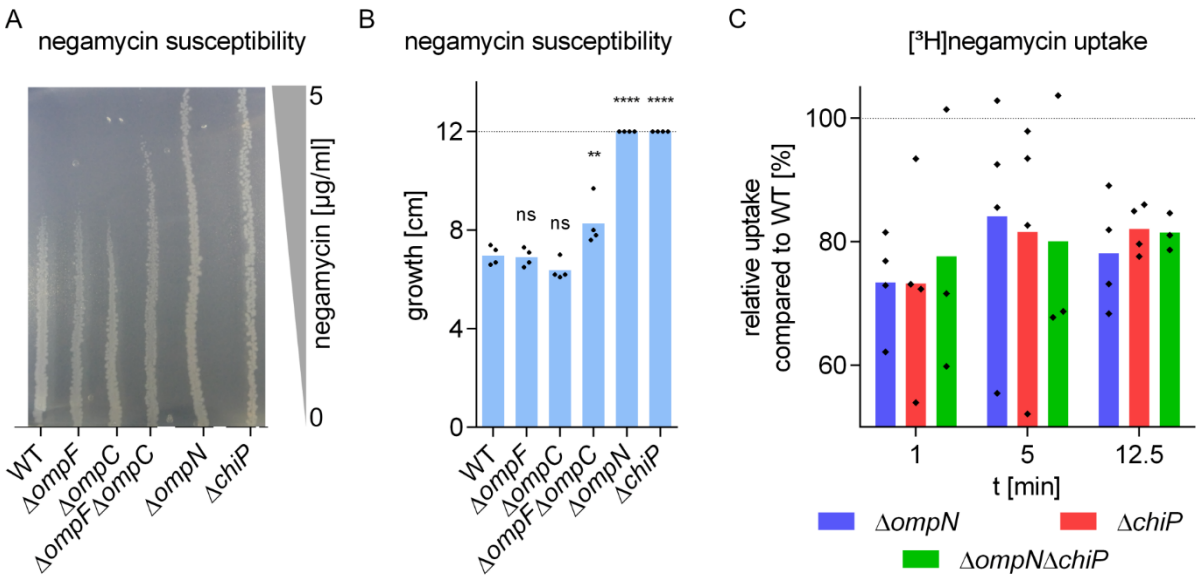

Figure 1. Negamycin susceptibility and [³H]negamycin uptake of *E. coli* porin mutants. (A) Growth of *E. coli* BW25113 porin mutants on PP agar with a linear negamycin gradient (0 – 5 µg/ml). One agar gradient plate is shown exemplarily (A) and the average of four independent experiments as a summary (B). The dotted line marks the limit of detection at the end of the plate. Statistical significance shows comparison of the respective gene deletion mutant to the WT. (C) Uptake measurements of [³H]negamycin in *E. coli* ATCC 25922 porin mutants. 32 µg/ml negamycin (specific activity: 0.052 Ci/mmol) was added and accumulation of [³H]negamycin of *E. coli* ATCC 25922 porin mutants was compared to its isogenic wildtype strain at 1, 5 or 12.5 min. Each diamond shows an independent measurement of susceptibility (B) or [³H]negamycin uptake (C) with the average displayed as a bar. Statistical significance was determined using unpaired Student's *t test* with Holm-Bonferroni correction. ns (not significant), $P > 0.05$; **, $P \leq 0.01$; ****, $P \leq 0.0001$.

As other uptake routes across the outer membrane of *E. coli* must be available and negamycin's physicochemical properties are perfectly suited for porin passage, we searched for further porin genes in the *E. coli* genome. Negamycin MIC was determined in these deletion mutants in the *E. coli* BW25113 background and we found multiple porin genes, namely *ompN*, *chiP*, *lamB*, *ompG*, *ompW* and *ompA*, where the gene deletion led to a 2-fold increase in MIC (Table 2). The addition of PMBN to these porin gene deletion mutants reversed the effect of decreased susceptibility to a level of WT with PMBN treatment, hinting that the deletion of these porin genes had an effect on the barrier function of the outer membrane. Further research focused on the two porin genes *ompN* and *chiP*, as the OmpN porin showed high similarity to the major porins OmpF and OmpC,[17] and the effect on negamycin susceptibility of Δ*ompN* and Δ*chiP* was reliably seen in both M9 and PP media. To test the

relevance of *ompN* and *chiP* in other *E. coli* species, single-gene mutations were generated in *E. coli* ATCC 25922. In contrast to the laboratory K-12 strain, from which BW25113 is derived, the ATCC 25922 strain originates from a clinical isolate.[18] Within the outer membrane, *E. coli* ATCC 25922 contains an intact O-antigen and thereby a more stabilized outer membrane barrier, in contrast to the K-12 strain and its derivatives, as here the O-antigen is missing.[1] In ATCC 25922, the deletion of the *ompN* or *chiP* gene led to a two-fold negamycin MIC increase as well, from 16 to 32 µg/ml in PP and 1 to 2 µg/ml in M9 (Table 2). Additionally, double-deletion mutants, lacking both *ompN* and *chiP*, were generated in *E. coli* BW25113 and *E. coli* ATCC 25922, as an additive effect on negamycin MIC might be expected. However, negamycin MIC was not increased further and stayed at the same level as single-gene deletion strains in both strain backgrounds (Table 2).

Table 2. Effects of gene deletions of porin genes, which are less described for antibiotic susceptibility, on negamycin MIC. Deletion of specific minor porin genes influences negamycin activity, both in *E. coli* BW25113 and ATCC 25922. The increased MIC by the porin gene deletion could be reversed by the addition of 15 µg/ml PMBN to a level similar to WT treated with PMBN.

	negamycin MIC [µg/ml]			
strain	PP	PP+PMBN	M9[a]	M9+PMBN[a]
E. coli BW25113 (WT)	8	2	4	4
E. coli BW25113 Δ*ompN*	16	2-4	8	4
E. coli BW25113 Δ*chiP*	16	2-4	8	4
E. coli BW25113 Δ*lamB*	16	4	ng	ng
E. coli BW25113 Δ*ompG*	16	2	4	nd
E. coli BW25113 Δ*ompW*	16	2	4-8	nd
E. coli BW25113 Δ*ompA*	ng	ng	4-8	nd
E. coli BW25113 Δ*phoE*, Δ*ompL*, Δ*bglH*, Δ*tsx*, Δ*fadL*, Δ*nanC*, Δ*ychO*, Δ*yfiB*, Δ*yfaZ*, Δ*yiaT*	8	nd	4	nd
E. coli BW25113 Δ*ompN*Δ*chiP*	16	2	8	nd
E. coli ATCC 25922 (WT)	16	4	1	1
E. coli ATCC 25922 Δ*ompN*	16-32	4	1-2	1
E. coli ATCC 25922 Δ*chiP*	32	4	2	1
E. coli ATCC 25922 Δ*ompN*Δ*chiP*	16-32	2	2	nd

[a] M9 was supplemented with 1 µg/ml thiamine for *E. coli* ATCC 25922. ng, no growth. nd, not determined

The deletion of these porin genes decreased negamycin accumulation in *E. coli* ATCC 25922. When *ompN*, *chiP* or both genes were deleted, on average 20% less radioactive-labeled [^{3}H]negamycin was accumulating in *E. coli* ATCC 25922 within 15 min after the addition of 32 µg/ml negamycin (Figure 1C & S1). Similarly to MIC determinations, the double deletion of both *ompN* and *chiP* did not have

an additive effect on negamycin uptake, as [^{3}H]negamycin levels were similar in *E. coli* ATCC 25922 Δ*ompN*Δ*chiP* as in the single gene deletion strains. This additional porin gene deletion might not be enough to reach a certain threshold of resistance, as other porins are still available or a change in uptake is masked by efflux. Therefore, the role of efflux pumps on negamycin susceptibility was investigated.

Influence of efflux on negamycin susceptibility. The most important *E. coli* efflux pumps, in regard to antibiotic resistance, were tested by examining the corresponding deletion strains.[1] The activity of negamycin was measured in deletion strain mutants without *acrA*, *acrB*, *acrD*, *acrE*, *acrF*, *macA*, *macB* or *mdfA*. Negamycin MIC stayed either at wildtype level or the gene removal had no large impact on susceptibility (Table S1). The deletion of *acrA*, *acrB* or both genes had previously strong effects on novobiocin MIC in PP, as it decreased from 32 µg/ml to 1-2 µg/ml for the single gene deletion of *acrA* or *acrB* and down to 0.5 µg/ml in *E. coli* Δ*acrAB*.[8] Only the deletion of *tolC* increased negamycin activity higher than two-fold in PP to a MIC of 2-4 µg/ml, but not in M9. In another *E. coli* K-12 derivative, *E. coli* C600,[19] the *tolC* deletion mutant did not change the negamycin MIC in PP compared to the wildtype (4 µg/ml; Table S1). For TolC mediated efflux, a complex with subunits composed of a permease and membrane fusion protein is necessary.[20] As the deletion of single or multiple genes of these subunits did not affect negamycin MIC (Table S1), the effect of the Δ*tolC* mutant might not necessarily be efflux specific. It has previously been reported, that the deletion of *tolC* can lead to multiple defects on the outer and inner membrane integrity,[21] which could affect antibiotic susceptibility. Compared to other antibiotics, negamycin accumulation is not strongly hindered by the common *E. coli* efflux systems.[22] Based on the results of the porin gene deletion strains with whole *E. coli* cells, we were interested to investigate the porin-mediated uptake on a protein level.

Negamycin translocation through porins by reversal potential determination. To check for permeation of negamycin through the porins OmpN, ChiP, OmpF and OmpC in an *in vitro* system, porin proteins were purified and antibiotic permeability was determined by reversal potential measurements under tri-ionic conditions in the presence of salts. The OmpN porin was analyzed in

detail and we could confirm previous conductance of the channel (Figure S2 & Table S2).[17] General properties of the OmpN porin, e. g. channel conductance and ion selectivity, are described in detail in the supplemental information (Figure S2, S3, S4 & Table S2, S4).

Under tri-ionic conditions, the reversal potentials were determined for OmpN, ChiP, OmpF and OmpC, when negamycin was added. Negamycin passed through OmpN, ChiP, OmpF and OmpC, in this order from fastest to slowest transport (Table 3 & Table S3). For quantification of negamycin translocation through OmpN, single channel measurements with OmpN and negamycin could not be obtained, as blockage of the ion current by negamycin addition could not be detected (Figure S5), however, a rough estimate suggests that ten to hundred molecules/s/monomer may permeate at a 1 µM negamycin gradient. The β-lactams ertapenem and cefotaxime (Table 3) and, as previously shown, the aminoglycoside kanamycin,[4] did not translocate through OmpN. The major *E. coli* porins OmpF and OmpC were not as selective as OmpN and permeable for ertapenem (Table 3) and kanamycin.[4]

Table 3. Permeability ratios of the antibiotics negamycin, ertapenem and cefotaxime through OmpN, ChiP, OmpF, or OmpC, under tri-ionic conditions with NaCl as determined by the electrophysiological assay (Table S3). Negamycin is able to pass through all the porins tested, whereas ertapenem and cefotaxime were not able to translocate through OmpN.

	permeability ratio (Na^+ : Cl^- : **antibiotic**)		
	negamycin	ertapenem	cefotaxime
OmpN	2 : 1 : 0.75	2 : 1 : **<0.0001**	2 : 1 : **0.000001**
ChiP	1 : 6 : 0.35	nd	nd
OmpF	5 : 1 : 1.35	5 : 1 : **1.85**	nd
OmpC	3 : 1 : 0.5	8.5 : 1 : **4.2**	nd

nd, not determined

Based on the structure of negamycin, it is of no surprise that negamycin is able to permeate efficiently through OmpF and OmpC, but this observation is not reflected by previous MIC determinations (Table 1). The electrophysiological data suggest that OmpN is more selective compared to other porins and negamycin is exceptionally promiscuous in its translocation through various porins.

Structure of OmpN. To further understand the permeability restrictions of OmpN, we determined the X-ray crystal structure of the protein using data to a resolution of 2.6 Å (Figure 2). Structurally, OmpN is very similar to OmpF and OmpC, but there are a few differences (Figure S6). The loop L7 outside the cell is elongated compared to OmpF and OmpC and Thr101 is substituted by Glu102 in the helix

of the otherwise conserved loop L3 within the constriction region of OmpN (Figure 2 & S6). This change to an acidic residue renders the OmpN porin more cation selective. At the extracellular mouth of the porin, the ertapenem binding site at R167 and R168 in OmpF is modified in OmpN (Figure S6).[23] In the same region in OmpC only one arginine is present (Arg174). On the other hand, in OmpN no basic residues are present at this location, but only His173 and a longer loop with two acidic residues (Asp248 and Asp250), thus making this region an attractor for positively charged molecules (Figure 2). Based on previous conductance measurements of OmpN (58 ± 17 pS, with 20 mM K2SO4 at +100 mV), a smaller constriction zone compared to OmpC (180 ± 30 pS) and OmpF (240 ± 27 pS) was expected.[4] Surprisingly, the minimal size of the constriction zone of OmpN (2.8 ± 1.1 Å) is similar to OmpC (2.8 ± 1.1 Å) and OmpF (3.1 ± 1.1 Å) (see also the comparison of minimal radius distribution of OmpN and OmpF in figure S7).[3] Therefore, the differences observed in conductance measurements from the actual pore size must base on electrostatic properties of the channel.

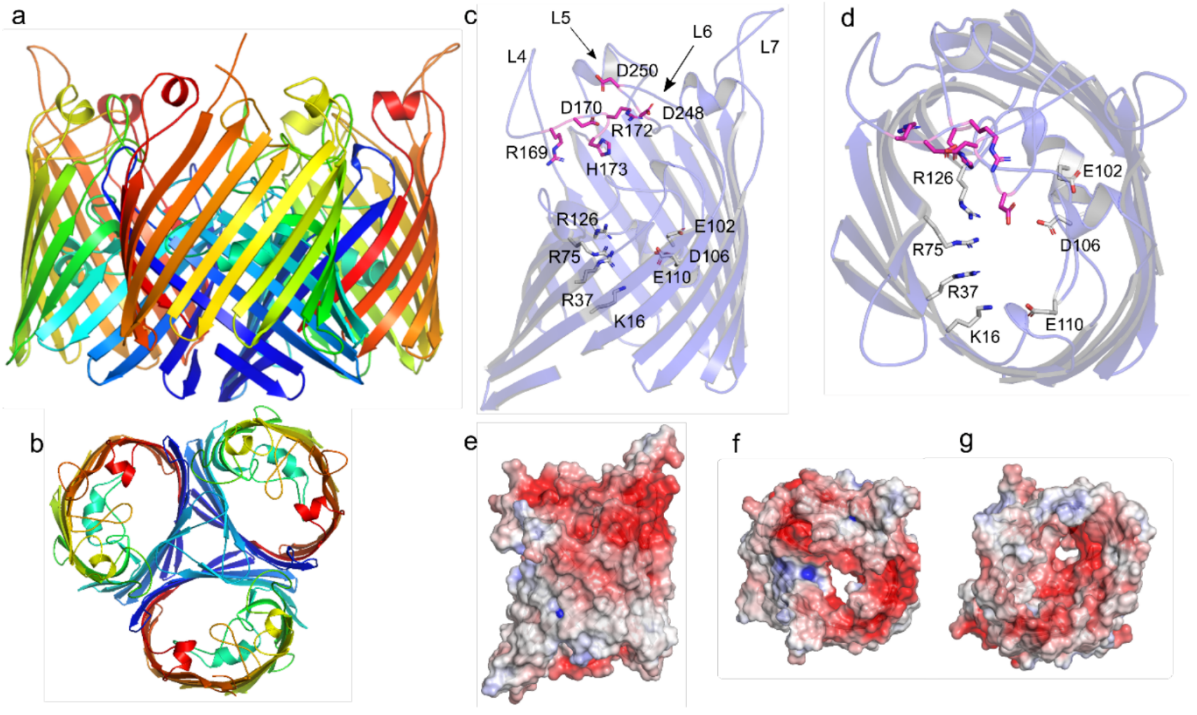

Figure 2. Structure of OmpN as resolved by X-ray crystallography. (a, b) Cartoon representation of OmpN, structures are shown in rainbow with N-terminus (blue) and C-terminus (red) for each monomer. (c) side view and top view from extracellular side (d) of OmpN monomer with highlighted residues from the constriction zone and extracellular mouth region. Electrostatic surfaces ($-5\ kTe^{-1}$ to $5\ kT\ e^{-1}$) of the OmpN monomer generated via ABPS server viewed from (**e**) the plane of the OM (**f**) the outside of the cell and the periplasmic space (**g**). All crystal structure figures were generated with PyMOL.

Translocation mechanism through OmpN (molecular dynamics). The structure of OmpN allowed us to conduct numerical simulations on a molecular level, which enabled us to investigate interactions of negamycin with the porin. As suggested by PROPKA for modelling the condition at pH 7 we protonated two residues at the constriction region, Glu261 and Asp308.[24] In OmpF and OmpC only one residue is protonated, corresponding to Asp308. To check the reliability of the double protonation state, we performed molecular dynamics simulations with an external electric field to assess the ionic current as a function of voltage. The predicted conductance is in good accordance with experimental data measured at pH 7 and 1 M NaCl (Figure S8 & Table S2).

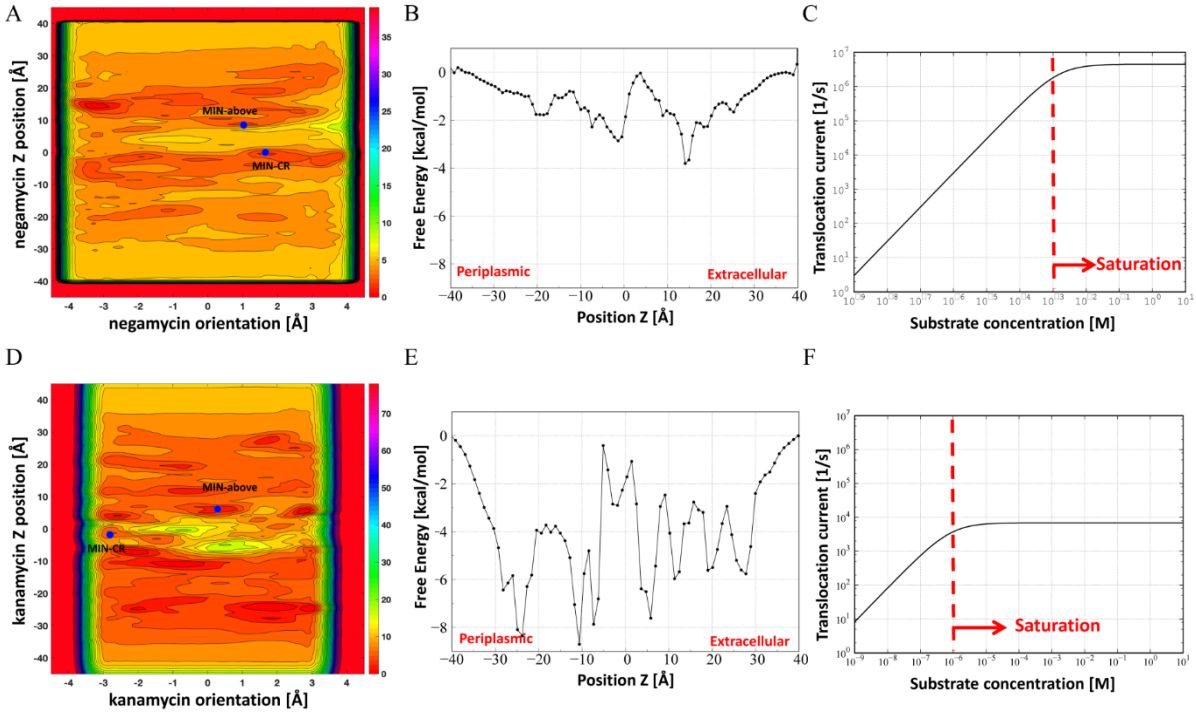

Figure 3. Molecular dynamics showing negamycin and kanamycin translocation through OmpN. Free energy surface (FES) of negamycin (A) and kanamycin (D) shown within the OmpN porin, depending on position and orientation of the antibiotics within the porin. FES depending on negamycin (B) and kanamycin (E) position within OmpN. Translocation current shown depending on substrate concentration of negamycin (C) or kanamycin (F).

Negamycin translocation through OmpN was simulated using well-tempered metadynamics with 8 walkers and the free energy surface was determined after sampling 32 µs, 4 µs per walker. Inspecting the 2-dimensional free energy surface we see two main minima, one at the constriction region (Figure 3A & 3B, Min-CR at Z-position = -2 Å, -4 kcal/mol with respect to outside) and the other one in the extracellular region, just above the constriction region (Figure 3A & 3B, Min-above at Z-position = 10 Å, -3 kcal/mol with respect to outside).

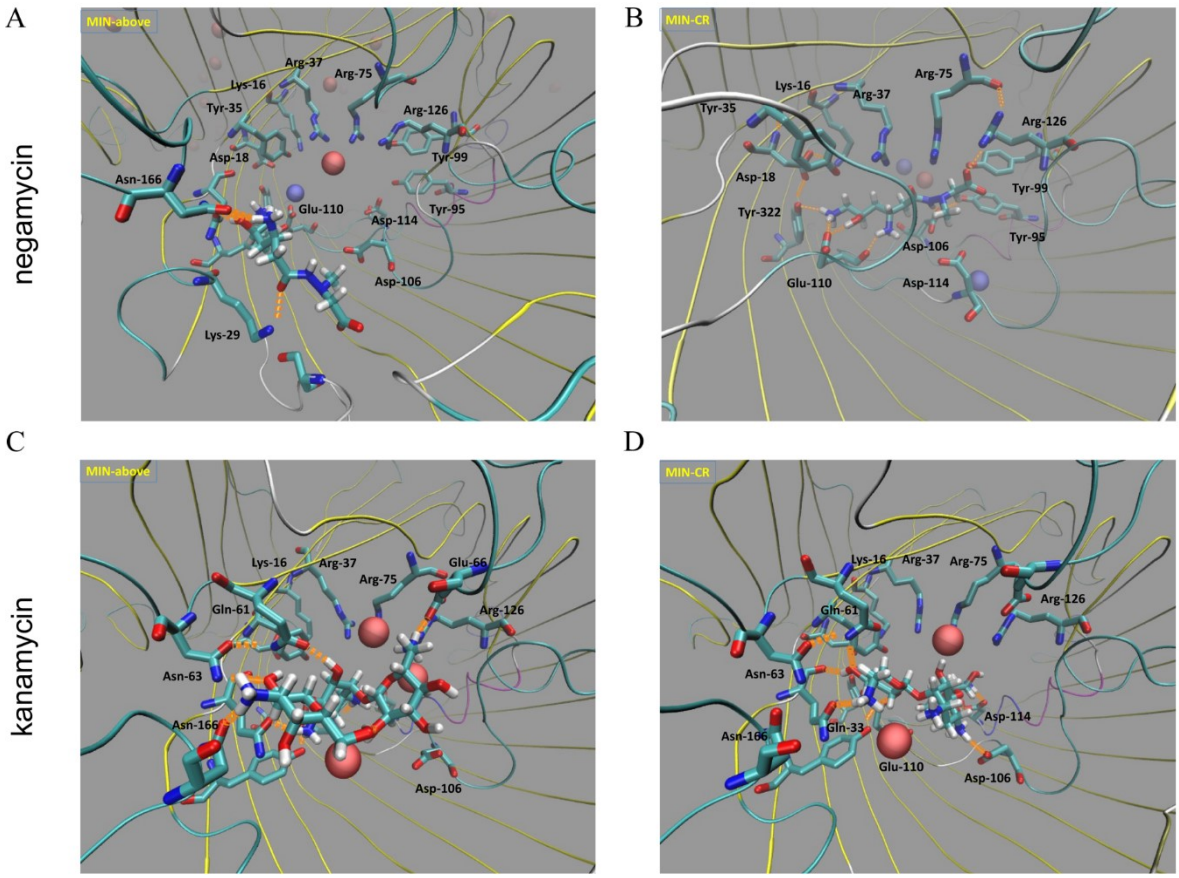

Figure 4. Interaction of negamycin and kanamycin within the barrel structure of the porin OmpN. (A) Negamycin at the extracellular mouth region of OmpN interacting with Lys29 and Asn166. (B) At position Min-CR, the positively charged groups of negamycin interact with Asp106 and Glu110 within loop L3 of OmpN, and the carboxylic group with Arg126. (C) Kanamycin in contact with Glu66, Asn166, Gln61 of OmpN and three chloride ions at position Min-above. (D) Kanamycin interactions at position Min-CR with Asp106, Asp114 and Glu110 of OmpN and additionally with two chloride ions. Chloride ions are shown as red and sodium ions as blue dots.

Another minimum is present at Z = 15 Å, with negamycin trapped in the same extracellular mouth region where ertapenem was co-crystallized in OmpF.[23] We focused on the two minima closer to the constriction region. In Min-CR, negamycin interacts strongly with the loop L3 via contacts with Asp106 and Glu110 (Figure 4A). The carboxylic group is in contact with Arg126. Starting with negamycin placed there, we recalculated the ionic current at positive and negative voltages (+100 mV and -100 mV) obtaining a reduction of one third with respect to the empty system, as expected when one monomer is blocked (Table S5). On the other hand, when negamycin is in Min-above (interaction with Lys29 and Asn166) the pore is completely free and we only see one chloride ion close to negamycin (Figure 4A).

The flux of negamycin from the cis to trans side was determined imposing a gradient concentration among the two cells. The flux was very high, with a residence time inside of less than 0.1 μs (Figure 3C), which might be too low to be measured in the single channel measurement setup (Figure S5). Saturation was only reached in a milimolar concentration range (Figure 3C).

In order to understand the apparent electrostatic barrier in OmpN, we investigated by numerical simulations the translocation of kanamycin, a large (minimum average radius of 5.5 Å) and highly (+4e) cationic molecule. Experimentally, the extremely low level of conductance using the reversal potential method was already shown.[4] Simulations were performed exactly as for negamycin, with the well-tempered metadynamics now using 16 walkers, for a total simulation time of 100 μs. The 2-dimensional free energy surface shows an affinity site just above the constriction region (Min-above at Z = 6 Å, -6 kcal/mol with respect to the exterior) and a weaker one at the constriction region (Min-CR at Z = -2 Å, -4 kcal/mol with respect to the exterior) (Figure 3D & 3E). The favourable interaction between the high charge of kanamycin and the acidic environment of OmpN is probably the origin of the electrostatic barrier or the extremely low measured flux (Figure 4C & 4D). To note that in Min-above kanamycin is in contact (3 Å) with three chloride ions, while it interacts with Glu66, Asn166 and Gln61. On the other hand, when in Min-CR there are two close chloride ions, while it interacts with Asp106, Asp114 and Glu110 of OmpN.

The predicted flux as function of gradient concentrations is in absolute value three orders of magnitude lower for kanamycin than for negamycin (because of the different size and strong interaction with the acidic residues, see figure S7) and, more interestingly, saturation of kanamycin is reached already at µM concentrations (Figure 3F).

This computational data is in accordance with the *in vitro* data. To understand how *E. coli* reacts to negamycin treatment, we set out to investigate the transcriptome of *E. coli* when exposed to the antibiotic.

***ompN* and *chiP* expression under negamycin treatment.** The results on a protein level clearly showed translocation of negamycin through OmpF and OmpC (Table 3), but this was not reflected in MIC measurements (Table 1). Although these major porins are described to be highly abundant,[1] only a small decrease in negamycin susceptibility could be detected, when *E. coli* Δ*ompF*Δ*ompC* was streaked on agar containing a linear negamycin gradient (Figure 1A & 1B). Therefore, we were interested how *E. coli* reacts to negamycin exposure. For this, the transcriptome of *E. coli* BW25113 was investigated by RNA-Seq. Total RNA was isolated from exponentially growing *E. coli* cells, treated with a negamycin concentration equivalent to 4x MIC for 45 min and expression was compared to an untreated sample. Additionally, gene deletion mutants lacking either *ompN*, *chiP* or both porin genes were investigated by RNA-Seq as well.

E. coli reacted to negamycin exposure by strongly decreasing the expression of multiple transporters, especially the ones responsible for translocation across the cytoplasmic membrane (Table 4). The gene *malK*, the ATP binding subunit of a maltose ABC transporter, was affected the strongest by a downregulation of over 500-fold upon negamycin treatment. However, negamycin activity was not dependent on *malK*, as *E. coli* Δ*malK* showed the same MIC as the wildtype (8 µg/ml in PP). Negamycin uptake might potentially still be affected by this operon, as the downstream gene of *malK* is *lamB*, a porin which we had associated with negamycin susceptibility in this study (Table 2) and whose expression was also decreased 48.8 times by negamycin treatment (Tables 4). Furthermore, peptide transporters were affected by negamycin treatment as well, as the transcripts encoding the dipeptide transporter Dpp were strongly decreased (Table 4). In previous studies, the Dpp transporter

was described as one of the main uptake pathways for negamycin across the cytoplasmic membrane.[8, 16] Negamycin treatment also induced expression of the efflux pump subunits *acrE*, *acrF* and *mdfA* and decreased expression of *acrD* slightly (Table 4). As mentioned above, *E. coli* Δ*acrE*, *E. coli* Δ*acrF* or *E. coli* Δ*mdfA* as well as deletions of other efflux pump subunit genes, did not increase negamycin activity (Table S1). Transcripts of *tolC*, *acrA*, *acrB*, *macA* and *macB* were not affected significantly under negamycin treatment. The expression of *bshA*, associated with stress response,[25] was strongly increased, but could not be linked to a resistance mechanism against negamycin, as the deletion of the gene did not alter negamycin susceptibility and MIC stayed at wildtype level of 8 µg/ml.

At the outer membrane, the negamycin treatment reduced expression of the *ompF* transcript by 2.6 fold, compared to the untreated sample (Table 4). *ompC* expression was not affected significantly. At the same time, *ompN* and *chiP* expression increased 3.6 and 5.1 fold, respectively (Table 4). Among the porin genes, *ompG* expression was increased the strongest with a 13.6 fold change. In contrast, *ompW* expression was reduced 2 times, but both *ompG* as well as *ompW* genes were associated with negamycin susceptibility (Table 2). As *E. coli* reacts to the antibiotic pressure, it might compensate the reduction of OmpF through other, more restrictive porins. Uptake of various antibiotics might therefore be decreased in *E. coli*, but not of negamycin, as we could show permeation through freely available minor porins like OmpN and ChiP (Table 3). Although these trends in porin gene expressions could be clearly seen, it has to be noted that average expression of *ompF* (1308.08 transcripts per million) was stronger than *ompN* (0.34 transcripts per million) across both treated and untreated samples (Table 4).

Table 4. Transcript expression fold changes of selected genes affected by negamycin treatment measured by RNA-Seq. Average fold change of transcripts shown from three independent biological experiments comparing treated to untreated *E. coli* BW25113 cells grown in PP. The strongest affected transcripts by negamycin treatment (> 30x fold change) are listed in Table S8 and the complete RNA-Seq dataset is available as supplementary data SI2.

	Transcript fold change[A]	**MIC fold change[C]**	**Average TPM (transcripts per million)**
Gene	***E. coli* BW25113 + negamycin[B]**	***Gene deletion mutant compared to WT***	***Average of both untreated and negamycin treated samples***
Porins			
ompN	3.6	2	0.3
chiP	5.1	2	3.1
ompF	-2.6	1	1308.1
ompC	ns	1	
ompG	13.6	2	0.3
ompA	2.6		1.8
lamB	-48.8	2	59.2
ompW	-2.0	2	13.3
Cytoplasmic membrane transporters			
malK	-546.9	1	91.6
dppB	-86.2	1[D]	61.5
dppD	-84.0	1[D]	94.4
dppC	-71.7	1[D]	72.2
dppF	-63.6	1[D]	40.7
dppA	-19.0	1[D]	192.2
Efflux			
acrD	-2.8	1	2.6
acrE	39.6	1	0.1
acrF	2.3	1	1.1
mdfA	3.4	1	21.2
Stress response			
ydbK	-2.3	2	4.8
pspB	62.7	nd	198.6
bhsA	105.3	1	1.8
soxS	1054.0	1	181.1

[A]Compared to untreated *E. coli* BW25113. [B]*E. coli* BW25113 treated with 16 µg/ml negamycin (4x MIC) in PP for 45 min. [C]Negamycin MIC fold change determined in PP, comparing the respective gene deletion mutant to the WT. [D]MIC changed four fold in peptide free media.[1] ns, not significant (FDR corrected p-value > 0.05); nd, not determined.

soxS, a transcriptional activator upon oxidative stress,[26] was overall the strongest increased transcript (with more than 1,000 fold) after negamycin treatment. Again, negamycin activity was not dependent on this specific stress reaction by the bacterial cell, as negamycin MIC for *E. coli* Δ*soxS* was at wildtype level (8 µg/ml). Interestingly, *soxS* dependent activation of the *ompN* gene was described previously.[27] Although *soxS* was proposed to be an activator of the *ydbK-ompN* operon,[27] negamycin treatment showed a different trend. YdbK has been described as an oxidoreductase and has been associated with superoxide resistance, but not with antibiotic resistance.[27, 28] The strong induction of *soxS* did not increase *ydbK* transcript levels, but actually reduced *ydbK* expression by 2.3 fold (Table 4). The MIC of negamycin increased two-fold in a Δ*ydbK* mutant (Table 4).

To confirm the increases of *ompN* and *chiP* transcripts on a protein level, outer membrane protein fractions from exponential growth phase were extracted and applied for detection via Western blot. *E. coli* was treated at early exponential phase with negamycin equivalent to concentrations between 0.125x to 8x MIC, and samples were taken at different time points after negamycin exposition. No OmpN or ChiP could be detected, neither in untreated nor treated samples (Figure S9). Although the *ompN* and *chiP* transcripts were clearly increased after negamycin treatment (Table 4), it has to be noted, that the transcript amounts of *ompN* were very low (Table 4, Supplemental information 2). Protein levels might not be sufficient for Western blot detection. Additionally, various porin gene deletion mutants were investigated, as the removal of *ompF*, *ompC* or both genes might be compensated by increased expression of OmpN, but the latter could not be shown by Western blot (Figure S9). Under the tested conditions, OmpN or ChiP were never expressed to a degree, where we were able to detect the proteins via Western blot.

To investigate if the deletion of *ompN*, *chiP* or both genes affected expression of other genes, which could indirectly influence negamycin susceptibility, the transcripts of the strains *E. coli* Δ*ompN*, *E. coli* Δ*chiP* and *E. coli* Δ*ompN*Δ*chiP* were examined under the same conditions as the wildtype strain before. The gene deletions did not lead to a significant change of expression of other porin genes, with the exception of the *chiP* transcript, which was reduced 2.3 fold in *E. coli* Δ*ompN* (Table S6). The change in negamycin susceptibility in *E. coli* Δ*ompN* or *E. coli* Δ*chiP* might therefore not be

due to a change in expression of other porins. Furthermore, other transcripts were not strongly affected by these gene deletions (Supplemental information 2). When *ompN* transcripts were compared between *E. coli* Δ*ompN* and its isogenic wildtype strain, no decrease in *ompN* transcripts could be observed, which would have been expected when the gene is removed. This indicates a very low basal expression of *ompN* in the wildtype strain. Although expression of OmpN and ChiP could not be shown on a protein level, the transcriptional analysis did not reveal unrelated changes of the transcriptome when *ompN* or *chiP* was deleted, which could affect negamycin susceptibility.

Porins are the main uptake pathways for nutrients across the outer membrane of *E. coli*, but antibiotics are not limited to these channels. Other mechanisms, interfering with the outer membrane integrity, have been proposed for certain antibiotic classes.[29] Negamycin's ability to use this self-promoted-uptake mechanism was investigated.

Analysis of the self-promoted uptake as a translocation mechanism for negamycin. For polycationic antibiotics, like aminoglycosides, it has been shown that they disrupt the outer membrane briefly, which led to an increase of the antibiotic itself.[29] This self-promoted uptake is an alternative translocation mechanism across the outer membrane of Gram-negative bacteria. As negamycin possesses two amine groups, negamycin might be able to use this channel-independent uptake mechanism. The self-promoted uptake pathway was investigated by uptake measurements of 1-N-phenyl-naphthylamine (NPN).[30, 31] Fluorescence signal of NPN increases strongly when it is able to interact with phospholipids of the cytoplasmic membrane. Here, polymyxins and aminoglycosides increased NPN passage through the outer membrane about 9 and 5 times, respectively, whereas negamycin addition did not increase signal above background level (Table S7). This result does not exclude, that negamycin might briefly disrupt the outer membrane, but at least not to a degree which could be measured by the employed NPN uptake assay. Outer membrane disruptors, like the tested polymyxins and aminoglycosides, could show a more severe effect on the outer membrane integrity, as molecules of these antibiotic classes are bigger and possess more amine groups. For negamycin the translocation across the outer membrane via porins seems most likely.

Discussion

Previous studies on negamycin uptake in *E. coli* showed multiple pathways across the inner membrane, both transporter dependent and independent.[8, 16] For a hydrophilic, small compound like negamycin, outer membrane translocation might be dependent on specific porins. In this study we report on multiple porins available for negamycin translocation across the outer membrane. Negamycin susceptibility was decreased when *ompN*, *chiP*, *lamB*, *ompG*, *ompW* or *ompA* were deleted (Table 2). The single gene deletion of *ompF* or *ompC* had no effect on negamycin MIC, and only a small increase in growth could be observed when the double knockout mutant was growing on a linear negamycin concentration gradient (Figure 1A & 1B). Negamycin was able to diffuse through OmpF, OmpC, ChiP and OmpN (Table 3). Although single channel conductance of OmpN was described to be similar to OmpC,[17] it is a more restrictive porin, as the OmpC-permeable antibiotics ertapenem and cefotaxime could not pass through OmpN (Table 3).[32] These various uptake routes of negamycin across the first barrier of bacterial defense in Gram-negatives make resistance development at this barrier unlikely, both through spontaneous resistance development as well as by cross resistance from previous antibacterial treatment, as usually the major porins OmpF and OmpC are affected.[5] The outer membrane of *E. coli* does not seem to be the primary limiting barrier in cellular uptake of negamycin, as previous isolated *E. coli* cells exposed to negamycin exclusively showed mutations in genes encoding the dipeptide permease Dpp in peptide free media.[8] In this study, we also observed that negamycin treatment had a strong effect on the expression of peptide transporter genes located in the cytoplasmic membrane, mainly of the *dpp* operon (Table S8).

The permeability ratio, determined by electrophysiological measurements (Table 3), of negamycin compared to NaCl (Na : Cl : negamycin) was high for OmpN (2 : 1 : 0.75), ChiP (1 : 6 : 0.35) and lower for OmpF (5 : 1 : 1.35) and OmpC (3 : 1 : 0.5). Compared to previous electrophysiological studies with OmpF, permeability ratios of kanamycin (14 : 1, permeability of sulfate : kanamycin)[4] and ampicillin (1 : 4 : 0.75, permeability of Cl : K : ampicillin)[33] were lower. Inspection of table 3 reveals that the four investigated channels allow negamycin to permeate in a similar manner as sodium chloride. A very rough estimation for a concentration gradient of 4 to 16 µM, which is in range of the

MIC, negamycin resulted in about 50-500 molecules per second per channel to be translocated (Table S3 & S4). Note that such rates can only be obtained in a diluted system whereas bacteria have an additional LPS layer reducing the entry.[34] Furthermore, the periplasmic space is extremely crowded and already a few molecules without an inner membrane sink would escape.[35]

Based on previous conductance measurements,[4] a smaller pore was expected, but the size of the constriction region of OmpN (Figure 2) was similar to OmpF and OmpC.[3] As OmpN showed a different translocation pattern for antibiotics than OmpF and OmpC, other mechanisms, such as an electrostatic barrier, must explain differences in substrate specificity. A previous study with clinical *E. coli* isolates could indeed show that alterations in the *ompC* sequence had an impact on antibiotic resistance, although pore size was not strongly affected.[32] The differences in antibiotic translocation could be linked to the transverse electric field inside the OmpC porin, which was affected by subtle changes of residues within the barrel structure. From the structure of OmpN we could identify Asp248 and Asp250 protruding into the barrel (Figure 2C), which could increase cation selectivity.

The physiological role of OmpN in *E. coli* is not known. OmpN was only first described in 1998, as it has been overlooked in previous studies due to its low expression in standard laboratory media.[17] It has been proposed, that the *ydbK-ompN* operon is part of the oxidative stress response, yet the *ompN* gene deletion did not affect the oxidative stress sensitivity.[27] Fabrega et al. (2012) could experimentally show the existence of a single mRNA transcript containing both genes.[27] This is in contradiction to the transcriptomic data under our testing conditions, where we could find numerous copies of the *ydbK* transcript, but none or only a few copies of *ompN* when untreated or treated with negamycin, respectively (Supplemental information 2). If there is an operon containing both transcripts, which could not be detected under our growth conditions, additional single transcription units of both genes, an unidentified riboswitch between the two genes or post-transcriptional regulation of *ompN* are plausible. Detection of transcription start sites (TSS) in *E. coli* revealed an additional TSS for *ompN*.[36] Oxidative stress did not induce a putative *ompN* promoter, but increased the promoter signal of *ydbK*.[27] This indicates that if *ompN* is induced by oxidative stress, it is likely due to co-transcription with the upstream *ydbK*.[27] The transcriptomic data in this study showed an opposite trend when *E. coli* was

treated with negamycin (Table 4). Negamycin treatment increased *ompN* and decreased *ydbK* expression. At the same time, the transcriptional activator *soxS* was the strongest increased transcript in negamycin treated cells. Dam et al. (2017) chose the whole upstream region between *ompN* and *micC* in their study to include a potential promoter of *ompN*.[37] Although no distinct *ompN* promoter region was identified, their reporter plasmid containing the putative promoter sequence showed upregulation when *E. coli* was exposed to certain antibiotics, e.g., carbapenems and cephalosporins, but they could not detect the OmpN protein by Western blot in these samples.[37]

It has been proposed previously, that OmpN might act as a backup porin due to its similarity to OmpC, when expression of the major porins OmpF and OmpC is reduced.[7] In *Klebsiella pneumoniae*, such a mechanism has been observed with some clinical isolates.[38] When OmpK35 and OmpK36, orthologues of OmpF and OmpC, were missing, some isolates showed expression of OmpK37, a porin with high sequence similarity to OmpN. Even if OmpN would be similarly regulated as OmpK37, the absence of OmpC and OmpF might not necessarily lead to OmpN expression, as also not all *K. pneumoniae* isolates without OmpK35 or OmpK36 showed OmpK37 expression.[38] In this regard, it would be interesting to see whether negamycin might be a treatment option in *K. pneumoniae* isolates with major porin deficiencies, where uptake of β-lactams is limited due to reduced porin expression.

In this study we could show that negamycin uses the *E. coli* porins OmpN and ChiP, which so far have not been associated with antibiotic translocation across the outer membrane. The abundancy of multiple uptake pathways across the outer and inner membranes of *E. coli* makes cross-resistance development with other antibiotics unlikely. These newly identified pathways across the outer membrane shed light on alternative uptake routes for antibiotics, which so far have not been in the focus of the scientific community. These minor porins might be of further interest in cases, where antibiotic uptake is limited due to decreased translocation through the major porins of *E. coli*.

Materials and Methods

Bacterial strains and chemicals. Bacterial strains used in this study are listed in Table S9. Strains were grown in lysogeny broth (LB), 0.5% polypeptone (PP) in water (BD BBL polypeptone, catalog no. 211910) or M9 medium (47.74 mM $NaHPO_4$ x $2H_2O$, 22.04 mM KH_2PO_4, 8.56 mM NaCl, 18.7 mM NH_4Cl, 2 mM $MgSO_4$, 100 µM $CaCl_2$, 0.4% glucose) at 37°C. Negamycin (>95% purity) was synthesized by Squarix GmbH.[14, 39] based on published procedures. Cefotaxime was obtained from Sigma-Aldrich, colistin sulfate from Cayman Chemical, ertapenem sodium from Sigma-Aldrich, polymyxin B (PMB) sulfate from Fluka, polymyxin B nonapeptide (PMBN) from Sigma-Aldrich, cefoxitin from Carl Roth, neomycin trisulfate from Sigma-Aldrich, gentamicin sulfate from Applichem, and 1-N-phenyl-naphthylamine (NPN) from Sigma-Aldrich.

Determination of antibacterial activity. MIC was determined by standard broth dilution series according to CLSI guidelines.[18] Briefly, antibiotics were diluted in a two-fold dilution series. Bacterial cells, grown over night on LB agar plates, were diluted in saline (0.9% NaCl (w/v)) and added to a final inoculum of 5 x 10^5 cells/ml. Microtiter plates were incubated at 37°C and MIC was readout after incubation for 20 h for PP and 24 h for M9 medium. Negamycin susceptibility on PP agar (7.5 g/l) plates was determined by pouring two layers. The bottom layer was poured and solidified at an inclined position. The top layer, containing negamycin at a concentration of 5 µg/ml, was added afterwards at level position. After the top layer solidified, plates were left at 4°C overnight, which resulted in a linear negamycin concentration gradient plate. For the inoculation of the agar gradient plates, *E. coli* strains were grown overnight on LB agar. Colonies were taken from these agar plates and resuspended in saline (0.9% NaCl (w/v)). OD_{600} of the cell suspension was adjusted to 0.1 and subsequently streaked with a sterile cotton swab on the PP agar gradient plate.

Gene knockouts. For gene deletions in *E. coli*, the method by Datsenko and Wanner (2000) was used.[40] Briefly, primers with homologous sequences corresponding to the target gene were used to amplify a kanamycin resistance cassette from the pKD13 plasmid (Table S10). Electrocompetent *E. coli* cells containing the pKD46 plasmid were transformed with this PCR product and homologous recombination was initiated by λ Red recombinase from the pKD46 plasmid. Successful integration of

the resistance cassette was checked by growth on LB with kanamycin. Gene deletion mutants were confirmed by PCR and followed by Sanger sequencing.

[^{3}H]negamycin uptake. Accumulation of [^{3}H]negamycin in *E. coli* was performed as described previously.[8] Briefly, tritium-labeled negamycin was acquired with a specific activity of 16.6 Ci/mmol and mixed with unlabeled negamycin, resulting in a specific activity of 0.052 Ci/mmol. *E. coli* ATCC 25922 was grown in PP at 37°C under shaking conditions. At exponential growth phase, cells were harvested by centrifugation at room temperature and resuspended in 25 mM tris buffer (pH 7) to an OD_{600} of 5. The cell suspension was incubated for 5 min at 37°C under shaking conditions before 32 µg/ml [^{3}H]negamycin (specific activity: 0.052 Ci/mmol) was added and samples were taken at indicated time points. Samples were centrifuged in a pre-cooled centrifuge and resuspended in ice-cold 25 mM tris buffer (pH 7). This suspension was transferred in ice-cold silicone oil (two parts of AR 200 [Sigma-Aldrich], one part of AK 100 [Wacker]). After centrifugation, the aqueous and silicone phases were removed, the cell pellet resuspended in 25 mM tris buffer (pH 7) and transferred to a liquid scintillation counting vwial. 1 ml of Soluene (PerkinElmer) was added and samples were incubated over night. On the next day, 3 ml of Ultima Gold (PerkinElmer) was added, mixed thoroughly and measured using the liquid scintillation analyzer Tri-Carb 2500TR (Packard Bioscience). Negamycin amounts were determined by a previously determined concentration series of tritium-labeled negamycin and *E. coli* cell number by OD_{600} measurements.

***chiP* cloning.** For the overexpression of ChiP, the gene *chiP* was cloned in a first step from gDNA of *E. coli* BW25113. Using the primer pair chiP-pASK5 (Table S10), the porin gene sequence was integrated via Gibson cloning[41] in the plasmid pASK-IBA5 (IBA GmbH), which was beforehand digested with *Xba*I and *Xho*I. This resulted in the plasmid pASK-IBA5-chiP, which was used as the template for cloning the *chiP* gene into pET19b (Addgene) using the primer pairs pET19b-chiP and chiP-pet19b with the Gibson cloning method (Table S10). Correct insertion was confirmed by *Xba*I/*Xho*I digestion and Sanger sequencing. For further ChiP overexpression, *E. coli* BL21 (DE3) *omp8*[42] was transformed with pET19b-chiP.

ChiP & OmpN purification for electrophysiological analysis. An overnight preculture of *E. coli* BL21 (DE3) Omp8 containing pET19b-chiP was inoculated LB medium containing 200 µg/ml ampicillin at a OD_{600} of 0.1 and grown at 37°C (200 rpm) in Erlenmeyer flasks until OD_{600} of the bacterial culture reached 0.6. At this point, the expression of the protein was induced with 0.5 mM isopropyl β-D-1-thiogalactopyranoside (IPTG, Sigma-Aldrich) and the flask was further incubated at 37 °C (200 rpm). After 6 h cells were centrifuged (30 min, 3,000 g at 4°C). The pellet was stored at -20°C until extraction. For extraction, a pellet from a 500 ml of culture was resuspended in 10 ml per mg of culture pellet in lysis buffer (20 mM Tris pH 8, 2.5 mM $MgCl_2$, 0.1mM $CaCl_2$, 1 mM phenylmethylsulfonyl fluoride (PMSF), 10 µg/ml RNase A and 10 µg/ml DNase I) and disrupted by five passages at 15,000 psi in a French Press on ice. After removing the cell debris by centrifugation (30 min, 3,220 g at 4°C), the membranes were pelleted by ultracentrifugation (1 h, 100,000 g at 4 °C). The pellet was solubilized in 20 mM Tris/HCl pH 8, 0.15% Octyl POE (N-octylpolyoxyethylene from Bachem) using a Potter homogenizer and incubated for 1 h at 4°C under constant rotation. The remaining insoluble material was separated by a second ultracentrifugation (1h, 100,000 g at 4°C). ChiP was extracted by solubilizing this pellet with 20 mM Tris HCl pH 8, 3% Octyl POE and elimination of insoluble material by ultracentrifugation (1 h, 100,000 g at 4°C). This ultracentrifugation step was repeated two times. The supernatants of the last two ultracentrifugation steps contained the ChiP protein and were pooled and concentrated with an Amicon concentration unit (cut off at 30 kDa). To obtain pure protein, the concentrated sample was subjected to anion-exchange chromatography using a Mono Q® 5/50 GL prepacked column (5.7 x 1 ml) connected to BioLogic DuoFlow chromatography systems (Bio Rad). Proteins were eluted with a linear gradient from 0 to 1 M KCl in 20 mM phosphate buffer, pH 7.4 containing 0.2% (v/v) dodecyldimethylaminoxid (LDAO) as previously reported.[43] The purity of ChiP was confirmed by SDS-PAGE analysis and the native protein showed a slightly higher molecular mass unlike the former study.[43] The presence of the protein was confirmed by mass spectrometric analysis and Western blot analysis using an anti-ChiP antibody. OmpN overexpression and purification was performed as described previously.[4]

Electrophysiological assays for porin permeability determination. Planar lipid bilayer conferring to Montal and Mueller were formed as published.[44] Briefly, an aperture in a Teflon septum with a

diameter of 100-120 µm was pre-painted with hexadecane dissolved in n-hexane at 1-5% (v/v) and the cuvette compartments were dried for 30-35 min, in order to eliminate the solvent. The bilayer was made with 1,2- diphytanoyl-sn-glycero-phosphatidyl-choline at a concentration of 4-5 mg/ml in n-pentane. Stock solutions of the outer membrane porin OmpN (1-2 mg/ml) or ChiP (0.5 mg/ml) were added to the cis (ground) side chamber containing 2.5 ml of a salt solution. Standard Ag/AgCl electrodes were used to detect the ionic current. Furthermore, for measuring the electrophysiological reversal potential to allow for asymmetric condition we used the commercial calomel electrodes (Metrohm) containing a salt bridge. The cis side electrode of the cell was grounded, whereas the trans side electrode was linked to the headstage of an Axopatch 700B amplifier, used for the conductance measurements in the voltage clamp mode. Signals were filtered by an on board low pass Bessel filter at 10 kHz and with a sampling frequency of 50 kHz. Examination of the current recordings was completed using LABView (National Instruments). The current voltage relation of the individual experiments was calculated from single averaged currents at the given voltages. The relative permeability of cations vs solute anions in the tri-ionic case ($P_{cation}+ : P_{anion}- : P_{substrate}$) were obtained by fitting the experimental reversal potential value in the Goldman-Hodgkin-Katz current equation.[45]

Expression and purification of OmpN for crystallization. For crystallization studies, OmpN expression and purification was done as follows. Porin-deficient BL21 *omp8*[42] cells were transformed with pASK-IBA OmpN plasmid and plated onto LB agar containing 100 µg/mL ampicillin (Melford, UK). For overexpression, 6 L of cells in LB containing 100 µg/mL ampicillin were grown (37 °C, 180 rpm) until OD_{600} ~0.6, when protein expression was induced with 200 µg/L anhydro-tetracycline (Sigma, UK) for 3 h at 37 °C Cells were harvested by centrifugation (5,000 rpm, 20 minutes, 4 °C), and pellets were homogenized in TBS buffer (20 mM Tris 300 mM NaCl pH 8), and were broken by one pass through a cell disruptor (Constant Systems 0.75 kW operated at 23 kpsi). Total membranes and cell debris were centrifuged at 45,000 rpm for 1 h at 4 °C (45Ti rotor; Beckman), and the resulting total membrane pellet was extracted twice in 0.5 % sarkosyl in 20 mM HEPES pH 7.5 to selectively remove inner membrane proteins.[46] The resulting outer membrane pellet was homogenized in TBS buffer containing 1.5% Lauryl-dimethylamine oxide (LDAO) (Sigma, UK). Membrane proteins were extracted by stirring for 60 minutes, 4 °C and centrifuged at 42,000 rpm in 45Ti rotor for 30 minutes at

4°C. OmpN was purified by using anion exchange chromatography (HiTrap Q in 20 mM HEPES, 50 mM NaCl, 0.2 % LDAO, pH 7.5) and further polished using size exclusion chromatography (Superdex 200 16/600 in 20 mM HEPES, 100 mM NaCl, 0.05 % LDAO, pH 7.5). Peak fractions were pooled and concentrated and analysed on SDS-PAGE. Purified OmpN was buffer exchanged to 20 mM HEPES, 100 mM NaCl, 0.4 % C8E4, pH 7.5, flash frozen in liquid nitrogen and stored at -80 C.

Crystallization of OmpN. Initial crystal screens of OmpN at 18 mg/ml were set up using the sitting drop method by using Mosquito robot (TTP Labtech). Crystal hits were optimized to obtain good quality crystals. Diffracting crystals were obtained in 0.2 M Li_2SO_4, 0.05 M MES, pH 6.5 and 20% (v/v) PEG 400. Diffraction data were collected on beamline IO4 at the Diamond Light Source, Didcot, UK and were processed using Dials[47] (Space group P43 1 2 ; four OmpN trimers in the asymmetric unit). The crystal structure was solved by Molecular Replacement with Phaser[48] using data to 2.61 Å resolution using search model PDB 5FVN[49] (for OmpE36). Phenix[50, 51] was used for Refinement, COOT[52] for manual building and structure validation was carried out with MolProbity[53].

Molecular Simulations. We prepared the system for molecular simulations following the protocol already used for other general porins.[54] We placed the trimer as obtained from X-ray crystallography in a pre-equilibrated POPC (1-palmitoyl-2-oleoyl-sn-glycero-3-phosphocholine) symmetric bilayer of 220 lipids. The system was oriented in order to center the protein at the origin of the coordinate system and align the channel diffusion axis along the *z*-axis, hence *z* positive values refer to the extracellular vestibule (EV), and *z* negative values refer to the periplasmic vestibule (PV). According to pK calculations performed with PROPKA, we protonated two residues near the loop L3, Asp308 (aligned with Asp296 of OmpF) and Glu-261. Using the ACEMD code,[55] the system was equilibrated in the gas-phase, in order to force lipids to adhere the hydrophobic regions of the porins. After 1 ps of energy minimization (conjugate gradients), a slow heating from 10 to 300 K was carried out for 1 ns, with positional restraints on the protein's alpha carbons along the three dimensions and on the lipids phosphorus atoms along *z* only. The system was solvated with ~26,000 water molecules, and the total number of atoms was ~123,000 in a box with size 110 × 110 × 110 Å. A suitable number of sodium and chloride ions were added to reach the desired concentration (0.2M, 0.5M and 1.0M). An excess of

Na^+ ions was required to neutralize the total negative charge of the trimer (−63 e). After releasing the constraints in 20 ns, an equilibration stage of 5 ns in the NPT ensemble at 1.0 bar and 300 K was performed. Finally, 200 ns MD simulations were performed in the NVT ensemble without restraints with box size of 108 × 108 × 107 Å, with a time step of 4 fs. This long time step is allowed by the repartitioning of masses between heavy atoms and hydrogens (h − mass = 4 amu).[56] The Langevin thermostat (300 K) was used with 0.1 ps damping time, and the particle mesh Ewald (PME) method with 9 Å cutoff for electrostatic interactions. The Amber99SB-ILDN force field parameters were used for OmpF, the General Amber Force Field for negamycin, GAFFlipid for POPC, and the TIP3P model for waters.

Negamycin preparation for molecular simulations. The AMBER force field parameters of Negamycin were generated by using antechamber (AMBER 16) software and standard GAFF parameters.[57] The atomic charges were generated with the semiempirical (BCC) option and the net molecular charge of +1. The molecule was then solvated in a box of 1847 water molecules (TIP3P), 5 Na^+ and 6 Cl^- ions what corresponds to a 0.15 M ionic concentration. Then the all-atom MD simulations were performed by using the ACEMD 2016 software.[55] To speedup the simulations, the mass of all hydrogen atoms was set to 4 a.m.u. and the timestep was set to 4 fs [Fenstra]. The system was equilibrated in a NPT ensemble (300K, 1 bar) for 1.3 ps, and then, the production run of 1 microsecond was performed in a NVT ensemble (300 K) with the volume of the box fixed to the last value of the equilibration stage. The dipole moment of Negamycin molecule along the trajectory was calculated every 10 ns, and the distribution histogram was calculated together with the average value and the standard deviation. The minimal projection area of Negamycin molecule along the trajectory was calculated every 100 ns by using MARVIN software [Calculator Plugins were used for structure property prediction and calculation, Marvin 19.8.0, 2019, ChemAxon (http://www.chemaxon.com)], and the distribution histogram was calculated together with the average value and the standard deviation.

Electric field simulations. We applied a constant external electric field corresponding to a gradient of -200, -100, +100, and +200 mV on the equilibrated OmpN system at 0.2M, 0.5M, and 1.0M

concentration of NaCl (NVT ensemble), as described earlier.[58] For each value we performed three independent simulations 100 ns long. The average current was calculated for each voltage and used to build the conductance curve as function of ion concentration. With the same scheme we performed the calculations also in presence of negamycin in Min-CR.

Metadynamics simulations. We performed metadynamics simulations to sample the transport of negamycin through OmpN. We used Well-Tempered metadynamics with 8 walkers as implemented in Plumed 2.0 and coupled to ACEMD, simulating a total of 32 us, or 4 us/walker. We biased two variables, (i) the orientation of the molecule along the axis Z, calculated as the distance between two atoms (N2-C4) projected along the axis Z, and (ii) the relative Z position of the center of mass of negamycin with respect to the center of mass of the monomer one. Bias is added by deposing (gaussian) hills every 5 ps, with initial eight of 1 kcal/mol, bias factor 20, sigma 0.2 Å and 0.5 Å respectively for the two variables. At the end of the simulations the eight of hills decreased by a factor 1000 (0.001 kcal/mol).

Flux calculations. We calculated from the one-dimensional FES the diffusive current of molecules through a single pore as described previously,[54, 59] from EV to PV, at different molecule gradient concentrations. At a low substrate concentration, one can neglect the interaction between the substrate molecules. Then, the diffusion is described by the linear 1D Smoluchowski equation, and the diffusion current is proportional to the substrate concentration gradient and is given by a Kramers-type integral formula.[45, 60] At a higher substrate concentration, the probability to have two substrate molecules occupying at the same time the pore is not negligible, that leads to saturation of the current. To take into account saturation effects, we have bridged the diffusion scale model with the two-state Markov model, as described earlier.[54, 59]

RNA isolation and sequencing. For RNA extraction from *E. coli* BW25113, cells were grown in PP at 37°C (190 rpm) until early exponential growth phase. For negamycin treatment, the bacterial liquid culture was split into two. One culture remained untreated and to the other culture a final concentration of 16 µg/ml negamycin was added. Samples were incubated for further 45 min at 37°C (190 rpm). Cells were harvested by centrifugation (10 min, 4,600 g at 4°C) and resuspended in

DNA/RNA Shield buffer (Zymo research). RNA was isolated using the Quick-RNA Miniprep Plus Kit (Zymo Research) and stored at -80°C. 5 µg total RNA were treated with DNase I (Roche) for 20 min at 37 °C and the DNase-digested RNA was cleaned up with the RNA Clean&Concentrator-5 Kit (Zymo) according to the manufacturer's instructions. Per replicate, a total amount of 150 ng RNA was subjected to rRNA depletion, cDNA synthesis and subsequent library preparation using the Illumina Stranded Total RNA Prep with Ribo-Zero Plus Kit according to the manufacturer's instructions. Libraries were checked for correct fragment length on an Agilent 2100 Bioanalyzer and then sequenced as single-read (75 bp read length) on a NextSeq500 platform (Illumina) at a depth of 6.7–14.4 million reads each. Library preparation and sequencing procedures were performed by the same individual and a design aimed to minimize technical batch effects was chosen. Sequencing was performed by the Quantitative Biology Center QBiC and NGS Competence Center NCCT (Tübingen, Germany).

RNA-Seq data assessment and analysis. Sequencing statistics including the quality per base and adapter content assessment of resulting transcriptome sequencing data were conducted with FastQC v0.11.5.[61] All reads mappings were performed against the reference strain of *E. coli* K12 substr. MG1655 (RefSeq ID NC_000913.3). The mappings of all samples were conducted with HISAT2 v2.1.0.[62] Spliced alignment of reads was disabled (HISAT2 parameter --no-spliced-alignment). The resulting mapping files in SAM format were converted to BAM format using SAMtools v1.9.[63] Mapping statistics, including percentage of mapped reads and fraction exonic region coverage, were conducted with the RNA-Seq module of QualiMap2 v2.2.2-dev.[64] Gene counts for all samples were computed with featureCounts v1.6.4[65] based on the annotation of the respective reference genome, where the selected feature type was set to transcript records (featureCounts parameter -t transcript). To assess variability of the replicates of each condition, a principal component analysis (PCA) was conducted with the DESeq2 package v1.20.0.[66]

Differential gene expression, For the computation of genes differentially expressed between the wildtype and the negamicyn treated samples and the strains *E. coli* Δ*ompN*, *E. coli* Δ*chiP* and *E. coli* Δ*ompN*Δ*chiP*, repectively, DESeq2 v1.20.0[66] was applied to the absolute gene counts as computed

with featureCounts. Genes with low counts (less than 10 reads) over all replicates in both media were filtered prior to differential expression analysis. For differences between each condition genes with an adjusted p-value (FDR) < 0.05 and absolute log2 fold change (FC) > 1 were reported as differentially expressed. For normalized expression values, a TPM (transcripts per million) for each gene was computed.

Data availability. All high-throughput sequencing data have been deposited in NCBI's Gene Expression Omnibus and are accessible under accession number GSE183363.

Outer membrane protein extracts for Western blot detection. Outer membrane proteins extraction was based on a method described before.[67] Briefly, *E. coli* cells were grown in PP at 37°C under shaking conditions and harvested at exponential growth phase by centrifugation (10 min, 4,000 g at 4°C). Cell pellets were resuspended in 1 ml buffer containing 100 ml Tris-HCl and 20% sucrose (pH 8.0) and incubated on ice for 10 min. Samples were centrifuged (10 min, 16,000 g) and pellets were resuspended in 1 ml buffer containing 100 mM Tris-HCl, 20% sucrose and 10 mM EDTA (pH 8.0). Lysozyme was added to a final concentration of 100 µg/ml and samples were incubated on ice for 10 min. Samples were supplemented with 20 mM $MgSO_4$, 5 µg/ml DNase I and 5 µg/ml RNase A. Bacterial cells were lysed by seven repetitions of freezing at -80°C in EtOH and thawing in H_2O at RT. The last thawing step was done on ice. Samples were centrifuged (25 min, 16,000 g) and washed with 500 µl of 20 mM $NaPO_4$ (pH 7.0). Samples were centrifuged again and resuspended in 1 ml of 20 mM NaPO4 and 0.5% sarcosyl (pH 7.0). After incubation for 30 min at RT, samples were centrifuged (30 min, 16,000 g) and washed twice with 1 ml of 20 mM $NaPO_4$ (pH 7) (15 min, 15,000 rpm). After removal of the supernatant, the pellet was resuspended in 50 µl Laemmli buffer and heated for 10 min at 100 °C.[68] 10 µl were applied on a SDS PAGE (Bolt™ 4-12% Bis-Tris Plus, invitrogen) and further analyzed by Western blot detection.

Western blot analysis & antibodies. Immunoblotting was performed as described previously.[69] Outer membrane proteins were extracted as described in methods and detected with peptide-specific, polyclonal, primary antibodies from rabbits, provided by Eurogentec. Peptide sequence for anti-OmpN

(GGADNPAGVDDKDLVKYAD) was based on a previous publication[37] and sequence for anti-ChiP (ATWQSNPDAYYDKNRT) was derived on a loop outside of the barrel structure of the porin protein.

Self-promoted uptake. Permeabilization of the outer membrane by antibiotics was measured by uptake of 1-N-phenyl-naphthylamine (NPN) based on a method as described previously.[30, 31] Briefly, *E. coli* BW25113 was grown in PP at 37°C under shaking conditions until exponential growth phase. Cells were harvested by centrifugation (15 min, 3,000 g) and washed in the same volume with 5 mM HEPES (pH 7.2). The cell suspension was centrifuged again (15 min, 3,000 g) and resuspended in 5 mM HEPES to an OD_{600} of 0.5. In a black flat-bottom microtiter plate, 100 µl of the cell suspension and 50 µl of 40 µM NPN in 5 mM HEPES (for a final concentration of 10 µM in 200 µl) were added for each sample. Subsequently, 50 µl of an antibiotic solution in 5 mM HEPES was added and the microtiter plate was incubated under shaking conditions at 37°C for 5 min. Fluorescence was measured at an excitation wavelength of 350 nm and an emission wavelength of 420 nm. Permeability of NPN was determined by first subtracting the background fluorescence signal (NPN in buffer only) and dividing antibiotic treated samples by untreated samples (no antibiotic added).

Acknowledgments. The project and data management work for this project was supported by the Quantitative Biology Center (QBiC) of the University of Tübingen.

References

1. Nikaido, H., Molecular Basis of Bacterial Outer Membrane Permeability Revisited. *Microbiology and Molecular Biology Reviews* **2003,** *67* (4), 593-656.
2. Ruggiu, F.; Yang, S.; Simmons, R. L.; Casarez, A.; Jones, A. K.; Li, C.; Jansen, J. M.; Moser, H. E.; Dean, C. R.; Reck, F.; Lindvall, M., Size Matters and How You Measure It: A Gram-Negative Antibacterial Example Exceeding Typical Molecular Weight Limits. *ACS Infectious Diseases* **2019,** *5* (10), 1688-1692.
3. Acosta-Gutiérrez, S.; Ferrara, L.; Pathania, M.; Masi, M.; Wang, J.; Bodrenko, I.; Zahn, M.; Winterhalter, M.; Stavenger, R. A.; Pagès, J.-M.; Naismith, J. H.; van den Berg, B.; Page, M. G. P.; Ceccarelli, M., Getting Drugs into Gram-Negative Bacteria: Rational Rules for Permeation through General Porins. *ACS Infectious Diseases* **2018,** *4* (10), 1487-1498.
4. Bafna, J. A.; Sans-Serramitjana, E.; Acosta-Gutiérrez, S.; Bodrenko, I. V.; Hörömpöli, D.; Berscheid, A.; Brötz-Oesterhelt, H.; Winterhalter, M.; Ceccarelli, M., Kanamycin Uptake into Escherichia coli Is Facilitated by OmpF and OmpC Porin Channels Located in the Outer Membrane. *ACS Infectious Diseases* **2020,** *6* (7), 1855-1865.
5. Vergalli, J.; Bodrenko, I. V.; Masi, M.; Moynié, L.; Acosta-Gutiérrez, S.; Naismith, J. H.; Davin-Regli, A.; Ceccarelli, M.; van den Berg, B.; Winterhalter, M.; Pagès, J.-M., Porins and small-molecule translocation across the outer membrane of Gram-negative bacteria. *Nature Reviews Microbiology* **2020,** *18* (3), 164-176.
6. Misra, R.; Benson, S., Isolation and characterization of OmpC porin mutants with altered pore properties. *Journal of bacteriology* **1988,** *170* (2), 528-533.
7. Pagès, J.-M.; James, C. E.; Winterhalter, M., The porin and the permeating antibiotic: a selective diffusion barrier in Gram-negative bacteria. *Nature Reviews Microbiology* **2008,** *6* (12), 893-903.
8. Hörömpöli, D.; Ciglia, C.; Glüsenkamp, K.-H.; Haustedt, L. O.; Falkenstein-Paul, H.; Bendas, G.; Berscheid, A.; Brötz-Oesterhelt, H., The Antibiotic Negamycin Crosses the Bacterial Cytoplasmic Membrane by Multiple Routes. *Antimicrobial Agents and Chemotherapy* **2021,** *65* (4), e00986-20.
9. Hamada, M.; Tadeuchi, T.; KONDO, S.; IKEDA, Y.; NAGANAWA, H.; MAEDA, K.; OKAMI, Y.; UMEZAWA, H., A new antibiotic, negamycin. *The Journal of antibiotics* **1970,** *23* (3), 170-171.
10. Olivier, N. B.; Altman, R. B.; Noeske, J.; Basarab, G. S.; Code, E.; Ferguson, A. D.; Gao, N.; Huang, J.; Juette, M. F.; Livchak, S.; Miller, M. D.; Prince, D. B.; Cate, J. H.; Buurman, E. T.; Blanchard, S. C., Negamycin induces translational stalling and miscoding by binding to the small subunit head domain of the Escherichia coli ribosome. *Proc Natl Acad Sci U S A* **2014,** *111* (46), 16274-9.
11. Polikanov, Y. S.; Szal, T.; Jiang, F.; Gupta, P.; Matsuda, R.; Shiozuka, M.; Steitz, T. A.; Vazquez-Laslop, N.; Mankin, A. S., Negamycin interferes with decoding and translocation by simultaneous interaction with rRNA and tRNA. *Mol Cell* **2014,** *56* (4), 541-50.
12. McKinney, D. C.; Basarab, G. S.; Cocozaki, A. I.; Foulk, M. A.; Miller, M. D.; Ruvinsky, A. M.; Scott, C. W.; Thakur, K.; Zhao, L.; Buurman, E. T.; Narayan, S., Structural Insights Lead to a Negamycin Analogue with Improved Antimicrobial Activity against Gram-Negative Pathogens. *ACS Medicinal Chemistry Letters* **2015,** *6* (8), 930-935.
13. Kondo, S.; IINUMA, K.; YOSHIDA, K.; YOKOSE, K.; IKEDA, Y.; SHIMAZAKI, M.; UMEZAWA, H., Syntheses and properties of negamycin analogs modified the δ-hydroxy-β-lysine moiety. *The Journal of antibiotics* **1976,** *29* (2), 208-211.
14. Raju, B.; Mortell, K.; Anandan, S.; O'Dowd, H.; Gao, H.; Gomez, M.; Hackbarth, C.; Wu, C.; Wang, W.; Yuan, Z.; White, R.; Trias, J.; Patel, D. V., N- and C-terminal modifications of negamycin. *Bioorganic & Medicinal Chemistry Letters* **2003,** *13* (14), 2413-2418.
15. Uehara, Y.; HORI, M.; KONDO, S.; HAMADA, M.; UMEZAWA, H., Structure-activity relationships among negamycin analogs. *The Journal of antibiotics* **1976,** *29* (9), 937-943.
16. McKinney, D. C.; Bezdenejnih-Snyder, N.; Farrington, K.; Guo, J.; McLaughlin, R. E.; Ruvinsky, A. M.; Singh, R.; Basarab, G. S.; Narayan, S.; Buurman, E. T., Illicit transport via dipeptide

transporter Dpp is irrelevant to the efficacy of negamycin in mouse thigh models of Escherichia coli infection. *ACS infectious diseases* **2015,** *1* (5), 222-230.
17. Prilipov, A.; Phale, P. S.; Koebnik, R.; Widmer, C.; Rosenbusch, J. P., Identification and Characterization of Two Quiescent Porin Genes, nmpC and ompN, in Escherichia coli BE. *Journal of bacteriology* **1998,** *180* (13), 3388-3392.
18. Patel, J. B.; Cockerill, F.; Bradford, P.; Eliopoulos, G.; Hindler, J.; Jenkins, S.; Lewis, S.; Limbago, B.; Miller, A.; Nicolau, P., M07-A10 Methods for Dilution Antimicrobial Susceptibility Tests for Bacteria That Grow Aerobically; Approved Standard—. *Clinical Laboratory Standards Institute* **2015,** *35* (2).
19. Appleyard, R. K., Segregation of New Lysogenic Types during Growth of a Doubly Lysogenic Strain Derived from Escherichia Coli K12. *Genetics* **1954,** *39* (4), 440-52.
20. Nikaido, H.; Takatsuka, Y., Mechanisms of RND multidrug efflux pumps. *Biochim Biophys Acta* **2009,** *1794* (5), 769-81.
21. Zgurskaya, H. I.; Krishnamoorthy, G.; Ntreh, A.; Lu, S., Mechanism and Function of the Outer Membrane Channel TolC in Multidrug Resistance and Physiology of Enterobacteria. *Front Microbiol* **2011,** *2*, 189-189.
22. Koronakis, V.; Eswaran, J.; Hughes, C., Structure and Function of TolC: The Bacterial Exit Duct for Proteins and Drugs. *Annual Review of Biochemistry* **2004,** *73* (1), 467-489.
23. Ziervogel, B. K.; Roux, B., The binding of antibiotics in OmpF porin. *Structure* **2013,** *21* (1), 76-87.
24. Rostkowski, M.; Olsson, M. H. M.; Søndergaard, C. R.; Jensen, J. H., Graphical analysis of pH-dependent properties of proteins predicted using PROPKA. *BMC Structural Biology* **2011,** *11* (1), 6.
25. Zhang, X. S.; García-Contreras, R.; Wood, T. K., YcfR (BhsA) influences Escherichia coli biofilm formation through stress response and surface hydrophobicity. *J Bacteriol* **2007,** *189* (8), 3051-62.
26. Demple, B., Redox signaling and gene control in the Escherichia coli soxRS oxidative stress regulon--a review. *Gene* **1996,** *179* (1), 53-7.
27. Fàbrega, A.; Rosner, J. L.; Martin, R. G.; Solé, M.; Vila, J., SoxS-dependent coregulation of ompN and ydbK in a multidrug-resistant Escherichia coli strain. *FEMS microbiology letters* **2012,** *332* (1), 61-67.
28. Nakayama, T.; Yonekura, S.; Yonei, S.; Zhang-Akiyama, Q. M., Escherichia coli pyruvate:flavodoxin oxidoreductase, YdbK - regulation of expression and biological roles in protection against oxidative stress. *Genes Genet Syst* **2013,** *88* (3), 175-88.
29. Hancock, R. E. W., ALTERATIONS IN OUTER MEMBRANE PERMEABILITY. *Annual Review of Microbiology* **1984,** *38* (1), 237-264.
30. Farmer, S.; Li, Z.; Hancock, R. E., Influence of outer membrane mutations on susceptibility of Escherichia coli to the dibasic macrolide azithromycin. *Journal of Antimicrobial Chemotherapy* **1992,** *29* (1), 27-33.
31. Marshall, A. J. H.; Piddock, L. J. V., Interaction of divalent cations, quinolones and bacteria. *Journal of Antimicrobial Chemotherapy* **1994,** *34* (4), 465-483.
32. Lou, H.; Chen, M.; Black, S. S.; Bushell, S. R.; Ceccarelli, M.; Mach, T.; Beis, K.; Low, A. S.; Bamford, V. A.; Booth, I. R.; Bayley, H.; Naismith, J. H., Altered Antibiotic Transport in OmpC Mutants Isolated from a Series of Clinical Strains of Multi-Drug Resistant E. coli. *PLOS ONE* **2011,** *6* (10), e25825.
33. Ghai, I.; Bajaj, H.; Bafna, J. A.; Hussein, H. A. E. D.; Winterhalter, M.; Wagner, R., Ampicillin permeation across OmpF, the major outer-membrane channel in Escherichia coli. *Journal of Biological Chemistry* **2018,** *293* (18), 7030-7037.
34. Wang, J.; Terrasse, R.; Bafna, J. A.; Benier, L.; Winterhalter, M., Electrophysiological Characterization of Transport Across Outer-Membrane Channels from Gram-Negative Bacteria in Presence of Lipopolysaccharides. *Angewandte Chemie International Edition* **2020,** *59* (22), 8517-8521.
35. Prochnow, H.; Fetz, V.; Hotop, S.-K.; García-Rivera, M. A.; Heumann, A.; Brönstrup, M., Subcellular quantification of uptake in Gram-negative bacteria. *Analytical chemistry* **2018,** *91* (3), 1863-1872.

36. Ettwiller, L.; Buswell, J.; Yigit, E.; Schildkraut, I., A novel enrichment strategy reveals unprecedented number of novel transcription start sites at single base resolution in a model prokaryote and the gut microbiome. *BMC Genomics* **2016,** *17* (1), 199.
37. Dam, S.; Masi, M., Dual regulation of the small RNA MicC and the quiescent porin OmpN in response to antibiotic stress in Escherichia coli. *Antibiotics* **2017,** *6* (4), 33.
38. Doménech-Sánchez, A.; Hernández-Allés, S.; Martínez-Martínez, L.; Benedí, V. J.; Albertí, S., Identification and Characterization of a New Porin Gene of *Klebsiella pneumoniae*: Its Role in β-Lactam Antibiotic Resistance. *Journal of Bacteriology* **1999,** *181* (9), 2726-2732.
39. Wang, Y. F.; Izawa, T.; Kobayashi, S.; Ohno, M., Stereocontrolled synthesis of (+)-negamycin from an acyclic homoallylamine by 1,3-asymmetric induction. *Journal of the American Chemical Society* **1982,** *104* (23), 6465-6466.
40. Datsenko, K. A.; Wanner, B. L., One-step inactivation of chromosomal genes in Escherichia coli K-12 using PCR products. *Proceedings of the National Academy of Sciences* **2000,** *97* (12), 6640-6645.
41. Gibson, D. G., Synthesis of DNA fragments in yeast by one-step assembly of overlapping oligonucleotides. *Nucleic acids research* **2009,** *37* (20), 6984-6990.
42. Prilipov, A.; Phale, P. S.; Van Gelder, P.; Rosenbusch, J. P.; Koebnik, R., Coupling site-directed mutagenesis with high-level expression: large scale production of mutant porins from E. coli. *FEMS microbiology letters* **1998,** *163* (1), 65-72.
43. Soysa, H. S. M.; Suginta, W., Identification and functional characterization of a novel OprD-like chitin uptake channel in non-chitinolytic bacteria. *Journal of Biological Chemistry* **2016,** *291* (26), 13622-13633.
44. Montal, M.; Mueller, P., Formation of bimolecular membranes from lipid monolayers and a study of their electrical properties. *Proceedings of the National Academy of Sciences* **1972,** *69* (12), 3561-3566.
45. Ghai, I.; Pira, A.; Scorciapino, M. A.; Bodrenko, I.; Benier, L.; Ceccarelli, M.; Winterhalter, M.; Wagner, R., General method to determine the flux of charged molecules through nanopores applied to β-lactamase inhibitors and OmpF. *The journal of physical chemistry letters* **2017,** *8* (6), 1295-1301.
46. Filip, C.; Fletcher, G.; Wulff, J. L.; Earhart, C., Solubilization of the cytoplasmic membrane of Escherichia coli by the ionic detergent sodium-lauryl sarcosinate. *Journal of bacteriology* **1973,** *115* (3), 717-722.
47. Winter, G.; Waterman, D. G.; Parkhurst, J. M.; Brewster, A. S.; Gildea, R. J.; Gerstel, M.; Fuentes-Montero, L.; Vollmar, M.; Michels-Clark, T.; Young, I. D., DIALS: implementation and evaluation of a new integration package. *Acta Crystallographica Section D* **2018,** *74* (2), 85-97.
48. McCoy, A. J.; Grosse-Kunstleve, R. W.; Adams, P. D.; Winn, M. D.; Storoni, L. C.; Read, R. J., Phaser crystallographic software. *Journal of applied crystallography* **2007,** *40* (4), 658-674.
49. Arunmanee, W.; Pathania, M.; Solovyova, A. S.; Le Brun, A. P.; Ridley, H.; Baslé, A.; van den Berg, B.; Lakey, J. H., Gram-negative trimeric porins have specific LPS binding sites that are essential for porin biogenesis. *Proceedings of the National Academy of Sciences* **2016,** *113* (34), E5034.
50. Adams, P. D.; Afonine, P. V.; Bunkóczi, G.; Chen, V. B.; Davis, I. W.; Echols, N.; Headd, J. J.; Hung, L.-W.; Kapral, G. J.; Grosse-Kunstleve, R. W., PHENIX: a comprehensive Python-based system for macromolecular structure solution. *Acta Crystallographica Section D: Biological Crystallography* **2010,** *66* (2), 213-221.
51. Afonine, P. V.; Grosse-Kunstleve, R. W.; Echols, N.; Headd, J. J.; Moriarty, N. W.; Mustyakimov, M.; Terwilliger, T. C.; Urzhumtsev, A.; Zwart, P. H.; Adams, P. D., Towards automated crystallographic structure refinement with phenix. refine. *Acta Crystallographica Section D: Biological Crystallography* **2012,** *68* (4), 352-367.
52. Emsley, P.; Cowtan, K., Coot: model-building tools for molecular graphics. *Acta crystallographica section D: biological crystallography* **2004,** *60* (12), 2126-2132.

53. Chen, V. B.; Arendall, W. B.; Headd, J. J.; Keedy, D. A.; Immormino, R. M.; Kapral, G. J.; Murray, L. W.; Richardson, J. S.; Richardson, D. C., MolProbity: all-atom structure validation for macromolecular crystallography. *Acta Crystallographica Section D: Biological Crystallography* **2010,** *66* (1), 12-21.
54. Pira, A.; Scorciapino, M. A.; Bodrenko, I. V.; Bosin, A.; Acosta-Gutiérrez, S.; Ceccarelli, M., Permeation of β-Lactamase Inhibitors through the General Porins of Gram-Negative Bacteria. *Molecules* **2020,** *25* (23), 5747.
55. Harvey, M. J.; Giupponi, G.; Fabritiis, G. D., ACEMD: accelerating biomolecular dynamics in the microsecond time scale. *Journal of chemical theory and computation* **2009,** *5* (6), 1632-1639.
56. Feenstra, K. A.; Hess, B.; Berendsen, H. J., Improving efficiency of large time-scale molecular dynamics simulations of hydrogen-rich systems. *Journal of Computational Chemistry* **1999,** *20* (8), 786-798.
57. Wang, J.; Wang, W.; Kollman, P. A.; Case, D. A., Automatic atom type and bond type perception in molecular mechanical calculations. *Journal of molecular graphics and modelling* **2006,** *25* (2), 247-260.
58. Aksimentiev, A.; Schulten, K., Imaging α-hemolysin with molecular dynamics: ionic conductance, osmotic permeability, and the electrostatic potential map. *Biophysical journal* **2005,** *88* (6), 3745-3761.
59. Coines, J.; Acosta-Gutierrez, S.; Bodrenko, I.; Rovira, C.; Ceccarelli, M., Glucose transport via the pseudomonad porin OprB: Implications for the design of Trojan Horse anti-infectives. *Physical Chemistry Chemical Physics* **2019,** *21* (16), 8457-8463.
60. Bodrenko, I. V.; Salis, S.; Acosta-Gutierrez, S.; Ceccarelli, M., Diffusion of large particles through small pores: From entropic to enthalpic transport. *The Journal of chemical physics* **2019,** *150* (21), 211102.
61. S., A. FastQC: a quality control tool for high throughput sequence data. http://www.bioinformatics.babraham.ac.uk/projects/fastqc. (accessed August 2021).
62. Kim, D.; Paggi, J. M.; Park, C.; Bennett, C.; Salzberg, S. L., Graph-based genome alignment and genotyping with HISAT2 and HISAT-genotype. *Nature biotechnology* **2019,** *37* (8), 907-915.
63. Li, H.; Handsaker, B.; Wysoker, A.; Fennell, T.; Ruan, J.; Homer, N.; Marth, G.; Abecasis, G.; Durbin, R., The sequence alignment/map format and SAMtools. *Bioinformatics* **2009,** *25* (16), 2078-2079.
64. Okonechnikov, K.; Conesa, A.; García-Alcalde, F., Qualimap 2: advanced multi-sample quality control for high-throughput sequencing data. *Bioinformatics* **2016,** *32* (2), 292-294.
65. Liao, Y.; Smyth, G. K.; Shi, W., featureCounts: an efficient general purpose program for assigning sequence reads to genomic features. *Bioinformatics* **2014,** *30* (7), 923-930.
66. Love, M. I.; Huber, W.; Anders, S., Moderated estimation of fold change and dispersion for RNA-seq data with DESeq2. *Genome biology* **2014,** *15* (12), 1-21.
67. Knopp, M.; Andersson, D. I., Amelioration of the Fitness Costs of Antibiotic Resistance Due To Reduced Outer Membrane Permeability by Upregulation of Alternative Porins. *Molecular Biology and Evolution* **2015,** *32* (12), 3252-3263.
68. Laemmli, U. K., Cleavage of structural proteins during the assembly of the head of bacteriophage T4. *nature* **1970,** *227* (5259), 680-685.
69. Sambrook, J.; Fritsch, E. F.; Maniatis, T., *Molecular cloning: a laboratory manual*. Cold spring harbor laboratory press: 1989.

Supplemental information

Table S1. Negamycin MIC determinations in efflux gene deletion mutant strains. Negamycin activity is not dependent on the absence of efflux pumps in *E. coli* BW25113 and ATCC 25922. The deletion of the major efflux pump genes *acrA* and *acrB* did not or only marginally increase negamycin activity. Deletion of other efflux pump subunits did not decrease negamycin MIC.

	negamycin MIC [µg/ml]	
strain	PP	M9
E. coli BW25113	8	4
E. coli BW25113 Δ*acrA*	8	4
E. coli BW25113 Δ*acrB*	8	4
E. coli BW25113 Δ*acrAB*	16	2
E. coli BW25113 Δ*acrD*	8	4
E. coli BW25113 Δ*acrE*	8	4
E. coli BW25113 Δ*acrF*	8	4
E. coli BW25113 Δ*macA*	8	2-4
E. coli BW25113 Δ*macB*	8	4
E. coli BW25113 Δ*tolC*	2-4	ng
E. coli BW25113 Δ*mdfa*	8	4
E. coli ATCC 25922	16	nd
E. coli ATCC 25922 *ΔacrAB*	16	nd
E. coli HN817	8	nd
E. coli HN818 (Δ*acrAB*)	4	nd
E. coli C600	4	nd
E. coli C600 *tolC*::Tn10	4	nd

Table S2. The trimeric channel conductance of OmpN with 1 M KCl, 1 M NaCl or 1 M KCH_3CO_2 in 10 mM HEPES buffer at pH 7 revealed a stable conductance. In Figure S2, the red line is the Gaussian fit to the conductance histogram and their respective mean values are tabulated here. The measured channel conductance with 1 M NaCl is in accordance with previous results.[10]

Salt [1 M]	G_{trimer} (nS)	Number of steps
Potassium chloride (KCl)	2.3 ± 0.25	249
Sodium chloride (NaCl)	1.6 ± 0.15	291
Potassium acetate (KCH_3CO_2)	0.9 ± 0.15	161

Table S3. Determination of antibiotic translocation through OmpF, OmpC, OmpN and ChiP by reversal potential measurements. Permeability (P) of the antibiotics negamycin, ertapenem and cefotaxime were compared to permeability of Na and Cl. OmpN is permeable for negamycin, but not for ertapenem or cefotaxime. OmpF and OmpC are permeable to both negamycin and ertapenem. Additionally, permeation of negamycin through ChiP could be observed, but was lower compared to OmpN.

	Substrate	**Substrate (mM)**		**Charge**	**V_{rev} (mV ± SD)**	**P_{Na}:P_{Cl}:$P_{antibiotic}$**
		Cis	**Trans**			
OmpF - negamycin						
	Na	1	1	+1		
	Cl	1	1	-1	11.5 ± 3	5:1:1.35
	negamycin	2.5	0	+1		
OmpF - ertapenem						
	Na	3	1	+1		
	Cl	1	1	-1	7.5 ± 1.8	5:1:1.85
	ertapenem	3	0	-1		
OmpC - negamycin						
	Na	1	1	+1		
	Cl	1	1	-1	8.5 ± 2.2	3:1:0.5
	negamycin	2.5	0	+1		
OmpC - ertapenem						
	Na	3	1	+1		
	Cl	1	1	-1	3.5 ± 2.5	8.5:1:4.2
	ertapenem	3	0	-1		
OmpN - negamycin						
	Na	0.1	0.1	+1		
	Cl	0.1	0.1	-1	21 ± 4	2:1:0.75
	negamycin	0.5	0	+1		
OmpN - ertapenem						
	Na	2	1	+1		
	Cl	1	1	-1	24.5 ± 3.5	2 :1: <0.0001
	ertapenem	2	0	-1		
OmpN - cefotaxime						
	Na	25	10	+1		
	Cl	10	10	-1	33.2 ± 2	2:1:0.000001
	cefotaxime	25	0	-1		
ChiP - negamycin						
	Na	1	1	+1		
	Cl	1	1	-1	6 ± 2	1:6:0.35
	negamycin	2	0	+1		

Table S4. Bi-ionic measurements with OmpN. Permeability ratio of potassium to sulfate and sodium to chloride were determined by applying a concentration gradient between the two chambers, separated by a lipid layer with integrated OmpN proteins. The measured V_m for a fixed salt concentration was used to calculate the permeability ratio P_{cation}/P_{anion} with the help of Goldman-Hodgkin-Katz equation.[11]

	Substrate Cis (mM)		Substrate Trans (mM)		V_{rev} (mV)	Permeability ratio (P_{cation}:P_{anion})
Potassium sulfate	K^+	SO_4^{2-}	K^+	SO_4^{2-}		
Blank	20	10	20	10	33.5	21:1
Gradient	100	50	20	10		
Sodium chloride	Na^+	Cl^-	Na^+	Cl^-		
Blank	10	10	10	10	8	2:1
Gradient	25	25	10	10		

Table S5. Calculations of the simulated ionic current of OmpN when negamycin occupies Min-CR in the presence of 0.2 M NaCl at either +100 or -100 mV. The simulated ionic current is reduced by 1/3 and close to the supposed current.

	Average current without negamycin (3 x 150 ns)	**Supposed current with one monomer blocked**	**Average current with negamycin in Min-1 (4 x 140 ns)**
+100 mV	580 pA ± 40	390 pA	410 pA ± 60
-100 mV	600 pA ± 40	400 pA	440 pA ± 70

Table S6. Effects of *ompN* and *chiP* porin gene deletions on other porin gene transcripts of *E. coli* BW25113. The deletion of either *ompN*, *chiP* or the combined deletion of both genes did not have an impact on the gene expression of other porins, with the exception of chiP, which showed significant decreased expression in all three mutants.

	Fold change[A]		
Gene/strain	***E. coli* Δ*ompN***	***E. coli* Δ*chiP***	***E. coli* Δ*ompN*Δ*chiP***
ompF	ns	ns	ns
ompC	ns	ns	ns
ompN	ns	ns	ns
chiP	-2.28	-924.74	-500.66
ompG	ns	ns	ns
ompA	ns	ns	ns
lamB	ns	ns	ns
ompW	ns	ns	ns

[A]Compared to *E. coli* BW25113 (WT). ns, not significant (FDR corrected p-value > 0.05).

Table S7. The self-promoted uptake assay using 1-N-phenyl-naphthylamine (NPN) to determine disruptions of the outer membrane by substrate addition. Antibiotics were added to a final concentration of 64 µg/ml in the presence of NPN and incubated for 5 min before measurement. The increase in fluorescence signal was put in relation to an untreated sample and the mean of at least three independent measurements (± SD) is shown. The strongest increase in signal was observed with outer membrane permeabilizers colistin and polymyxin B (PMB), followed by aminoglycosides, which have also been described to translocate through the outer membrane by the self-promoted uptake mechanism.[2] Negamycin and the β-lactam cefoxitin did not increase the signal above background level.

	Signal ratio to background (± SD)
Colistin	9.99 ± 3.75
PMB	8.91 ± 3.32
Gentamicin	6.13 ± 2.68
Neomycin	5.76 ± 3.82
Negamycin	1.24 ± 0.73
Cefoxitin	0.94 ± 0.29

Table S8. Strongest changes (> 30x fold change) of the transcriptome of *E. coli* BW25113 after negamycin treatment. *E. coli* BW25113 cells were grown in PP until early exponential phase at 37°C and the bacterial liquid culture was split into two. One culture remained untreated, whereas the other culture was treated with 16 µg/ml, corresponding to 4x MIC under shaking conditions.[1] Cells were harvested after 45 min of incubation and RNA was extracted as described in methods. *E. coli* BW25113 reacted by reducing multiple transporter protein transcripts, most prominently those at the inner membrane. One of the strongest affected groups of transcripts was the *dpp* operon, which has previously been associated with negamycin uptake.[1] The complete list of significantly affected transcripts is available in supplemental information 2.

Gene	Description[A]	Fold change[B]
malK	maltose ABC transporter ATP binding subunit	-546.913322
dppB	dipeptide ABC transporter membrane subunit DppB	-86.1695059
dppD	dipeptide ABC transporter ATP binding subunit DppD	-84.0307185
dppC	dipeptide ABC transporter membrane subunit DppC	-71.6544141
dppF	dipeptide ABC transporter ATP binding subunit DppF	-63.5477396
lhgO	L-2-hydroxyglutarate oxidase	-62.5898167
prpR	DNA-binding transcriptional dual regulator PrpR	-62.0623088
cysJ	sulfite reductase. flavoprotein subunit	-60.3411264
fliJ	flagellar biosynthesis protein FliJ	-58.03132
tdcD	propionate kinase	-56.8560864
cysW	sulfate/thiosulfate ABC transporter inner membrane subunit CysW	-55.4337997
gabT	4-aminobutyrate aminotransferase GabT	-54.9744204
cysI	sulfite reductase, hemoprotein subunit	-50.0429702
malF	maltose ABC transporter membrane subunit MalF	-49.0177085
lamB	maltose outer membrane channel/phage lambda receptor protein	-48.7673527
tnaB	tryptophan:H(+) symporter TnaB	-47.6795088
gabP	4-aminobutyrate:H(+) symporter	-45.2387442
malM	maltose regulon periplasmic protein	-44.8974575
malE	maltose ABC transporter periplasmic binding protein	-43.1531039
lsrB	Autoinducer-2 ABC transporter periplasmic binding protein	-42.8836279
ydcT	putative ABC transporter ATP-binding protein YdcT	-40.901354
astE	succinylglutamate desuccinylase	-39.2896334
gabD	NADP(+)-dependent succinate-semialdehyde dehydrogenase	-38.8883411
fliF	flagellar basal-body MS-ring and collar protein	-33.8950783
tdcE	2-ketobutyrate formate-lyase/pyruvate formate-lyase 4	-33.7341616
ydcV	putative ABC transporter membrane subunit YdcV	-33.1285049
cysU	sulfate/thiosulfate ABC transporter inner membrane subunit CysU	-32.3004167
csiD	PF08943 family protein CsiD	-32.0322829
actP	acetate/glycolate:cation symporter	-31.8728591
ddpA	putative D,D-dipeptide ABC transporter periplasmic binding protein	-31.4700146
tdcF	putative enamine/imine deaminase	-30.4499997

Table 8S, *continued*

Gene	Description[A]	Fold change[B]
metN	L-methionine/D-methionine ABC transporter ATP binding subunit	34.3947818
acrE	multidrug efflux pump membrane fusion lipoprotein AcrE	39.623094
ibpA	small heat shock protein IbpA	40.8315531
ynbB	putative CDP-diglyceride synthase	44.6081198
metR	DNA-binding transcriptional dual regulator MetR	48.7587398
pspG	phage shock protein G	49.7664034
pspD	phage shock protein D	49.8693075
pspA	phage shock protein A	52.2579712
pspC	phage shock protein C	53.511095
ydeT	fimbrial usher domain-containing protein YdeT	59.9419091
pspB	phage shock protein B	62.7055176
bhsA	DUF1471 domain-containing multiple stress resistance outer membrane protein BhsA	105.302241
soxS	DNA-binding transcriptional dual regulator SoxS	1054.00369

[A]Gene function description from ecocyc.org.[9] [B]*E. coli* BW25113 treated with 16 µg/ml negamycin compared to untreated *E. coli* BW25113.

Table S9. Bacterial strains used in this study. *E. coli* BW25113 single deletion mutant strains are originated from the Keio collection.[3] For multiple gene deletion strains, the kanamycin resistance cassette was removed.[4]

strain	genotype/characteristics	reference
E. coli BW25113	wildtype; F-, Δ(*araD-araB*)*567*, Δ*lacZ4787*(::*rrnB*-3), *λ*-, *rph*-1, Δ(*rhaD-rhaB*)*568*, *hsdR514*	[4]
E. coli BW25113 Δ*ompF*	F-, *Δ(araD-araB)567*, *ΔlacZ4787*(::*rrnB*-3), *λ*-, *ΔompF746*, *rph-1*, *Δ(rhaD-rhaB)568*, *hsdR514*	[4]
E. coli BW25113 Δ*ompC*	F-, *Δ(araD-araB)567*, *ΔlacZ4787*(::*rrnB*-3), *λ*-, Δ*ompC*768, *rph-1*, *Δ(rhaD-rhaB)568*, *hsdR514*	[4]
E. coli BW25113 Δ*ompN*	F-, *Δ(araD-araB)567*, *ΔlacZ4787*(::*rrnB*-3), *λ*-, Δ*ompN*740, *rph-1*, *Δ(rhaD-rhaB)568*, *hsdR514*	[4]
E. coli BW25113 Δ*chiP*	F-, Δ(*araD-araB*)567, Δ*lacZ*4787(::*rrnB*-3), λ-, Δ*chiP*729, *rph-1*, Δ(*rhaD-rhaB*)568, *hsdR*514	[4]
E. coli BW25113 Δ*lamB*	F-, Δ(araD-araB)567, ΔlacZ4787(::*rrnB*-3), *λ*-, Δ*lamB*, rph-1, Δ(rhaD-rhaB)568, hsdR514	[4]
E. coli BW25113 Δ*ompG*	F-, *Δ(araD-araB)567*, *ΔlacZ4787*(::*rrnB*-3), *λ*-, *ΔompG756::kan*, *rph-1*, *Δ(rhaD-rhaB)568*, *hsdR514*	[4]
E. coli BW25113 Δ*ompW*	F-, *Δ(araD-araB)567*, *ΔlacZ4787*(::*rrnB*-3), *λ*-, Δ*ompW*764::kan, *rph-1*, *Δ(rhaD-rhaB)568*, *hsdR514*	[4]
E. coli BW25113 Δ*ompA*	F-, *Δ(araD-araB)567*, *ΔlacZ4787*(::*rrnB*-3), *λ*-, *ΔompA772::kan*, *rph-1*, *Δ(rhaD-rhaB)568*, *hsdR514*	[4]
E. coli BW25113 Δ*phoE*	F-, *Δ(araD-araB)567*, *ΔlacZ4787*(::*rrnB*-3), *λ*-, *ΔphoE759::kan*, ΔompC768::Kan, *rph-1*, *Δ(rhaD-rhaB)568*, *hsdR514*	[4]
E. coli BW25113 Δ*ompL*	F-, *Δ(araD-araB)567*, *ΔlacZ4787*(::*rrnB*-3), *λ*-, *ΔompL737::kan*, *rph-1*, *Δ(rhaD-rhaB)568*, *hsdR514*	[4]
E. coli BW25113 Δ*bglH*	F-, *Δ(araD-araB)567*, *ΔlacZ4787*(::*rrnB*-3), *λ*-, Δ*bglH*751::kan, *rph-1*, *Δ(rhaD-rhaB)568*, *hsdR514*	[4]
E. coli BW25113 Δ*tsx*	F-, *Δ(araD-araB)567*, *ΔlacZ4787*(::*rrnB*-3), *λ*-, Δ*tsx*773::kan, *rph-1*, *Δ(rhaD-rhaB)568*, *hsdR514*	[4]
E. coli BW25113 Δ*fadL*	F-, *Δ(araD-araB)567*, *ΔlacZ4787*(::*rrnB*-3), *λ*-, Δ*fadL*752::kan, *rph-1*, *Δ(rhaD-rhaB)568*, *hsdR514*	[4]
E. coli BW25113 Δ*nanC*	F-, *Δ(araD-araB)567*, *ΔlacZ4787*(::*rrnB*-3), *λ*-, Δ*nanC*779::kan, *rph-1*, *Δ(rhaD-rhaB)568*, *hsdR514*	[4]

Table S9, *continued*

strain	genotype/characteristics	reference
E. coli BW25113 Δ*ychO*	F-, *Δ(araD-araB)567*, *ΔlacZ4787*(::*rrnB*-3), λ-, Δ*ychO*731::kan, *rph-1*, *Δ(rhaD-rhaB)568*, *hsdR514*	[4]
E. coli BW25113 Δ*yfiB*	F-, *Δ(araD-araB)567*, *ΔlacZ4787*(::*rrnB*-3), λ-, Δ*yfiB*768::kan, *rph-1*, *Δ(rhaD-rhaB)568*, *hsdR514*	[4]
E. coli BW25113 Δ*yfaZ*	F-, *Δ(araD-araB)567*, *ΔlacZ4787*(::*rrnB*-3), λ-, Δ*yfaZ*731::kan, *rph-1*, *Δ(rhaD-rhaB)568*, *hsdR514*	[4]
E. coli BW25113 Δ*yiaT*	F-, *Δ(araD-araB)567*, *ΔlacZ4787*(::*rrnB*-3), λ-, Δ*yiaT*768::kan, *rph-1*, *Δ(rhaD-rhaB)568*, *hsdR514*	[4]
E. coli BW25113 Δ*ompF*Δ*ompC*	F-, *Δ(araD-araB)567*, *ΔlacZ4787*(::*rrnB*-3), λ-, *ΔompF746*, ΔompC768, *rph-1*, *Δ(rhaD-rhaB)568*, *hsdR514*	[5]
E. coli BW25113 Δ*ompN*Δ*chiP*	F-, Δ(*araD-araB*)567, Δ*lacZ*4787(::*rrnB*-3), λ-, Δ*ompN*740, Δ*chiP*729, *rph*-1, Δ(*rhaD-rhaB*)568, *hsdR*514	this study
E. coli BW25113 Δ*acrA*	F-, Δ(*araD-araB*)567, Δ*lacZ*4787(::*rrnB*-3), Δ*acrA*748, λ-, *rph*-1, Δ(*rhaD-rhaB*)568, *hsdR*514	[4]
E. coli BW25113 Δ*acrB*	F-, Δ(*araD-araB*)567, Δ*lacZ*4787(::*rrnB*-3), Δ*acrB*747, λ-, *rph*-1, Δ(*rhaD-rhaB*)568, *hsdR*514	[4]
E. coli BW25113 Δ*acrAB*	F-, Δ(*araD-araB*)567, Δ*lacZ*4787(::*rrnB*-3), Δ(*acrB*747 - *acrA*748)::*kan*, λ-, *rph*-1, Δ(*rhaD-rhaB*)568, *hsdR*514	[1]
E. coli BW25113 Δ*acrD*	F-, *Δ(araD-araB)567*, *ΔlacZ4787*(::*rrnB*-3), λ-, Δ*acrD*790::kan, *rph-1*, *Δ(rhaD-rhaB)568*, *hsdR514*	[4]
E. coli BW25113 Δ*acrE*	F-, *Δ(araD-araB)567*, *ΔlacZ4787*(::*rrnB*-3), λ-, Δ*acrE*783::kan, *rph-1*, *Δ(rhaD-rhaB)568*, *hsdR514*	[4]
E. coli BW25113 Δ*acrF*	F-, *Δ(araD-araB)567*, *ΔlacZ4787*(::*rrnB*-3), λ-, Δ*acrF*784::kan, *rph-1*, *Δ(rhaD-rhaB)568*, *hsdR514*	[4]
E. coli BW25113 Δ*macA*	F-, *Δ(araD-araB)567*, *ΔlacZ4787*(::*rrnB*-3), λ-, Δ*macA*779::kan, *rph-1*, *Δ(rhaD-rhaB)568*, *hsdR514*	[4]
E. coli BW25113 Δ*macB*	F-, *Δ(araD-araB)567*, *ΔlacZ4787*(::*rrnB*-3), λ-, Δ*macB*780::kan, *rph-1*, *Δ(rhaD-rhaB)568*, *hsdR514*	[4]
E. coli BW25113 Δ*tolC*	F-, *Δ(araD-araB)567*, *ΔlacZ4787*(::*rrnB*-3), λ-, Δ*tolC*732::kan, *rph-1*, *Δ(rhaD-rhaB)568*, *hsdR514*	[4]
E. coli BW25113 Δ*mdfA*	F-, *Δ(araD-araB)567*, *ΔlacZ4787*(::*rrnB*-3), λ-, Δ*mdfA*742::kan, *rph-1*, *Δ(rhaD-rhaB)568*, *hsdR514*	[4]
E. coli BW25113 Δ*malK*	F-, *Δ(araD-araB)567*, *ΔlacZ4787*(::*rrnB*-3), λ-, Δ*malK*731::kan, *rph-1*, *Δ(rhaD-rhaB)568*, *hsdR514*	[4]
E. coli BW25113 Δ*pspB*	F-, *Δ(araD-araB)567*, *ΔlacZ4787*(::*rrnB*-3), λ-, Δ*pspB*741::kan, *rph-1*, *Δ(rhaD-rhaB)568*, *hsdR514*	[4]
E. coli BW25113 Δ*bhsA*	F-, *Δ(araD-araB)567*, *ΔlacZ4787*(::*rrnB*-3), λ-, Δ*bhsA*774::kan, *rph-1*, *Δ(rhaD-rhaB)568*, *hsdR514*	[4]
E. coli BW25113 Δ*soxS*	F-, *Δ(araD-araB)567*, *ΔlacZ4787*(::*rrnB*-3), λ-, Δ*soxS*756::kan, *rph-1*, *Δ(rhaD-rhaB)568*, *hsdR514*	[4]
E. coli ATCC 25922	Clinical isolate, CLSI reference strain	[6]
E. coli ATCC 25922 Δ*ompN*	Δ*ompN*	this study
E. coli ATCC 25922 Δ*chiP*	Δ*chiP*	this study
E. coli ATCC 25922 Δ*ompN*Δ*chiP*	Δ*ompN*Δ*chiP::kan*	this study
E. coli ATCC 25922 Δ*acrAB*	Δ*acrAB::kan*	this study
E. coli HN817		[7]
E. coli HN818	Δ*acrAB*	[7]
E. coli C600	*F- galK thi-1 thr-1 leuB6 lacY1 tonA21 supE44*, *envA*::Tn10	[8]
E. coli C600 Δ*tolC*	*F- galK thi-1 thr-1 leuB6 lacY1 tonA21 supE44*, *tolC*::Tn10	[8]

Table S10. Primers used for knockout and expression strain generation in this study. Nucleotides marked in bold are homologous sequences flanking the kanamycin resistance cassette of plasmid pKD13.[4]

Oligonucleotide	Intended purpose	Sequence (5‘-3‘)
Knockout generation		
BW-ompN_for	Deletion of *ompN* in *E. coli* BW25113	TAACAGCGGGCAGGAGGATTTAGAACTGATA AACCAGACC**ATTCCGGGGATCCGTCGACC**
BW-ompN_rev		GATAAAAGGCAAATAAAATAACTAAAGGATT TATTCAATG**TGTAGGCTGGAGCTGCTTCG**
ATCC-ompN_for	Deletion of *ompN* in *E. coli* ATCC 25922	AGAAAAAGCCCGCCAAAACAGCGGGCAGGG GGATTTAGAACTGAT**ATTCCGGGGATCCGT**
ATCC-ompN_rev		GATGAAAGGCAAATAAAATAACTAAAGGATT TATTCAATG**TGTAGGCTGGAGCTGCTTCG**
chiP_for	Deletion of *chiP* in *E. coli* BW25113 and *E. coli* ATCC 25922	TTGGTGCAGCAATTTATACGTCAAAGAGGAT TAACCCATG**ATTCCGGGGATCCGTCGACC**
chiP_rev		AAACCTGCCGCGTCGGGCATCAGAAGATGGT GAATGGTGC**TGTAGGCTGGAGCTGCTTCG**
acrAB_for	Deletion of *acrAB* in *E. coli* BW25113 and *E. coli* ATCC 25922	CCATTGACCAATTTGAAATCGGACACTCGAG GTTTACATATGAAC**TGTAGGCTGGAGCTG**
acrAB_rev		CGGCCTTAGTGATTACACGTTGTATCAATGAT GATCGACAGTATG**ATTCCGGGGATCCGT**
Expression strain generation		
chiP-pASK-IBA5_for	Cloning *chiP* from *E. coli* BW25113 into the pASK-IBA5 plasmid	ATGAATAGTTCGACAAAAATCTAGATGC GTACGTTTAGTGGC
chiP-pASK-IBA5_rev		GGTCCCCCTGCAGGTCGACCTCGAGTCA GAAGATGGTGAATGG
pET19b-chiP_for	Cloning *chiP* from pASK-IBA5-chiP into the pET19b plasmid	ACGTACGCATGGTATATCTCCTTC
pET19b-chip_rev		CATCTTCTGACATATGCTCGAGGATCC
chiP-pET19b_for		GAGATATACCATGCGTACGTTTAGTGGC
chiP-pET19b_rev		CGAGCATATGTCAGAAGATGGTGAATG GTG

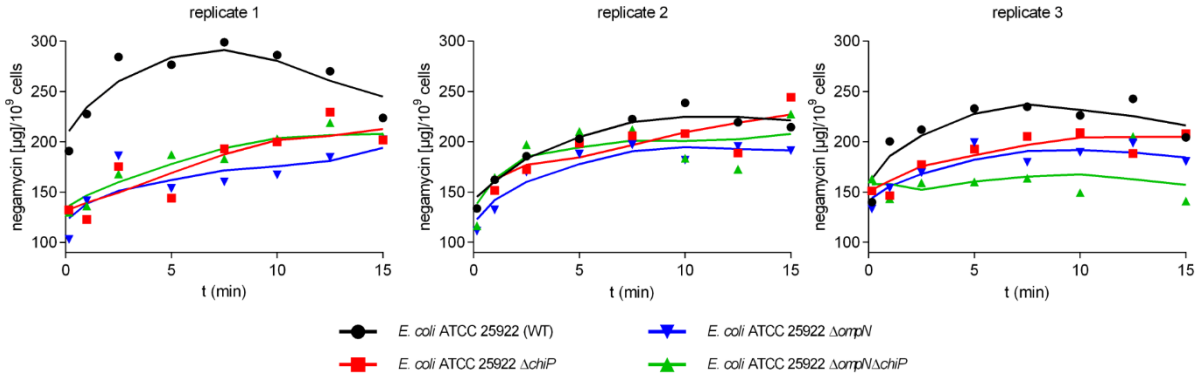

Figure S1. Negamycin uptake measurements in *E. coli* ATCC 25922 porin mutants using radioactive labeled [^{3}H]negamycin. Three replicates are shown exemplarily and the summary of this data displayed in Figure 1C. [^{3}H]negamycin (specific activity: 0.052 Ci/mmol) was added and accumulation was determined over 15 min. Negamycin accumulation was reduced in the *E. coli* gene deletion strain mutants without *ompN* or *chiP*. The deletion of both *ompN* and *chiP* had no additive effect on negamycin accumulation, as negamycin concentration in *E. coli* Δ*ompN*Δ*chiP* was at a similar level as the single gene deletion strains *E. coli* Δ*ompN* or *E. coli* Δ*chiP*.

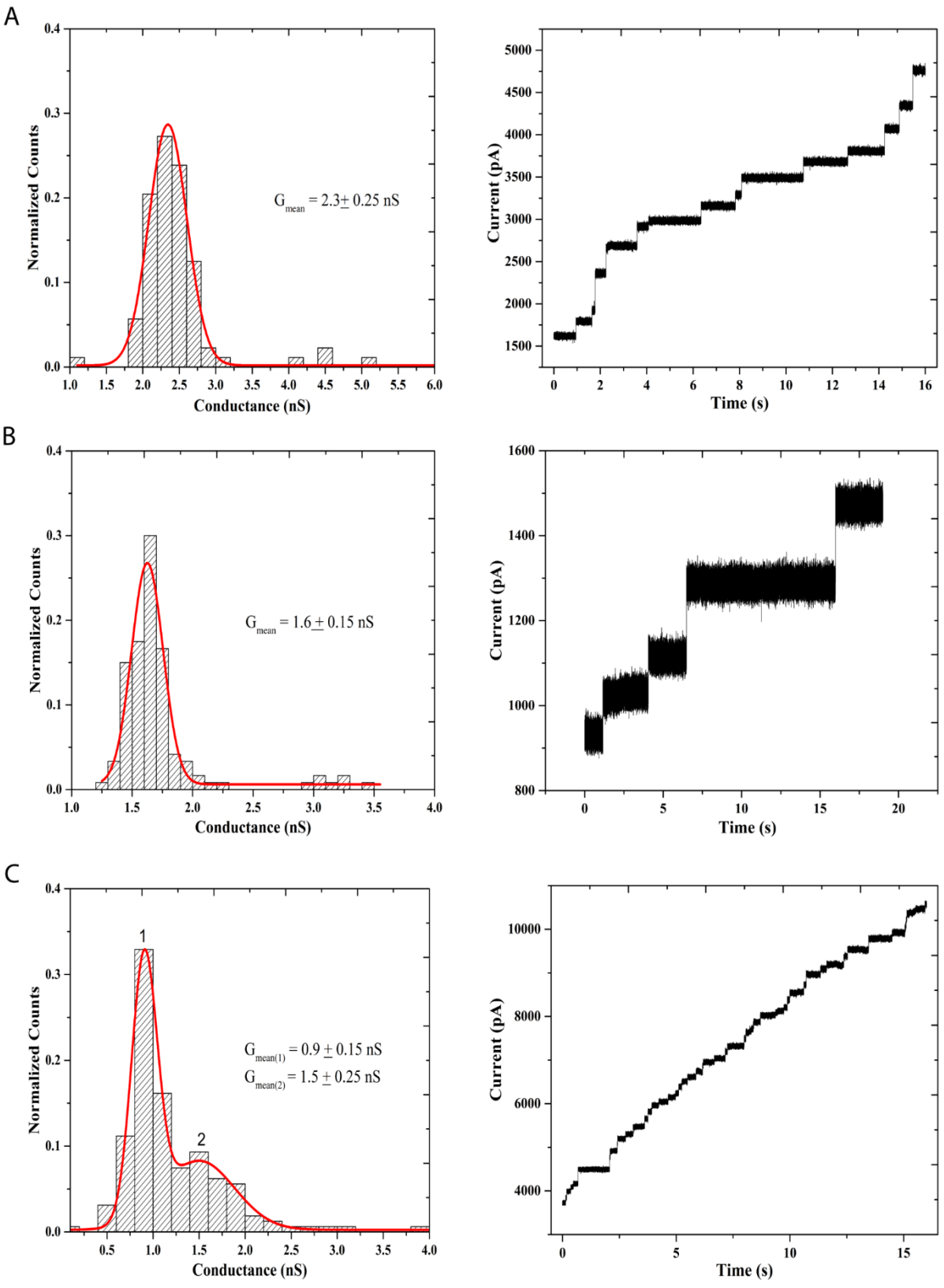

Figure S2. In a first series of measurement we characterized the OmpN single channel conductance. Purified OmpN porin were added on the cis (ground) side of the chamber and inserted stepwise into the planar lipid bilayer (A) Conductance histogram (left) of 1 M KCl with respect to its insertion steps (right). (B) Conductance histogram of 1 M NaCl (left) with respect to its insertion steps (right). (C) Conductance histogram of 1 M CH_3CO_2K with respect to its insertion steps (right).

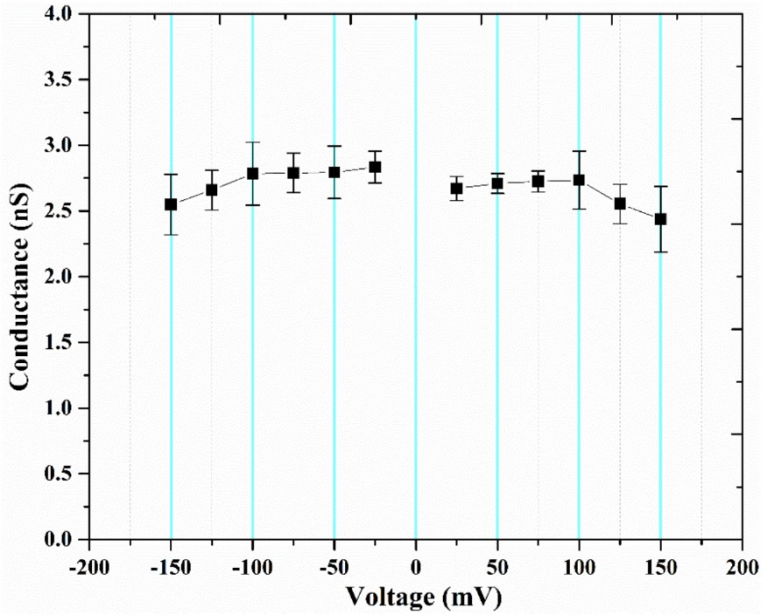

Figure S3. Trimeric OmpN conductance as a function of applied voltage with 1 M NaCl. The channel conductance remains stable up to ± 100 mV, and above ± 100 mV the conductance deviates towards the lower end. Error bars show SD from 3 individual measurements with a single OmpN channel.

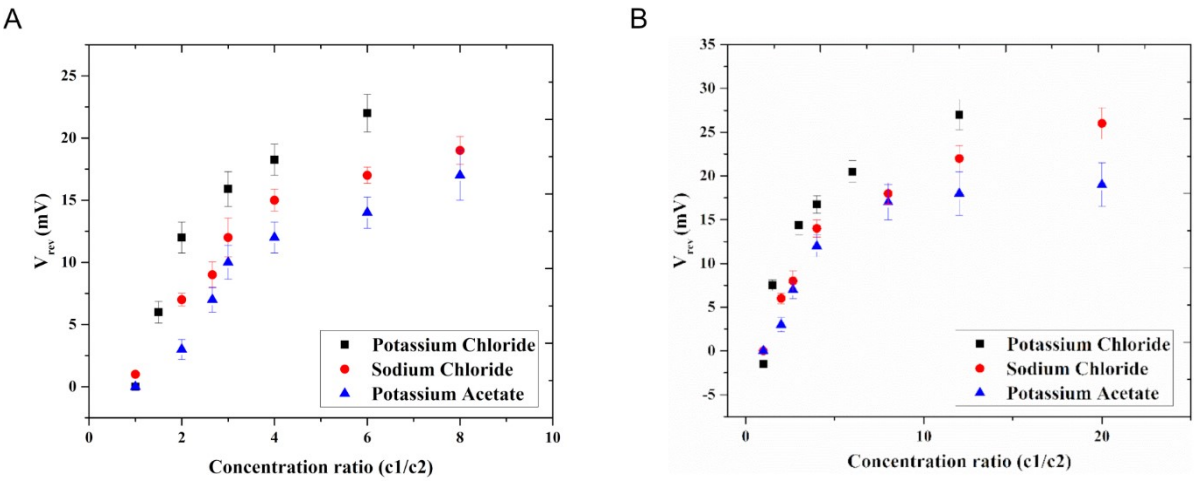

Figure S4. Selectivity test of the OmpN porin. Ion selectivity in a channel is not a single parameter but depends on the ion-pairs as well as on their concentration. To check the general selectivity of the porin, we performed a Zero-current potential experiment: measuring the ion current *vs.* voltage in the presence of a salt gradient. Low salt (A): we started with 10 mM salt on both sides and titrated the stock solution on one side and the initial buffer on the other side until we reach a tenfold concentration gradient (c1: 10 mM to 100 mM; c2: 10 mM). High salt (B): we started with 100 mM salt on both sides and titrated the stock solution on one side and the initial buffer on the other side until we reach a tenfold concentration gradient (c1: 100 mM to 2 M; c2: 100 mM salt). The selectivity was measured for three different salts (KCl, NaCl and KCH_3CO_2 with 10mM HEPES as a buffer at pH 7).

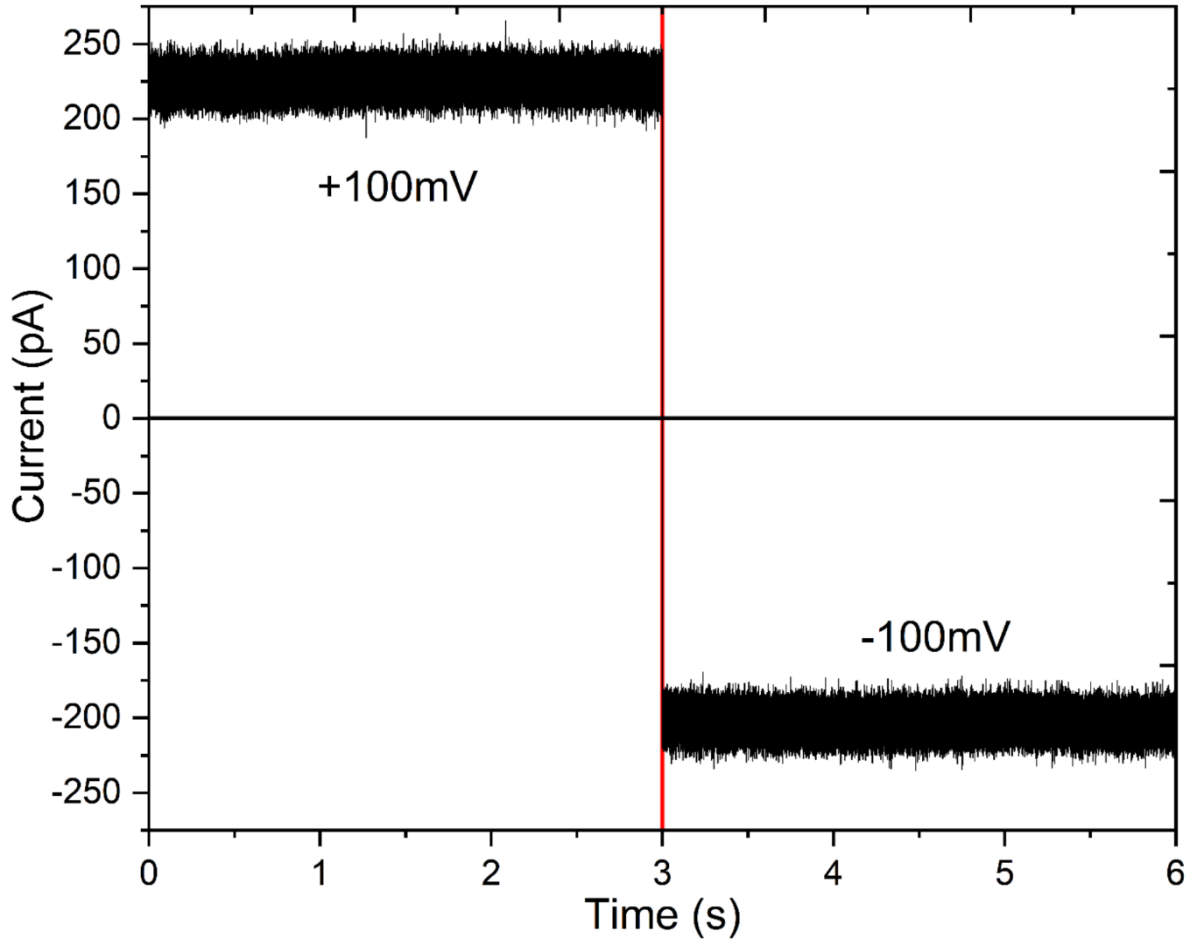

Figure S5. Single channel measurements with OmpN in the presence of 0.25 mM negamycin on the cis side at +100 or -100 mV. The addition of negamycin did not lead to blockage of the ion flux through the porin channel.

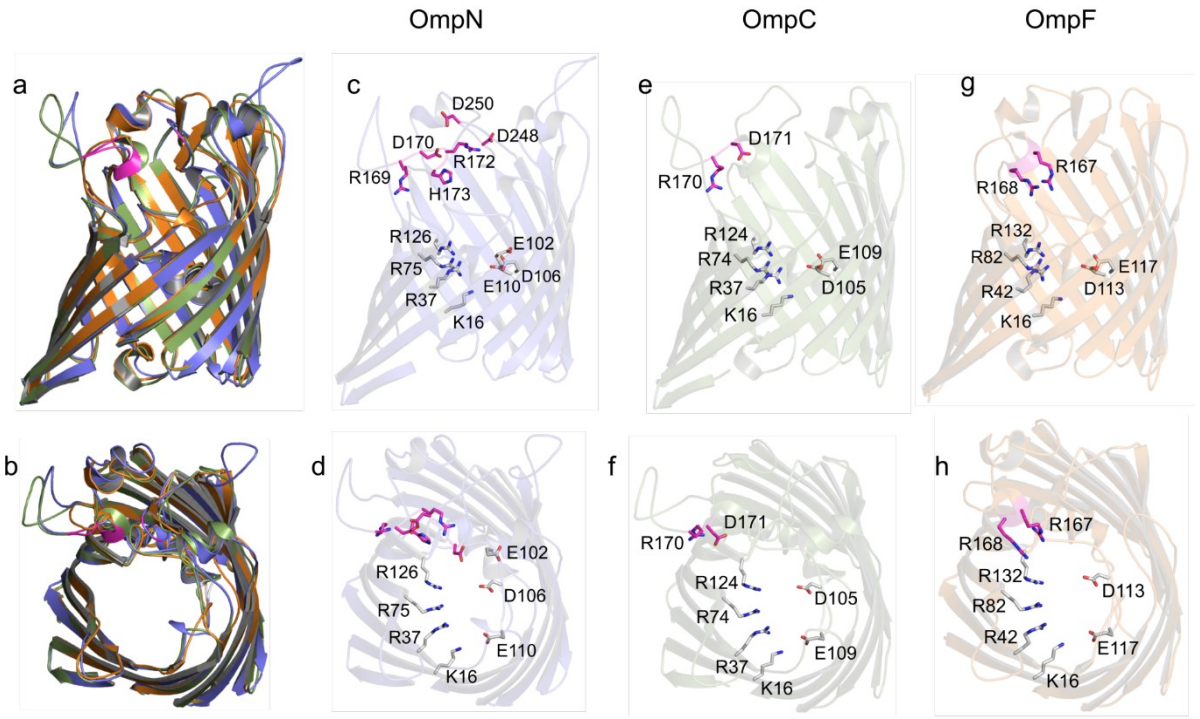

Figure S6. Structural differences between OmpN, OmpC and OmpF. (a,b) Superimposed cartoon representations of OmpN (blue), OmpC (green, PDB: 2JIN) and OmpF (orange, PDB: 4GCP) monomers. Side view and top view from extracellular side of OmpN (c,d); OmpC (e,f) and OmpF (g,h) monomers with highlighted residues from the constriction zone and extracellular mouth region.

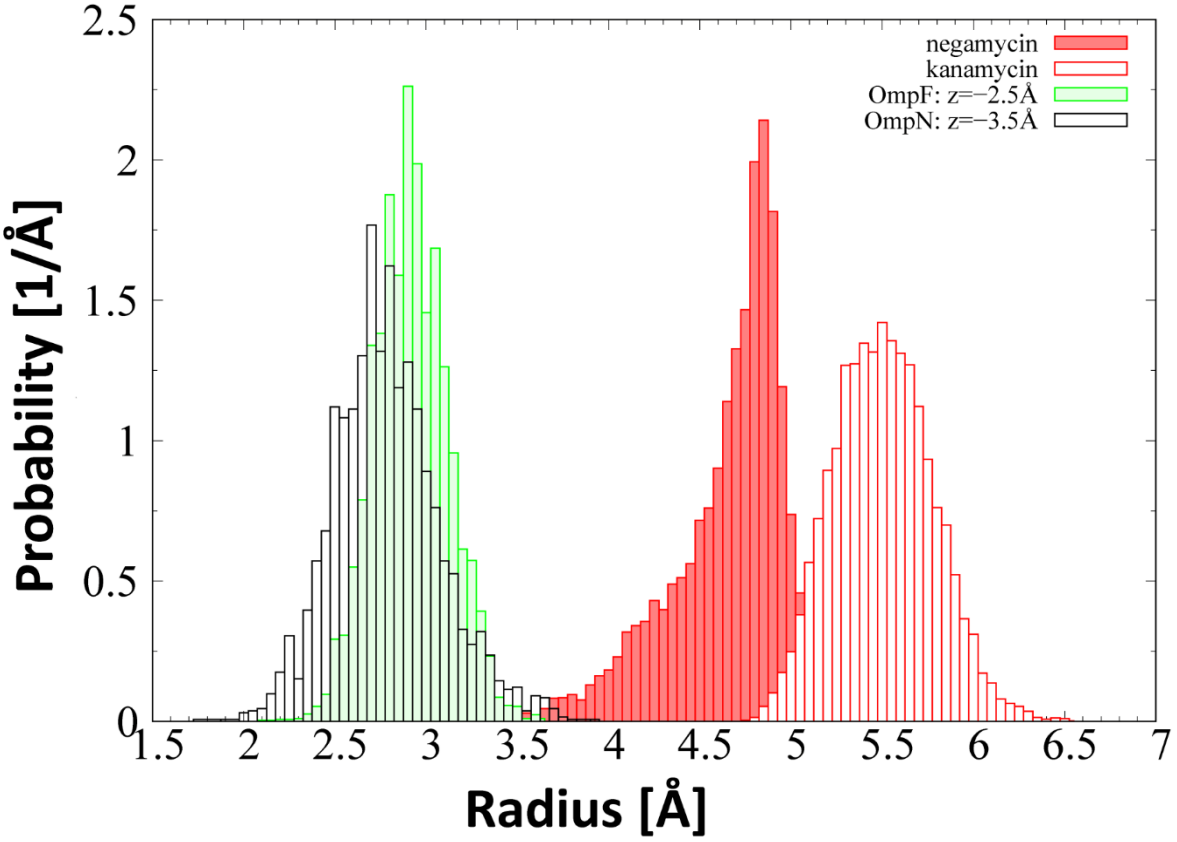

Figure S7. Probability distribution of the calculated minimal internal radius of OmpF (green) and OmpN (black) compared with the probability distribution of minimal radius of negamycin (filled red) and kanamycin (open red). Distributions were obtained from simulation trajectories of 200 ns and 1 µs in the NVT ensemble for OmpF/OmpN and negamycin/kanamycin, respectively. Noteably for negamycin the long tail overlaps with the distribution of porins, which is not the case for kanamycin.

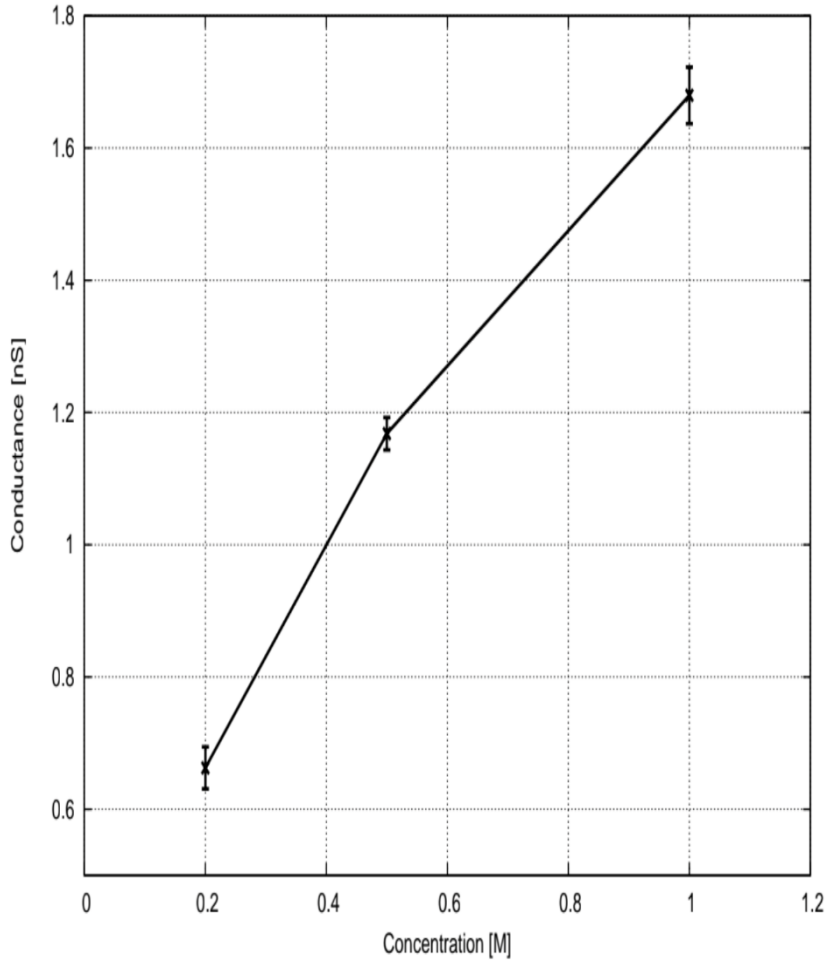

Figure S8. Simulated conductance of OmpN in the presence of 0.2, 0.5 or 1 M NaCl. The conductance simulations were in accordance with the measurements at 1 M NaCl with the purified OmpN protein (Table 2E, 1.6 ± 0.15 nS) and previous results (1.63 ± 0.06 nS).[10]

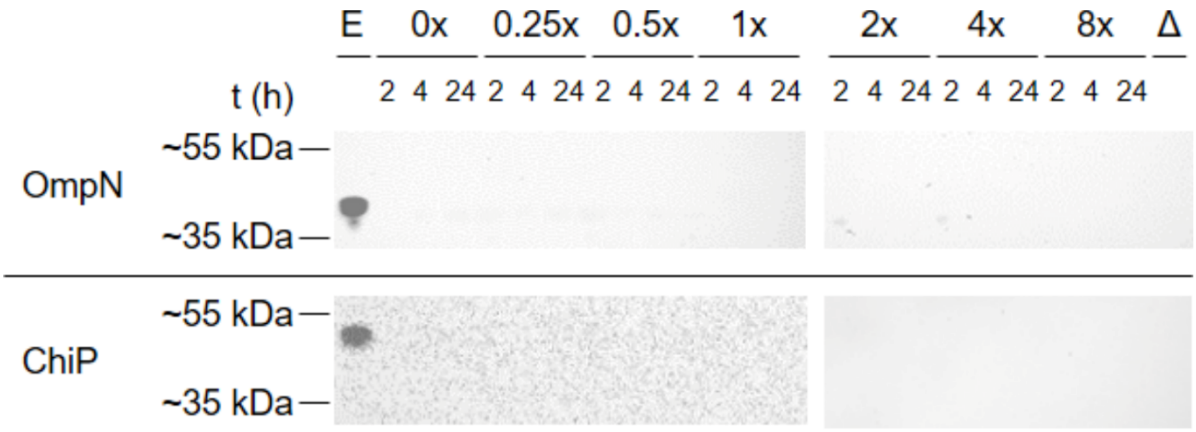

Figure S9. The effect of negamycin treatment or the gene deletions of *ompF* and *ompC* on the expression of OmpN and ChiP. OmpN and ChiP expression was investigated in *E. coli* BW25113, grown in PP. Outer membrane proteins were extracted as described in methods. Negamycin was added at early exponential growth phase at 0.25x to 8x MIC („1x“ corresponds to a negamycin MIC of 4 µg/ml). Samples were taken after 2, 4 and 24 h of incubation and are displayed in this order from left to right within each concentration. Only in the sample with a plasmid mediated *ompN* or *chiP* induction could a signal by Western blot be detected („E“). The deletion of both major porin genes *ompF* and *ompC* in *E. coli* BW25113 („Δ“) did not lead to OmpN or ChiP expression. Protein size was estimated by use of the Thermo Scientific PageRuler Plus Prestained Protein Ladder.

References (Supplemental information)

1. Hörömpöli, D.; Ciglia, C.; Glüsenkamp, K.-H.; Haustedt, L. O.; Falkenstein-Paul, H.; Bendas, G.; Berscheid, A.; Brötz-Oesterhelt, H., The Antibiotic Negamycin Crosses the Bacterial Cytoplasmic Membrane by Multiple Routes. *Antimicrobial Agents and Chemotherapy* **2021,** *65* (4), e00986-20.
2. Serio, A.; Keepers, T.; Andrews, L.; Krause, K., Aminoglycoside Revival: Review of a Historically Important Class of Antimicrobials Undergoing Rejuvenation. *EcoSal Plus* **2018**.
3. Baba, T.; Ara, T.; Hasegawa, M.; Takai, Y.; Okumura, Y.; Baba, M.; Datsenko, K. A.; Tomita, M.; Wanner, B. L.; Mori, H., Construction of Escherichia coli K-12 in-frame, single-gene knockout mutants: the Keio collection. *Molecular systems biology* **2006,** *2* (1), 2006.0008.
4. Datsenko, K. A.; Wanner, B. L., One-step inactivation of chromosomal genes in Escherichia coli K-12 using PCR products. *Proceedings of the National Academy of Sciences* **2000,** *97* (12), 6640-6645.
5. Bafna, J. A.; Sans-Serramitjana, E.; Acosta-Gutiérrez, S.; Bodrenko, I. V.; Hörömpöli, D.; Berscheid, A.; Brötz-Oesterhelt, H.; Winterhalter, M.; Ceccarelli, M., Kanamycin Uptake into Escherichia coli Is Facilitated by OmpF and OmpC Porin Channels Located in the Outer Membrane. *ACS Infectious Diseases* **2020,** *6* (7), 1855-1865.
6. Patel, J. B.; Cockerill, F.; Bradford, P.; Eliopoulos, G.; Hindler, J.; Jenkins, S.; Lewis, S.; Limbago, B.; Miller, A.; Nicolau, P., M07-A10 Methods for Dilution Antimicrobial Susceptibility Tests for Bacteria That Grow Aerobically; Approved Standard—. *Clinical Laboratory Standards Institute* **2015,** *35* (2).
7. Srikumar, R.; Kon, T.; Gotoh, N.; Poole, K., Expression of Pseudomonas aeruginosa multidrug efflux pumps MexA-MexB-OprM and MexC-MexD-OprJ in a multidrug-sensitive Escherichia coli strain. *Antimicrobial agents and chemotherapy* **1998,** *42* (1), 65-71.
8. Appleyard, R. K., Segregation of New Lysogenic Types during Growth of a Doubly Lysogenic Strain Derived from Escherichia Coli K12. *Genetics* **1954,** *39* (4), 440-52.
9. Keseler, I. M.; Mackie, A.; Santos-Zavaleta, A.; Billington, R.; Bonavides-Martínez, C.; Caspi, R.; Fulcher, C.; Gama-Castro, S.; Kothari, A.; Krummenacker, M., The EcoCyc database: reflecting new knowledge about Escherichia coli K-12. *Nucleic acids research* **2017,** *45* (D1), D543-D550.
10. Prilipov, A.; Phale, P. S.; Koebnik, R.; Widmer, C.; Rosenbusch, J. P., Identification and Characterization of Two Quiescent Porin Genes, nmpC and ompN, in Escherichia coli BE. *Journal of bacteriology* **1998,** *180* (13), 3388-3392.
11. Ghai, I.; Pira, A.; Scorciapino, M. A.; Bodrenko, I.; Benier, L.; Ceccarelli, M.; Winterhalter, M.; Wagner, R., General method to determine the flux of charged molecules through nanopores applied to β-lactamase inhibitors and OmpF. *The journal of physical chemistry letters* **2017,** *8* (6), 1295-1301.
12. Ziervogel, B. K.; Roux, B., The binding of antibiotics in OmpF porin. *Structure* **2013,** *21* (1), 76-87.

4.4. Manuscript 2

Two-step batch purification of negamycin from biosynthesis using cation exchange chromatography

Daniel Hörömpöli, Andreas Kulik, Karl-Heinz Glüsenkamp, Hamada Saad, Irina Helmle, Harald Gross, Anne Berscheid, Heike Brötz-Oesterhelt

Abstract

Negamycin is a natural product, isolated from a *Streptomyces purpeofuscus* related strain and described for the first time 50 years ago. In recent years it gained attention again, as its low toxicity and activity against Gram-negative bacteria made it interesting for further optimization. At the same time, it is also of interest for treatment of Duchenne muscular dystrophy, as negamycin‘s mode of action leads to miscoding, which could be used to compensate genomic defects. Various publications described total synthesis of negamycin, but chemical synthesis is costly. Therefore, we investigated the biosynthesis and batch purification of negamycin to establish a scalable procedure for further usage. For this, the original purification method by (Hamada et al. 1970) and Umezawa et al. (1972) was adjusted. Fermentation was performed using the negamycin producer strain *S. purpeofuscus* ATCC 21477. A two-step batch purification method by cation exchange chromatography was established, which resulted in 13 mg of pure negamycin (>95% purity) and additional 58 mg of semi-pure negamycin from a 2 l production culture.

Introduction

Streptomycetaceae have long been of interest as a source for new antibiotics (Hopwood 1999; Claessen et al. 2006). About two third of all clinically used antibiotics are derived from *Streptomyces* strains (Champness 1999). Although new antibiotic classes are nowadays rarely found, the potential to find new antibiotics is still there, as most *bacterial* strains cannot be grown in the lab (Lewis 2013). This leads to an estimate that over 100.000 different antibiotics could exist within the *Streptomyces* genus (Watve et al. 2001). These antibiotics can also be used as a basis for further derivatization, to get improved analogues with higher activity. This can either be achieved by genetic modification of the producer strain, feeding studies or by chemically modifying the molecule of interest. For this latter case, large amounts of the compounds are needed. For the molecule of our interest, the natural product negamycin, various studies described total synthetic pathways (Shibahara et al. 1972; Streicher et al. 1978; Hayashi et al. 2008; Hayashi et al. 2009), but acquiring larger amounts remains difficult and expensive.

Negamycin was first described 1970 after isolation from a *Streptomyces purpeofuscus* strain (Hamada et al. 1970). By binding to the small subunit of the ribosome, negamycin hinders translocation and stabilizes nearby tRNA, leading to a miscoding activity (Olivier et al. 2014; Polikanov et al. 2014). It

is a dipeptide-like antibiotic, therefore rather small (248.28 g/mol). Its high hydrophilicity complicates purification, but the original discoverers established multiple protocols for purification from biosynthesis (Hamada et al. 1970; Umezawa et al. 1972). As the previously described but rather ancient technique to use activated carbon to separate negamycin from the bacterial culture did not work for us, we focused on purification by multiple ion exchange chromatography steps. On the basis of the previous studies, we established a purification protocol for our lab and reduced purification steps from four to two. Purity was confirmed by high-performance liquid chromatography (HPLC), mass spectrometry (MS), thin layer chromatography (TLC) and nuclear magnetic resonance (NMR).

Materials and methods

Chemicals and strains used. Negamycin was synthesized by Squarix GmbH based on published procedures (Wang et al. 1982; Raju et al. 2003). Column material Amberlite IRC-50 (The Dow Chemical Company) was kindly provided by Andreas Kulik (University of Tübingen) and Amberlite CG50 (The Dow Chemical Company) was acquired from Sigma Aldrich. The negamycin production medium (NPM) is based on the medium described by Hamada et al. (1970). NPM consists of 2% starch, 2% soybean flour, 0.5% yeast extract, 0.5% NaCl, 0.7% $CaCO_3$, 20% glucose, 5 mg/L $CuSO_4$ x 5 H_2O, 5 mg/L $MnCl_2$ x 4 H_2O, 50 mg/L $ZnSO_4$ x 7 H_2O. pH was adjusted to 7.2 using NaOH. Glucose, $CuSO_4$, $MnCl_2$ and $ZnSO_4$ were sterilized separately by filtration. The producer strain *S. purpeofuscus* ATCC 21477 was purchased from ATCC.

Negamycin bioactivity determination by agar diffusion and MIC determination. Negamycin activity was determined by an agar diffusion assay, where bioactivity was tested against *E. coli* in a minimal medium with 0.5% polypeptone (BBL polypeptone peptone, BD) and 2.5 mM $CaCl_2$. Agar plates with polypeptone (polypeptone 0.5% (w/v), $CaCl_2$ 2.5 mM, agar-agar 7.5 g/l, pH 7.0), inoculated with *E. coli* BW25113 (OD_{600nm} adjusted to 0.2, 100 µl cell suspension per 10 ml agar) were prepared. After polymerization, holes with a volume of 50 µl were punched and filled either with crude extract or purified samples. Plates were incubated at 37°C overnight and activity determined by measuring the clear inhibition zone on the next day. The CLSI protocol for MIC determination by broth microdilution ((CLSI) 2006) was adjusted for negamycin as described before (Hörömpöli et al. 2021). Briefly, the cell suspension of a final inoculum of 5 x 10^5 colony forming units (CFU)/ml was incubated with a concentration series of negamycin in M9 medium (47.74 mM Na_2HPO_4 x $2H_2O$, 22.04 mM KH_2PO_4, 8.56 mM NaCl, 18.7 mM NH_4Cl, 2 mM $MgSO_4$, 100 mM $CaCl_2$, 0.4% glucose) for 24 h at 37°C, followed by the readout of the MIC.

Fermentation of the negamycin producer strain. This method is based on the first description of negamycin biosynthesis (Hamada et al. 1970; Umezawa et al. 1972). The following protocol was

optimized for a total volume of 2 l of the negamycin production medium (NPM). A first culture of *S. purpeofuscus* ATCC 21477 was grown in 125 ml NPM in a baffled flask by inoculating with 25 µl of a dense spore suspension. The culture was grown for 3-4 days (27°C, 130 rpm), until a clear shift to a darker color of the culture could be observed. This preculture was used to inoculate the production culture in fresh NPM with a final inoculum of 0.5%. This culture was grown in a volume of 125 ml in 500 ml baffled flasks. Bigger flasks with the same volume ratio also led to negamycin production, albeit with a lower yield of negamycin per volume. This main production culture was incubated for 4 days (27°C, 130 rpm) and the culture was harvested, when the color of the medium turned darker. pH of the harvested culture was adjusted to 4.0 using HCl. The sample was centrifuged (20 min, 4,800 g), the supernatant was additionally filtered with a paper filter and afterwards applied to the first cation exchange chromatography using Amberlite IRC-50.

Cation exchange chromatography with Amberlite IRC-50. Of the column material Amberlite IRC-50 (Na^+ form), 160 ml were applied to a glass column (⌀ 2.5 cm). Before each usage, 500 ml of 10% NaCl (w/v) were applied at a slow flow rate to regenerate the column material. Afterwards, the column was washed with 100 ml of dH_2O. The filtered sample was applied carefully and run through the column at a slow flow rate (~ 1 ml/min). The column was washed with 3 l of dH_2O at a high flow rate. Afterwards, the column was washed with 3 l of 0.064% NH_4OH and fractions of 1 l were collected after the dead volume of 130 ml, as parts of negamycin could elute early, depending on the amounts of negamycin within the biosynthesis sample. Negamycin was eluted with 4.5 l of 0.256% NH_4OH and fractions of 250/500 ml were collected after the dead volume. All fractions were tested for bioactivity and the uncolored fractions with bioactivity were pooled together. Subsequently, the pooled sample was carefully concentrated by rotary evaporation to a total volume of ~10 ml.

Cation exchange chromatography with Amberlite CG50. Of the column material Amberlite CG50 (NH_4^+ form), 900 ml were applied to a glass column (⌀ 3.125 cm). Before each usage, 1 l of 1% NH_4OH was applied at a slow flow rate to regenerate the column material. Afterwards, the column was washed with 500 ml of dH_2O. The concentrated sample from the first cation exchange column (Amberlite IRC-50) was applied carefully on the Amberlite CG50 column and run through at a slow flow rate (~1.5 ml/min). Negamycin was eluted with 3 l of dH_2O and fractions of 15 ml were collected. Fractions were tested for negamycin content by the bioactivity assay. Fractions with strongest activity were found between the fractions 85 and 123. To remove residual column material, samples were centrifuged (14,000 g, 5 min) and the supernatant was used for further analysis. Samples were frozen and subsequently freeze-dried. Purity was examined by bioactivity, HPLC-MS, TLC and NMR.

High-performance liquid chromatography (HPLC), mass spectrometry (MS), thin layer chromatography (TLC) and nuclear magnetic resonance (NMR). HPLC for MS analysis was performed with HP1090M (Hewlett-Packard Instruments) with a Nucleosil 100 C18 (3 µm, 100 x 2 mm ID) column (mobile phase: A = 0.1% formic acid, B = 0.06% formic acid in acetonitrile; gradient: t_{0min} -> t_{3min} = 0% B; t_{10min} -> t_{12min} = 100% B; flow rate: 400 µl/min; column temperature: 40°C; injection volume: 2.5 µl). MS analysis was coupled to HPLC and performed with the LC/MSD Ultra Trap System XCT 6330 (Agilent). For negamycin detection, MS^2 in positive mode for *m/z* 249 was screened and compared to a negamycin standard from chemical synthesis. Further HPLC analysis was performed with a Luna Omega Polar C18 (Phenomenex, 5 µm, 250 x 10 mm) column (mobile phase: A = acetonitrile, B = 0.1% trifluoroacetic acid; gradient: t_{0min} -> t_{10min} = 5% A; t_{10min} -> t_{15min}: 15% A; t_{15min} -> t_{25min}: 35% A; t_{30min} -> t_{35min}: 100% A; flow rate: 2.0 ml/min). Thin layer chromatography (TLC) was performed using TLC silica gel 60 F254 (Merck) with chloroform:methanol:25% aqueous ammonia (2:2:1) as the mobile phase. 6 µl of samples, containing 10 mg/ml of negamycin, were applied to the plate. After developing, the plate was dried at 60°C and treated with ninhydrin for visualization. For NMR analysis, negamycin was solubilized in D_2O/DCl (pH 1.0). ^1H NMR spectra of the synthetic negamycin were recorded with a Bruker NMR spectrometer at 600 Mhz. ^1H NMR spectra of the biosynthesized negamycin were recorded on a 400 MHz Bruker AVANCE III NMR spectrometer operating at 400.17 MHz, respectively, which was equipped with a 5 mm broadband SmartProbe and an AVANCE III HD Nanobay console. All NMR spectra were recorded in D_20 + DCl (pH 1), the residual solvent signal (resonance at δ_H 4.89) was used as internal reference.

Results

Negamycin production & batch purification. Negamycin biosynthesis was performed with the producer strain *Streptomyces purpeofuscus* ATCC 21477 and growing conditions based on the original publication (Hamada et al. 1970; Umezawa et al. 1972). Within our previous studies, we could not identify a strain or a nutrient medium with a higher production yield, with the exception of exchanging soybean meal by soybean flour (Hörömpöli 2016). The general procedure of negamycin biosynthesis and purification is shown in a schematic overview in figure 1 and one exemplary run is described here.

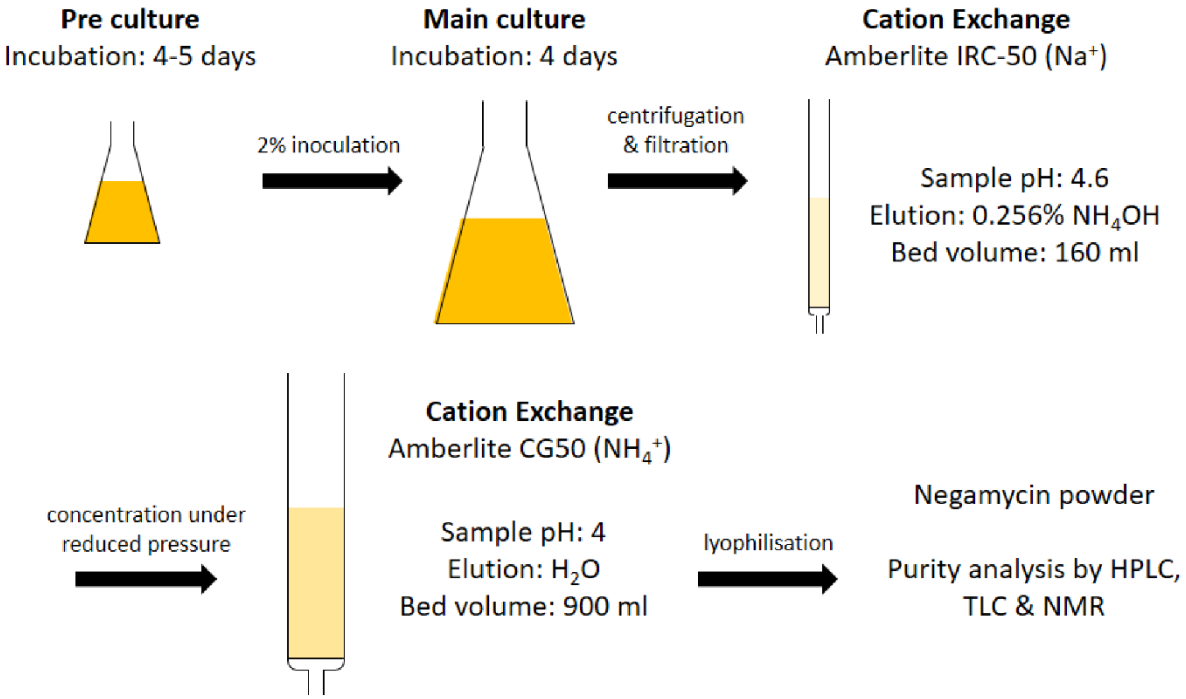

Figure 1. Schematic overview of the production and purification process of negamycin. A first culture is used to inoculate a bigger main production culture. The supernatant of this culture is purified in two cation exchange chromatography steps.

Fermentation of the negamycin producer strain under the above mentioned conditions led to a yield of roughly 125 mg/l, which was determined by bioactivity and compared to a standard curve based on a concentration gradient with negamycin from chemical synthesis (Figure S1). The biosynthesis sample was prepared for cation exchange chromatography as described in methods and applied to the Amberlite IRC-50 (Na^+ form) column (Table 1). Negamycin could be detected in fractions with NH_4OH, both at concentrations of 0.064% and 0.256%. The initial eluates of the washing steps looked impure, as the color of these eluates was yellow(ish), although showed strong bioactivity compared to the following eluate fractions. After initial washing with 0.064% NH_4OH, fractions eluting with

0.256% NH_4OH looked clear. All fractions with bioactivity were pooled together for further purification.

Table 1. Samples of the cation exchange chromatography using Amberlite IRC-50. The supernatant of the fermentation batch was applied after preparation for the column as described in methods.

Sample	V [l]	Bioactivity[a] [mm]	Color of the fraction
Supernatant	2.2	7	
Flow through		0	
Washing (H_2O)	3	0	
W1 (0.064% NH_4OH)	1	0	yellow
W2	1	6	yellow
W3	1	6	yellowish
E1 (0.256% NH_4OH)	0.25	7	clear
E2	0.25	6	clear
E3	0.25	5.5	clear
E4	0.25	4	clear
E5	0.25	3.5	clear
E6	0.25	3	clear
E7	0.25	2	clear
E8	0.25	2	clear
E9	0.25	1	clear
E10	0.5	0.5	clear
E11	0.5	0	clear
E12	0.5	0	clear
E13	0.5	0	clear

[a]Bioactivity determined as described in methods by the agar diffusion method. Radius of the inhibition zone is stated here.

In contrast to the previous purification protocol (Umezawa et al. 1972), the anion exchange chromatography after the first cation exchange separation was left out. After concentration by rotary evaporation to a volume of approximately 10 ml, the sample was applied to the second cation exchange chromatography with Amberlite CG50 (NH_4^+ form). Fractions of ~15 ml were collected, and every fourth fraction was tested for bioactivity (Figure 2). Bioactivity could be detected from fraction 45 to 205, which was the last fraction collected. Residual negamycin might have been lost, but activity within these last fractions was low. Distribution of bioactivity looks normally distributed, with the highest concentration of bioactive compound in fractions surrounding sample 89.

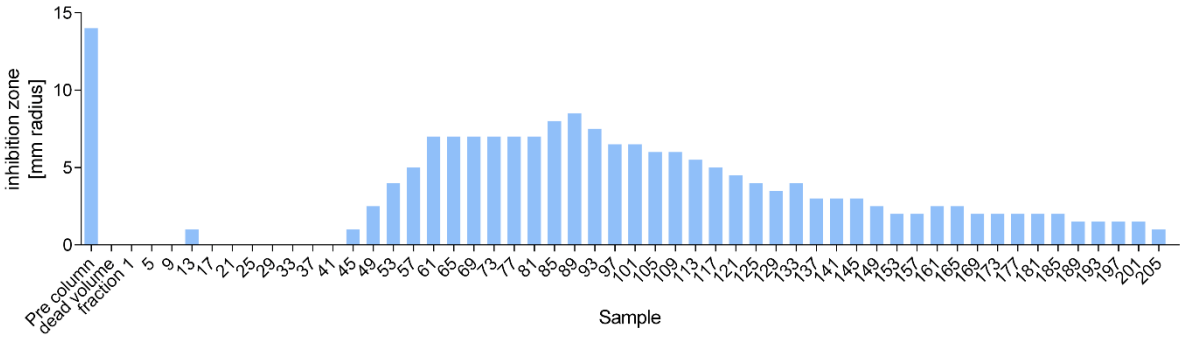

Figure 2. Fractions collected after the second cation exchange chromatography using Amberlite CG50. The "Pre column" sample originates from the first cation exchange chromatography using Amberlite IRC-50, which was concentrated before applying to this second chromatography step. Samples were applied to bioactivity determination by the agar diffusion assay as described in methods and the measured inhibition zone is displayed here.

For further characterization, fractions with bioactivity were pooled as shown in table 2. Subsequently, these sample pools were freeze-dried, resulting in 54.71, 12.98, 4.08 and 3.28 mg of substances in pools 1, 2, 3 and 4, respectively (Table 2). Samples from pool 1 to 3 showed characteristics similar to negamycin from total synthesis, as the freeze-dried samples were white powder. In contrast, the sample from pool 4 resembled brown grains. For the latter sample, bioactivity was lower compared to the total synthesis by a four-fold change when tested by MIC determination against *E. coli* BW25113 in M9 medium. Pool 1 and 3 had a MIC of 8 µg/ml, which is one dilution step worse than the MIC of the negamycin from total synthesis of 4 µg/ml. Pool 2 had the same MIC as the synthetic negamycin and was therefore used for investigation of its purity.

Table 2. Pooled fractions after cation exchange chromatography using Amberlite CG50 were further characterized after lyophilization. Fractions without bioactivity were not further investigated and are not shown here. MIC was compared to negamycin from total synthesis.

Sample	Fractions[a] (of 15 ml)	m [mg]	Characteristics	MIC[b] [µg/ml]
Pool 1	45-84	54.71	White powder, „fluffy“	8
Pool 2	85-123	12.98	White powder, „fluffy“	4
Pool 3	124-162	4.08	White powder, „fluffy“	8
Pool 4	162-205	3.28	Brown grains	16
Total synthesis			White powder, „fluffy“	4

[a]Fraction number corresponds to fractions shown in figure 2. [b]MIC against *E. coli* BW25113 in M9 medium.

Negamycin purity. The sample from pool 2 (Table 2) was applied to thin layer chromatography (TLC) and compared to the total synthetic negamycin (Figure 3A). Total synthetic negamycin showed three spots when detected with ninhydrin. Although purity of this total synthetic negamycin sample was reported to be at least 95%, the additional spots are intermediates from total synthesis with

protection groups, which could not be removed by purification. In contrast, the purified negamycin from the natural producer showed only one spot, which exhibited also the same retention factor (RF) as the strongest spot from the total synthesis. As ninhydrin detects amine groups, at least no other amine containing molecule could be found within the purified sample, indicating a high purity of this sample.

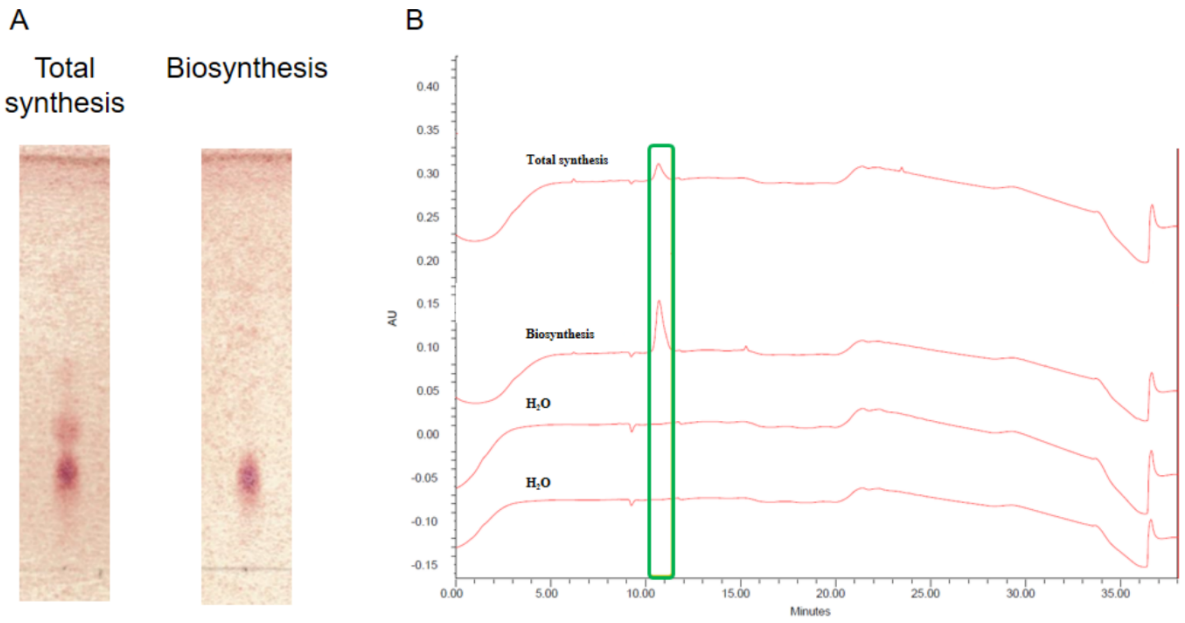

Figure 3. Control of purity of the purified sample from pool 2 by TLC and HPLC. (A) TLC comparing the negamycin standard from total synthetic (left) to the purified biosynthesized (right) negamycin sample (right). (B) The same samples were applied to HPLC analysis on a Luna Omega Polar column. The signal peak for negamycin is marked in a green box.

The sample was further applied to HPLC analysis using the Luna Omega Polar column (Figure 3B). At 11 min, the highest peak of the biosynthesis sample correlated with negamycin from total synthesis. An additional signal could be detected at 15 min, which was not seen in the standard sample from total synthesis, but the peak signal was much weaker than the negamycin signal. Lastly, the small signal at 23 min in the total synthesis sample was not seen in the purified material from biosynthesis. This signal could correlate to one of the other spots detected by TLC (Figure 3A).

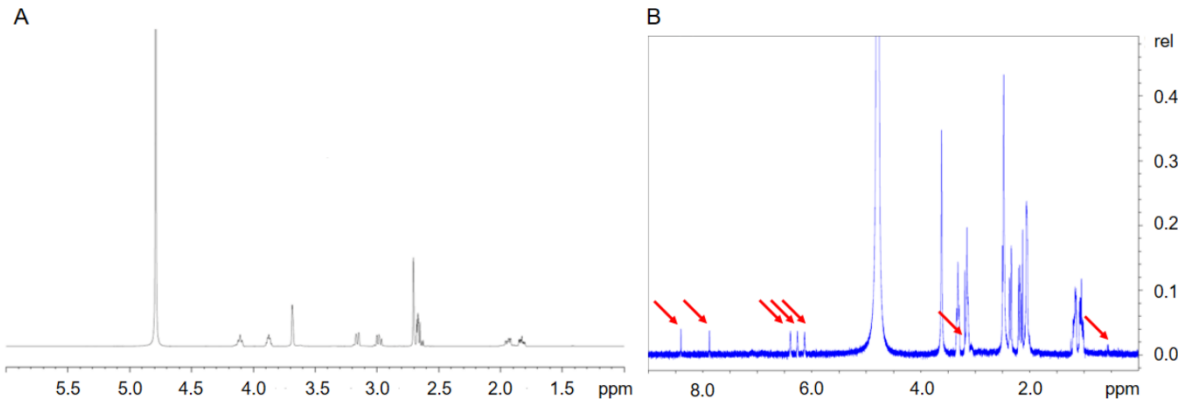

Figure 4. ^{1}H NMR spectra of negamycin from total synthesis (A) or purified from biosynthesis (B). Comparing the two spectra side by side, additional peaks in the biosynthetic negamycin, which could not be seen for negamycin from total synthesis, are highlighted by red arrows.

Finally, purity of the sample was determined by NMR as described in the methods. For comparison, an ^{1}H NMR spectrum of negamycin from total synthesis was kindly provided by Karl-Heinz Glüsenkamp (Squarix GmbH), which was not necessarily determined by a similar instrument. The total synthetic negamycin (Figure 4A) was compared to the purified negamycin (Figure 4B). Comparing the NMR spectra side by side, additional signals could be detected in the biosynthetic sample, indicated by red arrows. These signals on the left-hand side from the strongest signal could not be necessarily assigned to organic groups, which could mean, on a rather speculative note, that here some residual column material is contained within the sample. An additional signal could be seen at 3.25 ppm, indicating residual impurity of the sample. Calculating the integral of the signals of the biosynthetic sample, a purity of over 95% was determined by NMR analysis.

Discussion

The patent for negamycin described various methods for purification of the natural product from a *Streptomyces purpeofuscus* culture (Umezawa et al. 1972). The application to four ion exchange chromatography columns led to the best result. We adapted and improved this method by decreasing it to two cation exchange chromatography columns, leaving two anion exchange chromatography columns out (Figure 1). The purity could be confirmed by different methods, including NMR. Residual impurities could be detected, but were overall very low.

One exemplarily isolation process was shown in this study. Biosynthesis of negamycin varied from 60 to 150 µg/ml between fermentation runs. Yield of pure negamycin varied between 12 and 15.5 mg negamycin between different isolation procedures. From the 2.2 liter production culture with an estimated negamycin concentration of 125 µg/ml, we were able to purify about 13 mg of pure negamycin (>95% purity) and an additional 59 mg of semi-pure negamycin (Table 1 & Table 2).

Thereby we purified 72 mg (~26%) from the approx. 275 mg negamycin from the production medium, although it has to be mentioned that the exact negamycin concentration within the bacterial culture was only estimated. In comparison, Umezawa et al. (1972) achieved a concentration of 35 µg/ml in their 6 liter culture and purified 20 mg pure and 19 semi-pure (91% purity) negamycin after using four different ion exchange chromatography columns. This leads to 39 mg negamycin purified from a total of 210 mg contained within the bacterial production culture (~19%). Although their yield was a bit lower, it is within a similar range as our result. Further increase of negamycin amounts could be easily achieved by scaling up the fermentation and the batch purification, as bigger columns can be prepared.

An increase in yield and purity can probably be achieved by improving the purification steps, and not necessarily the fermentation. The production so far could not be improved, as previous adaptions to the negamycin production medium as well as alternative media did not increase negamycin concentration (Hörömpöli 2016). Other producer strains, e. g. *S. purpeofuscus* DSM 40283, were able to produce negamycin, but only in lower amounts compared to *S. purpeofuscus* ATCC 21477 (Hörömpöli 2016). As the biosynthetic gene cluster is not identified yet, further negamycin producing strains are not known and optimization of biosynthesis by heterologous expression or modification of regulation can be further improved, when the gene cluster has been found.

Purification could be optimized with modern column materials, although purification of very hydrophilic compounds remains tricky (Berlinck et al. 2019). Removal of large amounts of water is tedious and removal of salts and polar metabolites, like sugars and amino acids, is difficult. Hydrophilic interactions liquid chromatography (HILIC) columns have been proposed to be useful for isolation of hydrophilic natural products. HILIC was used for analysis before, but so far has not been reported for isolation of natural products (Berlinck et al. 2019). When used for negamycin analysis, a sharp peak with a good retention time could never be achieved (not shown). The column in this study used for analysis, Luna Omega Polar, might be of interest for semi-preparative HPLC. Such a purification step via HPLC could be performed in addition to the batch cation exchange chromatography, which might still be necessary, as a very rich medium has to be used for negamycin production.

Various total chemical synthesis methods for negamycin synthesis have been reported before (Shibahara et al. 1972; Streicher et al. 1978; Wang et al. 1982; Hayashi et al. 2008; Hayashi et al. 2009). Most methods are laborious, requiring 13 to 19 steps to achieve a yield of up to 26% (Wang et al. 1982; Hayashi et al. 2009). A more efficient method has been published as well, with only 8 steps leading to a yield of 42% (Hayashi et al. 2008), which would still need more working steps than the purification protocol described in this study. Residual impurities might also be difficult to remove, as we could observe when synthetic negamycin was analyzed (Figure 3A). Therefore, negamycin

biosynthesis followed by batch purification using cation exchange chromatography is a good alternative method to produce larger amounts of this natural antibiotic.

References

(CLSI), Clinical and Laboratory Standards Institute. 2006. 'Performance Standards for Antimicrobial Disk Susceptibility Tests; Approved Standard (M2-A9)', 9th Edition.

Berlinck, Roberto G. S., Afif F. Monteiro, Ariane F. Bertonha, Darlon I. Bernardi, Juliana R. Gubiani, Juliano Slivinski, Lamonielli F. Michaliski, Luciane A. C. Tonon, Victor A. Venancio, and Vitor F. Freire. 2019. 'Approaches for the isolation and identification of hydrophilic, light-sensitive, volatile and minor natural products', *Natural product reports*, 36: 981-1004.

Champness, Wendy. 1999. 'Actinomycete development, antibiotic production, and phylogeny: questions and challenges', *Prokaryotic Development*: 9-31.

Claessen, Dennis, Wouter De Jong, Lubbert Dijkhuizen, and Han AB Wösten. 2006. 'Regulation of Streptomyces development: reach for the sky!', *Trends in microbiology*, 14: 313-19.

Hamada, M., T. Takeuchi, S. Kondo, Y. Ikeda, and H. Naganawa. 1970. 'A new antibiotic, negamycin', *J Antibiot (Tokyo)*, 23: 170-1.

Hayashi, Yoshio, Shigenobu Nishiguchi, Magne O Sydnes, Thomas Regnier, Jun-ya Hasegawa, Takahiro Katoh, Tetsuya Kajimoto, Manabu Node, and Yoshiaki Kiso. 2009. 'A New Synthesis of (+)-Negamycin and Its Derivatives as a Potential Therapeutic Agent for Duchenne Muscular Dystrophy Treatment.' in, *Peptides for Youth* (Springer).

Hayashi, Yoshio, Thomas Regnier, Shigenobu Nishiguchi, Magne O Sydnes, Daisuke Hashimoto, Junya Hasegawa, Takahiro Katoh, Tetsuya Kajimoto, Masataka Shiozuka, and Ryoichi Matsuda. 2008. 'Efficient total synthesis of (+)-negamycin, a potential chemotherapeutic agent for genetic diseases', *Chemical communications*: 2379-81.

Hopwood, David A. 1999. 'Forty years of genetics with Streptomyces: from in vivo through in vitro to in silico', *Microbiology*, 145: 2183-202.

Hörömpöli, Daniel. 2016. 'Das Pseudopeptid-Antibiotikum Negamycin: Produktion in Streptomyces purpeofuscus und Rolle von Porinen bei der Aufnahme in *Escherichia coli* (Master thesis)', *Universität Tübingen*.

Hörömpöli, Daniel, Catherine Ciglia, Karl-Heinz Glüsenkamp, Lars Ole Haustedt, Hildegard Falkenstein-Paul, Gerd Bendas, Anne Berscheid, and Heike Brötz-Oesterhelt. 2021. 'The Antibiotic Negamycin Crosses the Bacterial Cytoplasmic Membrane by Multiple Routes', *Antimicrobial Agents and Chemotherapy*, 65: e00986-20.

Lewis, Kim. 2013. 'Platforms for antibiotic discovery', *Nature reviews Drug discovery*, 12: 371-87.

Olivier, N. B., R. B. Altman, J. Noeske, G. S. Basarab, E. Code, A. D. Ferguson, N. Gao, J. Huang, M. F. Juette, S. Livchak, M. D. Miller, D. B. Prince, J. H. Cate, E. T. Buurman, and S. C. Blanchard. 2014. 'Negamycin induces translational stalling and miscoding by binding to the small subunit head domain of the Escherichia coli ribosome', *Proc Natl Acad Sci U S A*, 111: 16274-9.

Polikanov, Y. S., T. Szal, F. Jiang, P. Gupta, R. Matsuda, M. Shiozuka, T. A. Steitz, N. Vazquez-Laslop, and A. S. Mankin. 2014. 'Negamycin interferes with decoding and translocation by simultaneous interaction with rRNA and tRNA', *Mol Cell*, 56: 541-50.

Raju, B., Kathleen Mortell, Sampathkumar Anandan, Hardwin O'Dowd, Hongwu Gao, Marcela Gomez, Corinne Hackbarth, Charlotte Wu, Wen Wang, Zhengyu Yuan, Richard White, Joaquim Trias, and Dinesh V. Patel. 2003. 'N- and C-terminal modifications of negamycin', *Bioorganic & Medicinal Chemistry Letters*, 13: 2413-18.

Shibahara, Seiji, Shinichi Kondo, Kenji Maeda, Hamao Umezawa, and Masaji Ohno. 1972. 'Total syntheses of negamycin and the antipode', *Journal of the American Chemical Society*, 94: 4353-54.

Streicher, Wolfgang, HELLMUTHR EINSHAGEN, and FRIEDERIKTEU RNOWSKY. 1978. 'Total synthesis of rac. negamycin and of negamycin analogs', *The Journal of antibiotics*, 31: 725-28.
Umezawa, Hamao, Shinichi Kondo, Kenji Takeuchi Maeda, and Masa Hamada. 1972. 'Negamycin (Patent US3679742 A)'.
Wang, Yi Fong, Toshio Izawa, Susumu Kobayashi, and Masaji Ohno. 1982. 'Stereocontrolled synthesis of (+)-negamycin from an acyclic homoallylamine by 1,3-asymmetric induction', *Journal of the American Chemical Society*, 104: 6465-66.
Watve, Milind G, Rashmi Tickoo, Maithili M Jog, and Bhalachandra D Bhole. 2001. 'How many antibiotics are produced by the genus Streptomyces?', *Archives of microbiology*, 176: 386-90.

Supplemental information

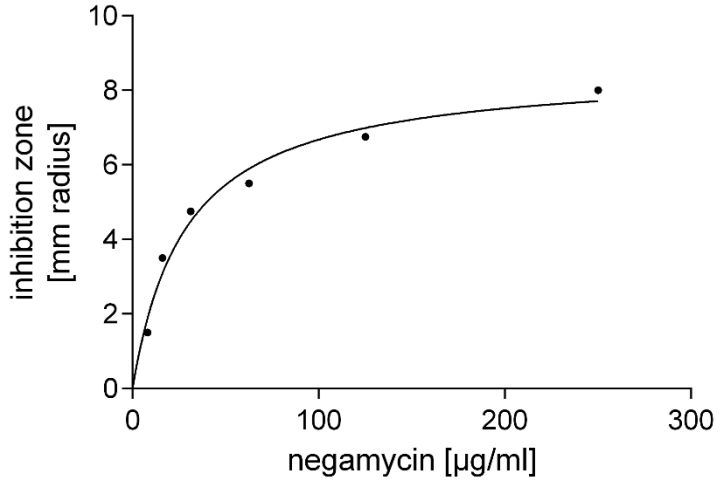

Figure S1. Negamycin bioactivity determined by the agar diffusion method. A concentration dilution series of the chemically synthesized negamycin was applied to the agar containing *E. coli* BW25113 under the conditions as described in methods.

4.5. Manuscript 3

Uptake of aminoglycosides through outer membrane porins in *Escherichia coli*

Eshita Paul[1], Ishan Ghai[1*], Daniel Hörömpöli[2], Heike Brötz-Oesterhelt[2,3], Mathias Winterhalter[1], Jayesh A Bafna[1],

[1] Department of Life Sciences and Chemistry, Jacobs University Bremen, Bremen, Germany.

[2] Department of Microbial Bioactive Compounds, Interfaculty Institute of Microbiology and Infection Medicine, University of Tu□bingen, Tu□bingen, Germany

[3]Cluster of Excellence Controlling Microbes to Fight Infection, Tübingen, Germany

*Correspondence: is.ghai@jacobs-university.de

Abstract

Aminoglycosides are important clinical antibiotics but their molecular uptake mechanism is still not completely understood. Here we quantify and compare the passive transport of three aminoglycosides (kanamycin, gentamicin, and amikacin) across general or sugar specific porins of *Escherichia coli* (OmpF, OmpC, LamB and ChiP). Our analysis revealed that permeation of aminoglycosides (Kanamycin/Gentamycin/Amikacin) is about the same through ChiP (≈5/3/2 molecules/s), OmpF (≈10/15/<1 molecules/s) and OmpC (≈11/8/<1 molecules/s). In contrast, LamB of smaller pore diameter has no significant permeation (≤1/1/1 molecules/s, all values recalculated for a gradient of 10 μM). Biological assays confirmed the relevance of these translocations for antibiotic potency.

Introduction

Gram-negative bacteria are enclosed by the complex multi-layered cell envelope containing the cytoplasmic membrane, the peptidoglycan layer and the outer membrane [1–3]. Among these chemically and structurally diverse layers, the outer membrane represents the first line of bacterial defense[4]. To overcome the outer membrane barrier, hydrophobic antibiotics take the slow lipid-mediated route, while the small hydrophilic ones – like β-lactams, tetracycline, chloramphenicol, and fluoroquinolones pass through general diffusion porins such as OmpF or OmpC[2]. Although most of these porins are constitutively expressed and present in open conformations allowing passive diffusion of small molecules with likely a defined exclusion limit (roughly <650 Da)[5], there are some porins which are solute-specific. Examples of such porins in *E. coli* include, but are not limited to, maltose and maltodextrin-specific LamB[6], sucrose specific SrcY[7], long chain fatty acid specific FadL[8], and nucleoside-specific Tsx[9], along with chitooligosaccharide-specific chitoporins[10].

Among the sugar-specific porins in *E. coli*, LamB has been extensively studied for maltosugar transport including maltodextrins as substrates. Another set of studies on sugar uptake has been performed on chitoporins (ChiP) that allow diffusion of chitooligosaccharides across the outer membrane of chitinolytic bacteria. First reported identifications of chitoporins came from marine species, including *Vibrio furnissii* (*Vf*ChiP)[10], which uses chitin as a natural source of energy via the N-acetylglucosamine pathway, followed by the chitoporin in *Vibrio cholerae* (*Vc*ChiP)[11]. Recently, Suginta and co-workers proved the physiological function of the outer membrane chitoporin from *Vibrio harveyi* (*Vh*ChiP)[12] by heterologous expression in *E. coli*, showing specifically a high translocation rate for chitohexose. The *chip* gene encoding chitoporin is conserved in non-chitinolytic bacterial species as well e.g. in *E. coli*[13]. Here the ChiP channel encoded by the *chiP* gene (formerly *ybfM*) has been shown to also facilitate the specific transport of chitin degradation products across the outer membrane[4]. Constitutive expression of *chiP* in *E. coli* is repressed by transcriptional and post-transcriptional control mechanisms by the ChiX sRNA[14]. In a *chiX* knock-out mutant, the presence of chitobiose/chitotriose induced the expression of *chip* resulting in increased cellular levels of both mRNA and protein [15]. ChiP of *E. coli* shows sequence homology to the OprD family of porins and a monomeric structure is predicted [4]. Surprisingly sequence comparison of ChiP from *E. coli* to ChiP from opportunistic pathogens like *Salmonella typhimurium*[15] (Q7CQY4) reveals 90% sequence identity, followed by 70% identity to *Serratia marcescens* ChiP[16] (L7ZIP1) and significantly lower identity (12-14%) to *Vibrio* ChiP sequences. At the same time ChiP of *E. coli* shows broad substrate specificity with a lower binding constant for chitooligosaccharides as compared to its *Vibrio* homologs. As per literature[4], ChiP functions in *E. coli* only under stress conditions unlike the constitutive activity of *Vibrio* ChiPs, e.g., during the utilization of chitin as a source of energy in glucose-scarce environment. This broad specificity for substrate might further make this a potential porin for allowing the transport of molecules with sugar-like structures.

Experimental investigations on bacterial antibiotic sensitivity revealed modifications in porin profiles, including reduction in the expression level or overexpression of functionally mutated porins, as an emerging mechanism in antibiotic resistant isolates[17]. This brings the study of the antibiotic influx process into the limelight. Here we focus on aminoglycosides, which are amino sugar containing aminocyclitols, binding to 16s/30s rRNA and in turn inhibiting protein synthesis by miscoding, inhibition of translocation or inhibiting recycling of ribosomal subunits and even disrupting biogenesis of the ribosome[18–21]. Uptake of clinically relevant aminoglycosides across the cytoplasmic membrane of Gram-negative bacteria is a

two-step energy dependent process and prior to that, additional transport across outer membrane has to be achieved[22–24]. These polycationic aminoglycosides have been shown to follow the species-specific self-promoted uptake mechanism[25]. The polycations displace divalent cations cross-bridging neighboring LPS molecules by competitive binding, which results in destabilization and permeabilization of the outer membrane[25]. Our recent study[26] demonstrated the contribution and relevance of the major outer membrane porins OmpF and OmpC in the molecular uptake of kanamycin, one of the most abundantly used aminoglycosides, into *E. coli*, showing a new diffusion route of these aminoglycosides through outer membrane porins.

With the sugar-like structure of the aminoglycosides in mind, we were interested whether these aminoglycosides are recognized as a substrate for translocation through the sugar specific minor porin ChiP of *E. coli*. So far only major porins have been studied in great details for their contribution to antibiotic transport[27]. To identify the contribution of this specific minor porin, we used single channel electrophysiology experiments. In the presence of low concentrations of antibiotics, we were unable to detect the translocation events due to their fast pace. We confirmed and compared the uptake of above molecules through ChiP and other porins using bi-ionic reversal potential measurements and supported the relevance using whole-cell studies with a defined set of *E. coli* porin mutants. Our interdisciplinary study showed a robust uptake pathway for aminoglycosides through ChiP of *E. coli* shedding light on their nonspecific transport through this minor porin. This study increased our understanding of the aminoglycoside translocation into Gram-negative bacteria, which might be useful for improving their uptake.

Materials and Methods

Bacterial strains and chemicals. For native porin overexpression, we used *E. coli* BL21 (DE3) Omp8[28] strain lacking the major porins of *E. coli* (OmpF, OmpC, OmpA and LamB). These cells were transformed with the respective plasmids and grown at 37°C, 200 rpm in Luria-Bertani (LB) medium (Roth, Germany) or LB agar plates supplemented with ampicillin at 100 µg/mL for plasmid maintenance. Gentamicin sulfate was obtained from Carl Roth, kanamycin sulfate, amikacin disulfate, potassium chloride salt from Sigma-Aldrich (Dorset, United Kingdom), 1,2-diphytanoyl-sn-glycero-3-phosphocholine (PC) from Avanti Polar Lipids (Alabaster, AL) and all other chemicals used were procured from AppliChem.

Gene knockout generation. For gene deletions in *E. coli*, the method by Datsenko and Wanner was used[29]. Briefly, primers with homologous sequences corresponding to the target gene were used to amplify a kanamycin resistance cassette from the pKD13 plasmid (**Table S1**). Electrocompetent *E. coli* cells containing the pKD46 plasmid were transformed with this PCR product and homologous recombination was initiated by λ Red recombinase from the pKD46 plasmid. Successful integration of the resistance cassette was checked by growth on LB with 50 µg/ml kanamycin. Gene deletion mutants were confirmed by PCR and followed by Sanger sequencing.

Susceptibility measurements. The minimal inhibitory concentration (MIC) was determined as described by the standardized method of CLSI[30]. Briefly, an antibiotic two-fold concentration series was prepared in microtiter plates in cation adjusted Mueller Hinton broth II (MHBII), and *E. coli* cells were added to a final inoculum of 5 x 10^5 CFU/ml. The plates were incubated at 37°C and after 18 h of incubation, the MIC was defined as the lowest concentration completely inhibiting bacterial growth. For agar plates with a linear antibiotic concentration gradient, MHBII was supplemented with 7.5 g/L agar-agar. A first layer was poured at an inclined position into square 12 x 12 cm petri dishes. After polymerization of the agar, the second layer, containing the indicated antibiotic concentration, was added at an even position. After polymerization of this second layer, agar plates were stored over night at 4°C. On the next day, *E. coli* cells were streaked on the agar concentration gradient plates from a cell suspension in 0.9% NaCl (w/v), which was prepared from *E. coli* colonies grown on MHBII agar plates and where the optical density at 600 nm (OD_{600nm}) was adjusted to 0.1. Growth was measured after 18 h of incubation at 37°C.

Expression and purification of proteins. For the overexpression of ChiP, the gene *chiP* was cloned from genomic DNA of *E. coli* BW25113. Using the primer pair chiP-pASK5 (**Table S2**), the porin gene sequence was integrated via Gibson cloning[31] into the plasmid pASK-IBA5 (IBA GmbH), which was beforehand digested with XbaI and XhoI. This resulted in the plasmid pASK-IBA5-chiP which was further used as the template for cloning the *chiP* gene into pET19b plasmid (Addgene). This was done using the primer pairs pET19b-chiP and chiP-pET19b with the Gibson cloning method (**Table S2**). Correct insertion was confirmed by XbaI/XhoI digestion and Sanger sequencing. *E. coli* BL21 (DE3) Omp8 was transformed with pET19b-*chiP*.

For protein expression, an overnight preculture of *E. coli* BL21 (DE3) Omp8 containing pET19b-*Ec*ChiP was inoculated into Luria-Bertani medium containing 100 µg/mL ampicillin at OD_{600}=0.1 and grown at 37°C and 200 rpm in Erlenmeyer flasks till optical density of the culture reached 0.6. At this point, the expression of the protein was induced with 0.5 mM isopropyl β-D-1-thiogalactopyranoside (IPTG –

Sigma) and the flask was placed at 37°C, 200 rpm. After 6 hours, cells were centrifuged at 3220xg (Eppendorf centrifuge 5810 R, A-4-62 rotor) for 30min at 4°C. The pellet was stored at -20°C for the extraction steps. For extraction, a pellet from 500 ml of culture was resuspended in 10 ml lysis buffer (20 mM Tris pH 8, 2.5 mM $MgCl_2$, 0.1mM $CaCl_2$, 1 mM PMSF, 10 µg/ml RNase A and 10 µg/ml DNase I) and disrupted by five passages at 15000 psi in a French Press on ice. After removing the cell debris by 30min of centrifugation at 3220xg, 4°C, the membrane was pelleted by ultracentrifugation (1 hour, 100000xg at 4°C). The pellet was solubilized in 20 mM Tris/HCl pH 8, 0.15 % Octyl POE (N-octylpolyoxyethylene from Bachem) using a Potter homogenizer and incubated for 1 hour at 4°C on the wheel. The remaining insoluble material was separated by a second ultracentrifugation (100000xg, 4°C, 1 hour). ChiP was extracted by solubilization of this pellet with 20 mM Tris HCl pH 8, 3% Octyl POE and elimination of insoluble material by ultracentrifugation. This step was performed two times. The last supernatants containing the expected protein were pooled and concentrated with an Amicon concentration unit (cut off 30 kDa). The samples were supplemented with Laemmli sample buffer and heated at 95°C for 10 min (denaturing condition) or supplemented with Laemmli sample buffer lacking beta mercapto-ethanol (non-denaturing condition) and loaded on 12% SDS PAGE gel. The gels were stained with Coomassie Brilliant Blue G250. To obtain pure protein from the last supernatant, the concentrated sample was subjected to anion-exchange chromatography using a Mono Q® 5/50 GL prepacked column (5.7x1ml) connected to BioLogic DuoFlow chromatography system (Bio Rad). Proteins were eluted with a linear gradient of 0-1 M KCl in 20mM phosphate buffer, pH 7.4 containing 0.2% (v/v) lauryldimethylamine N-oxide (LDAO) as previously reported[4]. The purity of the ChiP was confirmed by SDS-PAGE analysis and on our gels the native protein showed a slightly higher molecular mass than in the former study[4]. The presence of the protein was confirmed by mass spectrometric analysis and Western blot analysis using an anti-ChiP antibody. OmpF and OmpC were expressed and purified according to the previously published protocol[32,33].

Planar lipid bilayer and electrical recording: Single and multichannel measurements. Planar lipid bilayers conferring to Montal and Mueller were formed as published[26,34]. Briefly, an aperture in a Teflon septum with a diameter of 100-120 µm was pre-painted with hexadecane dissolved in n-hexane at 1-5% (v/v) and the cuvette compartments were dried for 10-15 min, in-order to eliminate the solvent. Bilayers were made with 1,2- diphytanoyl-sn-glycero-phosphatidyl-choline at a concentration of 4-5 mg/ml in n-pentane. Stock solutions (0.5 mg/mL) of the outer membrane porins were diluted 10^3 to 10^4-fold using Genapol X-080 (1% v/v). A small volume from the dilution was added to the *cis* side of the chamber containing 2.5 ml of 1M KCl for single channel measurements. For reversal potential measurements the gradient was created with the pure antibiotic solution[26,36]. Throughout the experiments the pH was maintained at 7.0 ± 0.5. The *cis* side of the chamber was the virtual ground and the *trans* side was linked with a CV- 203BU Headstage of the Axopatch 200B (Molecular Devices, LLC) patch-clamp amplifier in V-clamp mode (whole cell $\beta = 1$). The output signal was filtered by a lowpass Bessel filter at 10 kHz and saved at a sampling frequency of 50 kHz using an Axon Digidata 1440A digitizer (Molecular Devices, LLC). Data analysis was performed with an in-house analysis suite created with the LabVIEW software suite (National Instruments) or using Clampfit (Axon Instruments). Standard Ag/AgCl electrodes were used to detect the ionic current in single channel experiments. For measuring Bi-ionic and tri-ionic reversal potentials (multichannel) to allow for asymmetric condition, we used commercial calomel electrodes (Metrohm) containing a salt bridge. The current voltage relation of the individual experiments was calculated from single averaged currents at the given voltage. The relative permeability of cations *vs*

solute anions in the bi-ionic case ($P_{antibiotic}^{+}/P_{sulfate}^{-}$) and in tri-ionic case ($P_{K}^{+}/P_{sulfate}^{-}$/ $P_{antibiotic}^{+}$) were obtained by fitting of the experimental I–V curves with the Goldman–Hodgkin–Katz[35] current equation[36].

$$I_x = P_x z_x^2 \frac{V_m F^2}{RT} \frac{[c_x]_{Cis} - [c_x]_{Trans} \exp\left(\frac{-z_x V_m F}{RT}\right)}{1 - \exp\left(\frac{-z_x V_m F}{RT}\right)} \text{----------(1)}$$

Results

Single channel and bi-ionic reversal potential measurement. In a series of measurements, we took the single channel conductance of OmpF, OmpC, ChiP and LamB in Kanamycin 20mM, Gentamicin 20mM and Amikacin 5mM respectively. Moreover, antibiotic ions have much lower conductances and thus the single channel conductance values for LamB are only estimates (**Table 1**). Further the single channel conductance of OmpF, OmpC, ChiP, LamB were also measured for 1M KCl (**Table S3**) which are in agreement with previous measurements[6,26,32,33]. For this we prepared lipid membranes in the respective electrolyte solution and added the respective protein on one side, usually the ground connected side. The subsequent increase in conductance steps were statistically analyzed and the smallest conductance peak was identified as single channel conductance.

In a second series of measurements, we made the lipid membrane in 1M KCl and inserted the respective single channel. Addition of small amounts of antibiotics resulted in channel blockages. A statistical analysis of the blockage lengths or dwell times as a function of external voltage is used to reveal an estimate for possible translocations through the channel. To begin with, the three porins of interest from the *E. coli* outer membrane (OmpF, OmpC, and ChiP) were reconstituted into a planar DPhPC bilayer (in individual experiments) from the electrically grounded or the *cis* side, and the single channel currents in the presence of 1M KCl at pH 7 were recorded. Single channel blockages were observed at a concentration of 100 μM gentamicin for ChiP when added to the *cis* side of the chamber, and a transmembrane potential of -100mV was applied on the *trans* side. (**Figure 1**). Such behavior is due to the cationic nature of gentamicin and with the application of negative potential, the molecules are pulled through the pore due to the electrophoretic force. Decreasing the magnitude of ΔV further decreased the number of blockages, as the gentamicin molecules were pulled at a slower rate across the channel by virtue of a weaker electrophoretic force. To quantify the findings, the event rate f_e was analyzed, which is the number of events per second, and the dwell (or residence) time of gentamicin molecules in the channel was analyzed as obtained from an exponential fit of the dwell time distribution (**Figure 2**). For both quantities, multiple events were analyzed for each transmembrane voltage applied in the range from -20 to -100 mV. In a similar manner, measurements were also performed for OmpF and OmpC, where adding 10 μM of gentamicin was enough to observe a significant number of blockages (**Figure 1**). Again, the event rates and dwell times were analyzed for these two porins, but we did not observe any trend in dwell time change, although raising the negative voltage increased the overall number of events. As mentioned in our previous paper, an event rate itself is not sufficient to conclude translocation and a decrease of the dwell time with higher voltage is a hallmark of translocation[26]. The independent behavior of dwell time in the given range of transmembrane voltage indicated for OmpF and OmpC, that most events are rather simple blockages and not actual translocations.

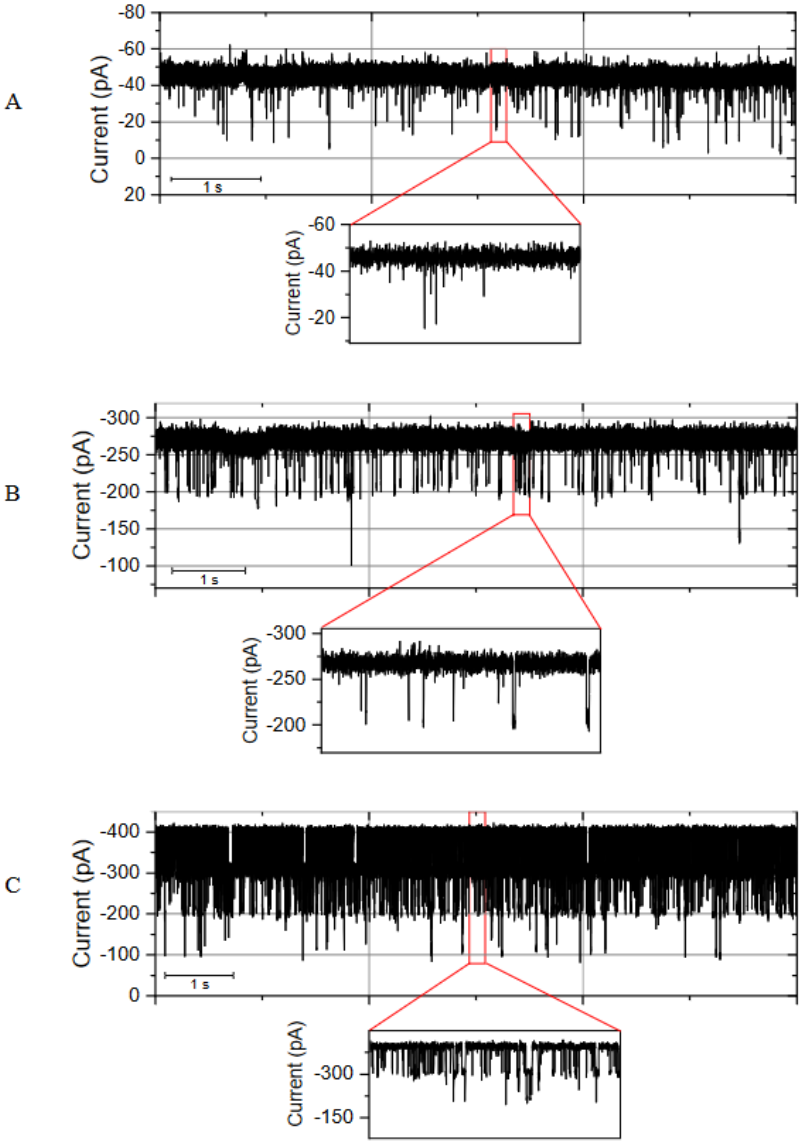

Figure 1. Examples of ion current traces through a single porin channel in the presence of gentamicin at -100 mV applied transmembrane volatge. **A:** ChiP in presence of 100 μM, **B:** OmpC in presence of 10 μM, and **C:** OmpF in the presence of 10 μM gentamicin sulfate in 1 M KCl, 10 mM HEPES at pH 7. The insets show zoomed events. All experiments were performed at 25°C while the data were filtered at 1 KHz.

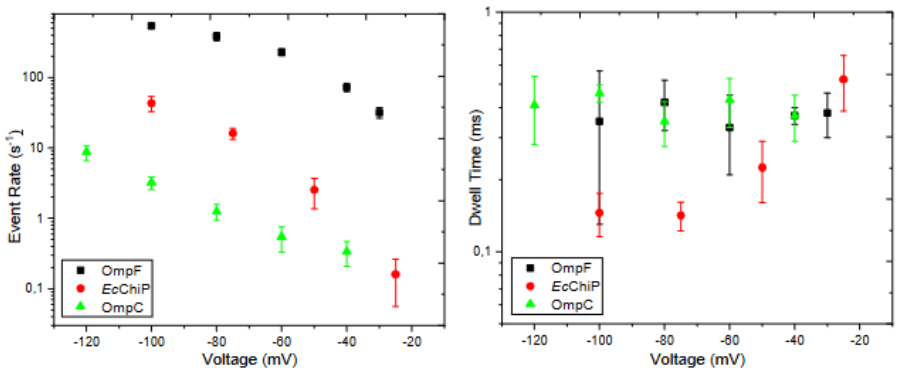

A B

Figure 2. Event rates and dwell times for gentamicin. Statistical analysis of the traces measured at different applied voltages for OmpF, OmpC, and ChiP. **A:** Event rate f_e *vs* applied negative voltages. Increasing the negative voltage pulls more cationic molecules into the channel. **B:** Dwell time analysis. In the case of ChiP, higher negative voltage drives gentamicin faster through the channel. In contrast, for OmpF and OmpC, increasing the voltage in the range of -20 to -100 mV does not affect the residence time significantly and the dwell time is independent of the voltage, indicating mainly non-translocating events or an overestimation of possible translocation.

In a third series of measurements, we followed a different approach previously used to reveal translocation for charged compounds as the current fluctuation analysis does not always identify successful transport by distinguishing translocation from binding or reflected events. To directly characterize quantitative transport of such charged molecules, the zero current assay or bi-ionic reversal potential assay is used. To distinguish permeability from short-lived bounce back events, we performed a concentration-driven relative permeation assay using bi-ionic reversal potentials for all the three antibiotics for each of the porins (**Table 1, Figure S2**). We produced a symmetrical bi-ionic antibiotic-sulfate condition on both sides of the porin reconstituted bilayer. A concentration gradient was then established by increasing the solute concentration on the *cis* (ground) side of the bilayer, and the induced zero-current membrane potential was observed. The permeability ratio of the antibiotic: sulfate through the OmpF, OmpC and ChiP were determined using the simplified GHK equation considering the effective charge of an antibiotic molecule as +4 for this bi-ionic situation. In this case, the reversal potentials for all the antibiotics are negative for the same ionic concentrations cis/trans for all the three porins, implying that anions permeate faster compared to cations through the three porin channels OmpF, OmpC and ChiP (**Table S5**).

Concentration gradient of Kanamycin Δ = 20 mM			
& V_{rev}	Conductance estimated	$P = P_{cation}^{4+} / P_{sulfate}^{2-}$	(molecules/sec/monomer) (Extrapolated to 10 µM gradient)
OmpF	16 ± 5 pS 9.6 mV	1:14	10
OmpC	13 ± 3 pS 5.1 mv	1:4.2	11
Chip	7± 3 pS 6.5 mV	1:6	5
LamB	3± 2 pS not measured	$\ll 10^7$	≤1
Gentamycin Δ = 20mM			
	Conductance estimated	$P = P_{cation}^{4+} / P_{sulfate}^{2-}$	
OmpF	24 ± 8 pS 15 mV	1:25	15
OmpC	15± 5 pS 16.5 mV	1:30	8
Chip	10± 4 pS 2 mV	1:3	3
LamB	4± 1 pS not measured	$\ll 10^7$	≤1
Amikacin Δ = 5 mM			
	Conductance estimated	$P = P_{cation}^{4+} / P_{sulfate}^{2-}$	
OmpF	14 ± 9 pS	$1:10^6$	≤1
OmpC	9 ± 5 pS	$1:10^6$	≤1
Chip	5± 4 pS 10 mV	1:10	20
LamB	2± 1 pS not measured	$\ll 10^7$	≤1

Table 1. Measured single channel conductance in presence of antibiotic salt under symmetric condition and reversal potential measurements for the indicated concentration gradient (5 and 20 mM). From these values we extrapolated the permeability ratio and the flux. Details of the flux calculations are outlined in the supplement.

For gentamicin the permeability ratios obtained were 1:25, 1:30 and 1:3 for OmpF, OmpC and ChiP. These ratios imply that while both sulfate and gentamicin molecules can permeate through these channels, for each gentamicin cation, the sulfates anions are permeating roughly 25, 30 and 3 times faster, respectively, until this flux is balanced by the reversal potential. This reversal potential approach is relatively simple to measure and provides a handle to qualitatively compare the translocation rate of a specific analyte across different porins. Further calculations from these measurements indicate that flux for gentamycin molecules is in a same range for ChiP as compared to OmpF and OmpC. While for

kanamycin the flux rates are higher for ChiP as compared to OmpF and OmpC, whereas for amikacin, the rate of translocation is significantly higher through ChiP than through the other porins. In this context, as a negative control we also checked for the permeation of these aminoglycosides through the major sugar specific porin of *E. coli* – LamB. The reversal potential value of V_{rev} within experimental error, measured in a tri-ionic conditions clearly shows that these large molecules cannot permeate through LamB. In **Table S4** supplementary file, calculated permeability ratios obtained under tri-ionic conditions are listed for kanamycin sulfate, gentamicin sulfate and amikacin sulfate respectively.

Whole cell assay. To validate the biological relevance of our *in vitro* experiments, we tested the antibiotic susceptibility of different *E. coli* porin mutants that had been constructed in the background of *E. coli* BW25113, a K-12 derived, broadly-used laboratory model strain. To quantify the antibacterial activity of the aminoglycosides, we measured the minimal inhibitory concentration (MIC) by a guideline-conform standardized method in liquid culture in microtiter plates (**Figure 3 A, B**, and **C**). The MIC results were

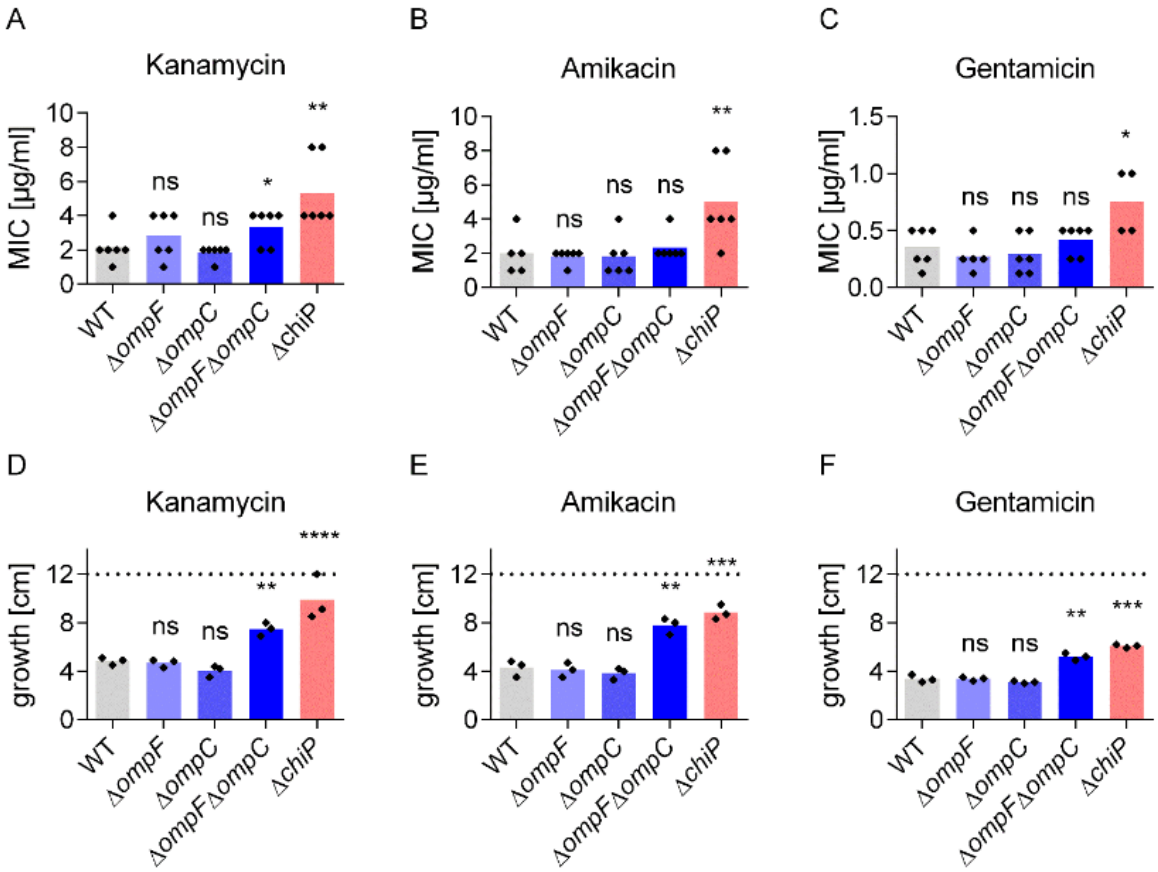

Figure 3. Susceptibility of *E. coli* BW25113 against the aminoglycosides kanamycin, amikacin or gentamicin. Aminoglycoside activity was measured by MIC determination (**A, B** & **C**) or growth on agar plates with a linear concentration gradient from 0 µg/ml to 3 µg/ml kanamycin (**D**), 0 to 2 µg/ml amikacin (**E**) or 0 to 0.75 µg/ml gentamicin (**F**). The limit of detection (i.e., the maximal stretch that a strain could grow given bei the breadth of the agar plate) is marked with a dotted line. Each diamond represents an

independent experiment and the mean average is shown as a colored bar. Statistical analysis was done using unpaired Student's t-test with Holm−Bonferroni correction, comparing the mutants to the wildtype (WT) strain. Not significant (ns), $P > 0.05$; **, $P \leq 0.01$; ***, $P \leq 0.001$.

complemented by streaking the *E. coli* strains on an agar plate containing a linear antibiotic gradient and measuring their distance of growth (**Figure 3D, E, F**). The deletion of only one of the major porin genes, i.e., either *ompF* or *ompC*, did not increase resistance of *E. coli* BW25113 against kanamycin, amikacin or gentamicin in the gradient agar assay, and the differences in the MIC assay were also weak. However, the combined deletion of both *ompF* and *ompC* led to a significant reduction of susceptibility in the gradient agar assay. In the case of *chiP*, already the single gene deletion increased resistance against all three aminoglycosides tested, and the effects were clearly visible on agar concentration gradient plates as well as in the MIC assay, which supports the involvement of the ChiP channel in translocation of this compound class. Notably, the overall impact of the *chiP* single gene deletion was even stronger than that of the combined Δ*ompF*Δ*ompC* double gene deletion, suggesting that ChiP plays a physiological role in the passage of all three aminoglycosides into *E. coli* BW25113. The *chiP* gene deletion was also tested within the *E. coli* ATCC 25922 strain background, which is a clinical isolate but, interestingly, in this strain the gene deletion had no effect on the resistance against kanamycin, amikacin or gentamicin when compared to its isogenic wild type strain (**Figure S3**). Differences in general outer membrane composition, the particular lipopolysaccharide structure, which differs between K12 strains and clinical isolates, or *chiP* expression might explain why different *E. coli* strain backgrounds are affected differently by the *chiP* gene deletion[42].

Discussion

The aim of this study was to quantify the possible flux of aminoglycosides through a few main *E. coli* porins. The electrophysiology technique provided quantitative information on the rate of transport and the nature of interaction at a single channel level. Furthermore, we combined *in vitro* techniques with bacterial growth inhibition assays to compare the permeation of three selected aminoglycosides side-by-side across several membrane channels located in the outer cell membrane of *E. coli*. Our data indicates that kanamycin, amikacin and gentamicin can all translocate through ChiP of *E. coli*. The permeation of kanamycin through OmpF and OmpC was already previously characterized[26] and revisited here. According to the reversal potential data presented here, OmpF and OmpC are more restrictive to gentamicin compared to ChiP and amikacin is even more strongly preferred by ChiP in relation to the other two porins. This special capacity of ChiP to allow the passage of aminoglycosides was also reflected in our cell-based assays. Among the three porins investigated in this study, only ChiP caused a consistent and clearly significant resistance phenotype upon single gene deletion in all of our assays. In the absence of the structural data, we can conclude that due to the sugar-like structure of these aminoglycosides, they are selected as a nonspecific substrate for the Chitoporin, which has not been shown to permeate any antibiotic previously. Although LamB represents the major sugar-specific porin in *E. coli*, it is poorly permeable to aminoglycosides. Thus, it is interesting that the permeation of these antibiotics is prominent through the minor porin ChiP as compared to the major ones, and even more so as antibiotic susceptibility loss was reproducibly associated with *chiP* single gene deletion in *E. coli* BW 25113. The reason, why this physiological phenotype only emerged in the K12 derivative *E. coli* BW 25113 is currently elusive and requires further extensive study. If the substantially shorter O-specific side chains inherent to the laboratory K12 linage plays a role is currently not known [42].

In this context it is also important to note that aminoglycosides have also porin-independent means of entering *E. coli*. A commonly assumed way for aminoglycoside penetration is their lipid mediated self-promoted uptake by destabilizing the outer membrane. Multiple options for cell entry may also explain, why aminoglycoside resistance is commonly associated with aminoglycoside modifying enzymes or 16S rRNA methyltransferases but not uptake mutations[37].

Nevertheless, inspection of the literature shows that the aminoglycoside class of antibiotics can also be affected by the porin mediated resistance[37]. For other antibiotic classed (carbapenems, cephalosporins multiple porins including OmpF, OmpC have been shown to play a role in developing resistance although they seem functionally redundant.[38–40] Most of the available studies are about the major porins OmpF or OmpC and only few reports on minor porins (e.g. NmpC) or specific porins (LamB) are available[41]. Our report on ChiP emphasizes that role of specific and minor porins concerning resistance development.

Here, we were able to demonstrate that at least three different aminoglycosides utilize the *E. coli* porin ChiP, which has not previously been linked to outer membrane antibiotic translocation. So far, the only known physiological role of ChiP in *E. coli* is chitooligosaccharide uptake under glucose-deficient conditions and ChiP was reported to be expressed at a low level in the absence of any inducer[4]. Although it is not as abundant as OmpF or OmpC, ChiP seems to contribute to aminoglycoside uptake, potentially due to its fast nonspecific permeation of the aminoglycosides investigated here. Especially considering the miscoding activity of the aminoglycosides and the common model of their entry in two phases[24], a minor porin with high permeation capacity could make a significant contribution. That means, a comparably small number of molecules entering first may be sufficient to trigger the production of non-functional membrane proteins by miscoding, thereby destabilizing the cell envelope to compound entry in a more general way. Present whole cell data also showed a difference in the effect of porin deletions between a nonpathogenic model strain and a clinical strain of *E. coli*, which emphasizes the need for follow-up studies on aminoglycoside uptake pathways in pathogenic isolates.

Acknowledgements

The Authors would like to acknowledge Dr. Claudio Piselli for experimental help with pET19b-*Ec*Chip expression plasmid generation. We received support from the JPIAMR network RESET-ME (BMBF-ERANET JPIAMR - 01KI1827B) and the JPIAMR Virtual Institute Translocation-Transfer 01KI1828. Moreover, financial support by the German Federal Ministry of Education and Reseach, though project Gram-Neg- Design, and by the German Center for Infection Research is gratefully acknowledged.

Author Contributions

E.P. and M.W., D.H. and H. B.-O. conceptualised and designed experiments. E.P prepared the proteins and performed single channel experiments. J.A.B performed and analysed bi-ionic reversal potentials and conductance. I.G. performed and analysed tri-ionic reversal potentials. D.H. performed and analysed whole cell assays. E.P. and M.W. wrote the article and I.G. J.A.B. D.H. and H.B.-O. edited the manuscript.

Bibliography

1. Rojas, E. R. *et al.* The outer membrane is an essential load-bearing element in Gram-negative bacteria. *Nature* **559**, 617–621 (2018).
2. Nikaido, H. Molecular Basis of Bacterial Outer Membrane Permeability Revisited. *Microbiol. Mol. Biol. Rev.* **67**, 593–656 (2003).
3. Nikaido, H. & Vaara, M. Molecular basis of bacterial outer membrane permeability. *Microbiol. Rev.* **49**, 1–32 (1985).
4. Soysa, H. S. M. & Suginta, W. Identification and Functional Characterization of a Novel OprD-like Chitin Uptake Channel in Non-chitinolytic Bacteria. *J. Biol. Chem.* **291**, 13622–13633 (2016).
5. Wang, J., Terrasse, R., Bafna, J. A., Benier, L. & Winterhalter, M. Electrophysiological Characterization of Transport Across Outer-Membrane Channels from Gram-Negative Bacteria in Presence of Lipopolysaccharides. *Angew. Chem. Int. Ed.* (2020) doi:10.1002/anie.201913618.
6. Benz, R., Schmid, A. & Vos-Scheperkeuter, G. H. Mechanism of sugar transport through the sugar-specific LamB channel ofEscherichia coli outer membrane. *J. Membr. Biol.* **100**, 21–29 (1987).
7. Schülein, K., Schmid, K. & Benz, R. The sugar-specific outer membrane channel ScrY contains functional characteristics of general diffusion pores and substrate-specific porins. *Mol. Microbiol.* **5**, 2233–2241 (1991).
8. Hearn, E. M., Patel, D. R., Lepore, B. W., Indic, M. & van den Berg, B. Transmembrane passage of hydrophobic compounds through a protein channel wall. *Nature* **458**, 367–370 (2009).
9. Bremer, E., Middendorf, A., Martinussen, J. & Valentin-Hansen, P. Analysis of the tsx gene, which encodes a nucleoside-specific channel-forming protein (Tsx) in the outer membrane of Escherichia coli. *Gene* **96**, 59–65 (1990).
10. Keyhani, N. O., Li, X.-B. & Roseman, S. Chitin Catabolism in the Marine Bacterium *Vibrio furnissii*: Identification and molecular cloning of a chitoporin. *J. Biol. Chem.* **275**, 33068–33076 (2000).
11. Meibom, K. L. *et al.* The Vibrio cholerae chitin utilization program. *Proc. Natl. Acad. Sci.* **101**, 2524–2529 (2004).
12. Suginta, W., Chumjan, W., Mahendran, K. R., Schulte, A. & Winterhalter, M. Chitoporin from Vibrio harveyi, a Channel with Exceptional Sugar Specificity. *J. Biol. Chem.* **288**, 11038–11046 (2013).
13. Rasmussen, A. A. *et al.* A conserved small RNA promotes silencing of the outer membrane protein YbfM. *Mol. Microbiol.* **72**, 566–577 (2009).
14. Plumbridge, J., Bossi, L., Oberto, J., Wade, J. T. & Figueroa-Bossi, N. Interplay of transcriptional and small RNA-dependent control mechanisms regulates chitosugar uptake in *E scherichia coli* and *S almonella*: Coregulation of a sugar porin and PTS transporter. *Mol. Microbiol.* **92**, 648–658 (2014).
15. Figueroa-Bossi, N., Valentini, M., Malleret, L. & Bossi, L. Caught at its own game: regulatory small RNA inactivated by an inducible transcript mimicking its target. *Genes Dev.* **23**, 2004–2015 (2009).
16. Takanao, S. *et al.* Construction and basic characterization of deletion mutants of the genes involved in chitin utilization by *Serratia marcescens* 2170. *Biosci. Biotechnol. Biochem.* **78**, 524–532 (2014).

17. Pagès, J.-M., James, C. E. & Winterhalter, M. The porin and the permeating antibiotic: a selective diffusion barrier in Gram-negative bacteria. *Nat. Rev. Microbiol.* **6**, 893–903 (2008).

18. Sabeti Azad, M. *et al.* Fluorescent Aminoglycoside Antibiotics and Methods for Accurately Monitoring Uptake by Bacteria. *ACS Infect. Dis.* **6**, 1008–1017 (2020).

19. Foster, C. & Champney, W. S. Characterization of a 30S ribosomal subunit assembly intermediate found in Escherichia coli cells growing with neomycin or paromomycin. *Arch. Microbiol.* **189**, 441–449 (2008).

20. Carter, A. P. *et al.* Functional insights from the structure of the 30S ribosomal subunit and its interactions with antibiotics. *Nature* **407**, 340–348 (2000).

21. Drew, R. H. Chapter 137 - Aminoglycosides. in *Infectious Diseases (Third Edition)* (eds. Cohen, J., Opal, S. M. & Powderly, W. G.) 1373–1381 (Mosby, 2010). doi:10.1016/B978-0-323-04579-7.00137-4.

22. Taber, H. W., Mueller, J. P., Miller, P. F. & Arrow, A. S. Bacterial uptake of aminoglycoside antibiotics. *Microbiol. Rev.* **51**, 439–457 (1987).

23. Ramirez, M. S. & Tolmasky, M. E. Aminoglycoside modifying enzymes. *Drug Resist. Updat. Rev. Comment. Antimicrob. Anticancer Chemother.* **13**, 151–171 (2010).

24. Krause, K. M., Serio, A. W., Kane, T. R. & Connolly, L. E. Aminoglycosides: An Overview. *Cold Spring Harb. Perspect. Med.* **6**, a027029 (2016).

25. Hancock, R. E., Farmer, S. W., Li, Z. S. & Poole, K. Interaction of aminoglycosides with the outer membranes and purified lipopolysaccharide and OmpF porin of Escherichia coli. *Antimicrob. Agents Chemother.* **35**, 1309–1314 (1991).

26. Bafna, J. A. *et al.* Kanamycin Uptake into *Escherichia coli* Is Facilitated by OmpF and OmpC Porin Channels Located in the Outer Membrane. *ACS Infect. Dis.* **6**, 1855–1865 (2020).

27. Hörömpöli, D. *et al.* The Antibiotic Negamycin Crosses the Bacterial Cytoplasmic Membrane by Multiple Routes. *Antimicrob. Agents Chemother.* **65**, (2021).

28. Prilipov, A., Phale, P. S., Gelder, P., Rosenbusch, J. P. & Koebnik, R. Coupling site-directed mutagenesis with high-level expression: large scale production of mutant porins from *E. coli*. *FEMS Microbiol. Lett.* **163**, 65–72 (1998).

29. Datsenko, K. A. & Wanner, B. L. One-step inactivation of chromosomal genes in Escherichia coli K-12 using PCR products. *Proc. Natl. Acad. Sci.* **97**, 6640–6645 (2000).

30. *Methods for dilution antimicrobial susceptibility tests for bacteria that grow aerobically: M07-A10□; approved standard*. (Committee for Clinical Laboratory Standards, 2015).

31. Gibson, D. G. Synthesis of DNA fragments in yeast by one-step assembly of overlapping oligonucleotides. *Nucleic Acids Res.* **37**, 6984–6990 (2009).

32. Lamichhane, U. *et al.* Peptide translocation through the mesoscopic channel: binding kinetics at the single molecule level. *Eur. Biophys. J.* **42**, 363–369 (2013).

33. Biró, I., Pezeshki, S., Weingart, H., Winterhalter, M. & Kleinekathöfer, U. Comparing the Temperature-Dependent Conductance of the Two Structurally Similar E. coli Porins OmpC and OmpF. *Biophys. J.* **98**, 1830–1839 (2010).

34. Montal, M. & Mueller, P. Formation of Bimolecular Membranes from Lipid Monolayers and a Study of Their Electrical Properties. *Proc. Natl. Acad. Sci.* **69**, 3561–3566 (1972).

35. Sullivan, H. Ionic Channels of Excitable Membranes, 2nd Ed. *Neurology* **42**, 1439 (1992).

36. Ghai, I. *et al.* General Method to Determine the Flux of Charged Molecules through Nanopores Applied to β-Lactamase Inhibitors and OmpF. *J. Phys. Chem. Lett.* **8**, 1295–1301 (2017).

37. Garneau-Tsodikova, S. & Labby, K. J. Mechanisms of resistance to aminoglycoside antibiotics: overview and perspectives. *MedChemComm* **7**, 11–27 (2016).

38. Prajapati, J. D., Kleinekathöfer, U. & Winterhalter, M. How to Enter a Bacterium: Bacterial Porins and the Permeation of Antibiotics. *Chem. Rev.* **121**, 5158–5192 (2021).

39. Fernández, L. & Hancock, R. E. W. Adaptive and Mutational Resistance: Role of Porins and Efflux Pumps in Drug Resistance. *Clin. Microbiol. Rev.* **25**, 661–681 (2012).

40. Delcour, A. H. Outer membrane permeability and antibiotic resistance. *Biochim. Biophys. Acta BBA - Proteins Proteomics* **1794**, 808–816 (2009).

41. Foudraine, D. E. *et al.* Exploring antimicrobial resistance to beta-lactams, aminoglycosides and fluoroquinolones in E. coli and K. pneumoniae using proteogenomics. *Sci. Rep.* **11**, 12472 (2021).

42. Rivera, M., Bertasso, A., McCaffrey, C. & Georgopapadakou, N. H. Porins and lipopolysaccharide of Escherichia coli ATCC 25922 and isogenic rough mutants. *FEMS Microbiology Letters* **108**, 183-187 (1993).